Supporting Information

P-Chiral Monophosphorus Ligands for Asymmetric Copper-Catalyzed Allylic Alkylation

Wenrui Xiong,[a] Guangqing Xu,[b] Xinhong Yu*[a] and Wenjun Tang*[a, b]

[a]Shanghai Key Laboratory of New Drug Design, School of Pharmacy, East China University of Science and Technology, 130 Meilong Road, Shanghai 200037, China

[b]State Key Laboratory of Bio-Organic and Natural Products Chemistry, Shanghai Institute of Organic Chemistry, Chinese Academy of Sciences, 345 Lingling Road, Shanghai 200032, China

*E-mail: tangwenjun@sioc.ac.cn

*E-mail: xhyu@ecust.edu.cn

Table of Contents

1. General Considerations

Unless otherwise noted, all commercial reagents were purchased from commercial suppliers and used without further purification. All reactions were carried out under nitrogen atmosphere in oven-dried glassware using standard Schlenk techniques. All solvents were purified and dried according to the standard methods prior to use. The ligands, copper complex and allyl substrates were prepared by following the indicated procedures described in the literature. Racemic products were synthesized by reaction of the allyl bromides with the corresponding Grignard reagent at −78 °C in dichloromethane in the presence of copper salt. Flash column chromatography was performed on silica gel (particle size 200–300 mesh, purchased from Canada) and eluted with petroleum ether/ethyl acetate.

^{1}H NMR, ^{13}C NMR, ^{31}P NMR and ^{19}F NMR spectra were recorded on a Bruker-Ultrashield PLUS400 NMR or a 500 MHz Agilent spectrometer with $CDCl_3$ as the solvent. ^{1}H chemical shifts were referenced to $CDCl_3$ at 7.26 ppm. ^{13}C chemical shifts were referenced to $CDCl_3$ at 77.16 ppm and obtained with ^{1}H decoupling. ^{31}P chemical shifts were referenced to 85% H_3PO_4 in D_2O at 0.0 ppm as external standard and obtained with ^{1}H decoupling. Multiplicities are abbreviated as follows: singlet (s), doublet (d), triplet (t), quartet (q), doublet-doublet (dd), triplet-doublet (td), quintet (quint), sextet (sextet), septet (septet), multiplet (m), and broad (br). MS was measured on Shimadzu LCMS-2010EV (EI) or Brukerdaltonics APEX III (HR-EI) mass spectrometers. Chiral HPLC analysis were performed on an Agilent 1200 system using chiral column described below in detail. Chiral GC analysis were performed on an Agilent 6890N GC using chiral column described below in detail. The optical rotations were measured on a Jacsco P-1010 polarimeter. Single crystals for X-ray structure determination were performed on SMART APEX CCD single-crystal diffractometer.

2. Procedure for the Preparation of (*E*)-Allyl Substrates

The unpurchased (*E*)-allyl substrates were synthesized from the corresponding aldehydes or ketones by a three-step Horner-Wadsworth-Emmonds olefination/DIBAL-H reduction/bromination or esterification sequence.

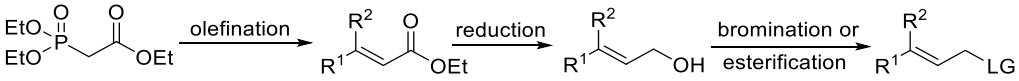

2.1 Procedure for the Horner-Wadsworth-Emmons Olefination

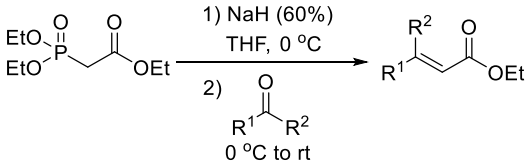

To a stirred suspension of NaH (60% in mineral oil, 1.6 equiv) in dry THF at 0 °C was added triethyl phosphonoacetate (1.6 equiv) dropwise and stirred for a further 1 h. The corresponding aldehydes or ketones (1.0 equiv) was dissolved in dry THF and added dropwise to the reaction mixture. After stirring for 24 h at rt, the solution was quenched with saturated NH_4Cl solution. The aqueous layer was extracted with EA and the combined organic layers were dried over anhydrous sodium sulfate, filtered and concentrated in vacuo to give the crude product as an *E*: *Z* mixture. The crude product was purified by column chromatography on silica gel with

*n*hexane/EA to give the desired (*E*)-allyl esters. ^{1}H NMR data of all compounds matched with those reports in the literature.[1]

2.2 Procedure for the DIBAL-H Reduction

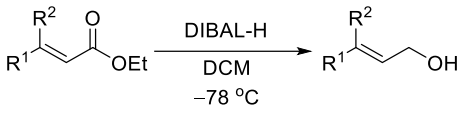

To a stirred solution of the corresponding (*E*)-allyl esters (1.0 equiv) in dry DCM at -78 °C was added dropwise DIBAL-H (1.5 M solution in toluene, 2.2 equiv). After the addition was complete, the solution was warmed to rt slowly and stirred overnight. Upon complete consumption of the starting material (as indicated by TLC), the reaction mixture was cooled to −78 °C and quenched with saturated aqueous NH_4Cl solution. After stirred at rt for 30 min, the reaction mixture was treated with anhydrous sodium sulfate and the resulting suspension was further at rt for 30 min. The suspension was passed through a pad of celite and the organic phased was separated from the filtrate, dried, and concentrated to provide crude (*E*)-allyl alcohols, which was used directly in next step without further purification. ^{1}H NMR data of all compounds matched with those reported in the literature.[2]

2.3 Procedure for the Bromination Reaction

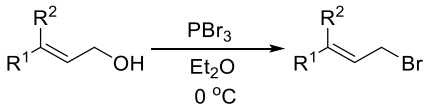

To a stirred solution of the corresponding (*E*)-allyl alcohols (1.0 equiv) in anhydrous Et_2O at 0 °C was added dropwise neat PBr_3 (1.05 equiv). After stirring at this temperature for 2 h, the reaction mixture was quenched with cold saturated aqueous NH_4Cl solution and warmed to rt. The organic layer was separated and washed with brine, dried over anhydrous sodium sulfate, filtered, and concentrated in vacuo to give the corresponding (*E*)-allyl bromides in nearly quantitative yield. NMR data of all compounds matched with those reported in the literature.[3]

(*E*)-3-(4'-(Trifluoromethyl)phenyl)-allylbromide (1b): 92% yield; yellow solid; ^{1}H NMR (500 MHz, $CDCl_3$) δ 7.58 (d, *J* = 7.9 Hz, 2H), 7.47 (d, *J* = 7.9 Hz, 2H), 6.67 (d, *J* = 15.6 Hz, 1H), 6.49 (dd, *J* = 15.5, 7.7 Hz, 1H), 4.15 (d, *J* = 7.6 Hz, 2H); ^{13}C NMR (126 MHz, $CDCl_3$) δ 139.3, 132.9, 130.0 (q, *J* = 32.6 Hz), 127.8, 126.9, 125.6 (q, *J* = 3.8 Hz), 125.1, 122.9, 32.4. The ^{1}H NMR and ^{13}C NMR spectra are in agreement with those reported in the literature.[3a]

(*E*)-3-(4'-Bromophenyl)-allylbromide (1c): 85% yield; grey solid; ^{1}H NMR (500 MHz, $CDCl_3$) δ 7.49–7.42 (m, 2H), 7.32–7.20 (m, 2H), 6.58 (d, *J* = 15.6 Hz, 1H), 6.38 (dt, *J* = 15.5, 7.7 Hz, 1H), 4.13 (dd, *J* = 7.7, 0.9 Hz, 2H); ^{13}C NMR (126 MHz, $CDCl_3$) δ 134.7, 133.3, 131.8, 128.2, 126.0, 122.2, 32.9. The ^{1}H NMR and ^{13}C NMR spectra are in agreement with those reported in the literature.[3a]

(*E*)-3-(4'-Chlorophenyl)-allylbromide (1d): 87% yield; white solid; ^{1}H NMR (500 MHz, $CDCl_3$) δ 7.33–7.27 (m, 4H), 6.60 (d, *J* = 15.6 Hz, 1H), 6.37 (dt, *J* = 15.5, 7.8 Hz, 1H), 4.14 (dd, *J* = 7.8, 0.9 Hz, 2H); ^{13}C NMR (126 MHz, $CDCl_3$) δ 134.3, 134.0, 133.2, 128.8, 127.9, 125.8, 33.0. The ^{1}H NMR and ^{13}C NMR spectra are in

agreement with those reported in the literature.[3a]

(*E*)-3-(4'-Methylphenyl)-allylbromide (1e): 82% yield; grey solid; ^{1}H NMR (500 MHz, $CDCl_3$) δ 7.28 (t, *J* = 8.9 Hz, 2H), 7.14 (d, *J* = 7.0 Hz, 2H), 6.62 (d, *J* = 15.5 Hz, 1H), 6.35 (dt, *J* = 15.2, 7.5 Hz, 1H), 4.17 (d, *J* = 7.5 Hz, 2H), 2.35 (s, 3H); ^{13}C NMR (126 MHz, $CDCl_3$) δ 138.3, 134.5, 133.0, 129.3, 126.7, 124.2, 33.8, 21.3. The ^{1}H NMR and ^{13}C NMR spectra are in agreement with those reported in the literature.[3c]

(*E*)-3-(3'-Bromophenyl)-allylbromide (1f): 89% yield; pale yellow oil; ^{1}H NMR (500 MHz, $CDCl_3$) δ 7.53 (s, 1H), 7.39 (d, *J* = 7.9 Hz, 1H), 7.29 (d, *J* = 7.8 Hz, 1H), 7.19 (t, *J* = 7.8 Hz, 1H), 6.56 (d, *J* = 15.6 Hz, 1H), 6.39 (dt, *J* = 15.5, 7.7 Hz, 1H), 4.13 (d, *J* = 7.7 Hz, 2H); ^{13}C NMR (126 MHz, $CDCl_3$) δ 137.9, 132.9, 131.2, 130.1, 129.5, 126.8, 125.4, 122.8, 32.6. The ^{1}H NMR and ^{13}C NMR spectra are in agreement with those reported in the literature.[3c]

(*E*)-3-(3'-Chlorophenyl)-allylbromide (1g): 92% yield; pale yellow oil; ^{1}H NMR (500 MHz, $CDCl_3$) δ 7.37 (s, 1H), 7.25 (s, 3H), 6.58 (d, J = 15.6 Hz, 1H), 6.40 (dt, *J* = 15.5, 7.7 Hz, 1H), 4.14 (d, *J* = 7.7 Hz, 2H); ^{13}C NMR (126 MHz, $CDCl_3$) δ 137.6, 134.6, 133.0, 129.9, 128.3, 126.7, 126.6, 124.9, 32.7. The ^{1}H NMR and ^{13}C NMR spectra are in agreement with those reported in the literature.[3c]

(*E*)-3-(3'-Methylphenyl)-allylbromide (1h): 85% yield; yellow oil; ^{1}H NMR (500 MHz, $CDCl_3$) δ 7.30–7.21 (m, 3H), 7.13 (d, *J* = 7.2 Hz, 1H), 6.64 (d, *J* = 15.6 Hz, 1H), 6.42 (dt, *J* = 15.6, 7.8 Hz, 1H), 4.19 (d, *J* = 7.8 Hz, 2H), 2.39 (s, 3H); 13C NMR (126 MHz, $CDCl_3$) δ 138.2, 135.8, 134.7, 129.2, 128.6, 127.5, 125.0, 124.0, 33.7, 21.4. The ^{1}H NMR and ^{13}C NMR spectra are in agreement with those reported in the literature.[3c]

(*E*)-3-(Cyclohexyl)-allylbromide (1i): 83% yield; colorless oil; ^{1}H NMR (500 MHz, $CDCl_3$) δ 5.71 (dd, *J* = 15.3, 6.4 Hz, 1H), 5.68–5.58 (m, 1H), 3.95 (d, *J* = 7.3 Hz, 2H), 1.99 (ddd, *J* = 11.2, 9.6, 3.2 Hz, 1H), 1.78–1.69 (m, 4H), 1.68–1.61 (m, 1H), 1.31–1.21 (m, 2H), 1.20–1.13 (m, 1H), 1.12–1.01 (m, 2H); ^{13}C NMR (126 MHz, $CDCl_3$) δ 142.1, 123.9, 40.2, 33.4, 32.4, 26.0, 25.6. The ^{1}H NMR and ^{13}C NMR spectra are in agreement with those reported in the literature.[3a]

(*E*)-3-(2'-Methylphenyl)-allylbromide (1l): 80% yield; yellow oil; ^{1}H NMR (500 MHz, $CDCl_3$) δ 7.45 (dd, *J* = 8.5, 4.5 Hz, 1H), 7.24–7.06 (m, 3H), 6.88 (d, *J* = 15.4 Hz, 1H), 6.30 (dt, *J* = 15.5, 7.8 Hz, 1H), 4.19 (dd, *J* = 7.8, 0.9 Hz, 2H), 2.37 (s, 3H); ^{13}C NMR (126 MHz, $CDCl_3$) δ 135.8, 134.8, 132.2, 130.4, 128.2, 126.5, 126.2, 125.9, 33.6. The ^{1}H NMR and ^{13}C NMR spectra are in agreement with those reported in the literature.[3a]

(*E*)-3-(1'-Naphthyl)-allylbromide (1m): 86% yield; grey solid; ^{1}H NMR (500 MHz, $CDCl_3$) δ 8.11 (d, *J* = 8.1 Hz, 1H), 7.87 (d, *J* = 7.8 Hz, 1H), 7.82 (d, *J* = 8.2 Hz, 1H), 7.63 (d, *J* = 7.1 Hz, 1H), 7.57–7.50 (m, 2H), 7.47 (t, *J* = 7.4 Hz, 1H), 7.42 (d, *J* = 15.3 Hz, 1H), 6.45 (dtd, *J* = 8.8, 7.7, 1.1 Hz, 1H), 4.28 (d, *J* = 7.7 Hz, 2H); ^{13}C NMR (126 MHz, $CDCl_3$) δ 133.6, 133.4, 131.6, 131.1, 128.7, 128.6, 128.3, 126.3, 125.9, 125.6, 124.3, 123.5, 33.4. The ^{1}H NMR and ^{13}C NMR spectra are in agreement with those reported in the literature.[3a]

(*E*)-3-(2'-Naphthyl)-allylbromide (1n): 85% yield; white solid; ^{1}H NMR (500 MHz, $CDCl_3$) δ 7.81 (t, *J* = 7.4 Hz, 3H), 7.75 (s, 1H), 7.59 (dd, *J* = 8.5, 1.1 Hz, 1H), 7.53–7.40 (m, 2H), 6.81 (d, *J* = 15.6 Hz, 1H), 6.53 (dt, *J* = 15.6, 7.8 Hz, 1H), 4.22 (d, *J* = 7.8 Hz, 2H); ^{13}C NMR (126 MHz, $CDCl_3$) δ 134.7, 133.4, 133.3, 133.2, 128.4, 128.1, 127.7, 127.1, 126.4, 126.3, 125.5, 123.5, 33.6. The ^{1}H NMR and ^{13}C NMR spectra are in agreement with those reported in the literature.[3c]

(*E*)-(4-Bromobut-2-en-2-yl)benzene (1o): 85% yield; pale yellow oil; ^{1}H NMR (400 MHz, $CDCl_3$) δ 7.43–7.37 (m, 2H), 7.37–7.30 (m, 2H), 7.30–7.23 (m, 1H), 6.08 (ddd, *J* = 8.5, 5.0, 1.3 Hz, 1H), 4.20 (d, *J* = 8.6 Hz, 2H), 2.14 (s, 3H); ^{13}C NMR (126 MHz, $CDCl_3$) δ 142.7, 141.5, 128.3, 127.8, 125.9, 122.8, 29.4, 15.6. The ^{1}H NMR and ^{13}C NMR spectra are in agreement with those reported in the literature.[3e]

(*E*)-1'-Bromo-4'-(4-bromobut-2-en-2-yl)benzene (1p): 88% yield; pale yellow oil; ^{1}H NMR (500 MHz, $CDCl_3$) δ 7.46 (d, *J* = 8.5 Hz, 2H), 7.27 (d, *J* = 8.3 Hz, 3H), 6.08 (t, *J* = 8.5 Hz, 1H), 4.17 (d, *J* = 8.5 Hz, 2H), 2.11 (s, 3H); ^{13}C NMR (126 MHz, $CDCl_3$) δ 141.0, 140.3, 131.4, 127.5, 123.4, 121.8, 28.9, 15.5. The ^{1}H NMR and ^{13}C NMR spectra are in agreement with those reported in the literature.[3e]

(*E*)-1'-Chloro-4'-(4-bromobut-2-en-2-yl)benzene (1q): 80% yield; pale yellow oil; ^{1}H NMR (500 MHz, $CDCl_3$) δ 7.35–7.28 (m, 4H), 6.07 (td, *J* = 8.5, 1.2 Hz, 1H), 4.18 (d, *J* = 8.5 Hz, 2H), 2.12 (s, 3H); ^{13}C NMR (126 MHz, $CDCl_3$) δ 140.6, 140.2, 133.6, 128.5, 127.2, 123.3, 29.0, 15.6. The ^{1}H NMR and ^{13}C NMR spectra are in agreement with those reported in the literature.[3b]

(*E*)-1'-Trifluoromethyl-4'-(4-bromobut-2-en-2-yl)benzene (1r): 91% yield; white solid; ^{1}H NMR (500 MHz, $CDCl_3$) δ 7.59 (d, *J* = 8.4 Hz, 2H), 7.50 (d, *J* = 8.1 Hz, 2H), 6.14 (t, *J* = 8.4 Hz, 1H), 4.18 (d, *J* = 8.5 Hz, 2H), 2.16 (s, 3H); ^{13}C NMR (126 MHz, $CDCl_3$) δ 145.7, 140.0, 129.8–129.3 (m), 127.4, 126.2, 125.4–125.1 (m), 124.8, 123.0, 28.4, 15.5. The ^{1}H NMR and ^{13}C NMR spectra are in agreement with those reported in the literature.[3f]

(*E*)-1'-Methyl-4'-(4-Bromobut-2-en-2-yl) benzene (1s): 80% yield; colourless oil; ^{1}H NMR (500 MHz, $CDCl_3$) δ 7.33 (d, *J* = 8.1 Hz, 2H), 7.21–7.19 (m, 1H), 7.19–7.15 (m, 2H), 6.09 (dd, *J* = 8.5, 7.5 Hz, 1H), 4.22 (d, *J* = 8.6 Hz, 2H), 2.37 (s, 3H), 2.15 (s, 3H). The ^{1}H NMR spectra is in agreement with those reported in the literature.[3b]

(*E*)-1'-Methyl-3'-(4-bromobut-2-en-2-yl)benzene (1t): 82% yield; yellow oil; ^{1}H NMR (500 MHz, $CDCl_3$) δ 7.28–7.19 (m, 3H), 7.13 (d, *J* = 7.0 Hz, 1H), 6.10 (t, *J* = 8.5 Hz, 1H), 4.22 (d, *J* = 8.6 Hz, 2H), 2.39 (s, 3H), 2.39 (s, 3H), 2.16 (s, 3H); ^{13}C NMR (126 MHz, $CDCl_3$) δ 142.2, 141.6, 137.9, 128.6, 128.2, 126.7, 123.1, 122.6, 29.6, 21.5, 15.7. The ^{1}H NMR and ^{13}C NMR spectra are in agreement with those reported in the literature.[3b]

(*E*)-1'-Bromo-3'-(4-bromobut-2-en-2-yl)benzene (1u): 90% yield; pale yellow oil; ^{1}H NMR (500 MHz, $CDCl_3$) δ 7.54 (d, *J* = 7.9 Hz, 1H), 7.30–7.24 (m, 1H), 7.13 (ddd, *J* = 15.5, 7.9, 1.5 Hz, 2H), 5.72 (td, *J* = 8.4, 1.3 Hz, 1H), 4.13 (t, *J* = 6.5 Hz, 2H), 2.08 (s, 3H); ^{13}C NMR (126 MHz, $CDCl_3$) δ 144.6, 142.5, 132.8, 129.6, 128.7, 127.3, 126.0, 121.8, 28.2, 17.5. The ^{1}H NMR and ^{13}C NMR spectra are in agreement with those reported in the literature.[3e]

(*E*)-1'-Chloro-3'-(4-bromobut-2-en-2-yl)benzene (1v): 89% yield; yellow oil; ^{1}H NMR (500 MHz, $CDCl_3$) δ 7.38 (s, 1H), 7.29–7.22 (m, 3H), 6.08 (t, *J* = 8.5 Hz, 1H), 4.16 (d, *J* = 8.5 Hz, 2H), 2.11 (s, 3H); ^{13}C NMR (126 MHz, $CDCl_3$) δ 144.0, 140.0, 134.3, 127.8, 126.1, 124.1, 123.9, 28.9, 15.5. The ^{1}H NMR and ^{13}C NMR spectra are in agreement with those reported in the literature.[3d]

(*E*)-1'-Trifluoromethyl-3'-(4-bromobut-2-en-2-yl)benzene (1w): 90% yield; yellow oil; ^{1}H NMR (500 MHz, $CDCl_3$) δ 7.65 (s, 1H), 7.58 (d, *J* = 7.7 Hz, 1H), 7.54 (d, *J* = 7.4 Hz, 1H), 7.46 (t, *J* = 7.8 Hz, 1H), 6.14 (t, *J* = 8.4 Hz, 1H), 4.19 (d, *J* = 8.5 Hz, 2H), 2.17 (s, 3H); ^{13}C NMR (126 MHz, $CDCl_3$) δ 143.0, 140.0, 129.2 (d, *J* = 1.1 Hz), 128.8, 124.4 (q, *J* = 3.4 Hz), 122.7 (q, *J* = 3.8 Hz), 28.4, 15.3. The ^{1}H NMR and ^{13}C NMR spectra are in agreement with those reported in the literature.[3b]

(*E*)-1'-Bromo-2'-(4-bromobut-2-en-2-yl)benzene (1x): 83% yield; pale yellow oil; ^{1}H NMR (500 MHz, $CDCl_3$) δ 7.54 (d, *J* = 7.9 Hz, 1H), 7.29–7.25 (m, 1H), 7.13 (ddd, *J* = 15.5, 7.9, 1.5 Hz, 2H), 5.72 (td, *J* = 8.4, 1.3 Hz, 1H), 4.13 (d, *J* = 8.4 Hz, 2H), 2.08 (s, 3H); ^{13}C NMR (126 MHz, $CDCl_3$) δ 144.7, 142.6, 132.9, 129.6, 128.7, 127.3, 126.0, 121.8, 28.2, 17.5. The ^{1}H NMR and ^{13}C NMR spectra are in agreement with those reported in the literature.[3b]

(*E*)-1'-(4-Bromobut-2-en-2-yl)naphthalene (1y): 88% yield; pale yellow oil; ^{1}H NMR (500 MHz, $CDCl_3$) δ 8.00–7.93 (m, 1H), 7.91–7.86 (m, 1H), 7.81 (t, *J* = 7.6 Hz, 1H), 7.54–7.50 (m, 2H), 7.46 (dd, *J* = 8.1, 7.2 Hz, 1H),

7.29 (dd, *J* = 7.0, 1.0 Hz, 1H), 5.93 (td, *J* = 8.5, 1.4 Hz, 1H), 4.28 (d, *J* = 8.5 Hz, 2H), 2.24 (d, *J* = 1.2 Hz, 3H); ^{13}C NMR (126 MHz, $CDCl_3$) δ 142.1, 142.0, 133.8, 130.9, 128.4, 127.6, 126.1, 126.0, 125.8, 125.4, 125.3, 124.7, 28.7, 18.8. The ^{1}H NMR and ^{13}C NMR spectra are in agreement with those reported in the literature.[3e]

(*E*)-2'-(4-Bromobut-2-en-2-yl)naphthalene (1z): 87% yield; white solid; ^{1}H NMR (500 MHz, $CDCl_3$) δ 7.85–7.79 (m, 4H), 7.58 (dd, *J* = 8.6, 1.8 Hz, 1H), 7.48 (ddd, *J* = 6.9, 5.7, 3.4 Hz, 2H), 6.26 (td, *J* = 8.5, 1.3 Hz, 1H), 4.27 (d, *J* = 8.5 Hz, 2H), 2.26 (d, *J* = 1.0 Hz, 3H); ^{13}C NMR (126 MHz, $CDCl_3$) δ 141.3, 139.3, 133.3, 132.9, 128.2, 127.9, 127.5, 126.3, 126.1, 124.9, 124.0, 123.3, 29.4, 15.6. The ^{1}H NMR and ^{13}C NMR spectra are in agreement with those reported in the literature.[3f]

(*E*)-(1-Bromohex-2-en-3-yl)benzene (1x'): 85% yield; colourless oil; ^{1}H NMR (500 MHz, $CDCl_3$) δ 7.36 (dd, *J* = 13.9, 6.9 Hz, 5H), 6.00 (t, *J* = 8.6 Hz, 1H), 4.22 (d, *J* = 8.6 Hz, 2H), 2.59 (dd, *J* = 16.3, 8.5 Hz, 2H), 1.42 (m, 2H), 0.91 (t, *J* = 7.2 Hz, 6H). The ^{1}H NMR spectra is in agreement with those reported in the literature.[3f]

(*E*)-(1-Bromo-4-methylpent-2-en-3-yl)benzene (1y'): 82% yield; pale yellow oil; ^{1}H NMR (500 MHz, $CDCl_3$) δ 7.33–7.27 (m, 3H), 7.18 (dd, *J* = 7.9, 1.6 Hz, 2H), 5.63 (t, *J* = 8.6 Hz, 1H), 4.18 (d, *J* = 8.6 Hz, 2H), 3.15 (dt, *J* = 14.0, 7.0 Hz, 1H), 1.10 (d, *J* = 7.0 Hz, 6H); ^{13}C NMR (126 MHz, $CDCl_3$) δ 152.9, 141.5, 128.2, 127.7, 126.9, 123.9, 29.2, 28.0, 21.6, 21.3. The ^{1}H NMR and ^{13}C NMR spectra are in agreement with those reported in the literature.[3e]

2.4 Procedure for the Esterification Reaction

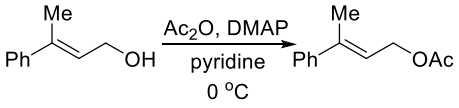

Allylic alcohol (1.8 mg, 12.4 mmol) and DMAP (76 mg, 0.62 mmol) were dissolved in pyridine (10 mL) at 0 °C. Acetic anhydride (5 mL) was added slowly at 0 °C. The solution was stirred at rt for 24 h and quenched with saturated aqueous $NaHCO_3$ solution. It was then diluted with water (10 mL), extracted with CH_2Cl_2 (3×20 mL), dried over anhydrous sodium sulfate and evaporated. The residue was purified by column chromatography on silica gel with *n*hexane/EA to afford the allylic acetate as liquid (85% yield). ^{1}H NMR (400MHz, $CDCl_3$) δ 7.27–7.45 (m, 5H), 5.93 (td, *J* = 1.2, 6.9 Hz, 1H), 4.82 (d, *J* = 6.9 Hz, 2H), 2.14 (s, 3H), 2.12 (s, 3H).

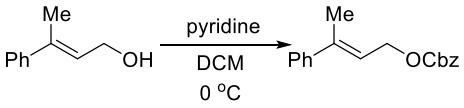

To a mixture of pyridine (2.4 mL, 30.0 mmol, 3.0 equiv), the allylic alcohol (1.5 g, 10.0 mmol, 1.0 equiv) and DCM (10 mL) was added benzyl chloroformate (2.8 mL, 20.0 mmol, 2.0 equiv) dropwise at 0 °C. The reaction mixture was allowed to warm to rt and stirred overnight (monitored by TLC). The mixture was then quenched with water (10 mL) and diluted with EA (10 mL). The organic layer was separated, washed sequentially with HCl solution (1M, 20 mL) and brine (20 mL), concentrated, and purified by column chromatography with *n*hexane/EA to give the allylic benzyl carbonate as a colorless oil (89% yield). ^{1}H NMR (400 MHz, $CDCl_3$) δ 7.39 (t, *J* = 1.8 Hz, 1H), 7.37 (s, 2H), 7.35 (t, *J* = 2.1 Hz, 2H), 7.34–7.32 (m, 2H), 7.32–7.28 (m, 2H), 7.28–7.25 (m, 1H), 5.90 (dd, *J* = 7.6, 6.4 Hz, 1H), 5.16 (s, 2H), 4.85 (d, *J* = 7.0 Hz, 2H), 2.10 (s, 3H).

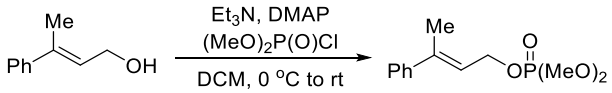

To a solution of allylic alcohol (1 g, 6.8 mmol, 1.0 equiv) and Et_3N (1.4 ml, 10.1 mmol, 1.5 equiv) in DCM (15 mL), $(MeO)_2P(O)Cl$ (0.9 ml, 8.1 mmol, 1.2 equiv) and DMAP (247 mg, 2.02 mmol, 0.3 equiv) were sequentially added at 0 °C. The reaction mixture was allowed to warm to rt, stirred for another 12 h and then diluted with EA (10 mL) and water (10 mL). The organic layer was separated and the aqueous layer was extracted with EA (10 mL). The combined organic layer was washed with water and brine, dried over anhydrous sodium sulfate, and concentrated to provide crude allylic phosphate as a yellow oil (80% yield). ^{1}H NMR (500 MHz, $CDCl_3$) δ 7.41 (d, *J* = 7.3 Hz, 2H), 7.34 (t, *J* = 7.4 Hz, 2H), 7.31–7.26 (m, 1H), 5.95 (td, *J* = 7.0, 1.1 Hz, 1H), 4.83–4.75 (m, 2H), 3.80 (s, 3H), 3.77 (s, 3H), 2.13 (s, 3H).

3. The Synthesis of P-Chiral Monophosphorus Ligands

Ligands **L1**–**L6**, **L9** and **L11** were prepared according to procedures described in our previous reports.[4-6] The synthesis of **L12**–**L18** was similar to the procedure for the synthesis of **L5** and **L6**.[6a] Ligands **L7**, **L8**, **L10** and **L19** were prepared according to procedures described as follows. The compound **A** was prepared according to a procedure described in our previous reports.[4]

3.1 The Synthesis of L7 and L8

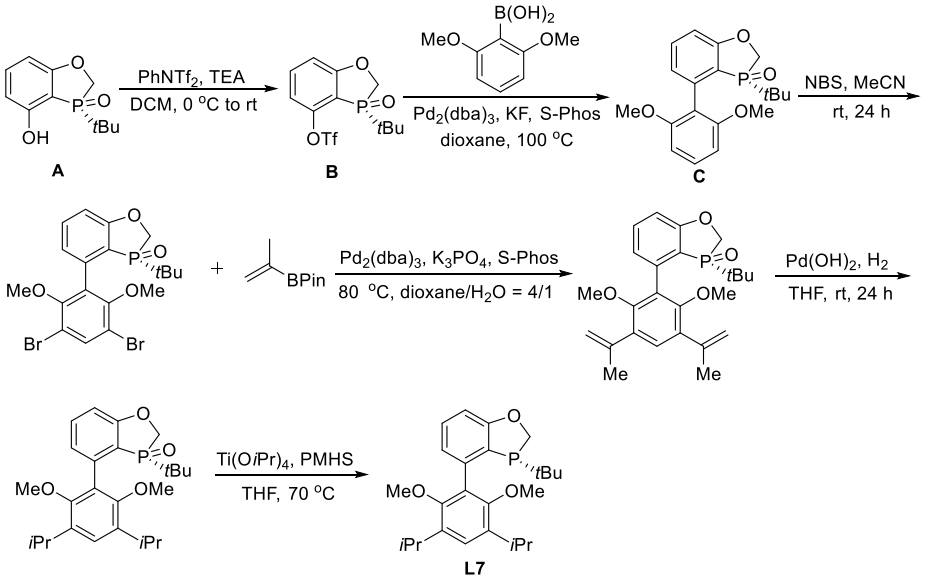

(1) To a solution of compound **A** (1.0 equiv) and triethylamine (4.0 equiv) in DCM at 0 °C was added Tf_2NPh (1.2 equiv). The mixture was stirred at rt for 5 h and then quenched with addition of water. The organic layer was separated, dried over anhydrous sodium sulfate, concentrated, and purified by column chromatography with *n*hexane/EA to give the triflate product as a white solid (94% yield). (2) To a solution of the triflate product (1.0 equiv) and 2, 6-dimethoxyphenylboronic acid (1.5 equiv), $Pd_2(dba)_3$ (1 mol %), S-Phos (3 mol %) and potassium fluoride (4.0 equiv) was charged degassed dioxane. The mixture was stirred at 100 °C under nitrogen for 10 h and then cooled to rt. The resulting mixture was removed most dioxane under a reduced pressure. And column chromatography was conducted with *n*hexane/EA to provide the coupling product as a white crystalline solid (90% yield). (3) The coupling product (1.0 equiv) and acetonitrile were charged into a flask. NBS (2.5 equiv) was added to the formed solution. The reaction mixture was stirred at rt for 16 h. Water and EA were added to the

reaction mixture. The mixture stirred for 20 min then the organic fraction is separated, washed with 2N HCl, dried over anhydrous sodium sulfate, filtered then concentrated. The crude product is purified by column chromatography with *n*hexane/EA to provide the desired bromide product as a white solid (82% yield). (4) To a solution of the bromide product (1.0 equiv) and isopropenylboronic acid pinacol ester (3.0 equiv), $Pd_2(dba)_3$ (3 mol %), S-Phos (6 mol %) and potassium phosphate (6.0 equiv) was charged degassed dioxane and water. The mixture was stirred at 80 °C under nitrogen for 18 h and then cooled to rt. The resulting mixture was removed most solvent under a reduced pressure. And column chromatography was conducted with *n*hexane/EA to provide the coupling product as a white crystalline solid (76% yield). (5) The hydrogenation of the coupling product was performed in the presence of $Pd(OH)_2$ and H_2 in THF at rt for 16 h. After concentrated, the resulting mixture was directly performed column chromatography with *n*hexane/EA to provide the oxidation state product as a white crystalline solid (85% yield). (6) The oxaphosphole oxide was added to a Schlenk flask equipped with magnetic stirring bar. THF was charged followed by addition of PMHS and $Ti(O\textit{i}Pr)_4$ (3.0 equiv). The reaction mixture was heated at 70 °C and monitored by ^{31}P NMR spectroscopy. The reaction mixture then was cooled to rt and quenched by dropwise addition of degassed 30 % NaOH at 0 °C, the resulting mixture was further stirred at 60 °C for 0.5 h. The aqueous layer was removed and subsequently extracted under nitrogen atmosphere. The combined organics were dried over anhydrous sodium sulfate then filtered through nitrogen-purged neutral alumina with Et_2O. The solvents were removed under reduced pressure to afford ligand **L7** as a colourless oil (80% yield). ^1H NMR (500 MHz, $CDCl_3$) δ 7.31 (t, *J* = 7.8 Hz, 1H), 7.13 (s, 1H), 7.03 (dd, *J* = 7.2, 2.9 Hz, 1H), 6.91 (dd, *J* = 8.1, 0.5 Hz, 1H), 4.82 (d, *J* = 12.5, 2.0 Hz, 1H), 4.57 (dd, *J* = 26.3, 12.5 Hz, 1H), 3.65 (s, 3H), 3.38 (dt, *J* = 13.8, 6.9 Hz, 1H), 3.32 (s, 3H), 3.25 (dt, *J* = 13.8, 6.9 Hz, 1H), 1.31 (d, *J* = 6.9 Hz, 3H), 1.27 (d, *J* = 7.0 Hz, 3H), 1.23 (d, *J* = 6.9 Hz, 3H), 1.12 (d, *J* = 6.9 Hz, 3H), 0.72 (d, *J* = 12.2 Hz, 9H); ^{13}C NMR (126 MHz, $CDCl_3$) δ 163.7, 153.6, 152.6, 139.7 (d, *J* = 17.7 Hz), 138.0, 137.3, 130.0, 129.0, 125.0 (d, *J* = 16.0 Hz), 123.4, 123.3 (d, *J* = 4.1 Hz), 109.7, 70.6, 70.4, 62.3, 61.1, 30.74 (d, *J* = 19.7 Hz), 29.7, 26.9 (d, *J* = 14.8 Hz), 26.6 (d, *J* = 4.7 Hz), 24.4 (d, *J* = 5.5 Hz), 23.4 (d, *J* = 5.1 Hz); ^{31}P NMR (121 MHz, $CDCl_3$) δ -4.8; ESI-MS: m/z 415.30 $[M+H]^+$; HRMS (ESI) m/z calcd for $C_{25}H_{36}O_3P$ $[M+H]^+$: 415.2402, found: 415.2397.

The synthesis of ligand **L8** was followed according to a similar experimental procedure. **L8**: 85% yield; White solid; ^1H NMR (500 MHz, $CDCl_3$) δ 7.34–7.30 (m, 1H), 7.15 (s, 1H), 7.03 (ddd, *J* = 7.5, 3.2, 0.8 Hz, 1H), 6.92 (dd, *J* = 8.1, 0.8 Hz, 1H), 4.83 (dd, *J* = 12.5, 2.0 Hz, 1H), 4.57 (dd, *J* = 26.3, 12.5 Hz, 1H), 3.66 (s, 3H), 3.44–3.37 (m, 1H), 3.34 (s, 3H), 3.28 (dd, *J* = 17.4, 9.9 Hz, 1H), 2.11–1.94 (m, 4H), 1.89–1.77 (m, 4H), 1.74–1.60 (m, 6H), 1.43–1.26 (m, 2H), 0.73 (d, *J* = 12.2 Hz, 9H); ^{13}C NMR (126 MHz, $CDCl_3$) δ 163.7, 154.4, 153.3, 139.71 (d, *J* = 17.7 Hz), 135.3, 134.8, 130.0, 128.9, 124.7, 123.3 (d, *J* = 4.1 Hz), 109.7, 70.7, 70.4, 62.4, 61.2, 38.6 (d, *J* = 12.0 Hz), 35.4, 34.7, 34.5, 34.2, 30.8 (d, *J* = 19.8 Hz), 26.9 (d, *J* = 14.7 Hz), 25.6 (dd, *J* = 17.3, 12.0 Hz); ^{31}P NMR (162 MHz, $CDCl_3$) δ -6.1; ESI-MS: m/z 467.30 $[M+H]^+$; HRMS (ESI) m/z calcd for $C_{29}H_{40}O_3P$ $[M+H]^+$: 467.2715, found: 467.2703.

3.2 The Synthesis of L10

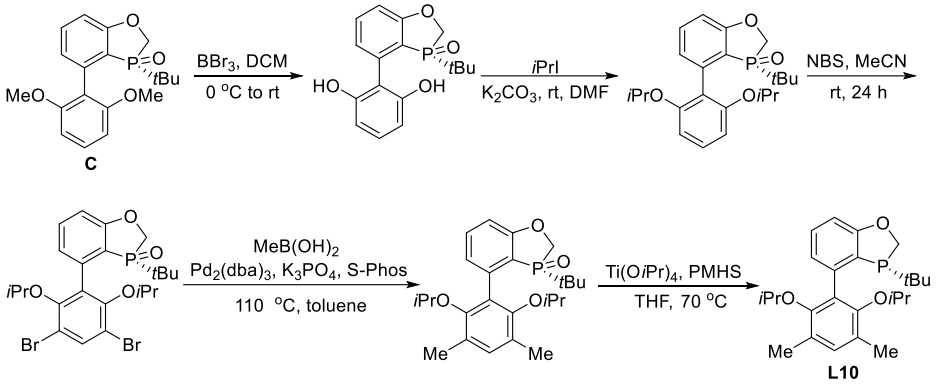

The synthesis of compound **B** was followed by the above description.

(1) Compound **B** (1.0 equiv) was placed in a dry Schlenk tube, then DCM was added and stirred to completely dissolve the material. The reaction system was transferred to an ice water bath and BBr_3 (2.5 equiv, 1.0 M in DCM) was slowly added at 0 °C. After the completion of the dropwise addition, the reaction system was warmed to room temperature, stirred overnight and monitored by TLC. The reaction was quenched by adding MeOH. The residue was purified by column chromatography with *n*hexane/EA to give a white crystal product (91% yield). (2) The white crystal product (1.0 equiv) and anhydrous K_2CO_3 (3.0 equiv) were placed in a dry Schlenk tube, DMF was added and stirred to dissolve the materials. *i*PrI (5.0 equiv) was then added to the reaction system. After complete conversion, the reaction mixture was concentrated and column chromatography was conducted with *n*hexane/EA to provide the product as a white solid (94% yield). (3) The product (1.0 equiv) and acetonitrile were charged into a flask. NBS (2.5 equiv) was added to the formed solution. The reaction mixture was stirred at rt for 16 h. Water and EA were added to the reaction mixture. The mixture stirred for 20 min then the organic fraction is separated, washed with 2N HCl, dried over anhydrous sodium sulfate, filtered then concentrated. The crude product is purified by column chromatography with *n*hexane/EA to provide the desired bromide product as a white solid (85% yield). (4) To a solution of the bromide product (1.0 equiv) and methyl-boric acid (3.0 equiv), $Pd_2(dba)_3$ (3 mol %), S-Phos (6 mol %) and potassium phosphate (6.0 equiv) was charged dry toluene. The mixture was stirred at 110 °C under nitrogen for 18 h and then cooled to rt. The resulting mixture was removed most solvent under a reduced pressure and filtered over celite. After concentrated, column chromatography was conducted with *n*hexane/EA to provide the coupling product as a white crystalline solid (76% yield). (5) The oxaphosphole oxide was added to a Schlenk flask equipped with magnetic stirbar. THF was charged followed by addition of PMHS and Ti(O*i*Pr)$_4$ (3.0 equiv). The reaction mixture was heated at 70 °C and monitored by ^{31}P NMR spectroscopy. The reaction mixture then was cooled to rt and quenched by dropwise addition of degassed 30 % NaOH at 0 °C, the resulting mixture was further stirred at 60 °C for 0.5 h. The aqueous layer was removed and subsequently extracted under nitrogen atmosphere. The combined organics were dried over anhydrous sodium sulfate then filtered through nitrogen-purged neutral alumina with Et_2O. The solvents were removed under reduced pressure to afford ligand **L10** as a colourless oil (87% yield). ^{1}H NMR (500 MHz, $CDCl_3$) δ 7.30 (t, *J* = 7.8 Hz, 1H), 7.16 (dd, *J* = 7.1, 3.6, 1H), 6.97 (s, 1H), 6.90 (dd, *J* = 8.0, 0.8 Hz, 1H), 4.86 (dd, *J* = 12.5, 1.9 Hz, 1H), 4.54 (dd, *J* = 26.4, 12.5 Hz, 1H), 3.88 (dt, *J* = 12.2, 6.1 Hz, 1H), 3.61 (dq, *J* = 12.3, 6.1 Hz, 1H), 2.27 (s, 3H), 2.22 (s, 3H), 1.07 (d, *J* = 6.1 Hz, 3H), 1.03 (d, *J* = 6.1 Hz, 3H), 0.98 (d, *J* = 6.1 Hz, 3H), 0.82 (d, *J* = 6.2 Hz, 3H), 0.78 (d, *J* = 12.2 Hz, 9H); ^{13}C NMR (126 MHz, $CDCl_3$) δ 163.9, 152.2, 151.8, 140.1, 139.9, 131.8, 130.2,

128.9, 127.3, 126.6, 124.3 (d, J = 4.3 Hz), 109.8, 75.4, 73.9, 70.5, 70.3, 30.8, 30.6, 27.1 (d, J = 14.9 Hz), 22.7 (d, J = 2.4 Hz), 22.4, 22.0, 17.1, 16.8; ^{31}P NMR (162 MHz, $CDCl_3$) δ -4.8; ESI-MS: m/z 415.30 $[M+H]^+$; HRMS (ESI) m/z calcd for $C_{25}H_{36}O_3P$ $[M+H]^+$: 415.2402, found: 415.2397.

3.3 The Synthesis of L19

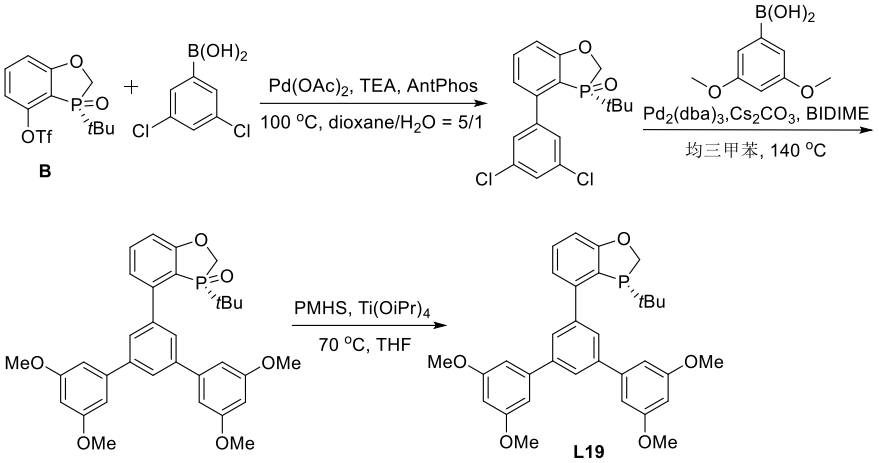

(1) To a mixture of compound **B** (1.0 equiv) and 3, 5-dichlorophenylboronic acid (2.0 equiv), $Pd(OAc)_2$ (5 mol %), Antphos (10 mol %) and TEA (3.0 equiv) was charged degassed dioxane/H_2O. The mixture was stirred under nitrogen for 24 h at 100 °C, concentrated, partitioned with water and DCM. The DCM layer was dried over anhydrous sodium sulfate, concentrated, and purified by column chromatography with *n*hexane/EA to provide pure product (55% yield). (2) To a solution of the pure product (1.0 equiv) and 3, 5-dimethoxyphenylboronic acid acid (6.0 equiv), $Pd_2(dba)_3$ (10 mol %), BI-DIME (20 mol %) and Cs_2CO_3 (8.0 equiv) was charged degassed mesitylene. The mixture was stirred at 140 °C under nitrogen for 24 h and then cooled to rt. The resulting mixture was concentrated and purified by column chromatography with *n*hexane/EA to provide the oxidation state of **L19** (92% yield). (3) To a solution of oxidation state of **L19** (1.0 equiv) in THF at rt was added PMHS (3.0 equiv) and Ti(O*i*Pr)$_4$ (3.0 equiv). The reaction mixture was heated at 70 °C and monitored by ^{31}P NMR spectroscopy. The reaction mixture then was cooled to rt and quenched by dropwise addition of degassed 30 % NaOH at 0 °C, the resulting mixture was further stirred at 60 °C for 0.5 h. The aqueous layer was removed and subsequently extracted under nitrogen atmosphere. The combined organics were dried over anhydrous sodium sulfate then filtered through nitrogen-purged neutral alumina with Et_2O. The solvents were removed under reduced pressure to afford ligand **L19** as a white solid (75% yield). ^{1}H NMR (500 MHz, $CDCl_3$) δ 7.97 (d, J = 1.6 Hz, 2H), 7.74 (t, J = 1.6 Hz, 1H), 7.41–7.37 (m, 1H), 7.13 (dd, J = 6.7, 3.5 Hz, 1H), 6.96 (dd, J = 8.1, 0.8 Hz, 1H), 6.87 (d, J = 2.3 Hz, 4H), 6.51 (s, 2H), 4.88 (dd, J = 12.6, 1.9 Hz, 1H), 4.63 (dd, J = 26.0, 12.6 Hz, 1H), 3.88 (s, 12H), 0.69 (d, J = 12.1 Hz, 9H); ^{13}C NMR (126 MHz, $CDCl_3$) δ 166.0 (d, J = 19.2 Hz), 161.2, 146.3 (d, J = 5.5 Hz), 142.9, 141.9, 141.5 (d, J = 1.5 Hz), 135.0, 127.6, 125.7, 123.3 (d, J = 7.9 Hz), 113.0 (d, J = 5.2 Hz), 105.6, 99.7, 65.7 65.2, 55.6, 34.3, 33.8, 24.1; ^{31}P NMR (162 MHz, $CDCl_3$) δ -10.6; ESI-MS: m/z 543.20 $[M+H]^+$; HRMS (ESI) m/z calcd for $C_{33}H_{36}O_5P$ $[M+H]^+$: 543.2300, found: 543.2302.

3.4 Characterization Data of New P-Chiral Monophosphorus Ligands

L12: 85% yield; White solid; ^{1}H NMR (500 MHz, $CDCl_3$) δ 7.34 (t, J = 7.8 Hz, 1H), 7.29 (s, 1H), 7.22 (s, 2H), 7.15 (s, 2H), 6.94 (dd, J = 11.4, 6.0 Hz, 4H), 4.88 (d, J = 12.3 Hz, 1H), 4.59 (dd, J = 25.5, 12.6 Hz, 1H), 3.36 (s,

3H), 3.26 (s, 3H), 2.35 (d, *J* = 3.7 Hz, 12H), 0.91 (d, *J* = 12.1 Hz, 9H); ^{13}C NMR (126 MHz, $CDCl_3$) δ 163.7, 155.3, 154.5, 139.6 (d, *J* = 18.1 Hz), 138.8, 138.6, 137.7, 137.5, 133.0, 130.8, 130.2 (d, *J* = 9.2 Hz), 128.5, 127.0, 126.5, 123.1 (d, *J* = 3.9 Hz), 109.7, 61.2, 60.9, 31.9, 30.9 (d, *J* = 19.2 Hz), 29.7 (d, *J* = 4.8 Hz), 29.3, 27.0 (d, *J* = 14.6 Hz), 22.7, 21.4, 14.1; ^{31}P NMR (121 MHz, $CDCl_3$) δ -11.1; ESI-MS: m/z 539.40 $[M+H]^+$; HRMS (ESI) m/z calcd for $C_{35}H_{40}O_3P$ $[M+H]^+$: 539.2715, found: 539.2716.

L13: 80% yield; White solid; ^{1}H NMR (500 MHz, $CDCl_3$) δ 7.44 (d, *J* = 1.7 Hz, 2H), 7.43 (s, 1H), 7.42 (d, *J* = 1.6 Hz, 2H), 7.39 (d, *J* = 1.8 Hz, 2H), 7.35 (d, *J* = 7.8 Hz, 1H), 6.98–6.96 (m, 1H), 6.94 (d, *J* = 8.1 Hz, 1H), 4.87 (d, *J* = 12.5 Hz, 1H), 4.54 (dd, *J* = 25.6, 12.6 Hz, 1H), 3.33 (s, 3H), 3.32 (s, 3H), 1.35 (s, 18H), 1.34 (s, 18H), 0.93 (d, *J* = 12.2 Hz, 9H); ^{13}C NMR (126 MHz, $CDCl_3$) δ 163.7, 155.3, 154.6, 150.7, 150.4, 140.2, 140.0, 138.0, 137.7, 132.9, 131.4, 130.3 (d, *J* = 10.2 Hz), 130.0, 123.6, 123.0 (d, *J* = 18.9 Hz), 120.7(d, *J* = 19.2 Hz), 109.7, 70.8, 70.6, 61.1(d, *J* = 5.4 Hz), 60.9, 34.9 (d, *J* = 2.0 Hz), 31.5 (d, *J* = 7.6 Hz), 30.9 (d, *J* = 19.4 Hz), 27.0 (d, *J* = 14.7 Hz); ^{31}P NMR (162 MHz, $CDCl_3$) δ -9.3; ESI-MS: m/z 707.45 $[M+H]^+$; HRMS (ESI) m/z calcd for $C_{47}H_{64}O_3P$ $[M+H]^+$: 707.4593, found: 707.4574.

L15: 83% yield; White solid; ^{1}H NMR (500 MHz, $CDCl_3$) δ 7.36–7.32 (m, 2H), 6.97–6.88 (m, 2H), 6.78 (d, *J* = 2.3 Hz, 2H), 6.70 (d, *J* = 2.3 Hz, 2H), 6.45 (t, *J* = 2.3 Hz, 2H), 4.87 (dd, *J* = 12.5, 1.6 Hz, 1H), 4.56 (dd, *J* = 25.5, 12.6 Hz, 1H), 3.82 (s, 6H), 3.80 (s, 6H), 3.42 (s, 3H), 3.30 (s, 3H), 0.89 (d, *J* = 12.1 Hz, 9H); ^{13}C NMR (126 MHz, $CDCl_3$) δ 163.7, 160.6 (d, *J* = 19.6 Hz), 155.6, 154.9, 140.7 (d, *J* = 15.7 Hz), 139.4 (d, *J* = 18.2 Hz), 132.5, 130.5, 130.4 (d, *J* = 1.2 Hz), 130.3, 129.7, 125.0 (d, *J* = 15.7 Hz), 122.8 (d, *J* = 3.9 Hz), 109.8, 107.3, 106.7, 99.3 (d, *J*=3.3 Hz), 70.8, 70.6, 61.2, 61.0 (d, *J*=4.2 Hz), 55.4 (d, *J* = 9.4 Hz), 30.9 (d, *J* = 19.4 Hz), 26.9 (d, *J* = 14.7 Hz); ^{31}P NMR (162 MHz, $CDCl_3$) δ -8.6; ESI-MS: m/z 603.40 $[M+H]^+$; HRMS (ESI) m/z calcd for $C_{35}H_{40}O_7P$ $[M+H]^+$: 603.2512, found: 603.2513.

L16: 86% yield; White solid; ^{1}H NMR (500 MHz, $CDCl_3$) δ 7.58 (d, *J* = 8.5 Hz, 2H), 7.48 (d, *J* = 8.6 Hz, 2H), 7.33 (t, *J* = 7.8 Hz, 1H), 7.30 (s, 1H), 6.94 (t, *J* = 8.3 Hz, 6H), 4.88 (d, *J* = 12.6 Hz, 1H), 4.60 (dd, *J* = 25.6, 12.5 Hz, 1H), 3.84 (d, *J* = 2.3 Hz, 6H), 3.36 (s, 3H), 3.19 (s, 3H), 0.89 (d, *J* = 12.1 Hz, 9H); ^{13}C NMR (126 MHz, $CDCl_3$) δ 163.6, 158.7 (d, *J* = 5.7 Hz), 155.1, 154.3, 139.5 (d, *J* = 18.1 Hz), 132.4, 131.2, 130.9, 130.5 (d, *J* = 7.6 Hz), 130.20 (d, *J* = 18.4 Hz), 129.8 (d, *J* = 16.2 Hz), 125.0 (d, *J* = 15.2 Hz), 123.0 (d, *J* = 4.0 Hz), 113.8, 113.6, 109.7, 70.7 ,70.5, 61.0, 60.6 (d, *J* = 2.7 Hz), 55.2, 30.9 (d, *J* = 19.3 Hz), 29.7, 27.0 (d, *J* = 14.7 Hz); ^{31}P NMR (121 MHz, $CDCl_3$) δ -6.9; ESI-MS: m/z 543.30 $[M+H]^+$; HRMS (ESI) m/z calcd for $C_{33}H_{36}O_5P$ $[M+H]^+$: 543.2300, found: 543.2302.

L17: 82% yield; White solid; ^{1}H NMR (500 MHz, $CDCl_3$) δ 7.37 (t, *J* = 14.6, 6.8 Hz, 1H), 7.35 (s, 1H), 6.95 (dd, *J* = 11.8, 5.3 Hz, 2H), 6.83 (s, 2H), 6.79 (s, 2H), 4.89 (dd, *J* = 12.6, 1.5 Hz, 1H), 4.56 (dd, *J* = 25.5, 12.6 Hz, 1H), 3.91 (s, 3H), 3.90 (s, 3H), 3.89 (s, 6H), 3.87 (s, 6H), 3.41 (s, 3H), 3.35 (s, 3H), 0.92 (d, *J* = 12.1 Hz, 9H); ^{13}C NMR (126 MHz, $CDCl_3$) δ 163.8, 155.3, 154.8, 153.1 (d, *J* = 16.7 Hz), 139.5 (d, *J* = 18.3 Hz), 137.2 (d, *J* = 2.1 Hz), 134.2 (d, *J* = 13.2 Hz), 132.2, 130.5, (d, *J* = 5.1 Hz), 129.7, 122.8, 110.0, 106.4, 105.8, 61.2, 61.0 (d, *J* = 6.1 Hz), 56.2 (d, *J* = 16.1 Hz), 31.0 (d, *J* = 19.1 Hz), 27.0 (d, *J* = 14.6 Hz); ^{31}P NMR (162 MHz, $CDCl_3$) δ -9.1; ESI-MS: m/z 663.30 $[M+H]^+$; HRMS (ESI) m/z calcd for $C_{37}H_{44}O_9P$ $[M+H]^+$: 663.2723, found: 663.2723.

L18: 83% yield; White solid; ^{1}H NMR (500 MHz, $CDCl_3$) δ 7.30 (d, *J* = 7.8 Hz, 1H), 7.22 (dd, *J* = 14.2, 5.9 Hz, 2H), 7.08 (dd, *J* = 7.1, 2.7 Hz, 1H), 6.91 (s, 1H), 6.88 (d, *J* = 8.0 Hz, 1H), 6.62 (dd, *J* = 15.0, 7.4 Hz, 4H), 4.83 (dd, *J* = 12.4, 2.0 Hz, 1H), 4.58 (d, *J* = 14.2 Hz, 1H), 3.82 (s, 3H), 3.78 (s, 3H), 3.76 (s, 3H), 3.65 (s, 3H), 3.36 (s, 3H), 3.20 (s, 3H), 0.88 (d, *J* = 12.0 Hz, 9H); ^{13}C NMR (126 MHz, $CDCl_3$) δ 163.7, 158.5 (d, *J* = 18.8 Hz), 158.1 (d, *J* = 4.3 Hz), 156.3, 155.0, 139.7 (d, *J* = 17.1 Hz), 135.7, 130.0, 128.6, 128.3, 128.1, 124.1 (d, *J* = 4.1 Hz), 123.0, 122.1, 117.4 (d, *J* = 12.1 Hz), 109.3, 105.3, 104.3 (d, *J* = 12.8 Hz), 103.9, 60.6 (d, *J* = 6.4 Hz), 56.0, 55.7 (d, *J* = 2.7 Hz), 30.8 (d, *J* = 17.4 Hz), 27.3 (d, *J* = 14.3 Hz); ^{31}P NMR (162 MHz, $CDCl_3$) δ -6.4; ESI-MS: m/z 603.30 $[M+H]^+$; HRMS (ESI) m/z calcd for $C_{35}H_{40}O_7P$ $[M+H]^+$: 603.2512, found: 603.2510.

4. Optimization of Reaction Conditions

Table S1. Cu-catalyzed asymmetric allylic alkylation of cinnamyl chloride (1) with EtMgBr (2a) by employing different copper salts and (*R*)-BIDIME.[a]

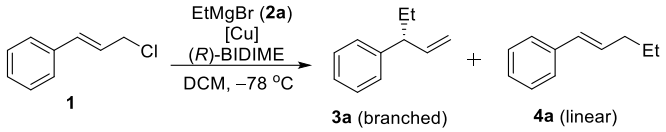

Entry	5 mol % [Cu]	6 mol % **L**	**3a**:**4a**[b]
1	--	--	23/77
2	CuI	(*R*)-BIDIME	7/93
3	CuBr	(*R*)-BIDIME	5/95
4	CuCl	(*R*)-BIDIME	0/100
5	$CuBr.SMe_2$	(*R*)-BIDIME	7/93
6	$[Cu(MeCN)_4]PF_6$	(*R*)-BIDIME	10/90
7	$Cu(OAc)_2$	(*R*)-BIDIME	9/91
8	CuOAc	(*R*)-BIDIME	0/100
9	$Cu(OTf)_2$	(*R*)-BIDIME	9/91
10	$(CuOTf)_2$·toluene	(*R*)-BIDIME	9/91
11	$(CuOTf)_2$·benzene	(*R*)-BIDIME	9/91
12	CuTc	(*R*)-BIDIME	0/100
13	CuCN	(*R*)-BIDIME	93/7
14[c]	CuCN	(*R*)-BIDIME	80/20
15[d]	CuCN	(*R*)-BIDIME	96/4

[a]Unless otherwise specified, the reactions were performed under nitrogen in DCM at −78 °C in the presence of 5 mol % [Cu] and 6 mol % **L** with cinnamyl chloride (**1**, 0.25 mmol, 1.0 equiv) and EtMgBr (3 M solution in diethyl ether, 0.5 mmol, 2.0 equiv). Slow addition of EtMgBr over 0.5 h. [b]All reactions gave full conversion. The ratios of **3a**/**4a** were determined by ^{1}H NMR spectroscopy. [c]The reaction was performed under nitrogen in DCM at −78 °C in the presence of 2.5 mol % CuCN and 3 mol % **L** with cinnamyl chloride (**1**, 0.25 mmol, 1.0 equiv) and EtMgBr (3 M solution in diethyl ether, 0.5 mmol, 2.0 equiv). [d]The reaction was performed under nitrogen in DCM at −78 °C in the presence of 10 mol % CuCN and 12 mol % **L** with cinnamyl chloride (**1**, 0.25 mmol, 1.0 equiv) and EtMgBr (3 M solution in diethyl ether, 0.5 mmol, 2.0 equiv).

Table S2. The preliminary investigation of different ligands for the copper catalyzed asymmetric allylic alkylation.[a]

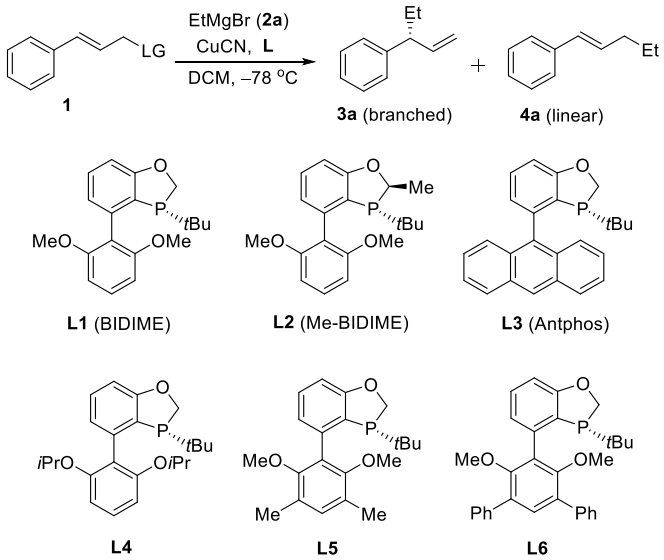

Entry	LG	5 mol % [Cu]	6 mol % **L**	**3a**:**4a**[b]	*er* (**3a**)[c]
1	Cl	CuCN	**L1**	93:7	53:47
2	Br	CuCN	**L1**	62:38	56:44
3	Cl	CuCN	**L2**	97:3	51:49
4	Br	CuCN	**L2**	60:40	53:47
5	Cl	CuCN	**L3**	91:9	53:47
6	Br	CuCN	**L3**	53:47	54:46
7	Cl	CuCN	**L4**	98:2	52:48
8	Br	CuCN	**L4**	28:72	53:47
9	Cl	CuCN	**L5**	93:7	64:36
10	Br	CuCN	**L5**	60:40	86:14
11	Cl	CuCN	**L6**	96:4	56:44
12	Br	CuCN	**L6**	72:28	85:15

[a]Unless otherwise specified, the reactions were performed under nitrogen in DCM at −78 °C in the presence of **5** mol % [Cu] and 6 mol % **L** with allyl substrates (**1**, 0.25 mmol, 1.0 equiv) and EtMgBr (3 M solution in diethyl ether, 0.5 mmol, 2.0 equiv). Slow addition of EtMgBr over 0.5 h. [b]All reactions gave full conversion. The ratios of **3a**/**4a** were determined by ^{1}H NMR spectroscopy. [c]The *er* values of **3a** were determined by chiral HPLC analysis.

Table S3. The further optimization of reaction conditions for the copper catalyzed asymmetric allylic alkylation.[a]

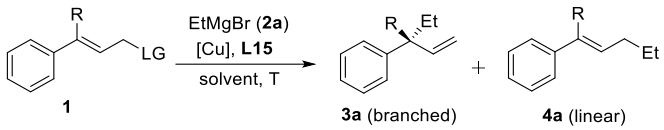

Entry	R	LG	[Cu]	L	3a:4a[b]	*er* (3a)[c]
1	H	Br	5 mol % CuCN	6 mol % **L15**	76:24	93:7
2[d]	H	Br	5 mol % CuCN	6 mol % **L15**	79:21	54:46
3[e]	H	Br	5 mol % CuCN	6 mol % **L15**	87:13	53:47
4[f]	H	Br	5 mol % CuCN	6 mol % **L15**	67:33	54:46
5[g]	H	Br	5 mol % CuCN	6 mol % **L15**	33:67	70:30
6	H	Br	5 mol % CuTc	6 mol % **L15**	80:20	96:4
7	H	Br	5 mol % $[Cu(CNMe)_4]PF_6$	6 mol % **L15**	70:30	94:6
8	H	Br	5 mol % CuCl	6 mol % **L15**	76:24	93:7
9	H	Br	5 mol % CuBr	6 mol % **L15**	71:29	93:7
10	H	Br	5 mol % $CuBr{\cdot}SMe_2$	6 mol % **L15**	83:17	81:19
11	H	Br	5 mol % CuI	6 mol % **L15**	80:20	94:6
12[h]	H	Br	5 mol % CuTc	6 mol % **L15**	74:26	93:7
13[i]	H	Br	5 mol % CuTc	6 mol % **L15**	71:29	86:14
14	H	Br	2.5 mol % CuTc	3 mol % **L15**	80:20	96:4
15	H	Br	1 mol % CuTc	1.2 mol % **L15**	82:18	95:5
16	H	Br	0.5 mol%CuTc	0.6 mol % **L15**	85:15	97:3
17	H	Br	0.1 mol%CuTc	0.12 mol % **L15**	60:40	96:4
18	H	Cl	0.5 mol%CuTc	0.6 mol % **L15**	40:60	77:23
19	H	Cl	0.5 mol % CuCN	0.6 mol % **L15**	88:12	61:39
20	Me	Br	5 mol % CuCN	6 mol % **L15**	74:26	68:32
21	Me	Br	5 mol % CuTc	6 mol % **L15**	74:26	95:5
22	Me	Br	2.5 mol % CuTc	3 mol % **L15**	67:33	82:18
23	Me	Br	1 mol % CuTc	1.2 mol % **L15**	69:31	79:21
24[j]	Me	OAc	5 mol % CuTc	6 mol % **L15**	--	--
25	Me	OCbz	5 mol % CuTc	6 mol % **L15**	14:86	42:58
26	Me	$OPO(OMe)_2$	5 mol % CuTc	6 mol % **L15**	25:75	44:56

[a]Unless otherwise specified, the reactions were performed under nitrogen in DCM at −78 °C in the presence of [Cu] and **L15** with allyl bromide and EtMgBr (3 M solution in diethyl ether, 2.0 equiv). Slow addition of EtMgBr over 0.5 h. [b]All reactions gave full conversion. The ratios of **3a**/**4a** were determined by ^{1}H NMR spectroscopy. [c]The *er* values of **3a** were determined by chiral HPLC analysis. [d]The reaction was performed in Et_2O. [e]The reaction was performed in MTBE. [f]The reaction was performed in THF. [g]EtMgBr (1 M solution in THF). [h]The reaction was performed at −40 °C. [i]The reaction was performed at −10 °C. [j]No reaction.

5. X-Ray Crystal Data of Copper Complex

CD 1906544 contain the supplementary crystallographic data for this paper. These data can be obtained free of charge via www.ccdc.cam.ac.uk/conts/retrieving.html (or from the Cambridge Crystallographic Data Centre, 12 Union Road, Cambridge CB21EZ, UK; fax: (+44)1223-336-033; or deposit@ccdc.cam.ac.uk).

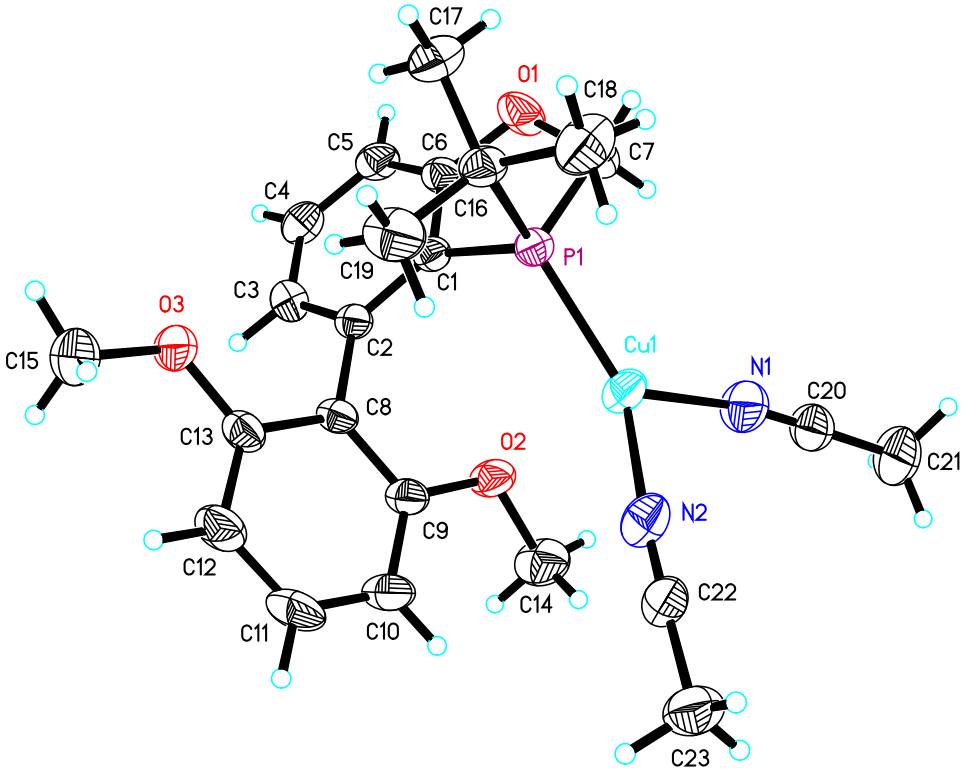

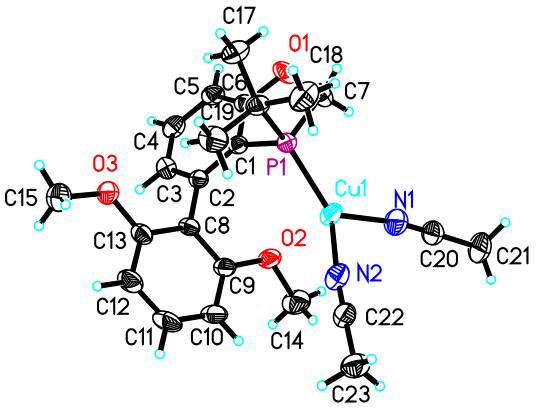

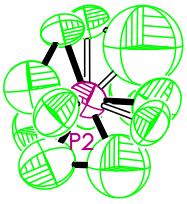

Crystal data and structure refinement for mo_d8v17470_0m.

Identification code	mo_d8v17470_0m	
Empirical formula	C23 H29 Cu F6 N2 O3 P2	
Formula weight	620.96	
Temperature	296(2) K	
Wavelength	0.71073 Å	
Crystal system	Orthorhombic	
Space group	P 21 21 21	
Unit cell dimensions	a = 8.5246(2) Å	= 90°.
	b = 10.5054(3) Å	= 90°.
	c = 30.1709(7) Å	= 90°.
Volume	2701.93(12) $Å^3$	
Z	4	
Density (calculated)	1.527 Mg/m^3	
Absorption coefficient	0.996 mm^{-1}	
F(000)	1272	
Crystal size	0.200 x 0.160 x 0.130 mm^3	
Theta range for data collection	2.053 to 25.499°.	
Index ranges	-9<=h<=10, -12<=k<=8, -33<=l<=36	
Reflections collected	14429	
Independent reflections	4984 [R(int) = 0.0255]	
Completeness to theta = 25.242°	99.0 %	
Absorption correction	Semi-empirical from equivalents	
Max. and min. transmission	0.7456 and 0.5766	
Refinement method	Full-matrix least-squares on F^2	
Data / restraints / parameters	4984 / 64 / 386	
Goodness-of-fit on F^2	1.078	
Final R indices [I>2sigma(I)]	R1 = 0.0440, wR2 = 0.1179	
R indices (all data)	R1 = 0.0523, wR2 = 0.1261	
Absolute structure parameter	-0.004(6)	
Extinction coefficient	0.018(3)	
Largest diff. peak and hole	0.258 and -0.602 e.	

6. References

(1) (a) Metternich, J. B.; Gilmour, R. A Bio-Inspired, Catalytic *E* → *Z* Isomerization of Activated Olefins. *J. Am. Chem. Soc*. **2015**, *137*, 11254−11257. (b) Simard-Mercier, J.; Jiang, J. L.; Ho, M. L.; Flynn, A. B.; Ogilvie, W. W. Single-Isomer Trisubstituted Olefins from a Novel Reaction of (*E*)-*β*-Chloro-*α*-Iodo-*α*, *β*-Unsaturated Esters and Amides. J. *Org. Chem.* **2008**, *73*, 5899−5906. (c) Kalkhambkar, R. G.; Laali, K. K. Arenediazonium Salts Immobilized in Imidazolium Ionic Liquids as Electrophilic Partners in the $Pd(OAc)_2$-Catalyzed Matsuda-Heck Arylation. *Tetrahedron Lett*. **2011**, *52*, 1733−1737. (d) Felluga, F.; Ghelfi, F.; Pitacco, G.; Roncaglia, F.; Valentin, E.; Venneri, C. D. Esterase-Mediated Synthesis of Optically Active GABA Analogues Containing a Stereogenic All-Carbon Quaternary Carbon Atom. *Tetrahedron: Asymmetry* **2010**, *21*, 2183−2191. (e) Dyker, G.; Grundt, P. Synthesis of Functionalized 4a-Methyl-1, 2, 3, 4, 4a, 9, 10, 10a-octahydrophenanthrenes. *Helv. Chim. Acta*, **1999**, *82*, 588−596. (f) Shevlin, M.; Friedfeld, M. R.; Sheng, H.-M.; Pierson, N. A.; Hoyt, J. M.; Campeau, L. C.; Chirik, P. J. Nickel-Catalyzed Asymmetric Alkene Hydrogenation of *α*, *β*-Unsaturated Esters: High-Throughput Experimentation-Enabled Reaction Discovery, Optimization, and Mechanistic Elucidation. *J. Am. Chem. Soc*. **2016**, *138*, 3562−3569. (g) Li, J.-Q.; Quan, X.; Andersson, P. G. Highly Enantioselective Iridium-Catalyzed Hydrogenation of *α*, *β*-Unsaturated Esters. *Chem. Eur. J*. **2012**, *18*, 10609−10616.

(2) Bernasconi, M.; Ramella, V.; Tosatti, P.; Pfaltz, A. Iridium-Catalyzed Asymmetric Hydrogenation of 3, 3-Disubstituted Allylic Alcohols in Ethereal Solvents. *Chem. Eur. J*. **2014**, *20*, 2440−2444.

(3) (a) van Zijl, A. W.; Arnold, L. A.; Minnaard, A. J.; Feringa, B. L. Highly Enantioselective Copper-Catalyzed Allylic Alkylation with Phosphoramidite Ligands. *Adv. Synth. Catal.* **2004**, *346*, 413−420. (b) Fañanás-Mastral, M.; Pérez, M.; Bos, P. H.; Rudolph, A.; Harutyunyan, S. R.; Feringa, B. L. Enantioselective Synthesis of Tertiary and Quaternary Stereogenic Centers: Copper/Phosphoramidite-Catalyzed Allylic Alkylation with Organolithium Reagents. *Angew. Chem. Int. Ed.* **2012**, *51*, 1922−1925. (c) Reichl, K. D.; Dunn, N. L.; Fastuca, N. J.; Radosevich. A. T. Biphilic Organophosphorus Catalysis: Regioselective Reductive Transposition of Allylic Bromides via P^{III}/P^{V} Redox Cycling. *J. Am. Chem. Soc*. **2015**, *137*, 5292−5295. (d) Fañanás-Mastral, M.; Vitale, R.; Pérez, M.; Feringa, B. L. Enantioselective Synthesis of All-Carbon Quaternary Stereogenic Centers via Copper-Catalyzed Asymmetric Allylic Alkylation of (Z)-Allyl Bromides with Organolithium Reagents. *Chem. Eur. J*. **2015**, *21*, 4209−4212. (e) Guduguntla, S.; Gualtierotti, J. B.; Goh, S. S.; Feringa, B. L. Enantioselective Synthesis of Di- and Tri-Arylated All-Carbon Quaternary Stereocenters via Copper-Catalyzed Allylic Arylations with Organolithium Compounds. *ACS Catal.* **2016**, *6*, 6591−6595. (f) Nguyen, T. N. T.; Thiela, N. O.; Teichert, J. F. Copper(I)-catalysed Asymmetric Allylic Reductions with Hydrosilanes. *Chem. Commun*. **2017**, *53*, 11686−11689.

(4) (a) Tang, W.; Qu, B.; Capacci, A. G.; Rodriguez, S.; Wei, X.; Haddad, N.; Narayanan, B.; Ma, S.; Grinberg, N.; Yee, N. K.; Krishnamurthy, D.; Senanayake, C. H. Novel, Tunable, and Efficient Chiral Bisdihydrobenzooxaphosphole Ligands for Asymmetric Hydrogenation. *Org. Lett.* **2010**, *12*, 176−179. (b) Tang, W.; Patel, N. D.; Xu, G.; Xu, X.; Savoie, J.; Ma, S.; Hao, M.-H.; Keshipeddy, S.; Capacci, A. G.; Wei, X.; Zhang, Y.; Gao, J. J.; Li, W.; Rodriguez, S.; Lu, B. Z.; Yee, N. K.; Senanayake, C. H. Efficient Chiral Monophosphorus Ligands for Asymmetric Suzuki-Miyaura Coupling Reactions. *Org. Lett.* **2012**, *14*, 2258−2261. (c) Tang, W.; Capacci, A. G.; Wei, X.; Li, W.; White, A.; Patel, N. D.; Savoie, J.; Gao, J. J.; Rodriguez, S.; Qu, B.; Haddad, N.; Lu, B. Z.; Krishnamurthy, D.; Yee, N. K.; Senanayake, C. H. A General and Special Catalyst for Suzuki-Miyaura Coupling Processes. *Angew. Chem. Int. Ed*. **2010**, *49*, 5879−5883.

(5) (a) Tang, W.; Keshipeddy, S.; Zhang, Y.; Wei, X.; Savoie, J.; Patel, N. D.; Yee, N. K.; Senanayake, C. H. Efficient Monophosphorus Ligands for Palladium-Catalyzed Miyaura Borylation. *Org. Lett.* **2011**, *13*, 1366−1369. (b) Zhao, Q.; Li, C.; Senanayake, C. H.; Tang, W. An Efficient Method for Sterically Demanding Suzuki-Miyaura Coupling Reactions. *Chem. Eur. J.* **2013**, *19*, 2261−2265. (c) Xu, G.; Fu, W.; Liu, G.; Senanayake, C. H.; Tang. W. Efficient Syntheses of Korupensamines A, B and Michellamine B by Asymmetric Suzuki-Miyaura Coupling Reactions. *J. Am. Chem. Soc.* **2013**, *136*, 570−573.

(6) (a) Haddad, N.; Mangunuru, H. P. R.; Fandrick, K. R.; Qu, B.; Sieber, J. D.; Rodriguez, S.; Desrosiers, J. N.; Patel, N. D.; Lee, H.; Kurouski, D.; Grinberg, N.; Yee, N. K.; Song, J.-H. J.; Senanayake, C. H. Reengineered BIDIME Ligand Core Based on Computer Modeling to Increase Selectivity in Asymmetric Suzuki-Miyaura Coupling for the Challenging Axially Chiral HIV Integrase Inhibitor. *Adv. Synth. Catal.* **2016**, *358*, 3522−3527. (b) Patel, N. D.; Sieber, J. D.; Tcyrulnikov, S.; Simmons, B. J.; Rivalti, D.; Duvvuri, K.; Zhang, Y.; Gao, D.-H. A.; Fandrick, K. R.; Haddad, N.; Lao, K. S.; Mangunuru, H. P.; Biswas, R. S.; Qu, B.; Grinberg, N.; Pennino, S.; Lee, H.; Song, J.-H. J.; Gupton, B. F.; Garg, N. K.; Kozlowski, M. C.; Senanayake, C. H. Computationally Assisted Mechanistic Investigation and Development of Pd-Catalyzed Asymmetric Suzuki-Miyaura and Negishi Cross-Coupling Reactions for Tetra-*ortho*-Substituted Biaryl Synthesis. *ACS Catal.* **2018**, *8*, 10190−10209.

7. NMR Spectra and HPLC chromatographs

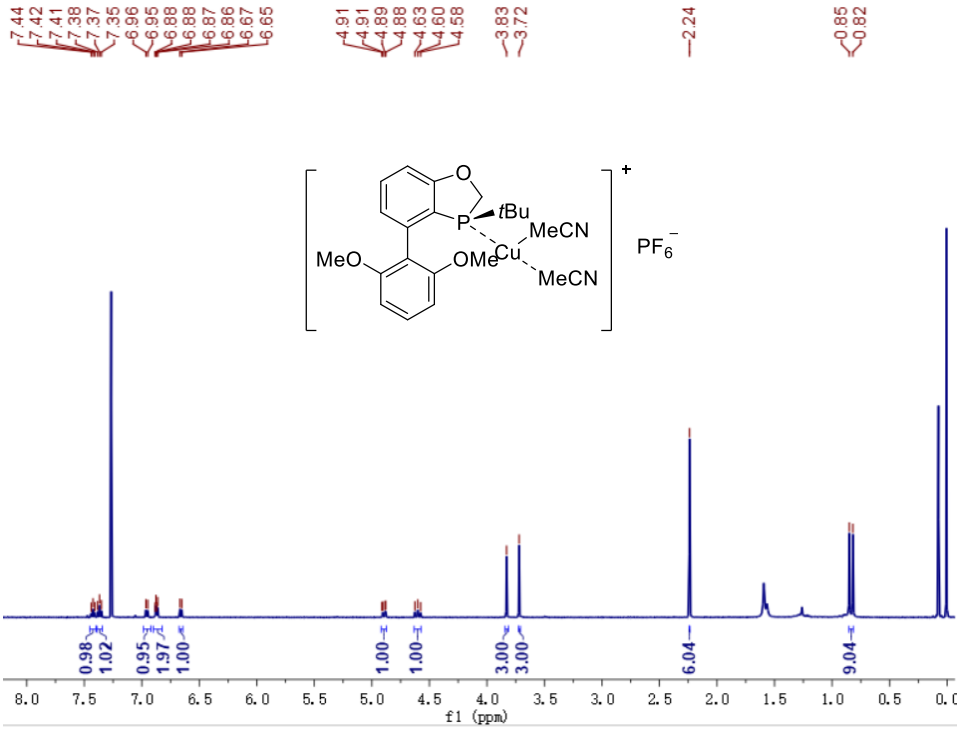

Figure S1: ^{1}H NMR (500 MHz, $CDCl_3$) spectrum of copper complex

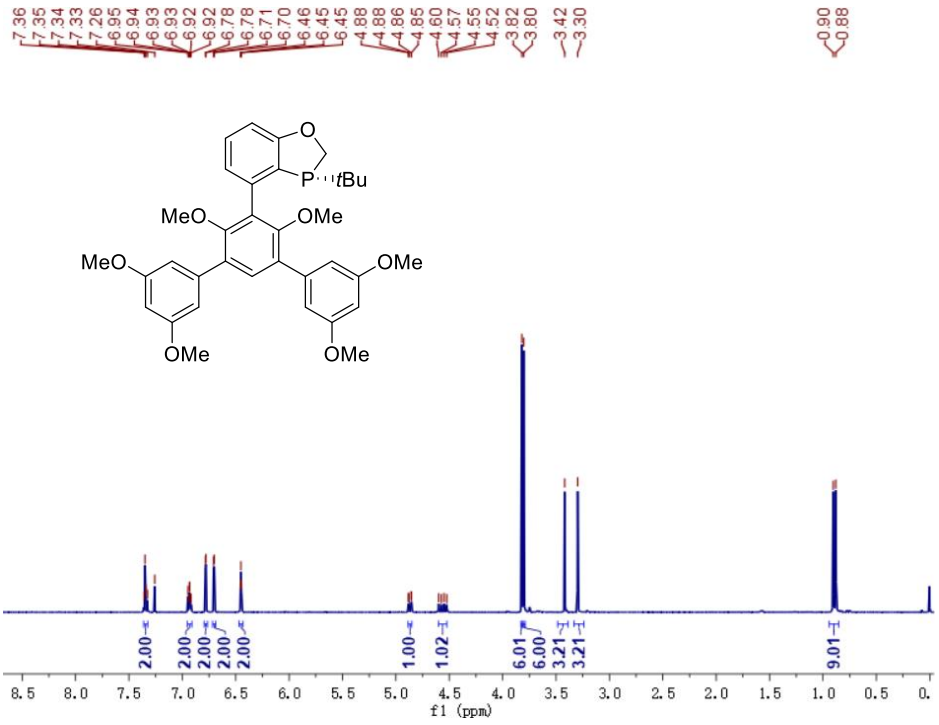

Figure S2: ^{1}H NMR (500 MHz, $CDCl_3$) spectrum of **L15**

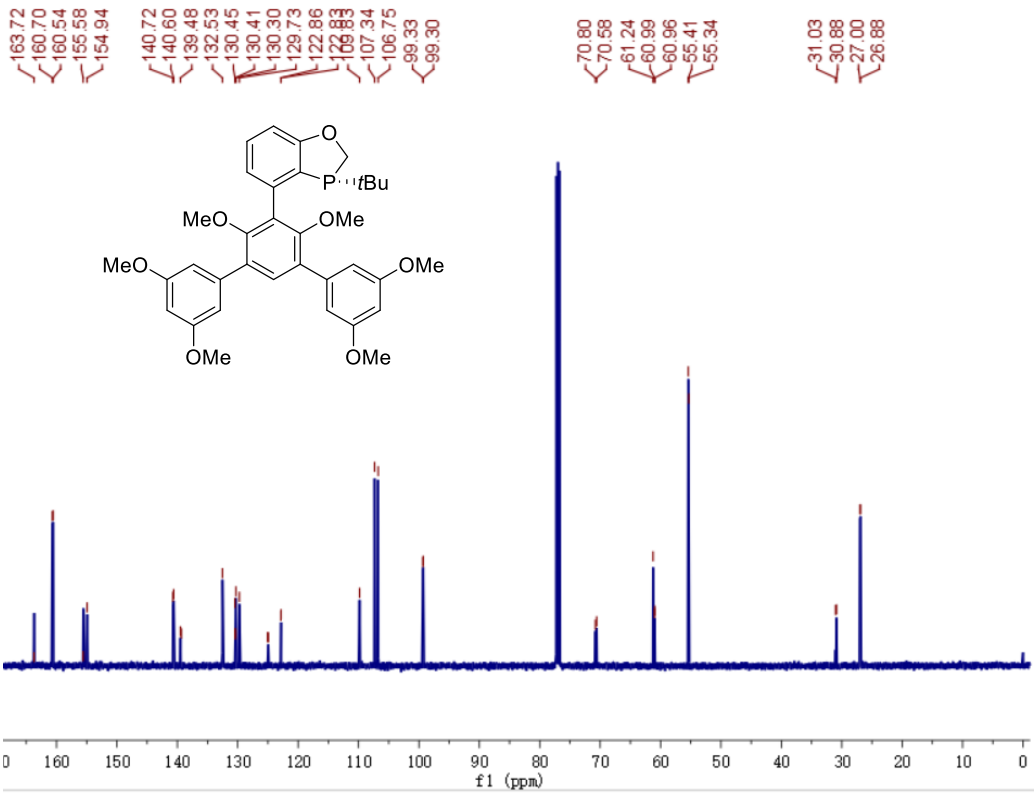

Figure S3: ^{13}C NMR (126 MHz, $CDCl_3$) spectrum of **L15**

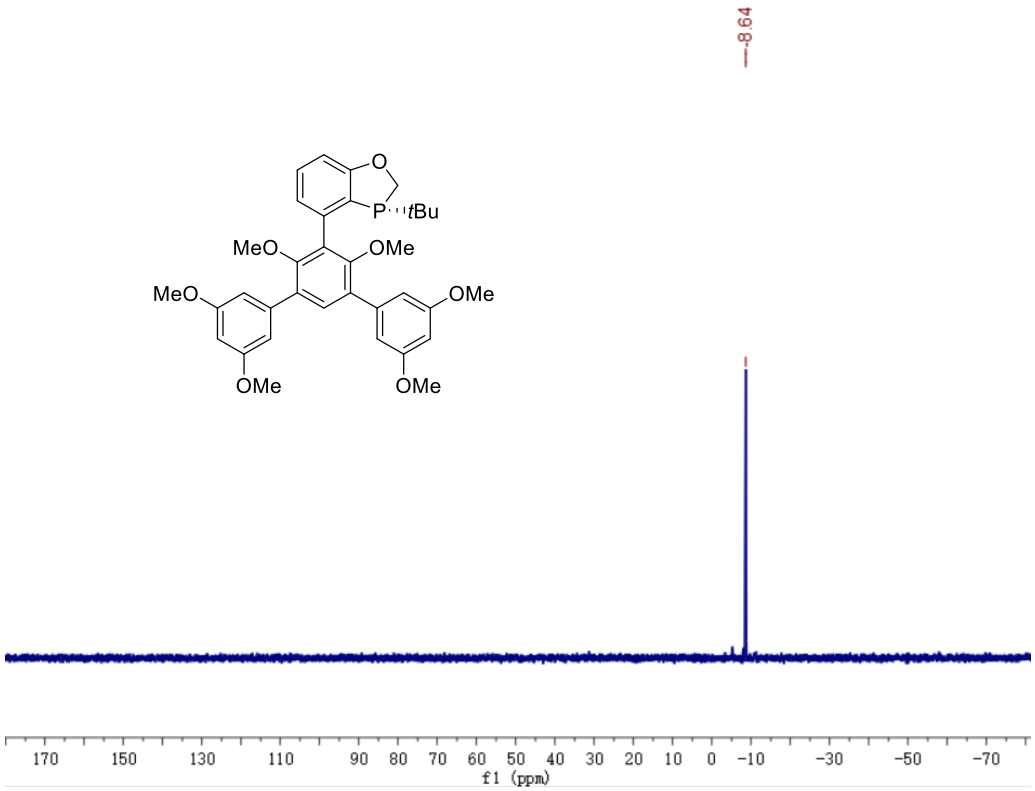

Figure S4: ^{31}P NMR (162 MHz, $CDCl_3$) spectrum of **L15**

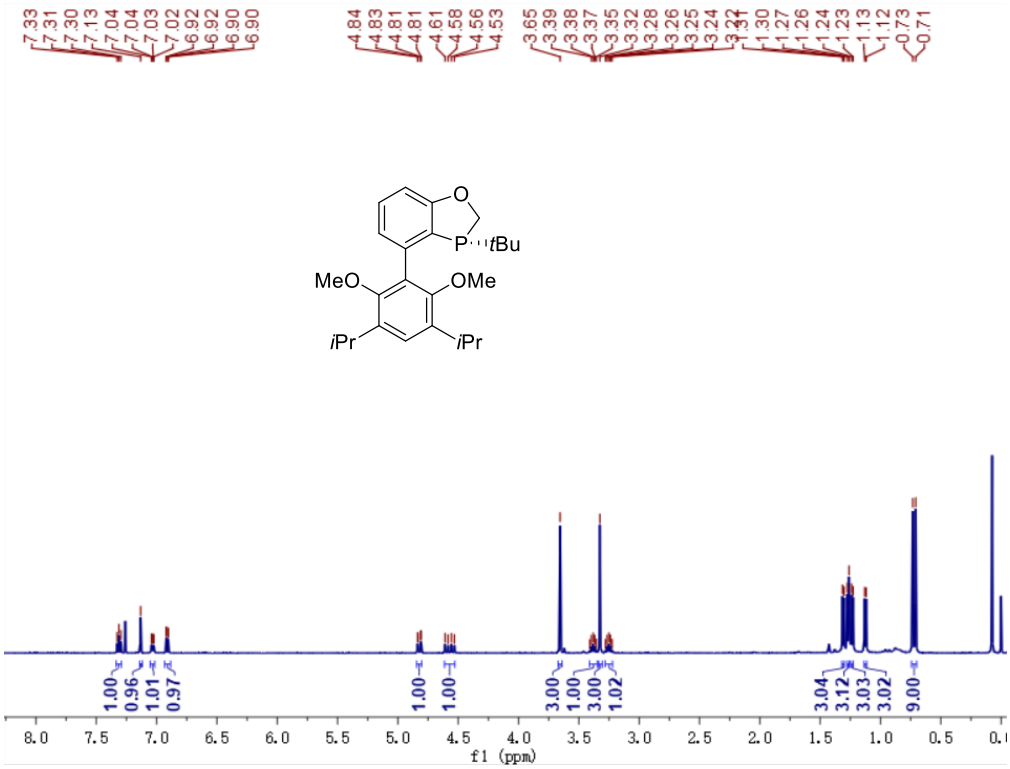

Figure S5: ^{1}H NMR (500 MHz, $CDCl_3$) spectrum of **L7**

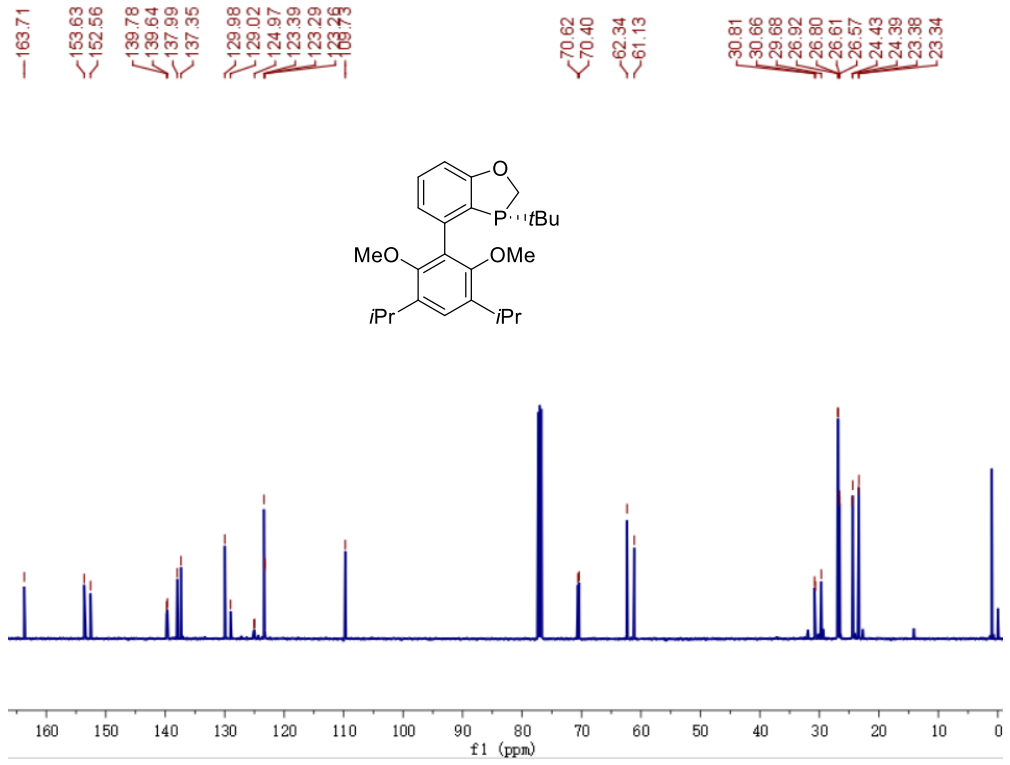

Figure S6: ^{13}C NMR (126 MHz, $CDCl_3$) spectrum of **L7**

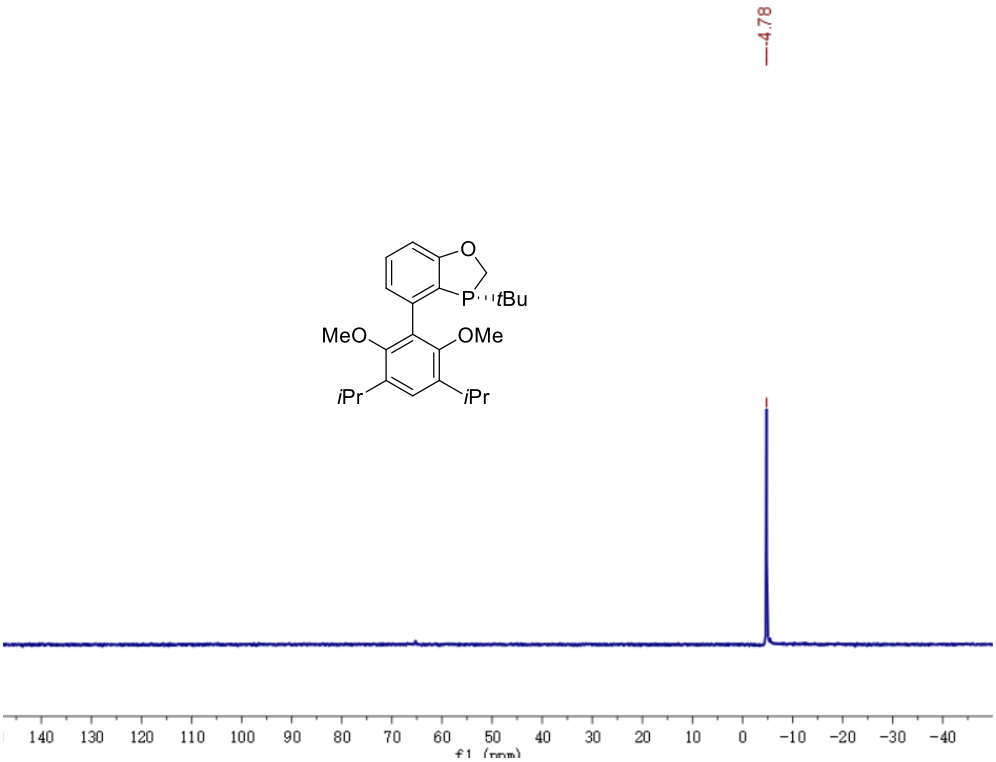

Figure S7: ^{31}P NMR (121 MHz, $CDCl_3$) spectrum of **L7**

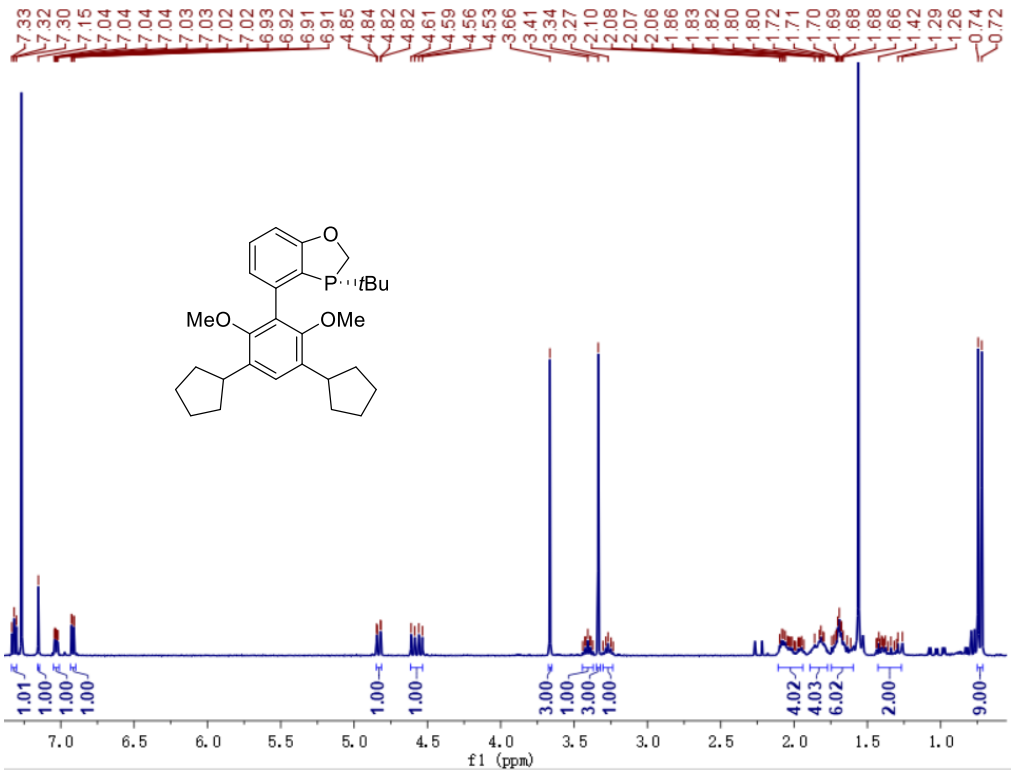

Figure S8: ^{1}H NMR (500 MHz, $CDCl_3$) spectrum of **L8**

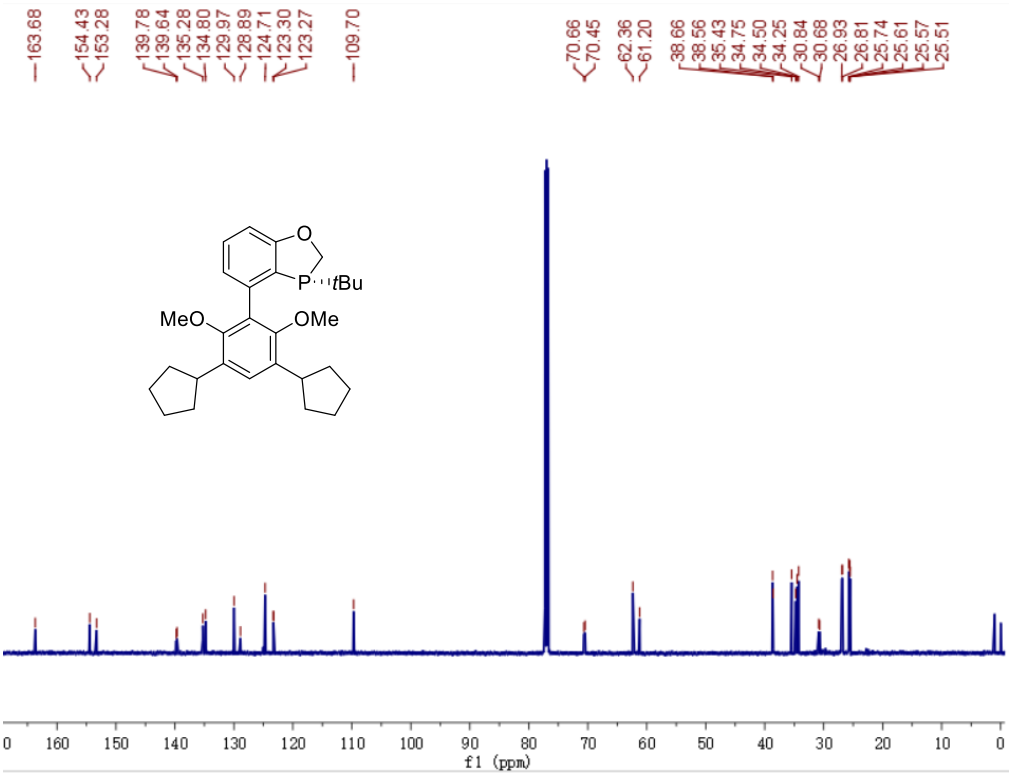

Figure S9: ^{13}C NMR (126 MHz, $CDCl_3$) spectrum of **L8**

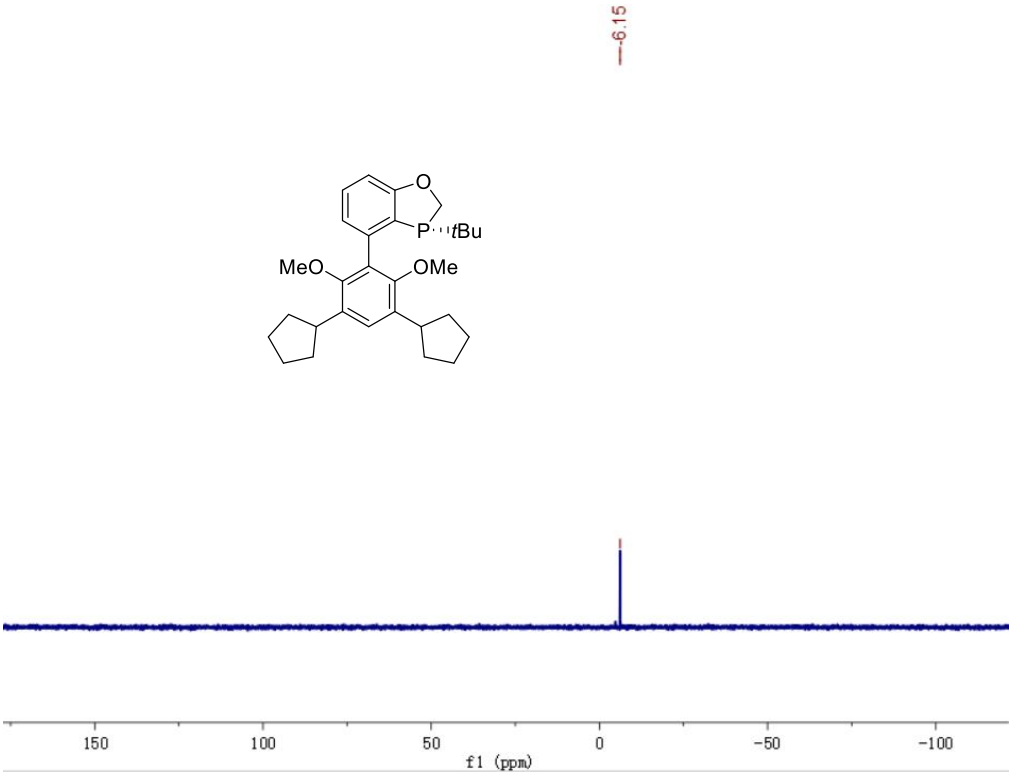

Figure S10: ^{31}P NMR (162 MHz, $CDCl_3$) spectrum of **L8**

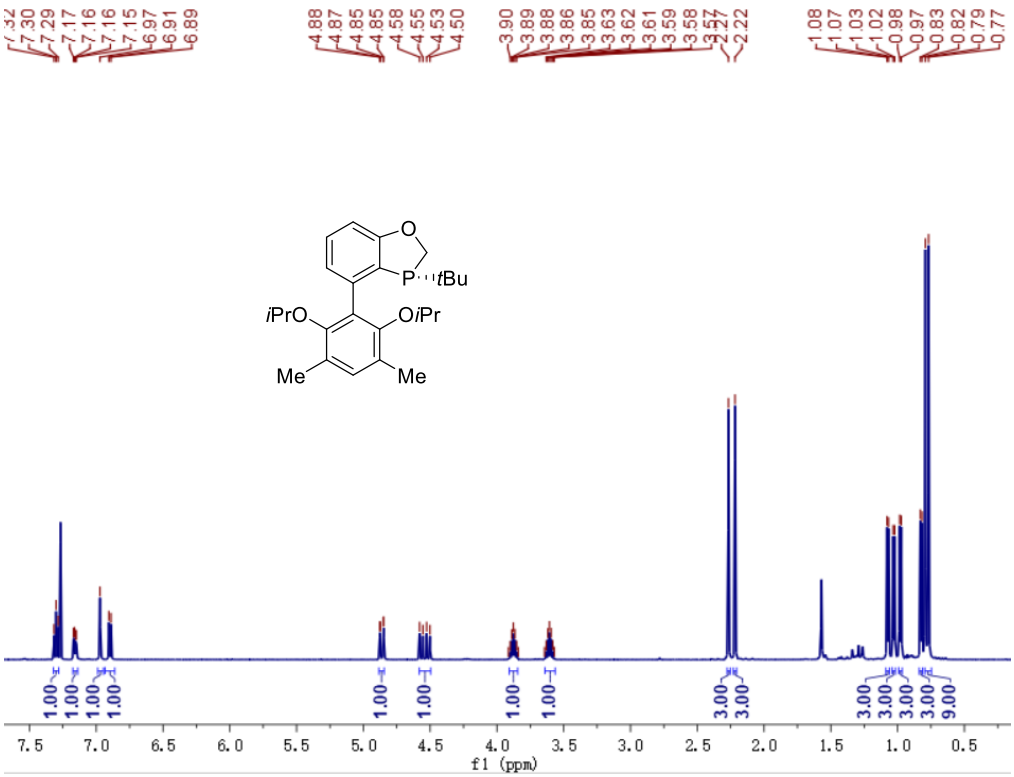

Figure S11: ^{1}H NMR (500 MHz, $CDCl_3$) spectrum of **L10**

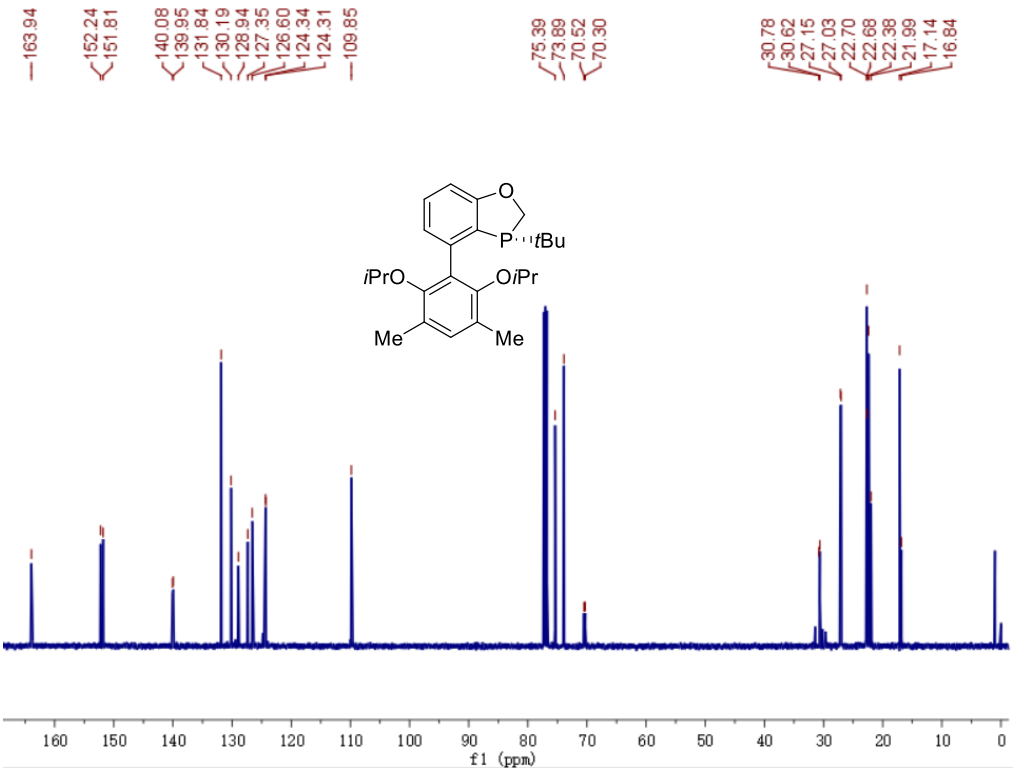

Figure S12: ^{13}C NMR (126 MHz, $CDCl_3$) spectrum of **L10**

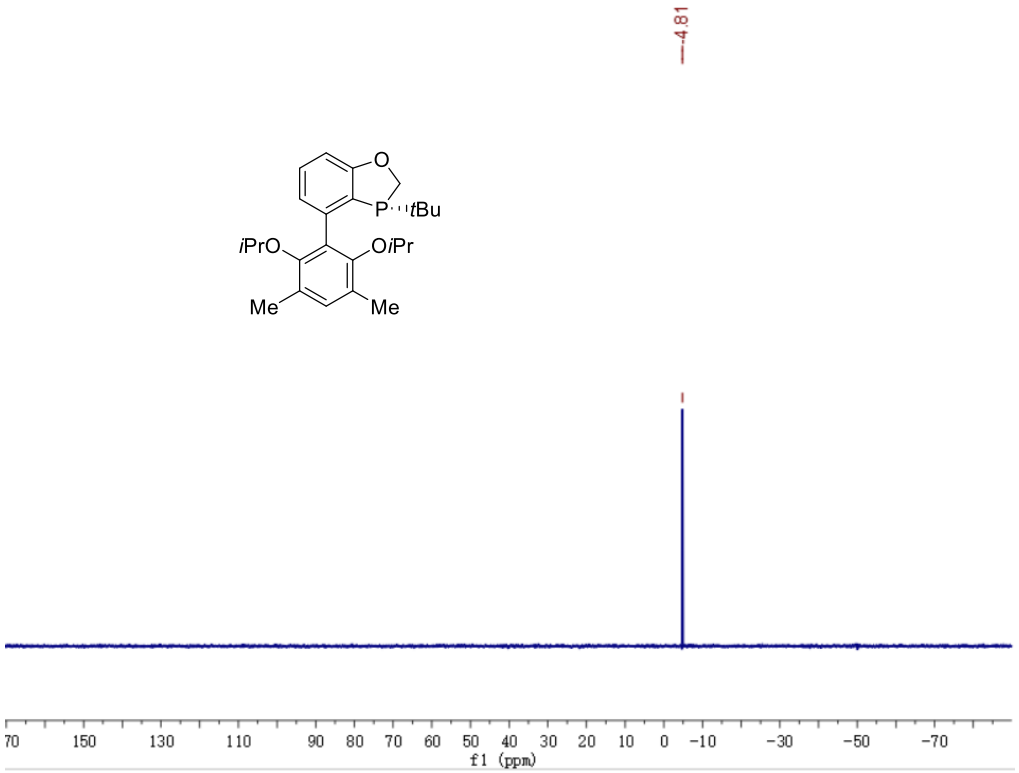

Figure S13: ^{31}P NMR (162 MHz, $CDCl_3$) spectrum of **L10**

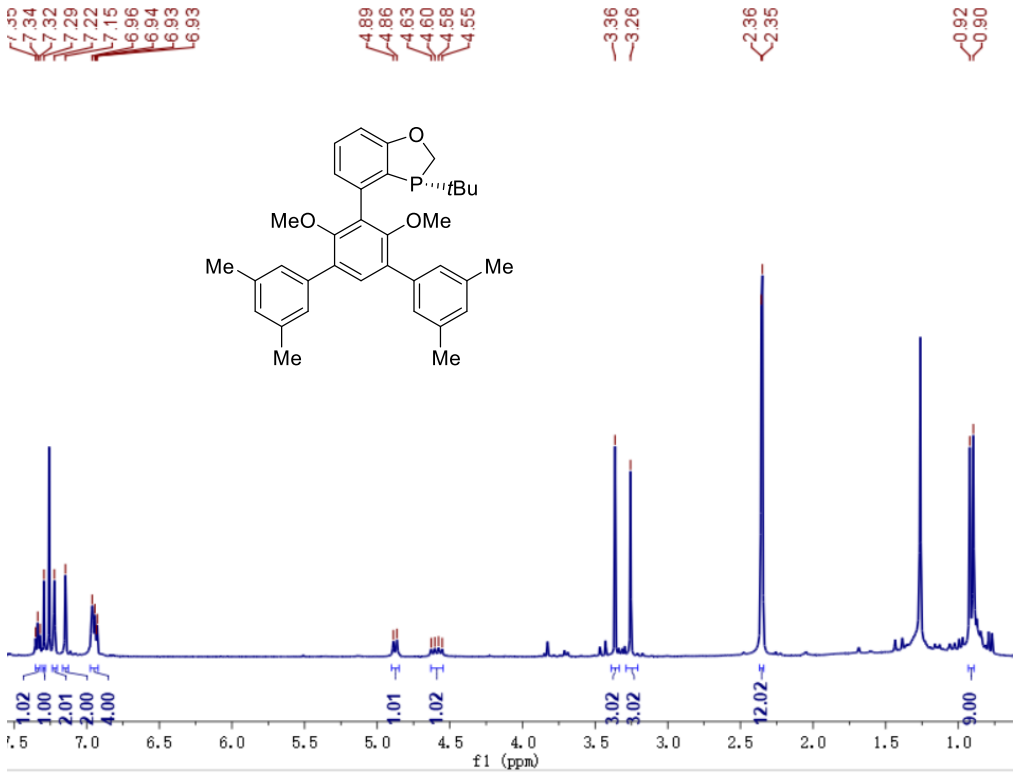

Figure S14: ^{1}H NMR (500 MHz, $CDCl_3$) spectrum of **L12**

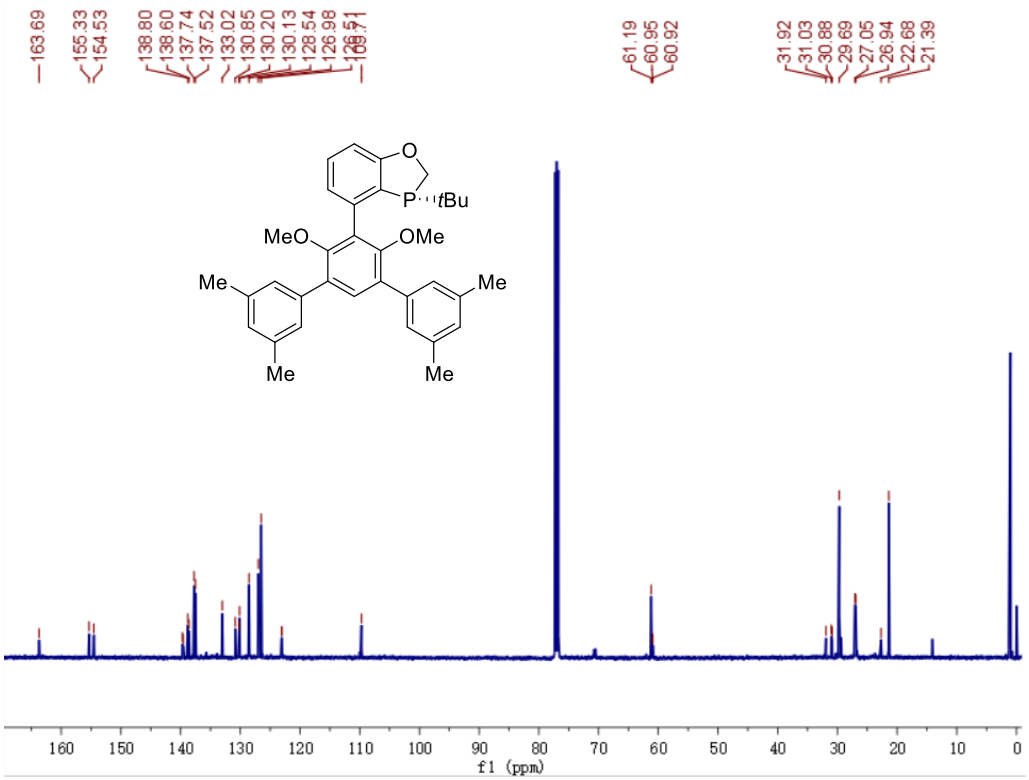

Figure S15: ^{13}C NMR (126 MHz, $CDCl_3$) spectrum of **L12**

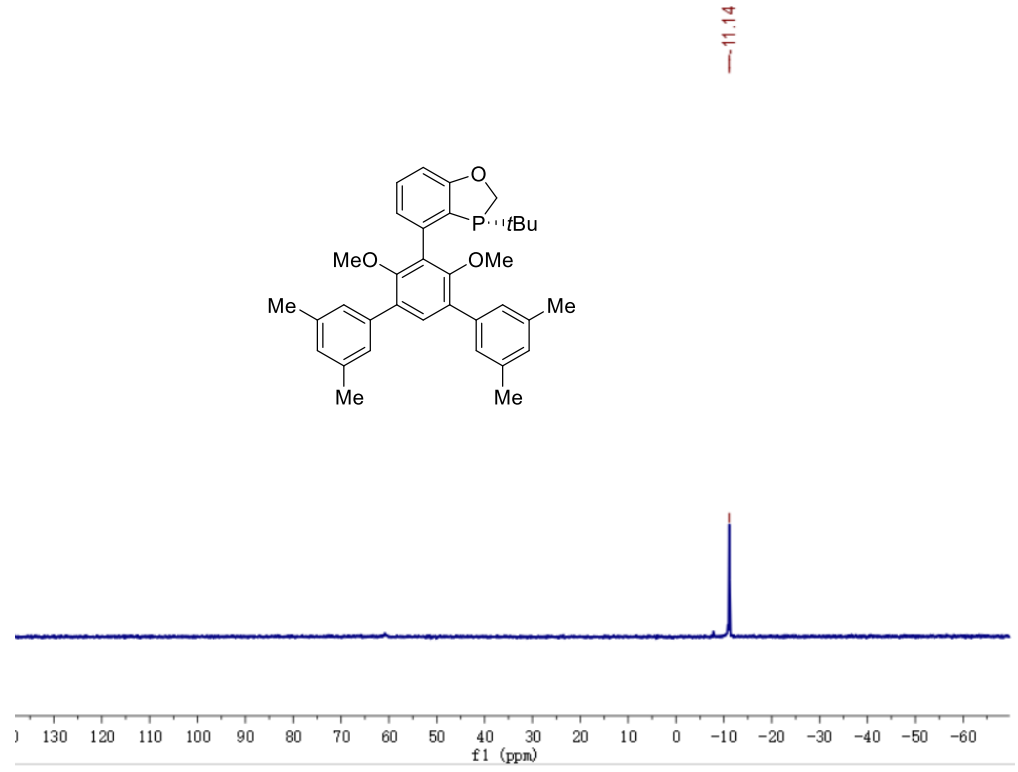

Figure S16: ^{31}P NMR (121 MHz, $CDCl_3$) spectrum of **L12**

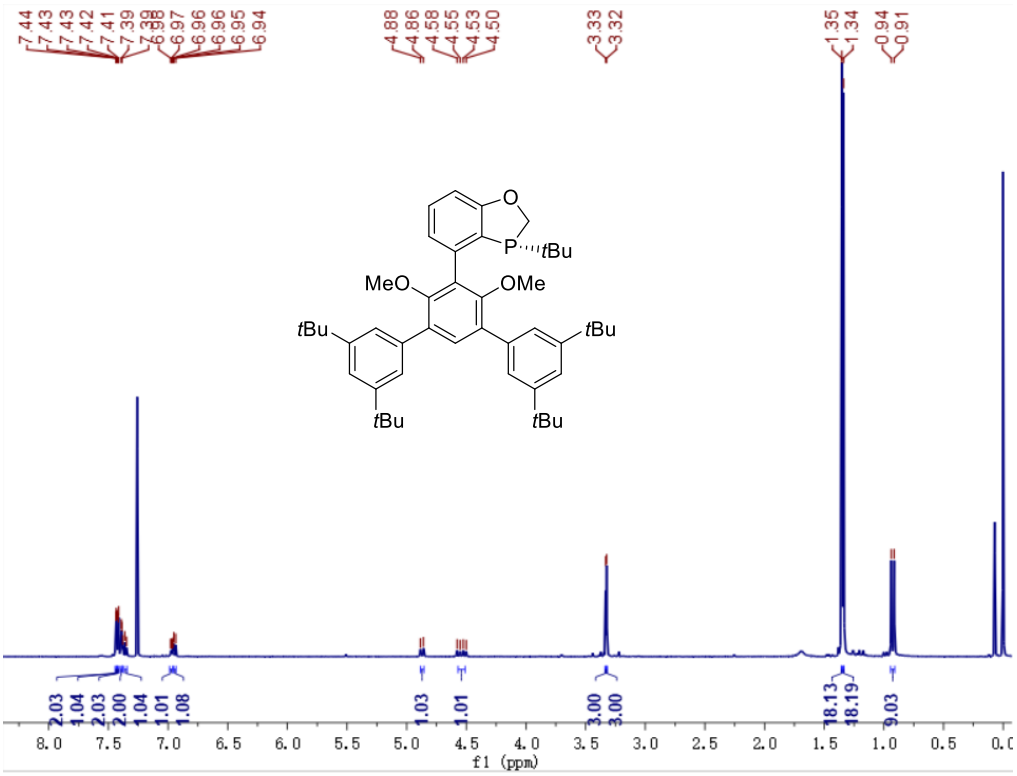

Figure S17: ^{1}H NMR (500 MHz, $CDCl_3$) spectrum of **L13**

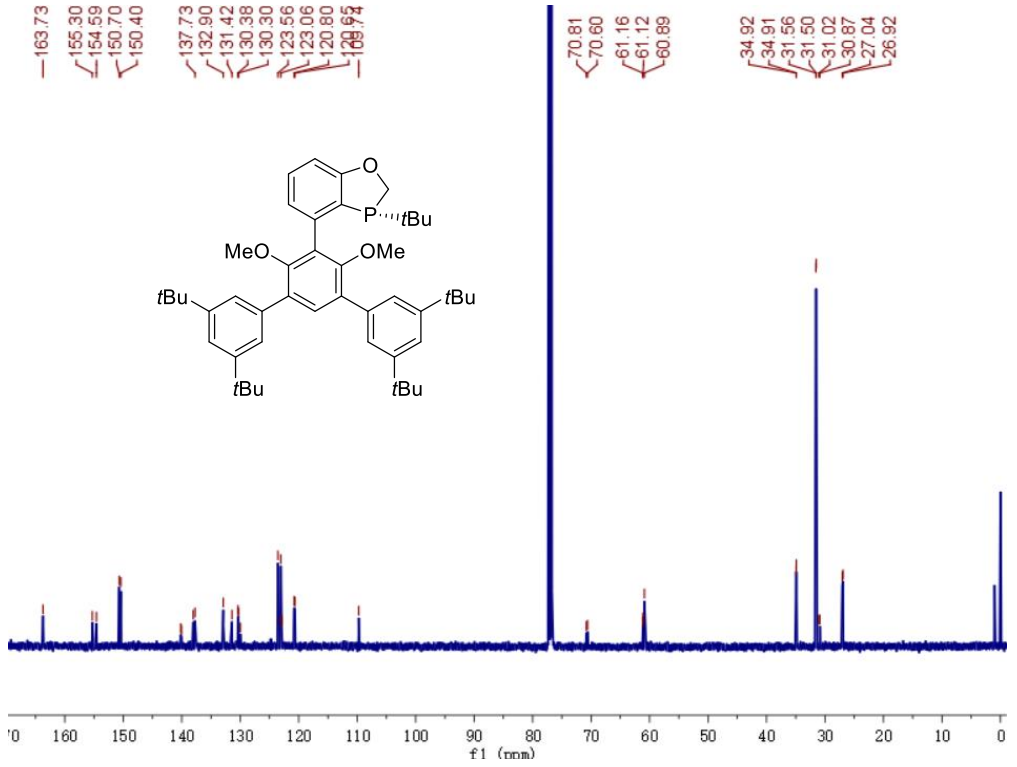

Figure S18: ^{13}C NMR (126 MHz, $CDCl_3$) spectrum of **L13**

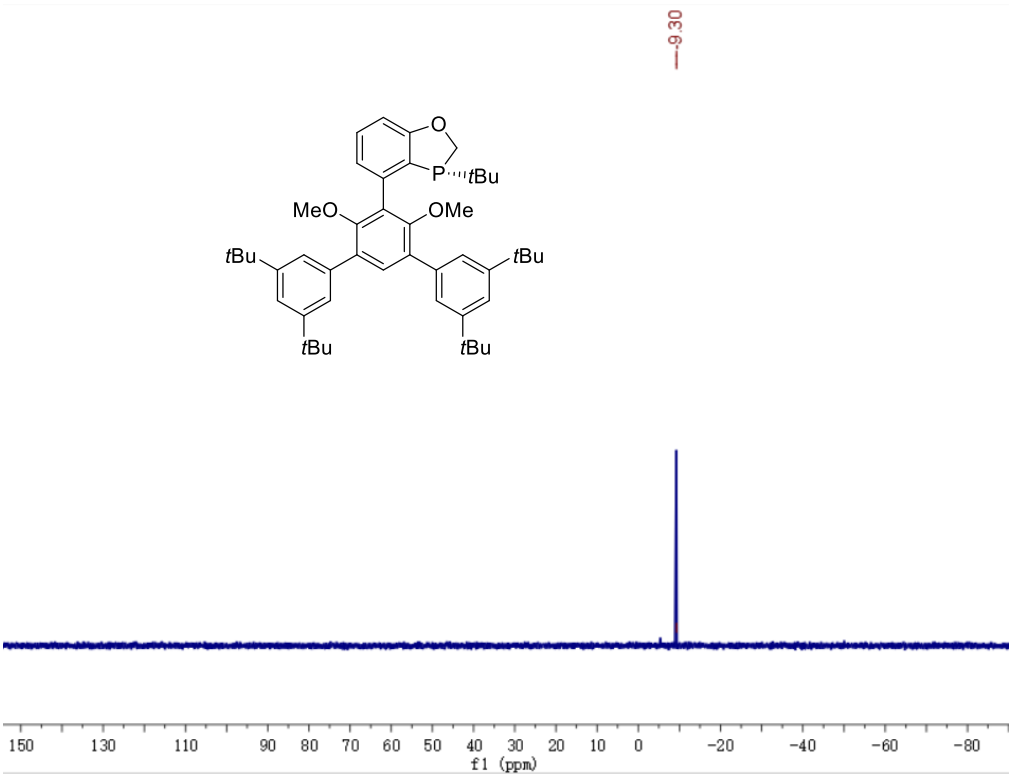

Figure S19: ^{31}P NMR (162 MHz, $CDCl_3$) spectrum of **L13**

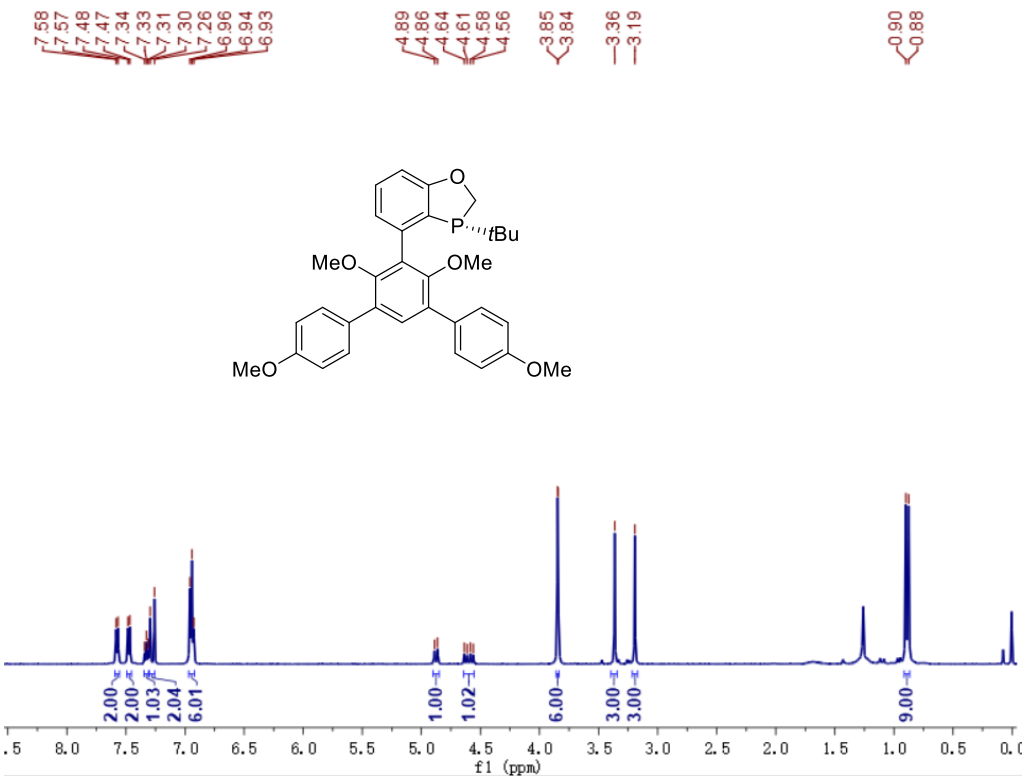

Figure S20: ^{1}H NMR (500 MHz, $CDCl_3$) spectrum of **L16**

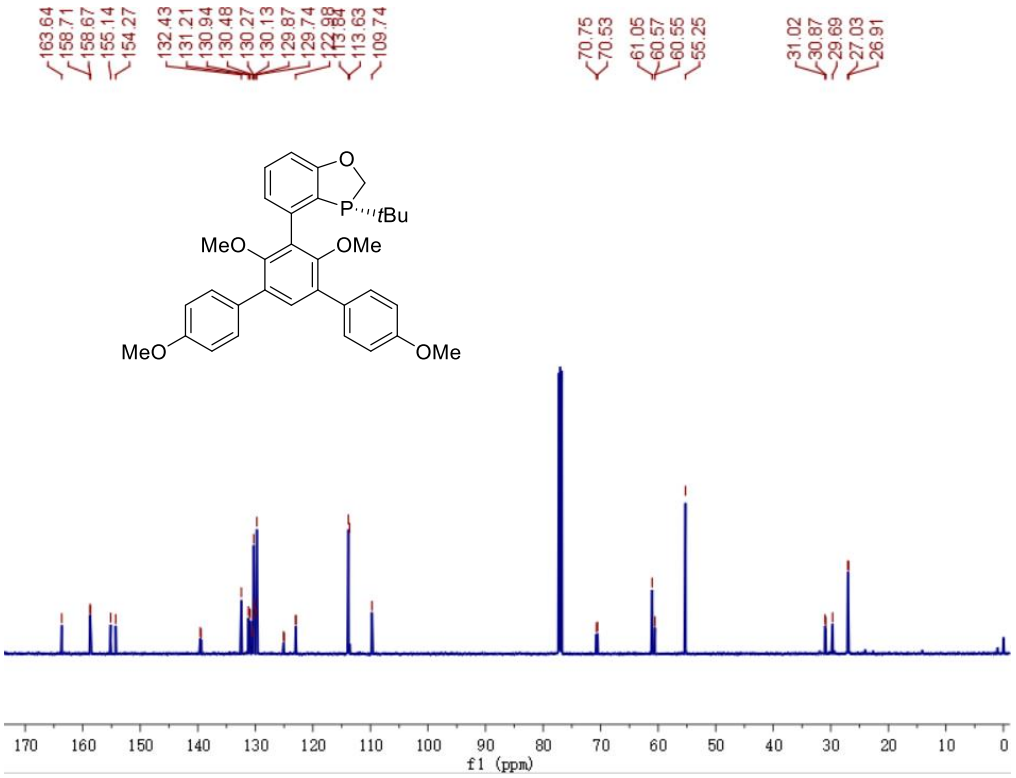

Figure S21: ^{13}C NMR (126 MHz, $CDCl_3$) spectrum of **L16**

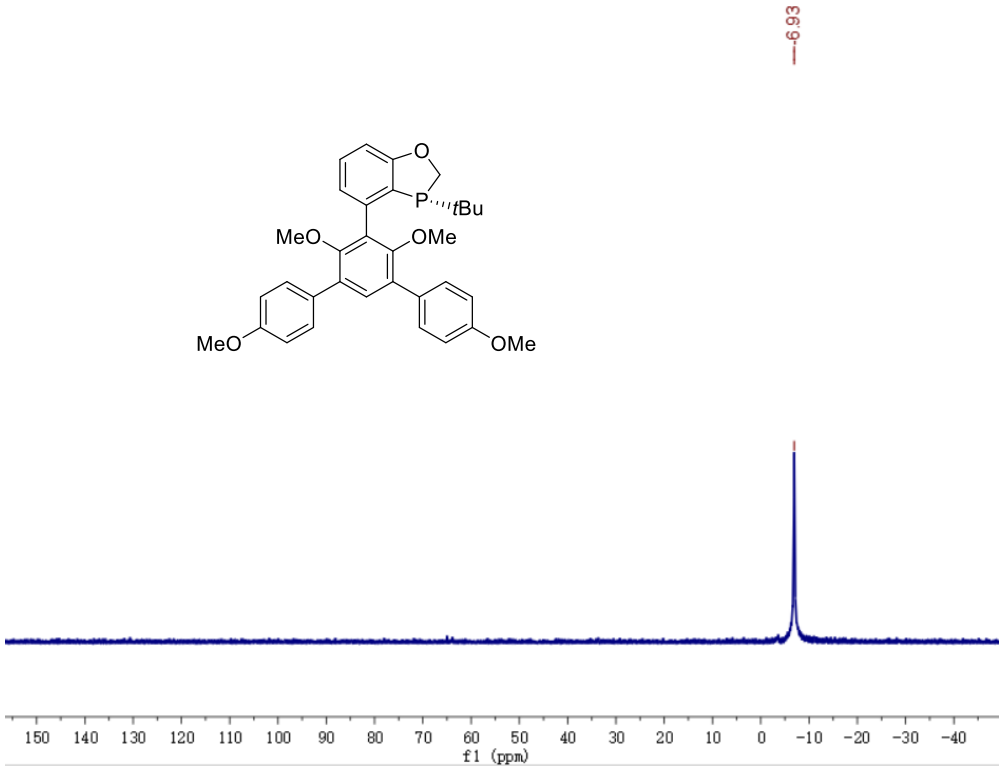

Figure S22: ^{31}P NMR (121 MHz, $CDCl_3$) spectrum of **L16**

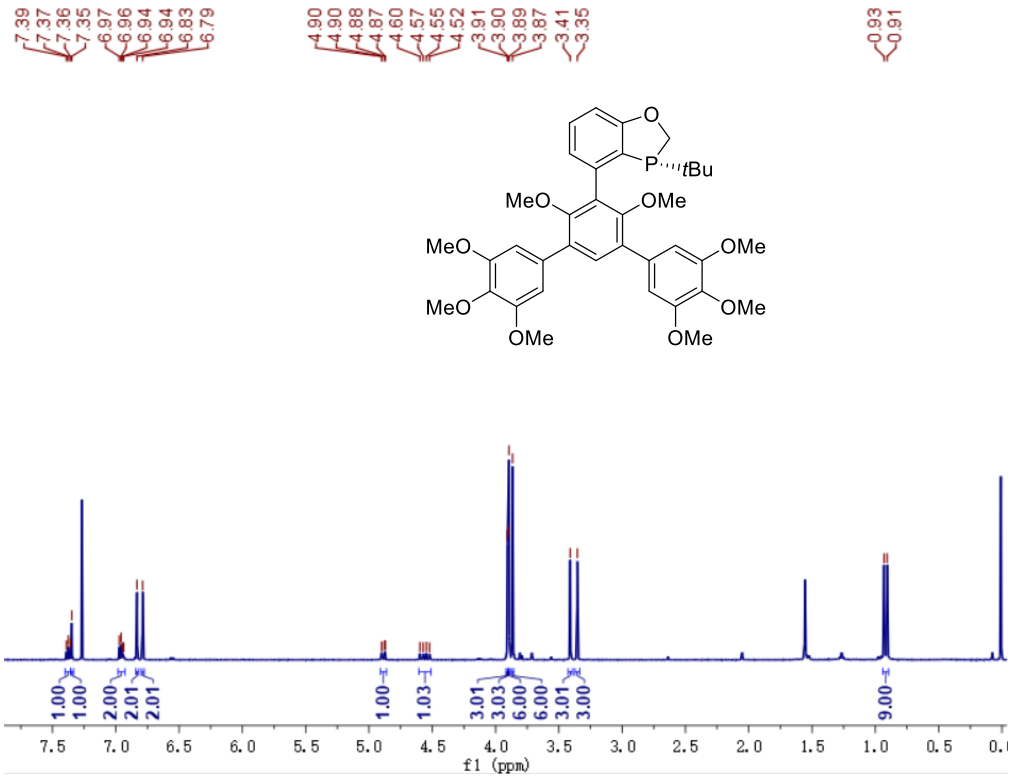

Figure S23: ^{1}H NMR (500 MHz, $CDCl_3$) spectrum of **L17**

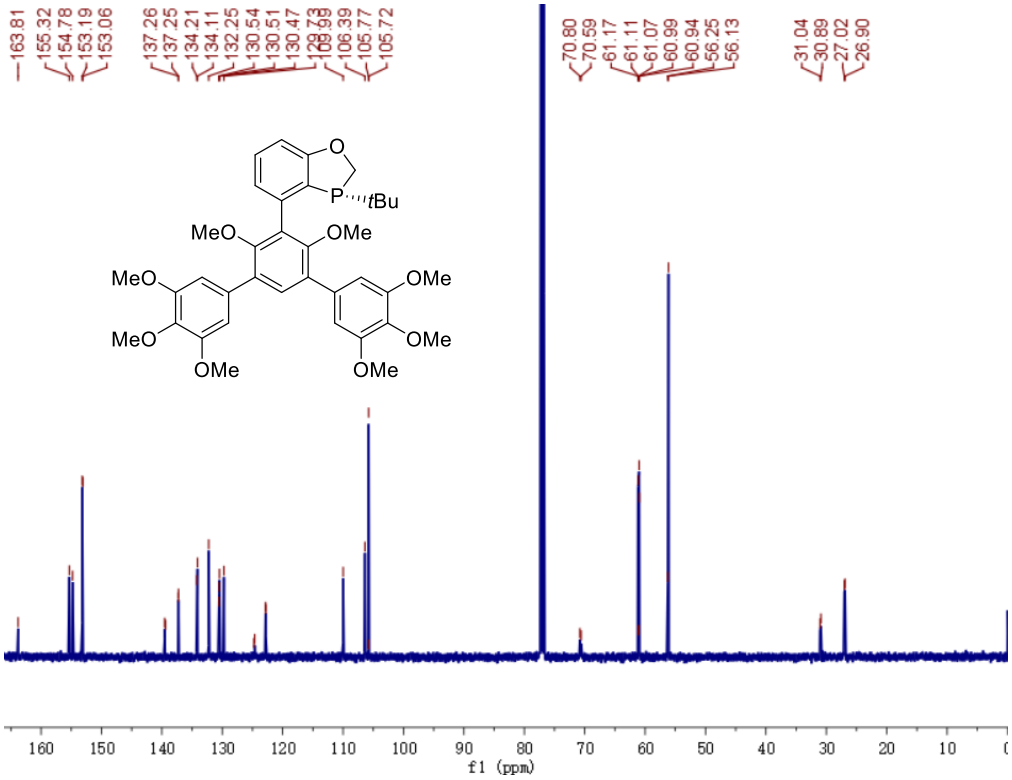

Figure S24: ^{13}C NMR (126 MHz, $CDCl_3$) spectrum of **L17**

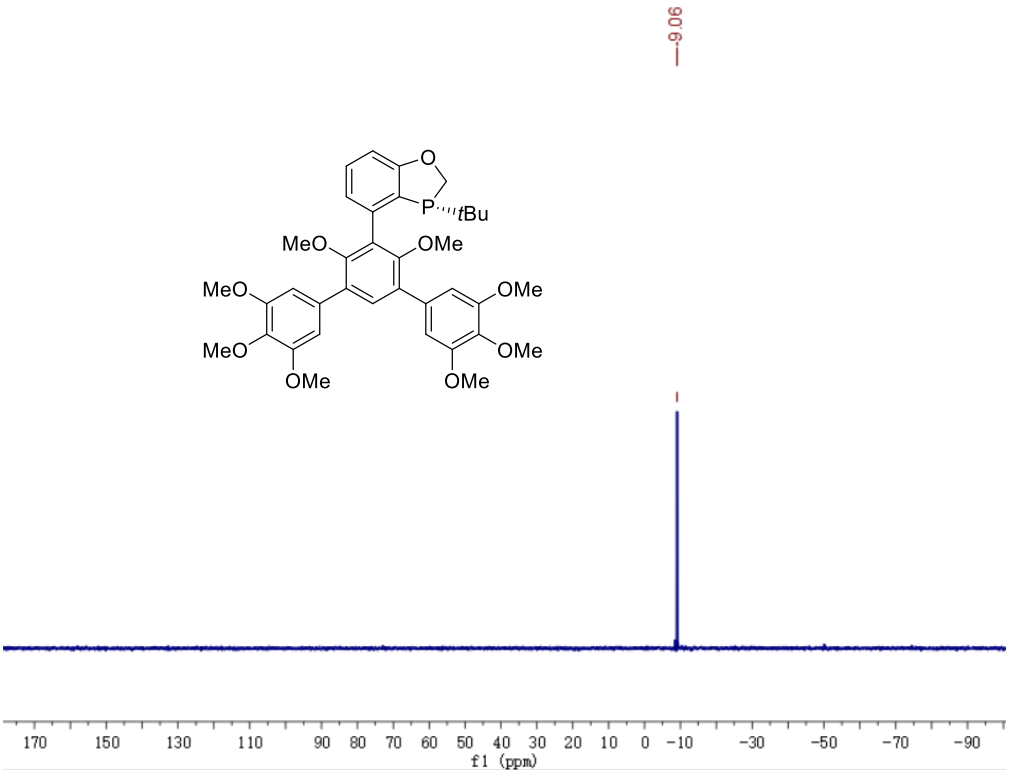

Figure S25: ^{31}P NMR (162 MHz, $CDCl_3$) spectrum of **L17**

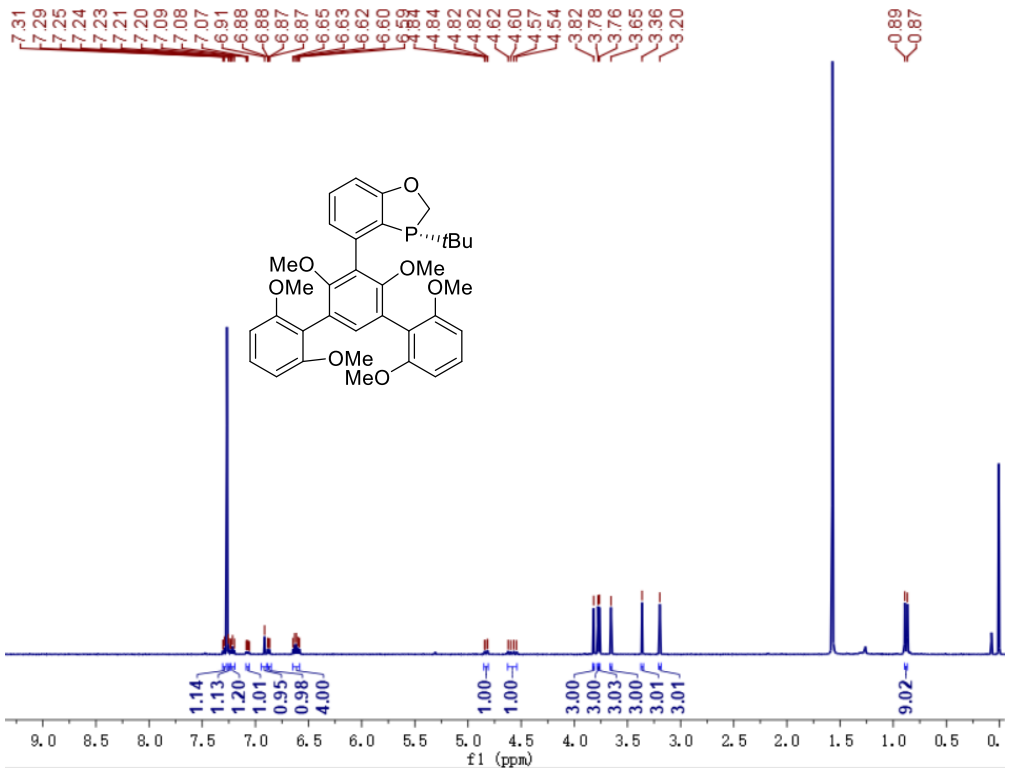

Figure S26: ^{1}H NMR (500 MHz, $CDCl_3$) spectrum of **L18**

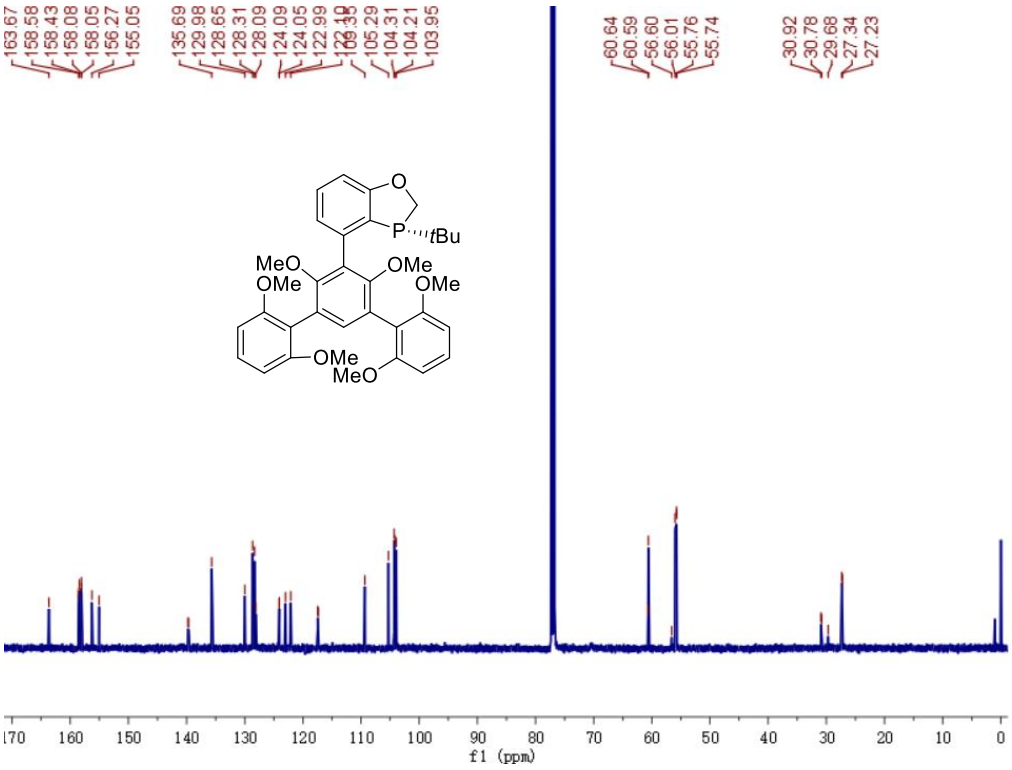

Figure S27: ^{13}C NMR (126 MHz, $CDCl_3$) spectrum of **L18**

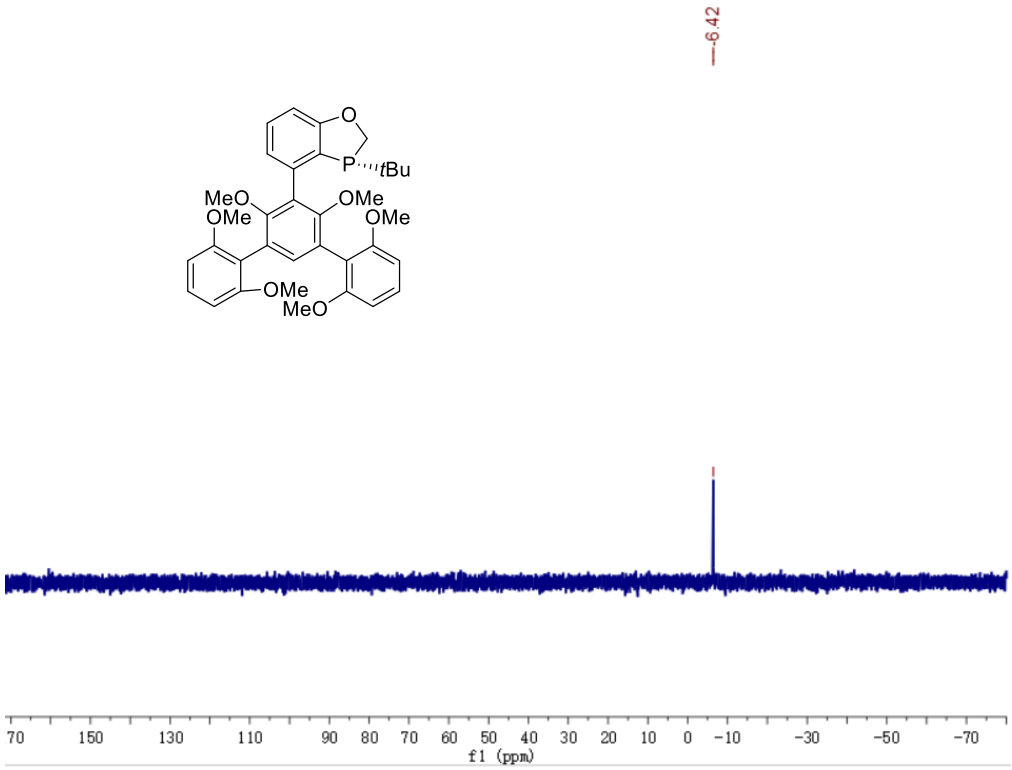

Figure S28: ^{31}P NMR (162 MHz, $CDCl_3$) spectrum of **L18**

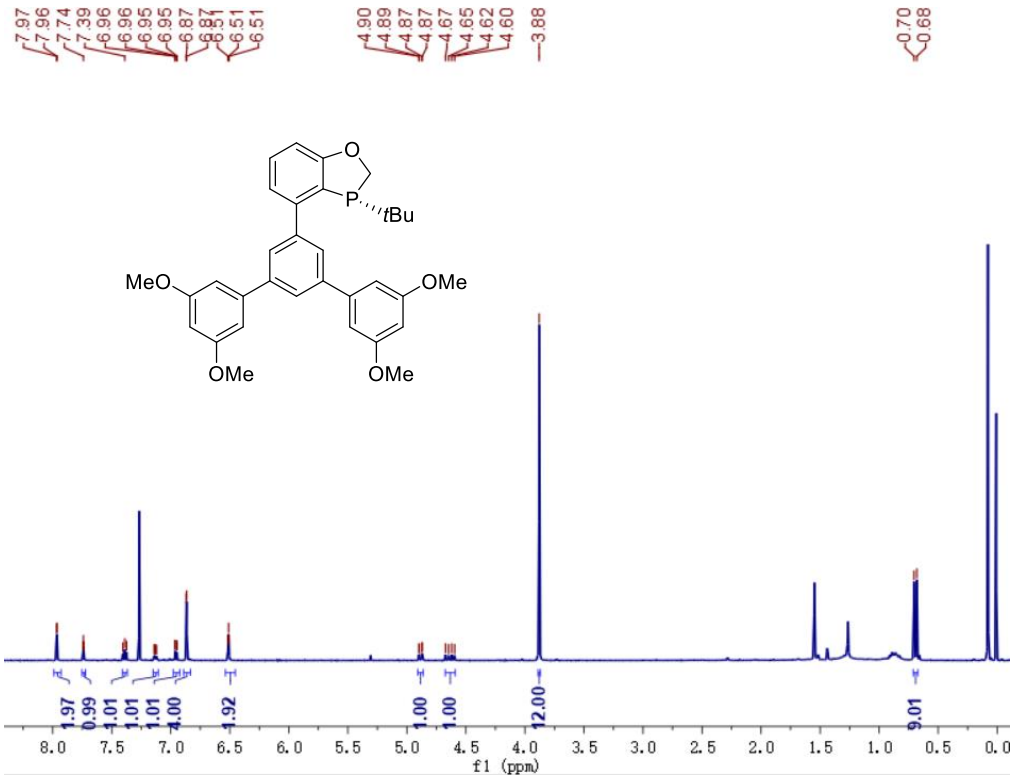

Figure S29: ^{1}H NMR (500 MHz, $CDCl_3$) spectrum of **L19**

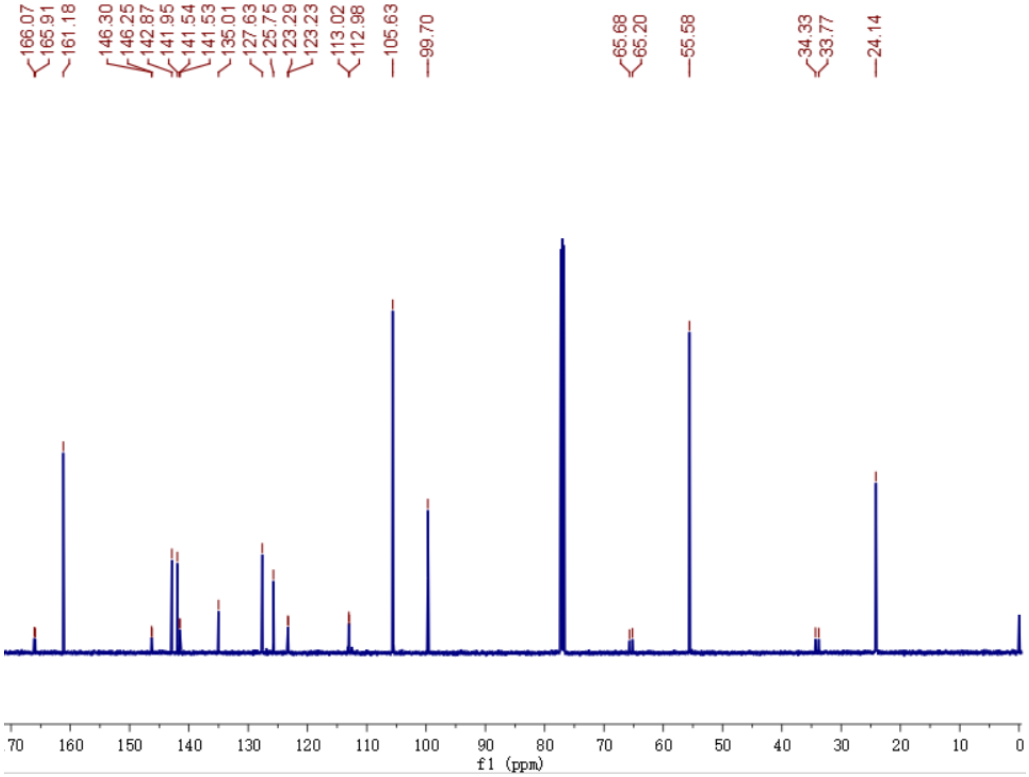

Figure S30: ^{13}C NMR (126 MHz, $CDCl_3$) spectrum of **L19**

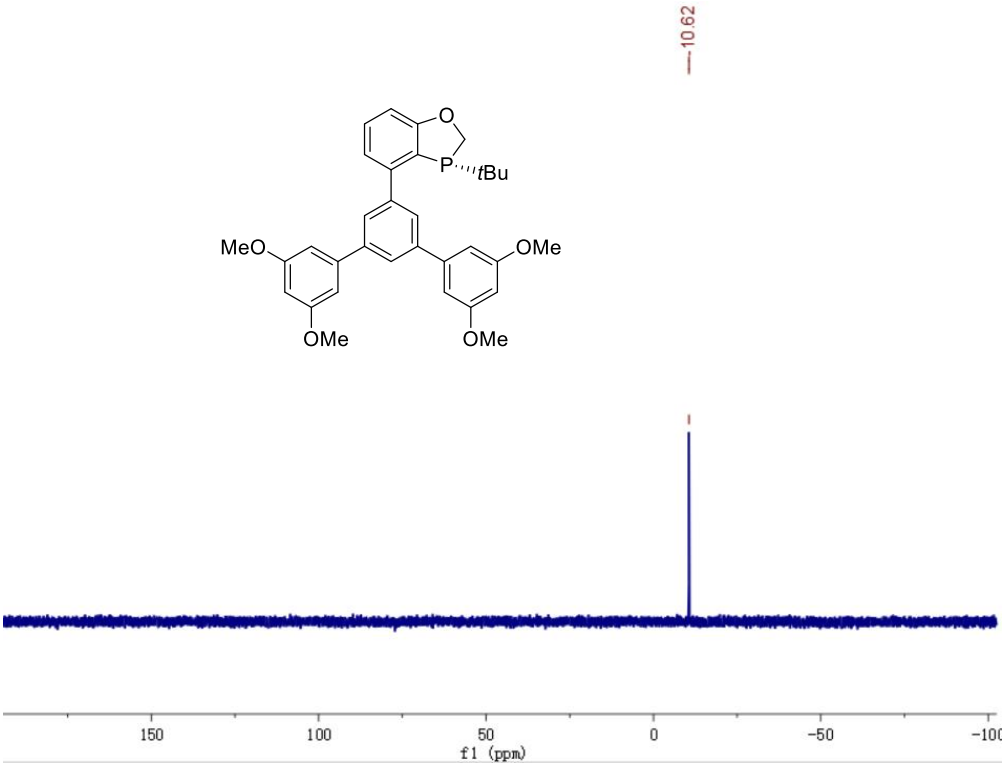

Figure S31: ^{31}P NMR (162 MHz, $CDCl_3$) spectrum of **L19**

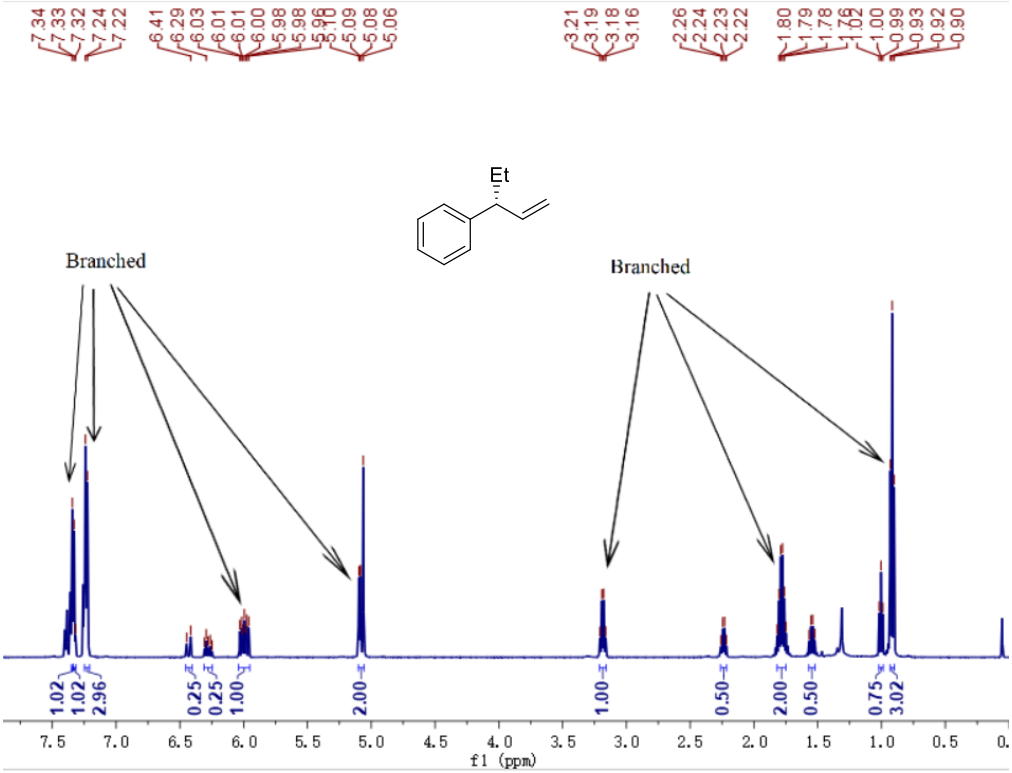

Figure S32: ^{1}H NMR (500 MHz, $CDCl_3$) spectrum of **3aa** and **4aa** (The left peaks are linear products.)

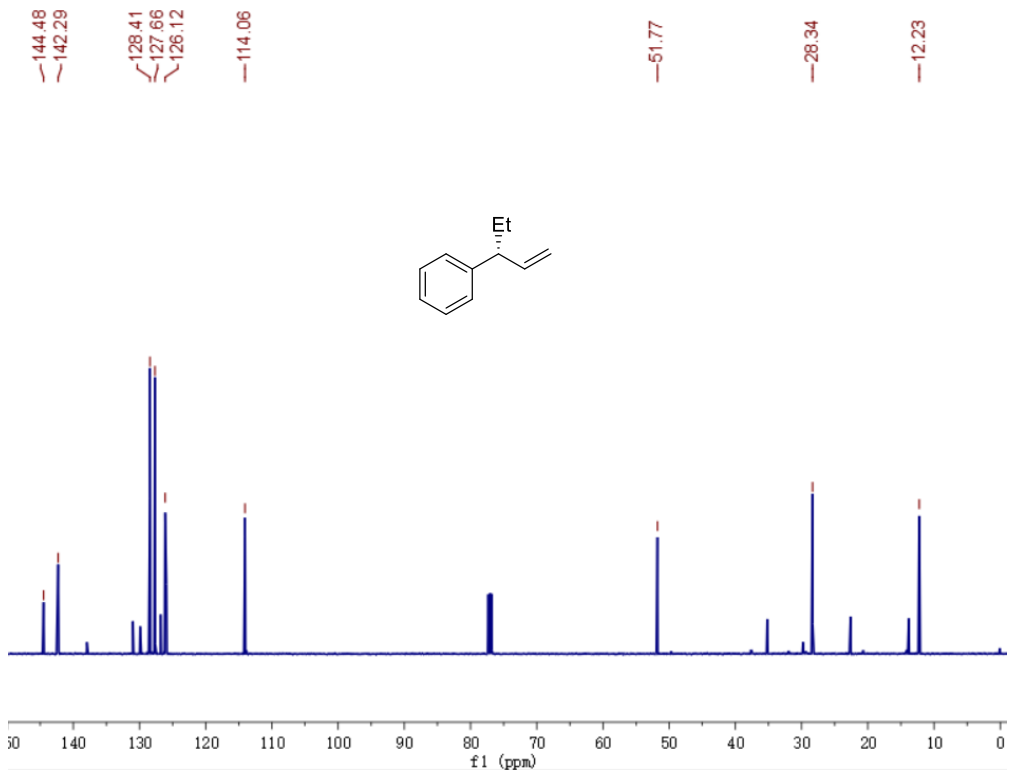

Figure S33: ^{13}C NMR (126 MHz, $CDCl_3$) spectrum of **3aa** and **4aa**

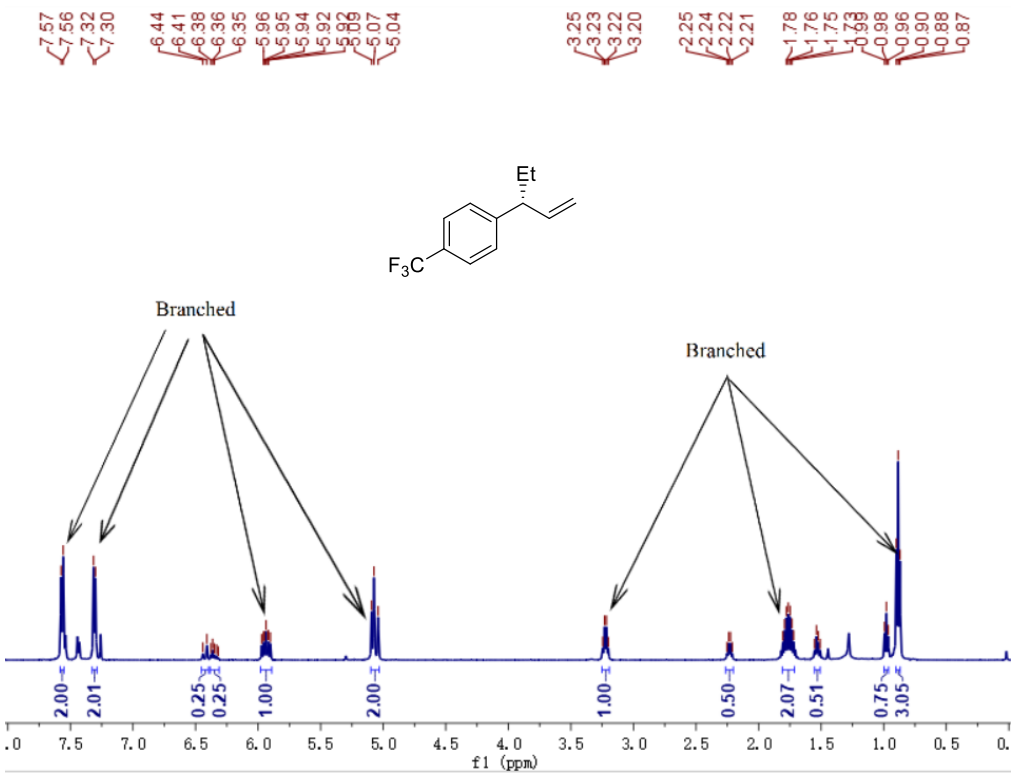

Figure S34: ^{1}H NMR (500 MHz, $CDCl_3$) spectrum of **3ba** and **4ba** (The left peaks are linear products.)

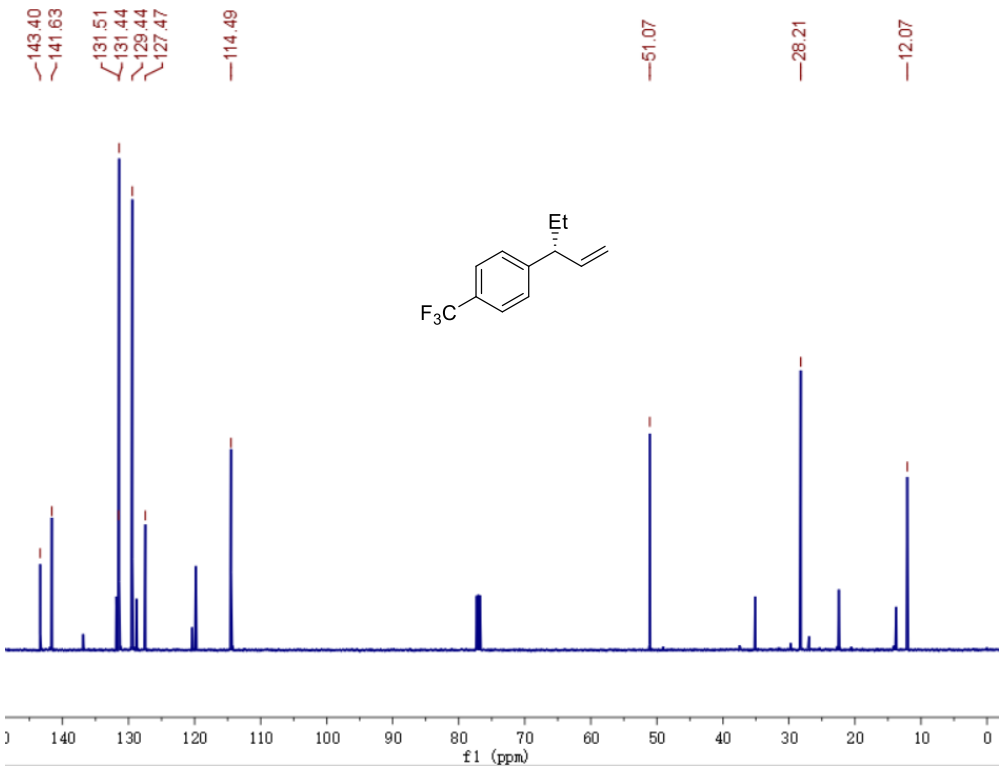

Figure S35: ^{13}C NMR (126 MHz, $CDCl_3$) spectrum of **3ba** and **4ba**

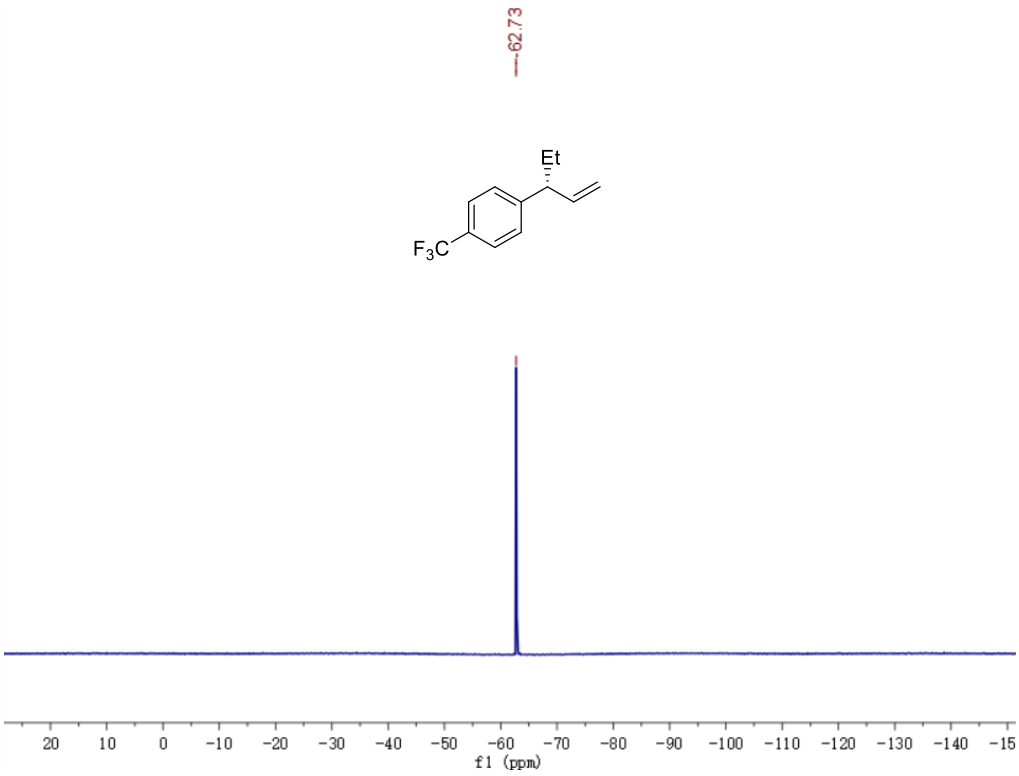

Figure S36: ^{19}F NMR (282 MHz, $CDCl_3$) spectrum of **3ba** and **4ba**

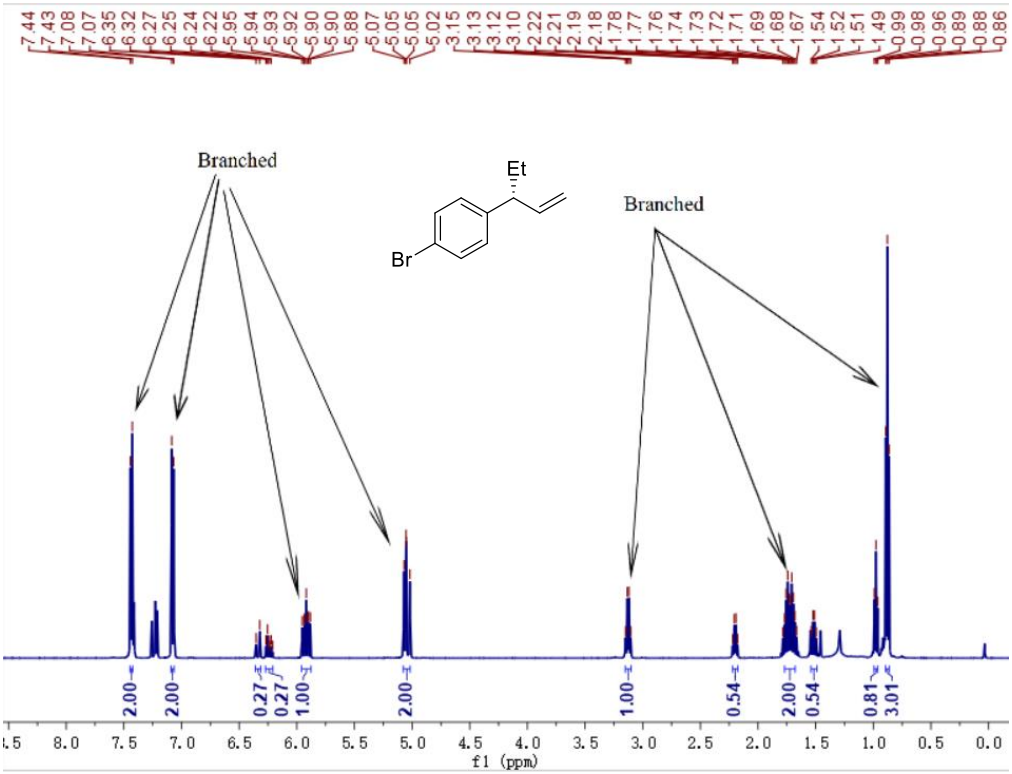

Figure S37: ^{1}H NMR (500 MHz, $CDCl_3$) spectrum of **3ca** and **4ca** (The left peaks are linear products.)

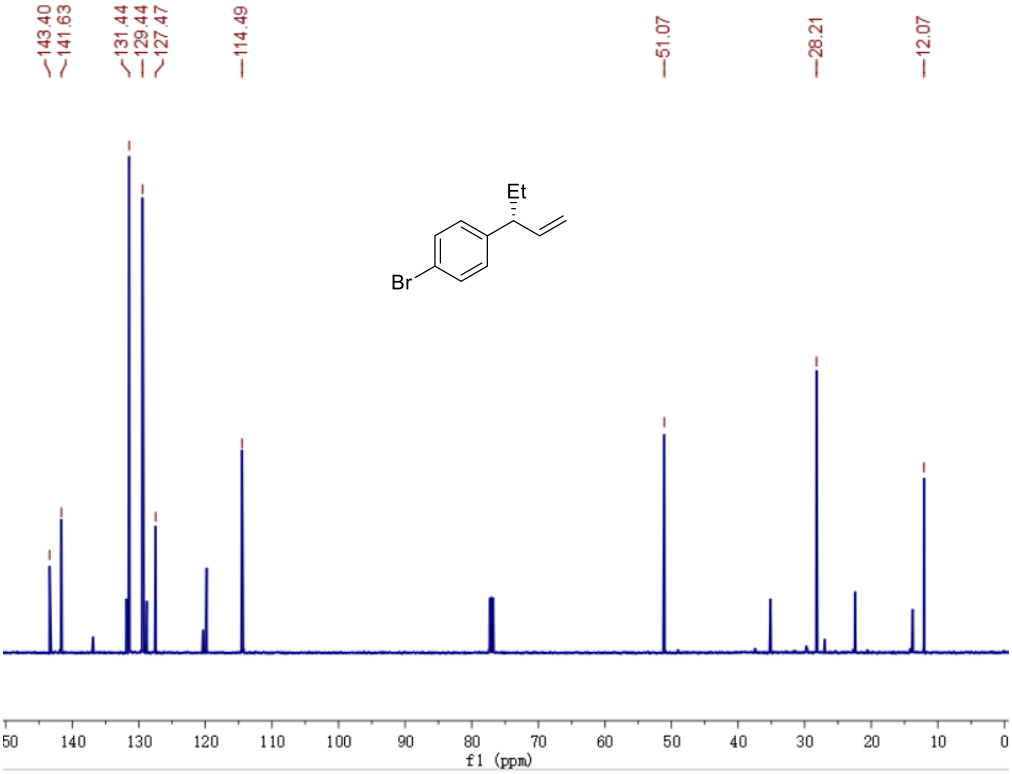

Figure S38: ^{13}C NMR (126 MHz, $CDCl_3$) spectrum of **3ca** and **4ca**

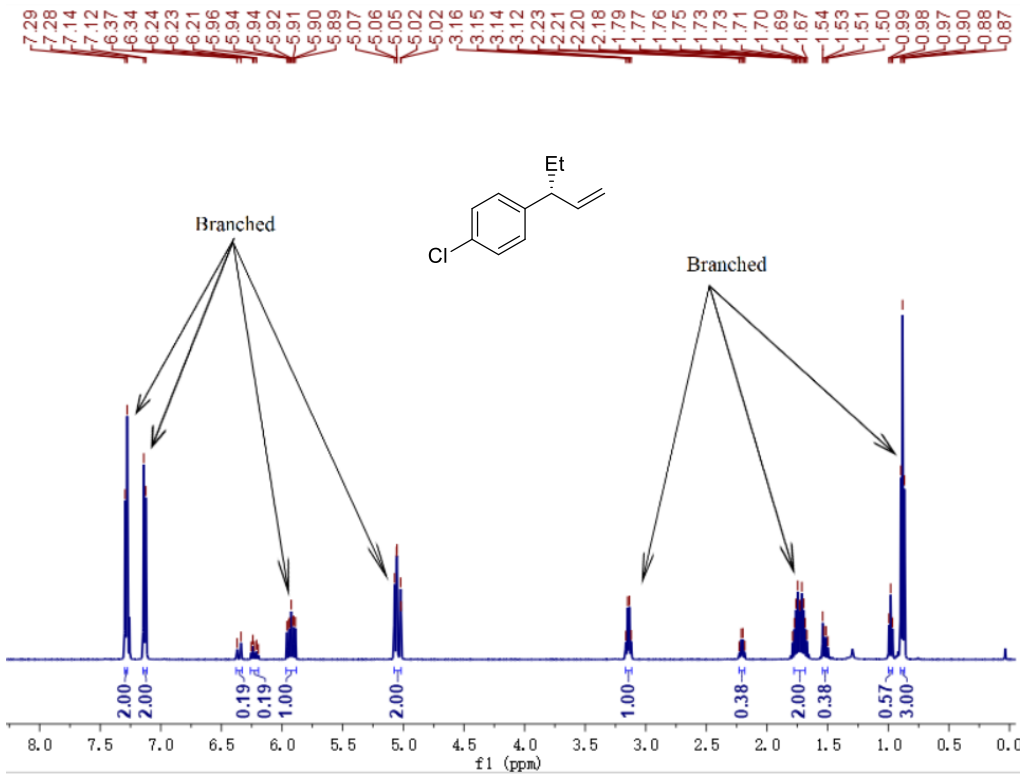

Figure S39: ^{1}H NMR (500 MHz, $CDCl_3$) spectrum of **3da** and **4da** (The left peaks are linear products.)

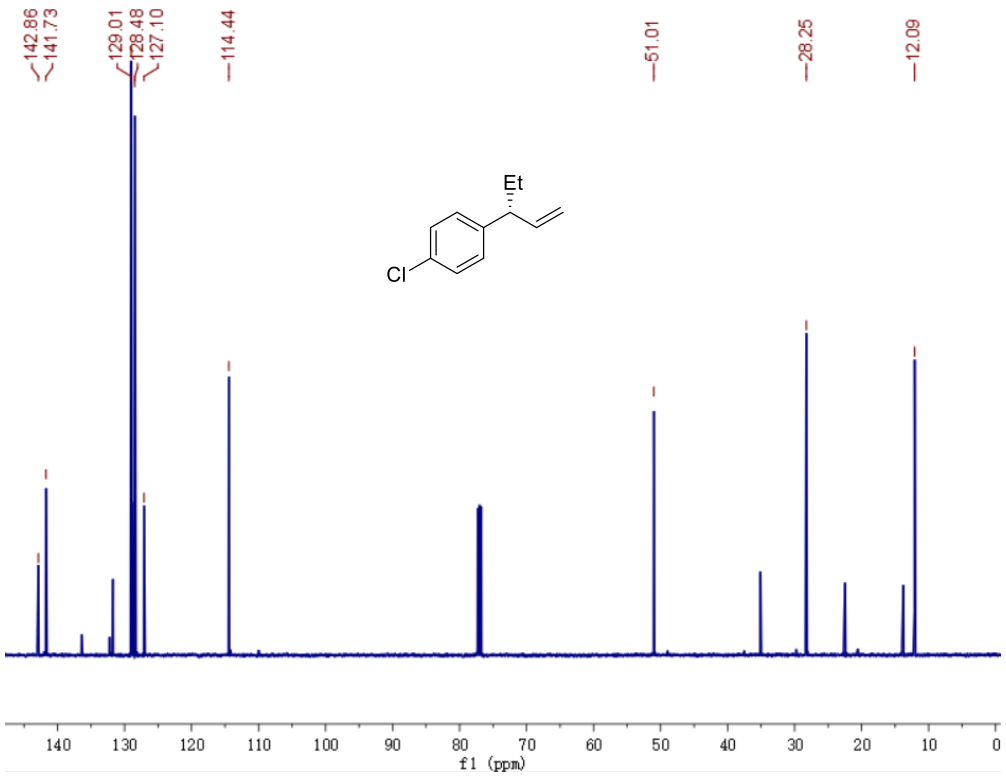

Figure S40: ^{13}C NMR (126 MHz, $CDCl_3$) spectrum of **3da** and **4da**

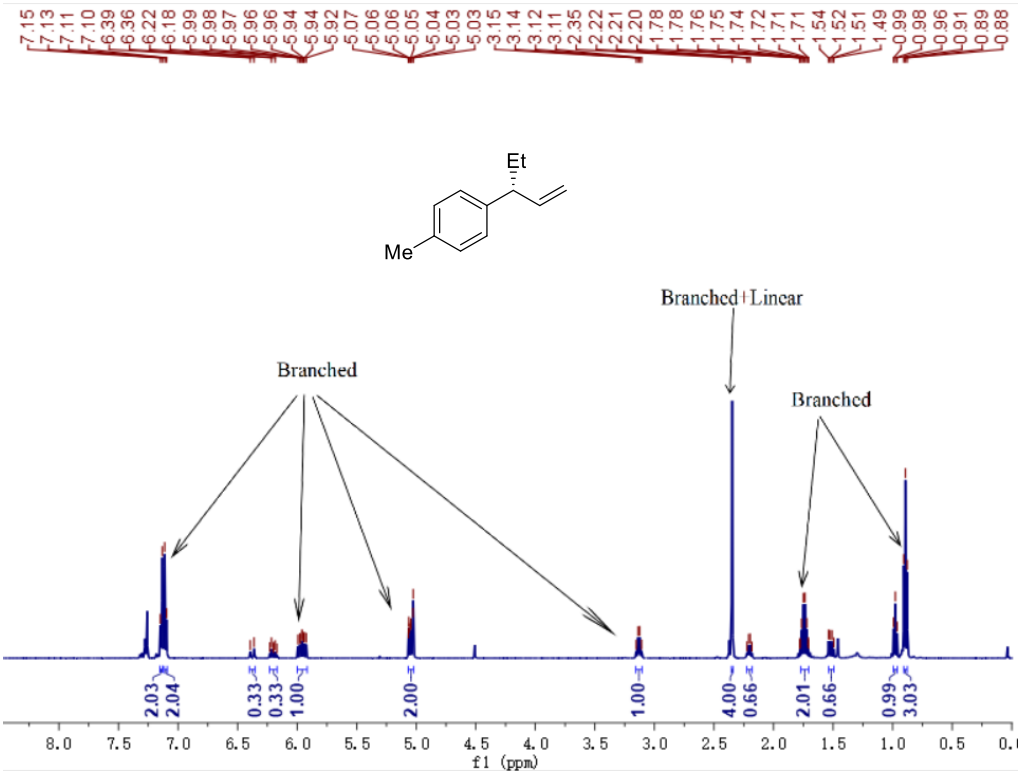

Figure S41: ^{1}H NMR (500 MHz, $CDCl_3$) spectrum of **3ea** and **4ea** (The left peaks are linear products.)

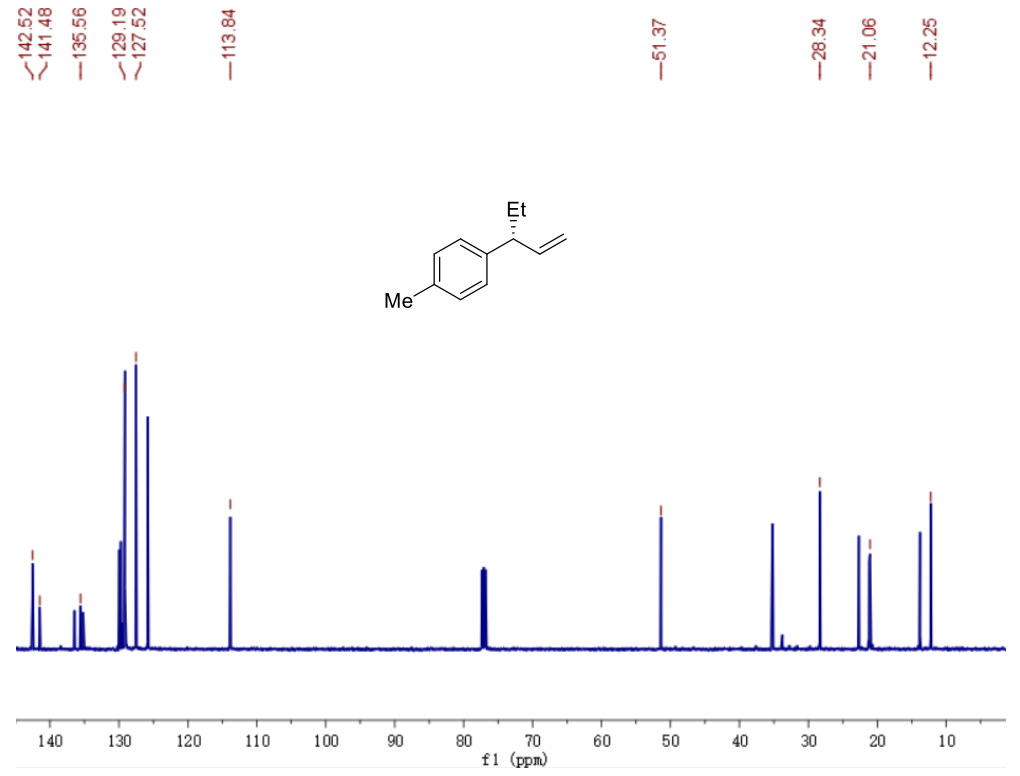

Figure S42: ^{13}C NMR (126 MHz, $CDCl_3$) spectrum of **3ea** and **4ea**

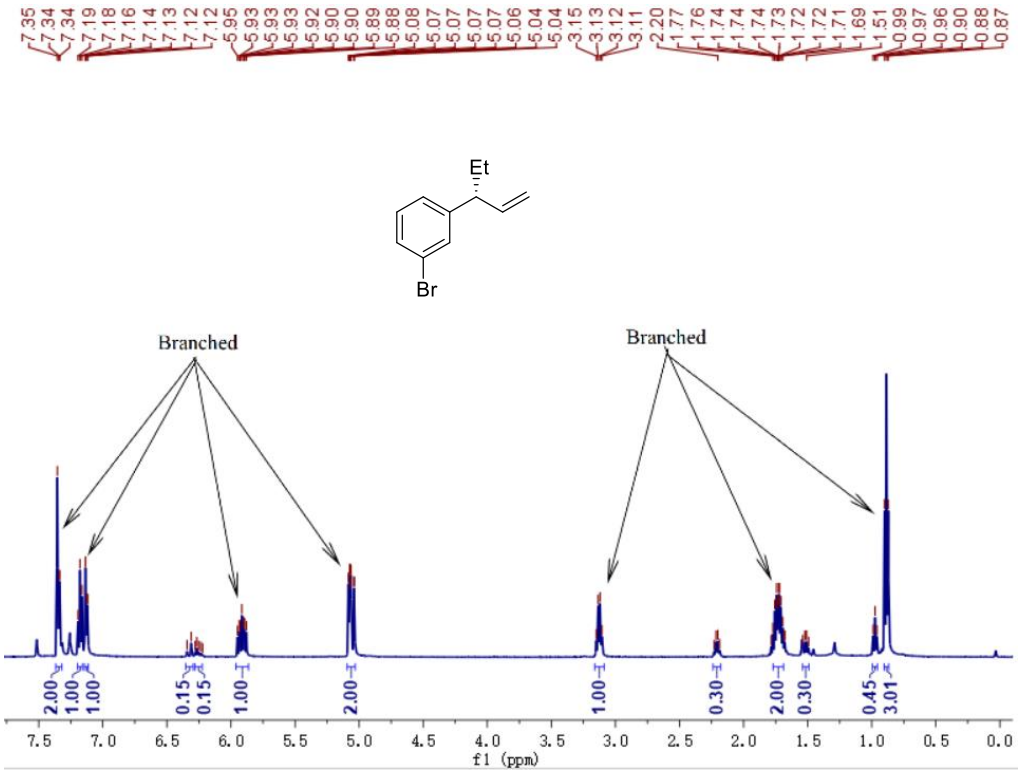

Figure S43: ^{1}H NMR (500 MHz, $CDCl_3$) spectrum of **3fa** and **4fa** (The left peaks are linear products.)

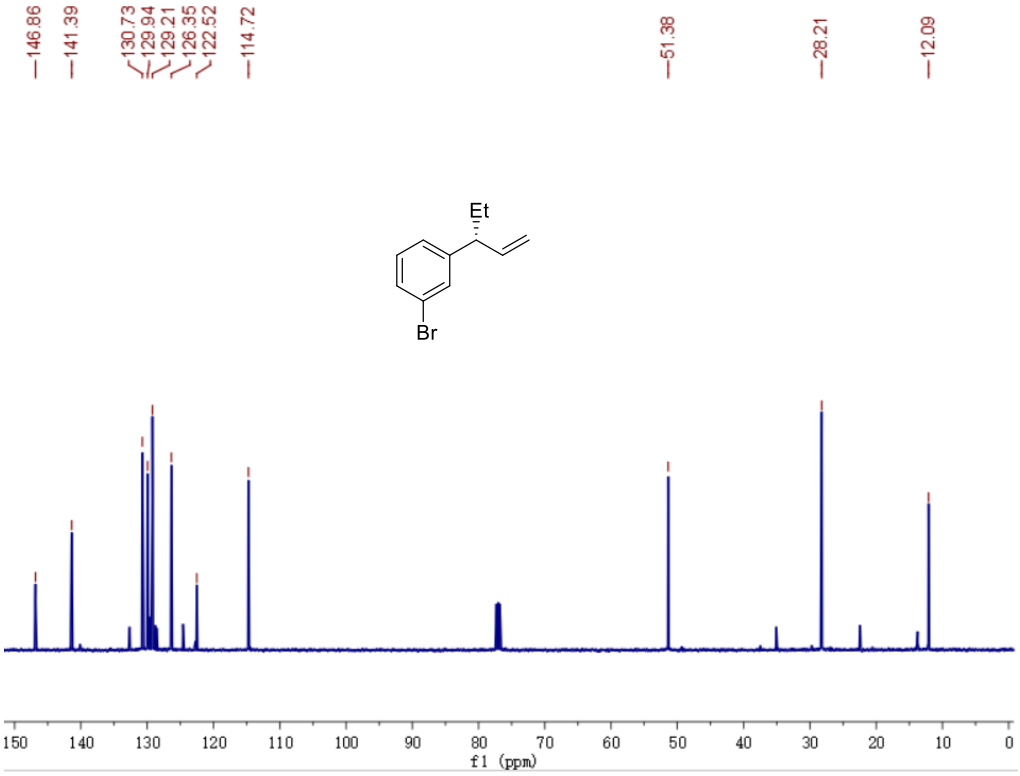

Figure S44: ^{13}C NMR (126 MHz, $CDCl_3$) spectrum of **3fa** and **4fa**

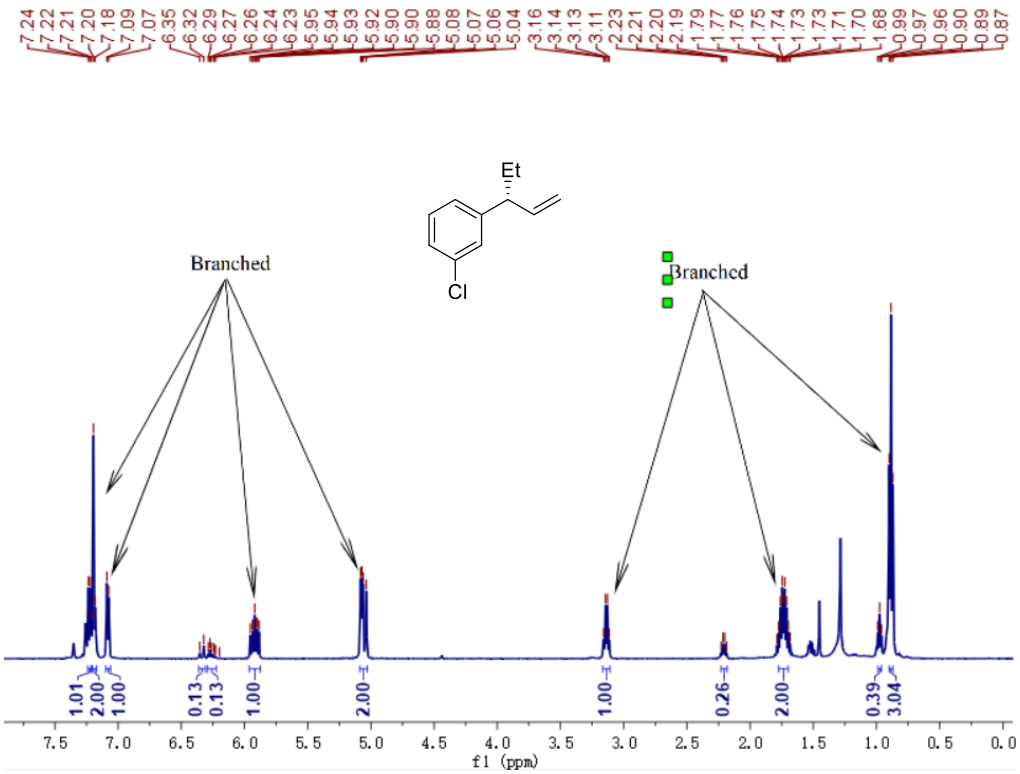

Figure S45: ^{1}H NMR (500 MHz, $CDCl_3$) spectrum of **3ga** and **4ga** (The left peaks are linear products.)

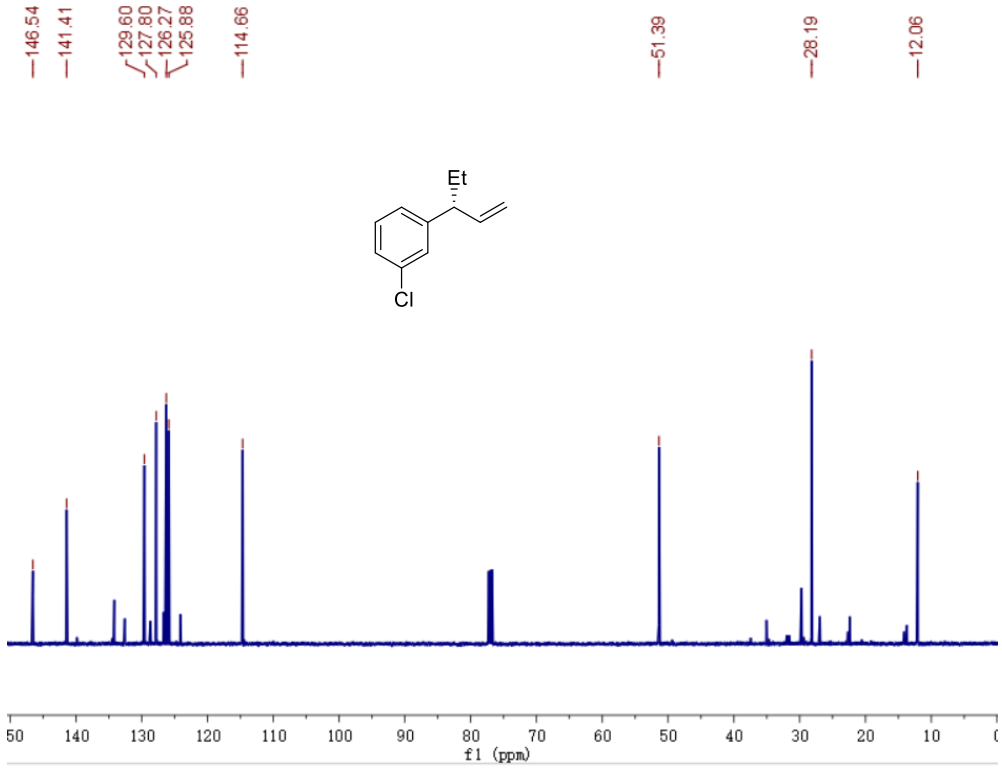

Figure S46: ^{13}C NMR (126 MHz, $CDCl_3$) spectrum of **3ga** and **4ga**

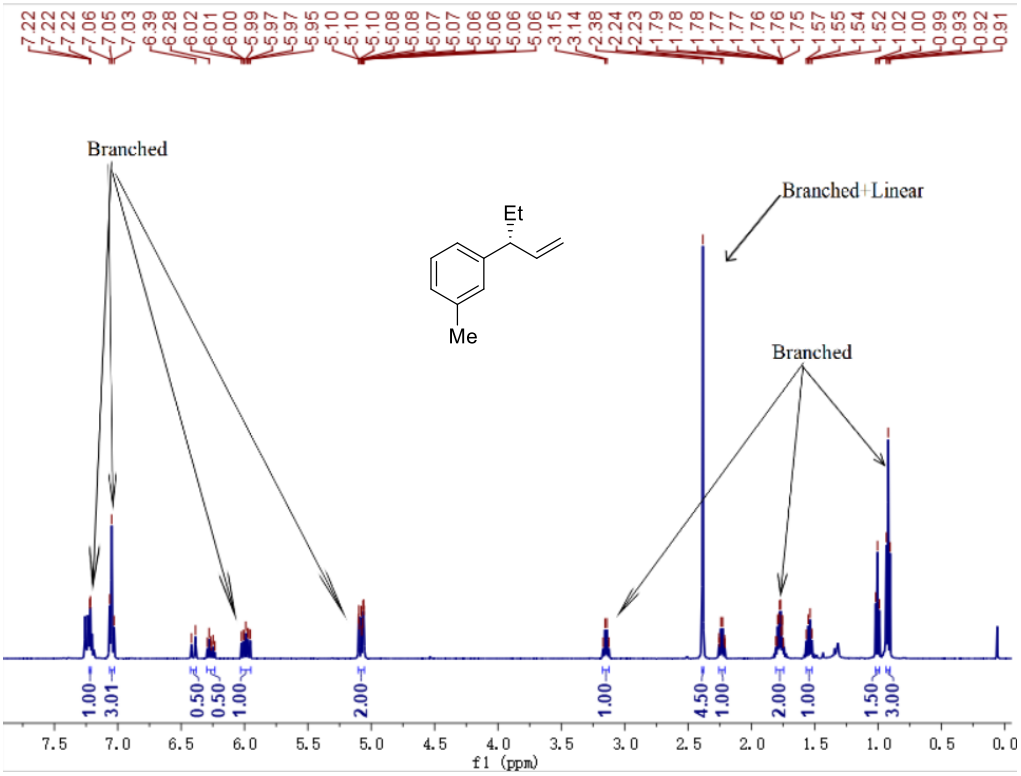

Figure S47: ^{1}H NMR (500 MHz, $CDCl_3$) spectrum of **3ha** and **4ha** (The left peaks are linear products.)

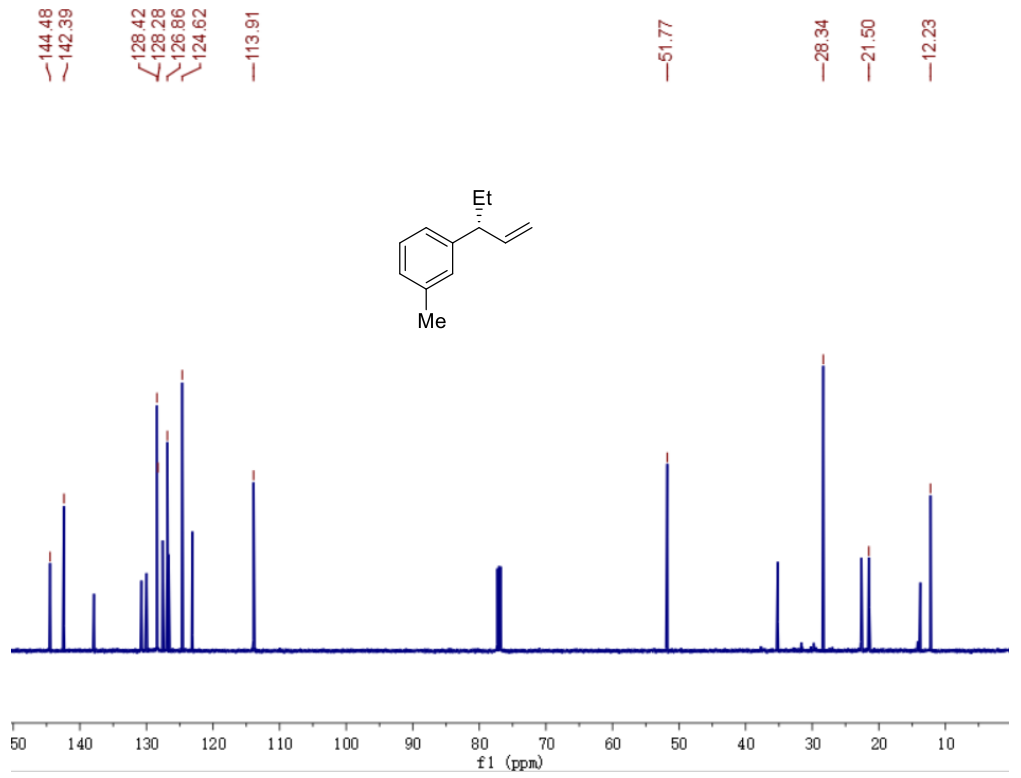

Figure S48: ^{13}C NMR (126 MHz, $CDCl_3$) spectrum of **3ha** and **4ha**

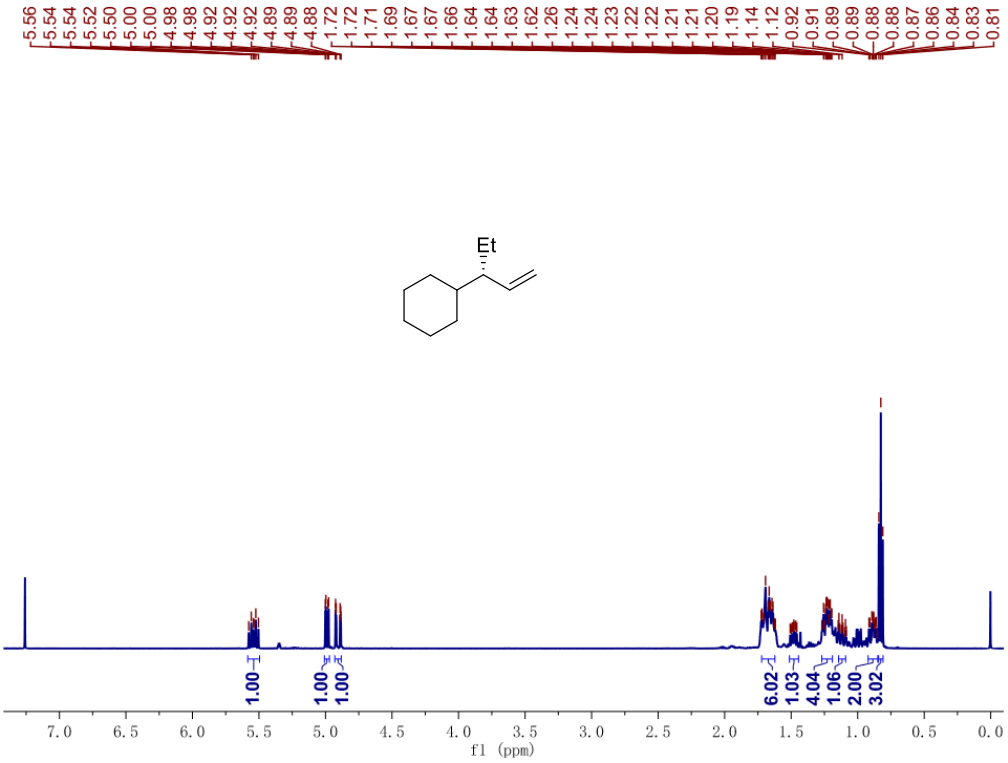

Figure S49: ^{1}H NMR (500 MHz, $CDCl_3$) spectrum of **3ia** and **4ia**

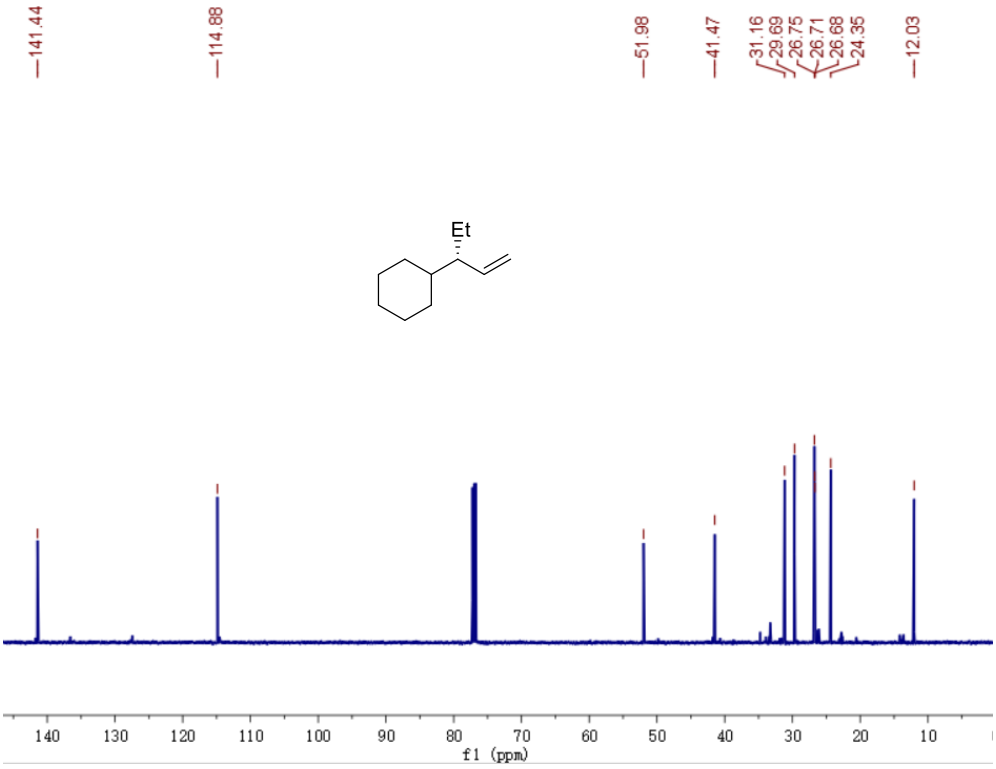

Figure S50: ^{13}C NMR (126 MHz, $CDCl_3$) spectrum of **3ia** and **4ia**

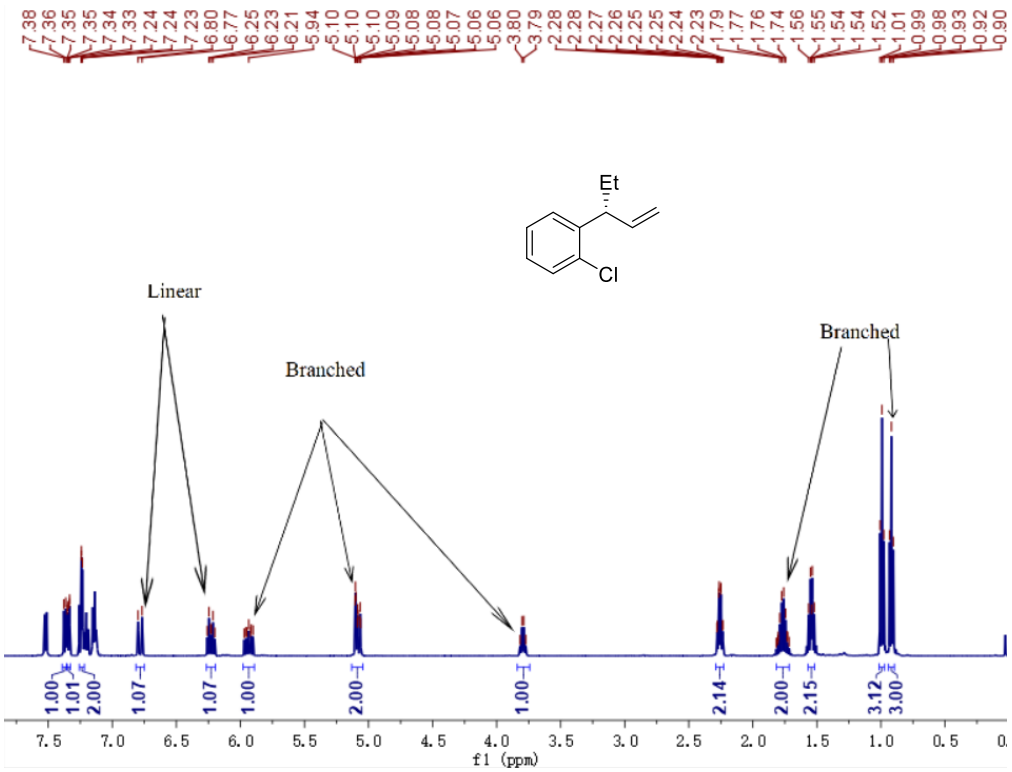

Figure S51: ^{1}H NMR (500 MHz, $CDCl_3$) spectrum of **3ja** and **4ja**

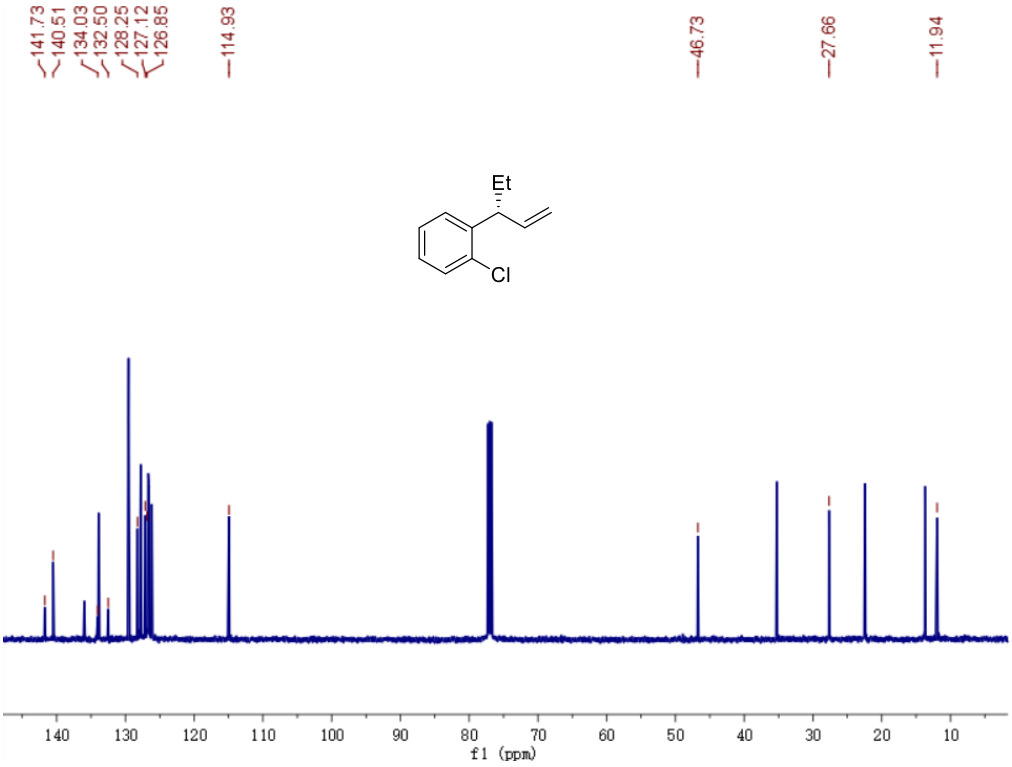

Figure S52: ^{13}C NMR (126 MHz, $CDCl_3$) spectrum of **3ja** and **4ja**

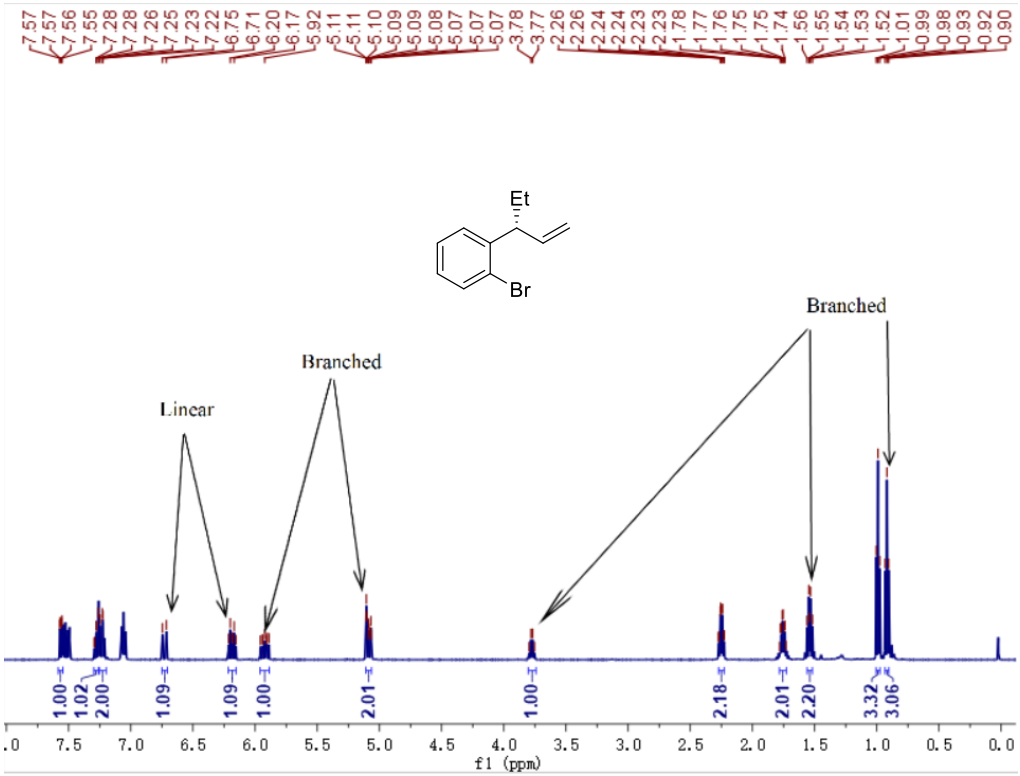

Figure S53: ^{1}H NMR (500 MHz, $CDCl_3$) spectrum of **3ka** and **4ka**

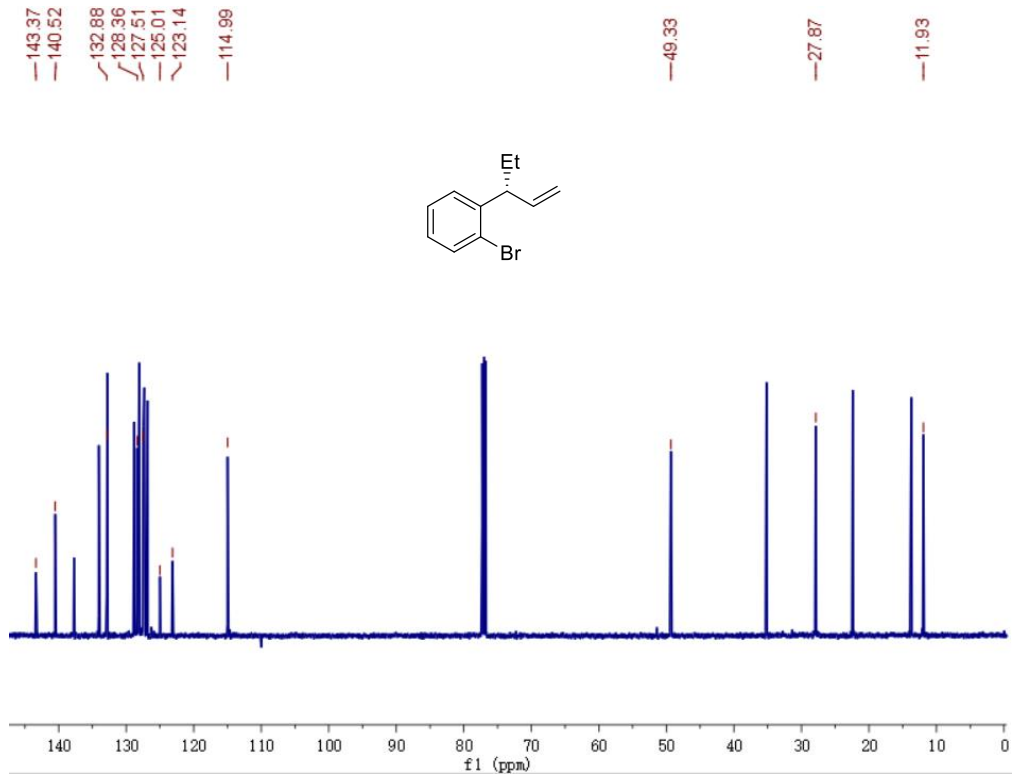

Figure S54: ^{13}C NMR (126 MHz, $CDCl_3$) spectrum of **3ka** and **4ka**

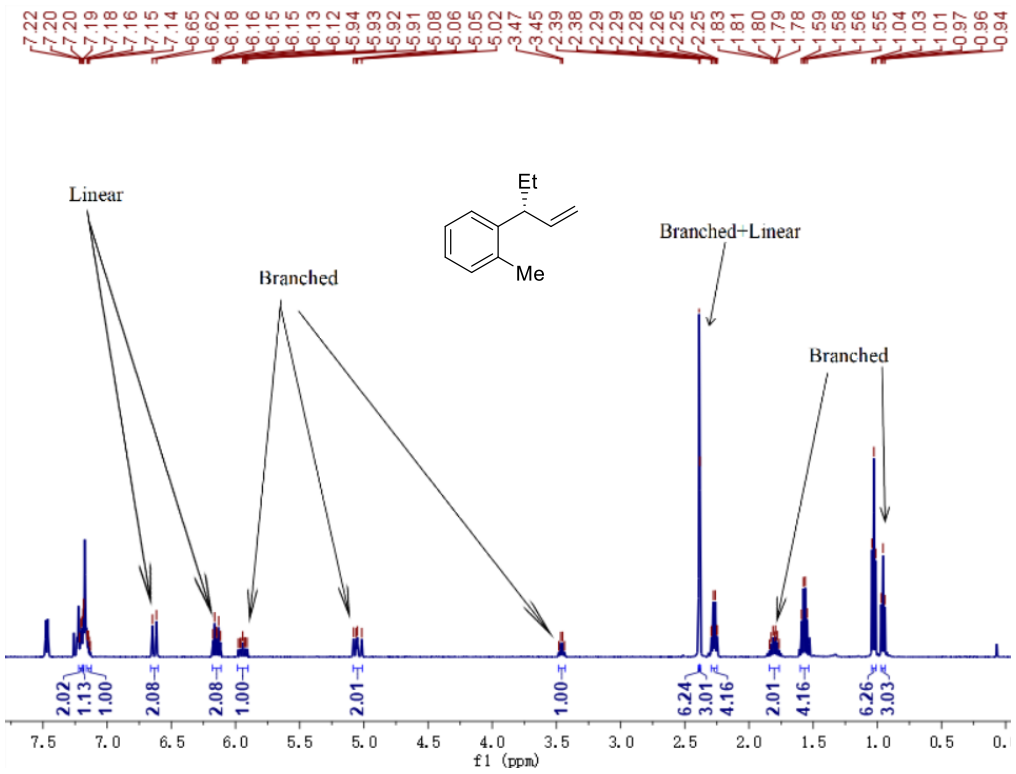

Figure S55: ^{1}H NMR (500 MHz, $CDCl_3$) spectrum of **3la** and **4la**

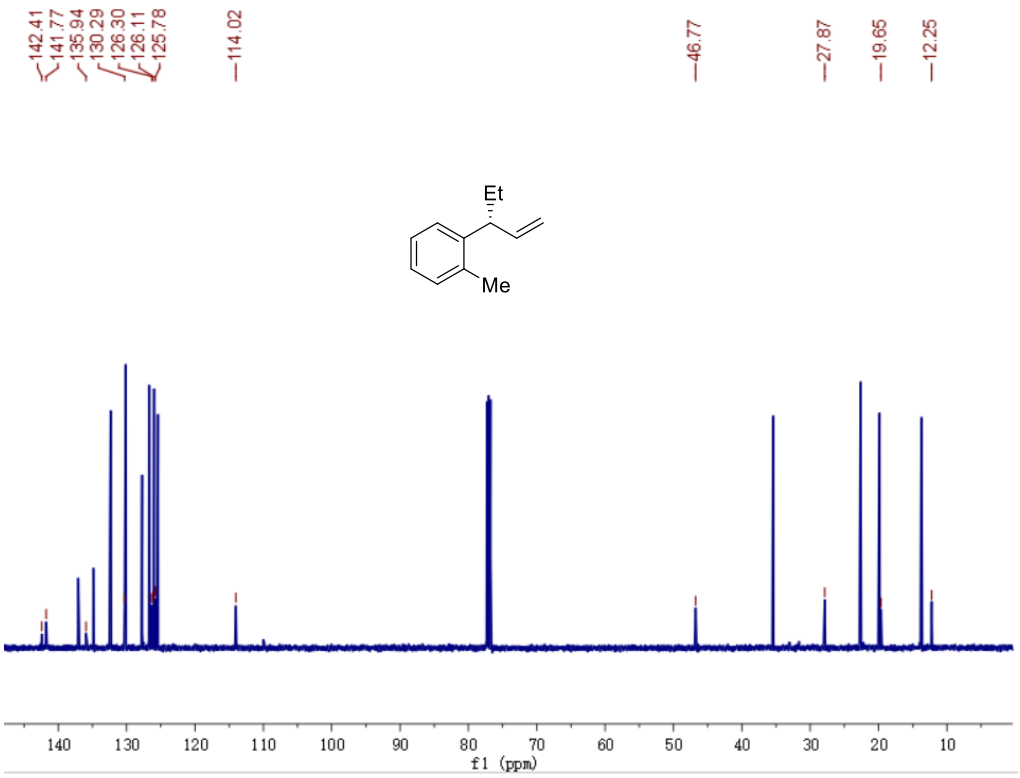

Figure S56: ^{13}C NMR (126 MHz, $CDCl_3$) spectrum of **3la** and **4la**

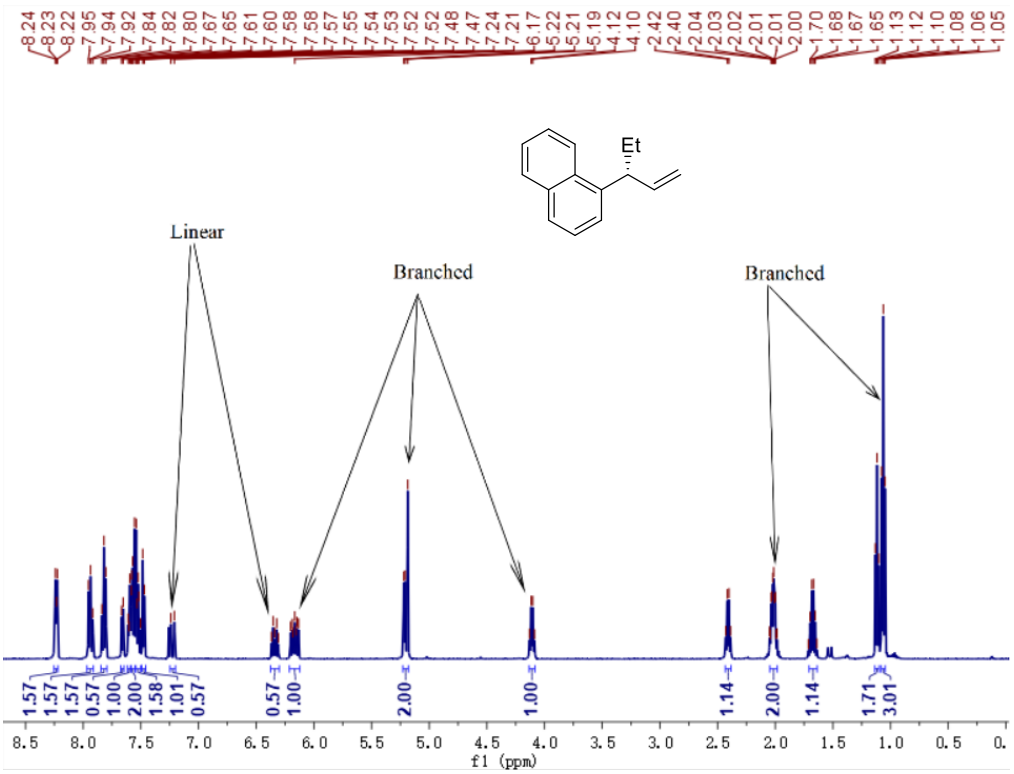

Figure S57: ^{1}H NMR (500 MHz, $CDCl_3$) spectrum of **3ma** and **4ma**

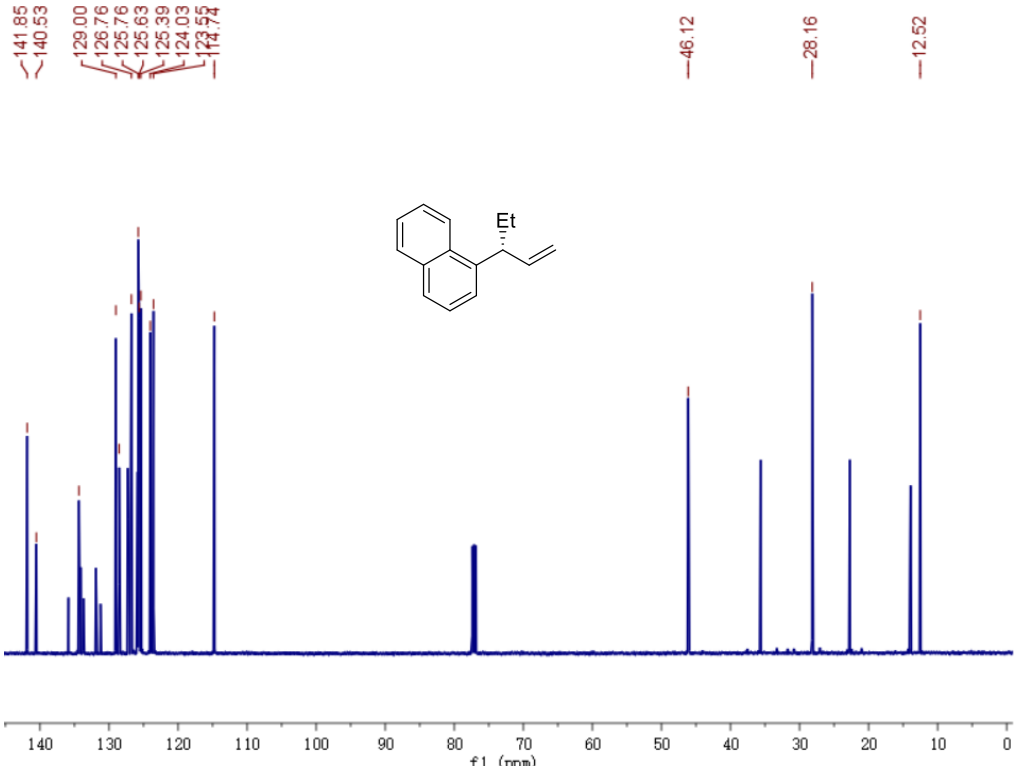

Figure S58: ^{13}C NMR (126 MHz, $CDCl_3$) spectrum of **3ma** and **4ma**

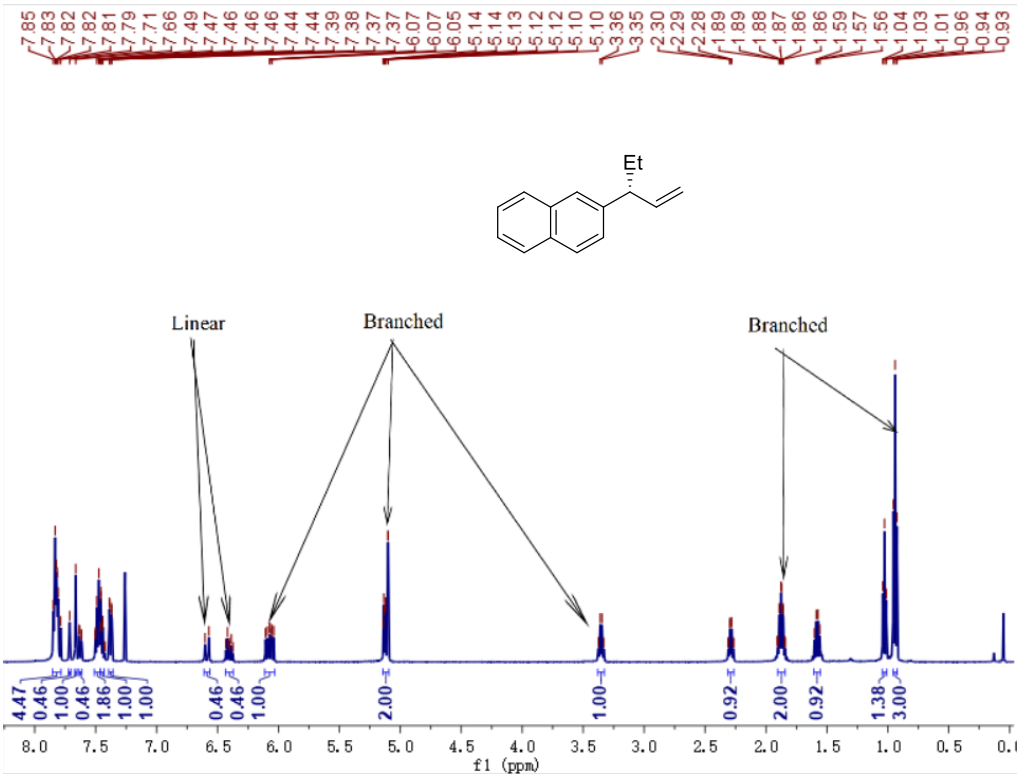

Figure S59: ^{1}H NMR (500 MHz, $CDCl_3$) spectrum of **3na** and **4na**

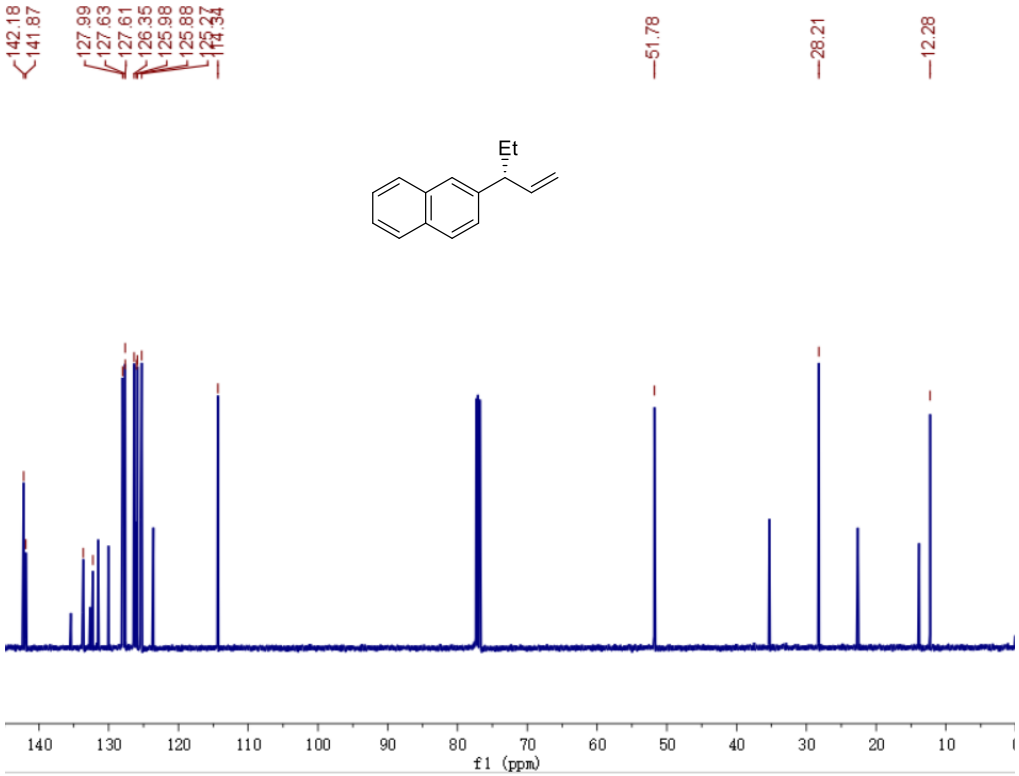

Figure S60: ^{13}C NMR (126 MHz, $CDCl_3$) spectrum of **3na** and **4na**

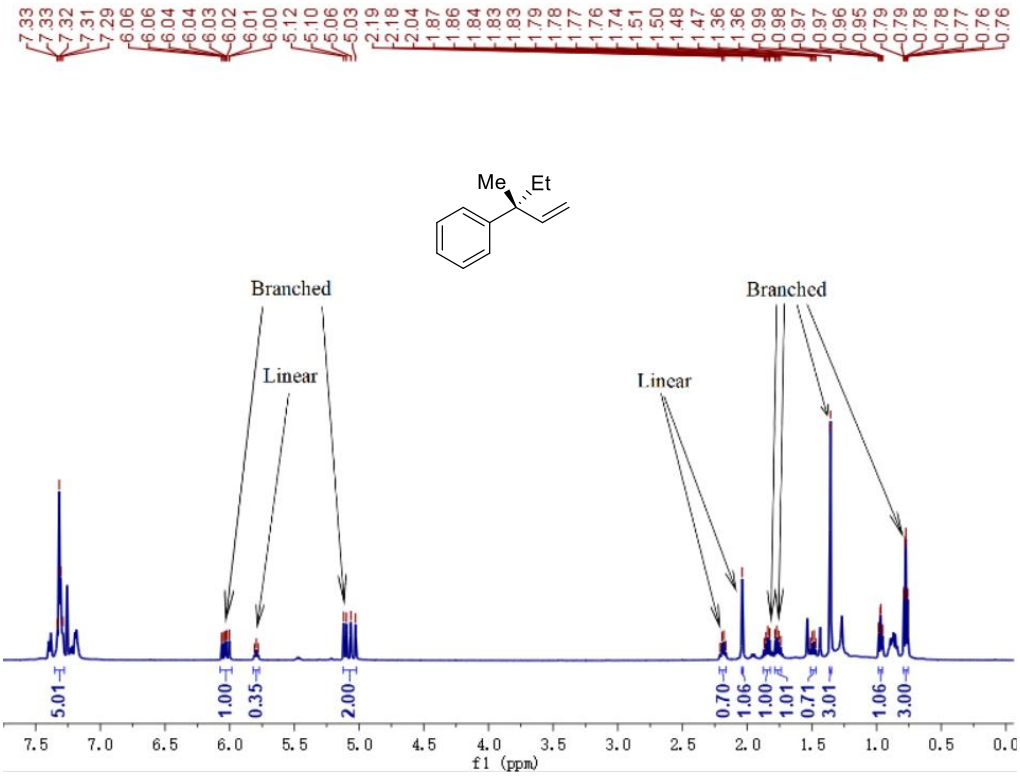

Figure S61: ^{1}H NMR (500 MHz, $CDCl_3$) spectrum of **3oa** and **4oa**

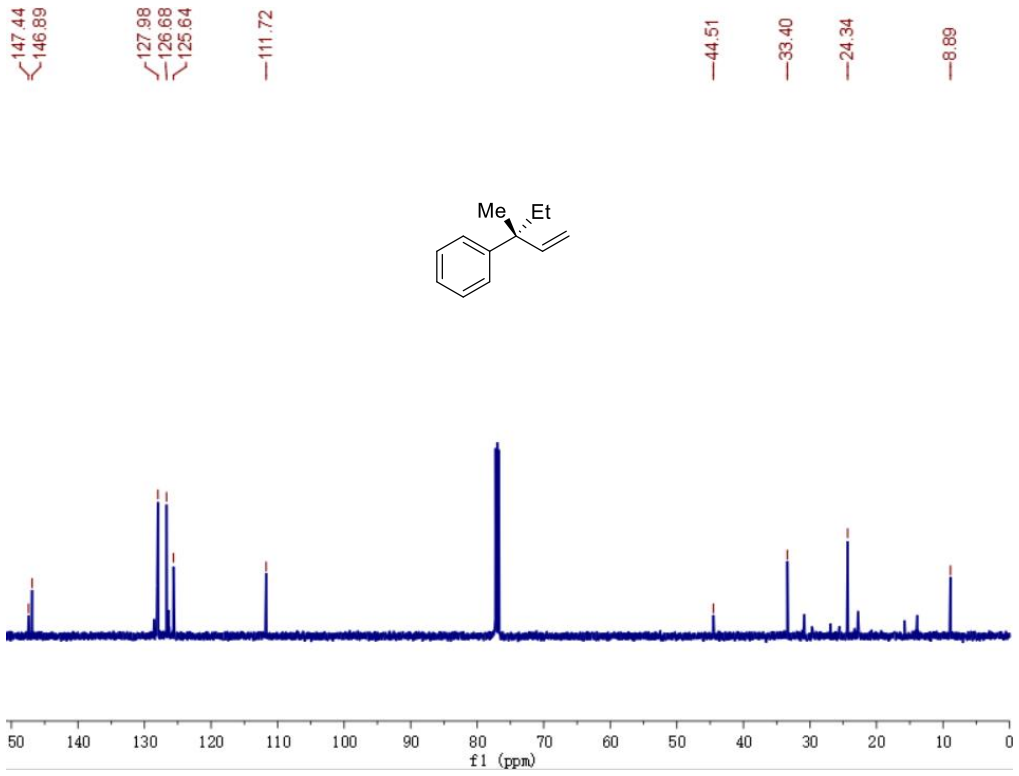

Figure S62: ^{13}C NMR (126 MHz, $CDCl_3$) spectrum of **3oa** and **4oa**

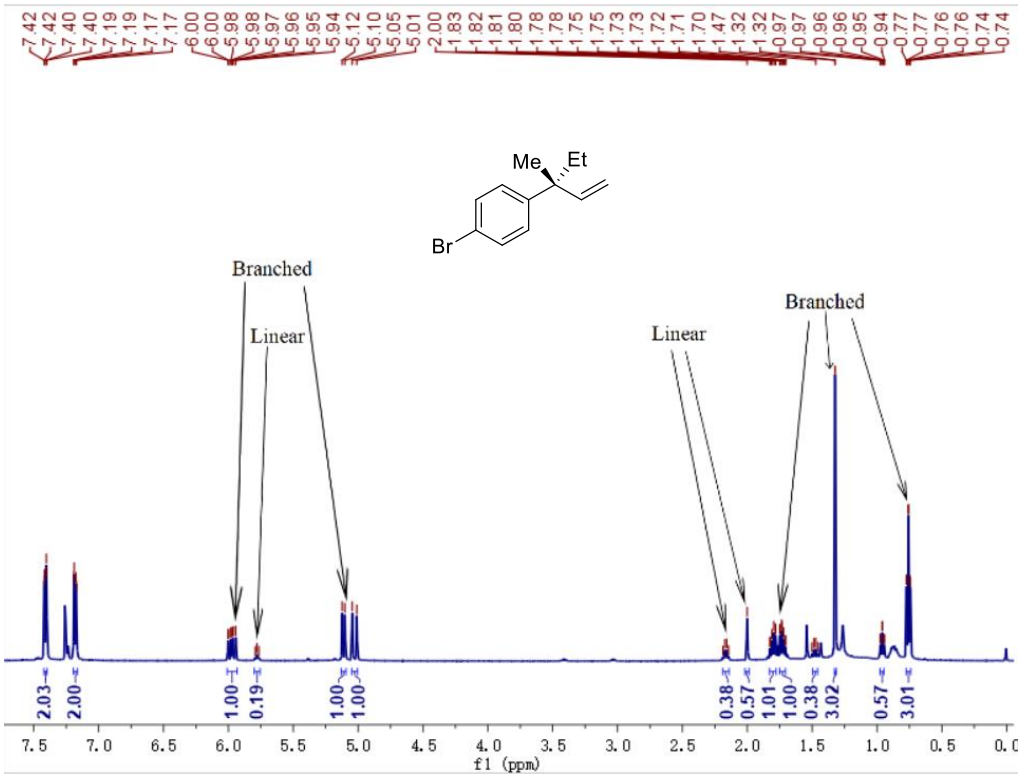

Figure S63: ^{1}H NMR (500 MHz, $CDCl_3$) spectrum of **3pa** and **4pa**

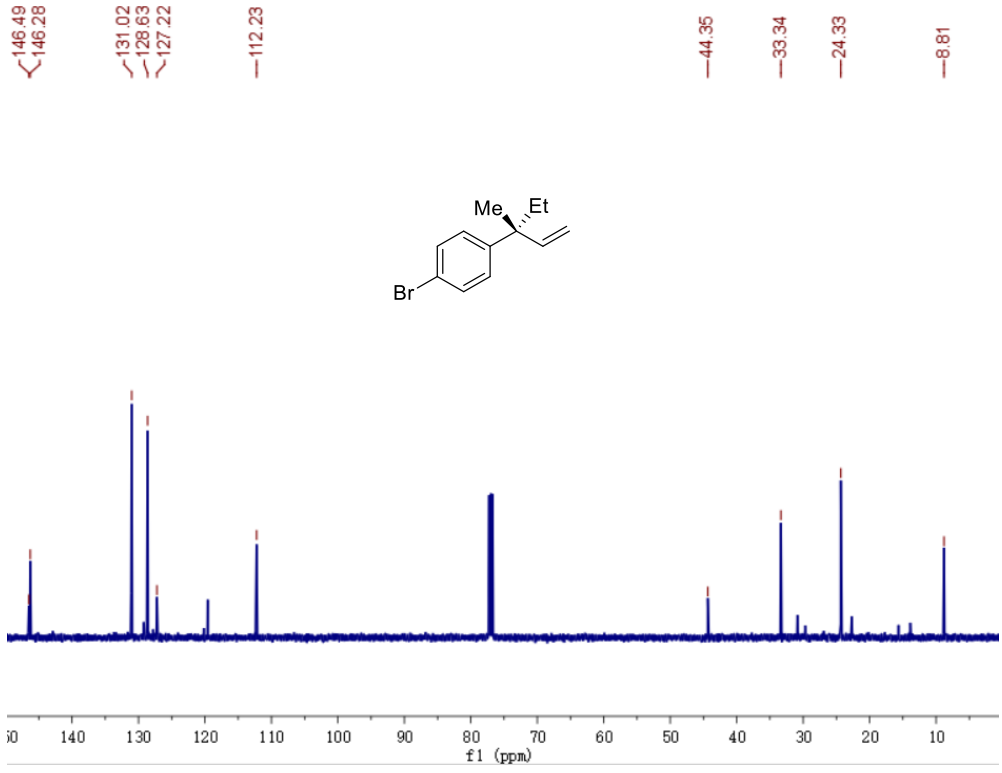

Figure S64: ^{13}C NMR (126 MHz, $CDCl_3$) spectrum of **3pa** and **4pa**

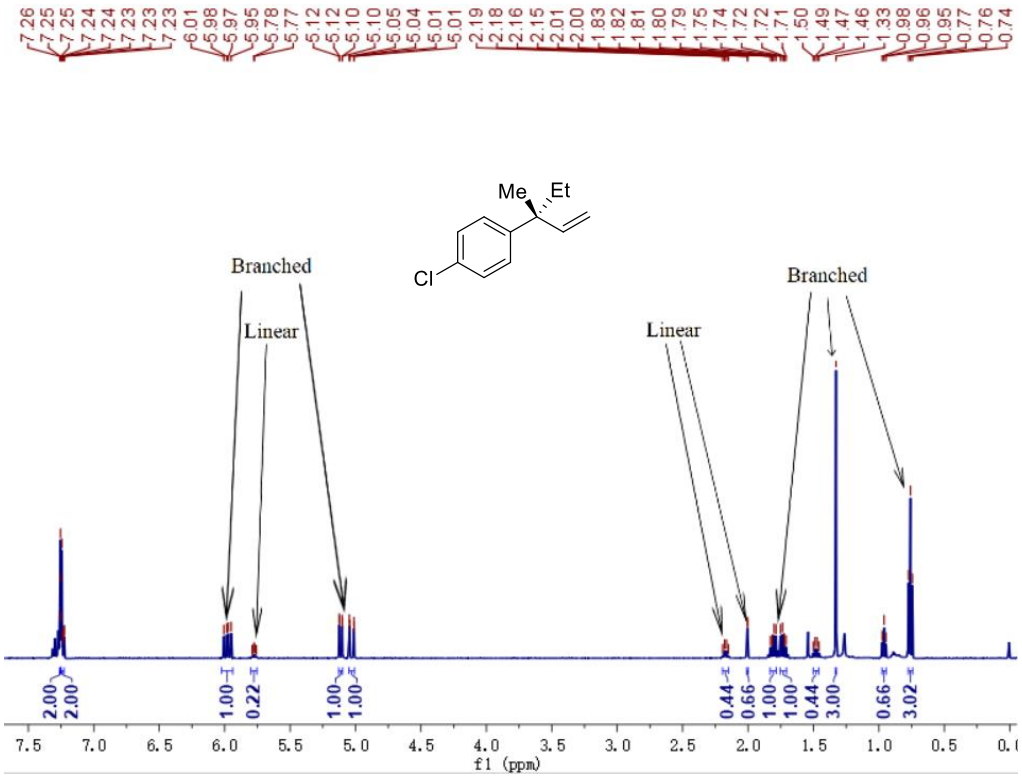

Figure S65: ^{1}H NMR (500 MHz, $CDCl_3$) spectrum of **3qa** and **4qa**

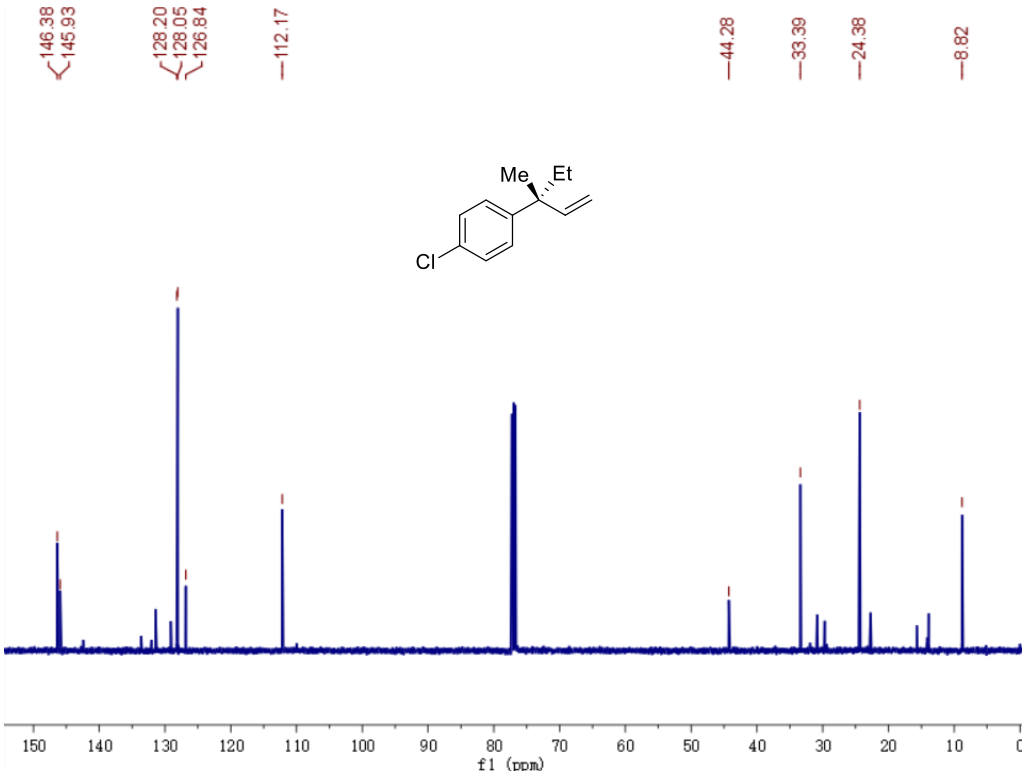

Figure S66: ^{13}C NMR (126 MHz, $CDCl_3$) spectrum of **3qa** and **4qa**

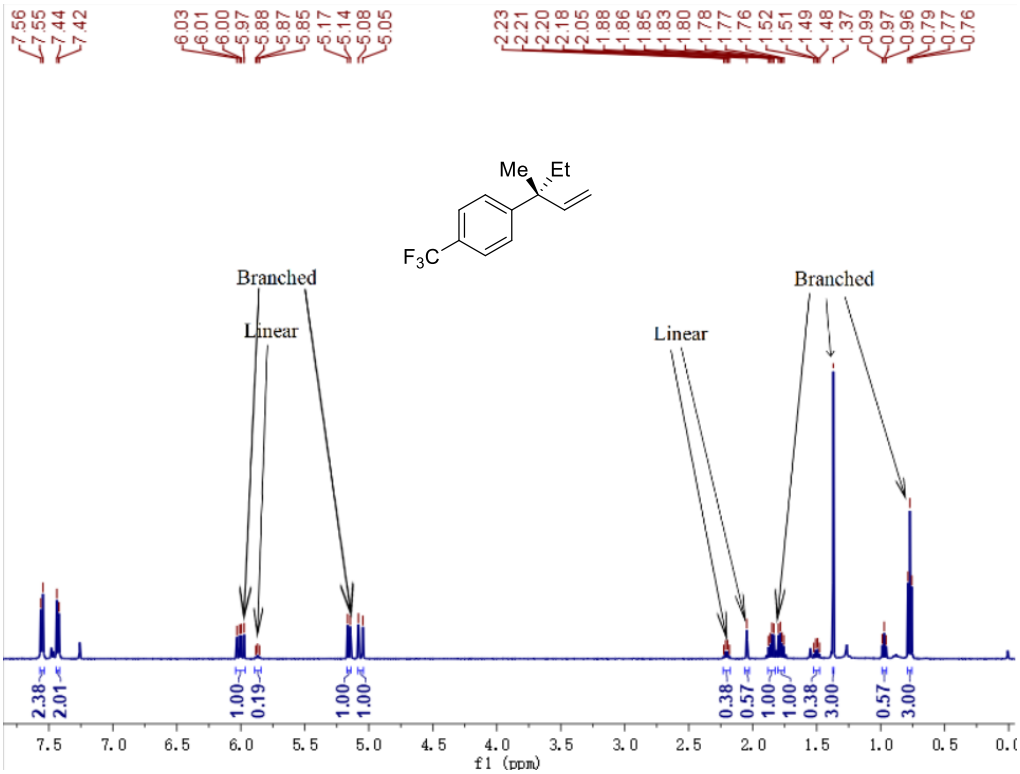

Figure S67: ^{1}H NMR (500 MHz, $CDCl_3$) spectrum of **3ra** and **4ra**

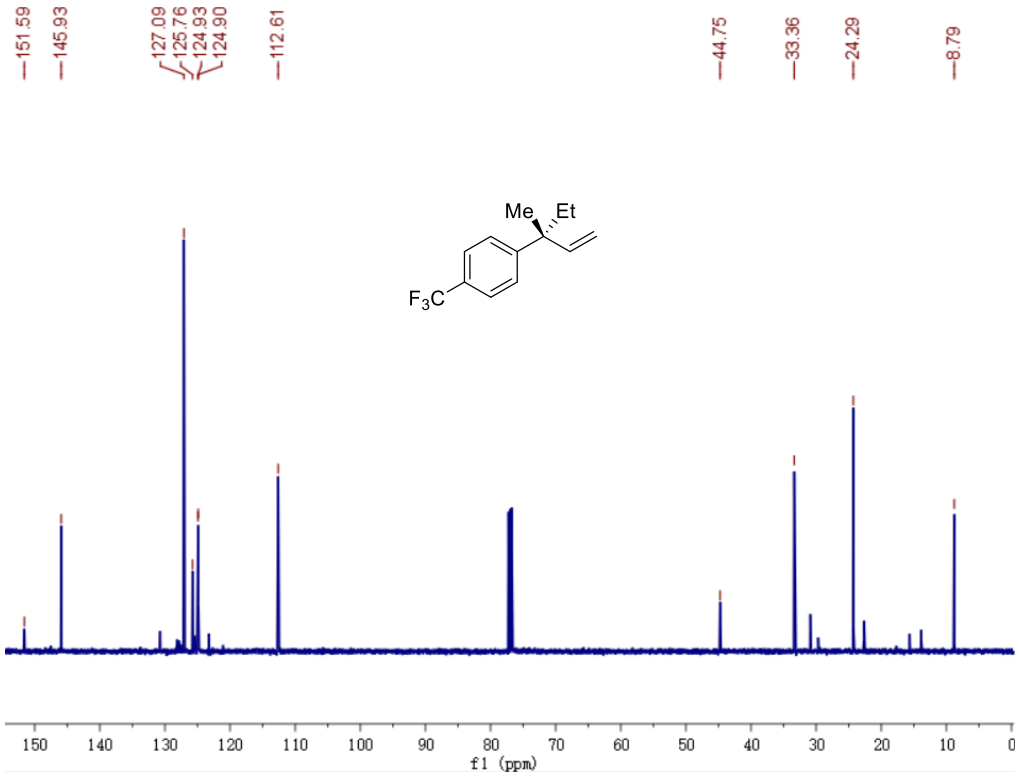

Figure S68: ^{13}C NMR (126 MHz, $CDCl_3$) spectrum of **3ra** and **4ra**

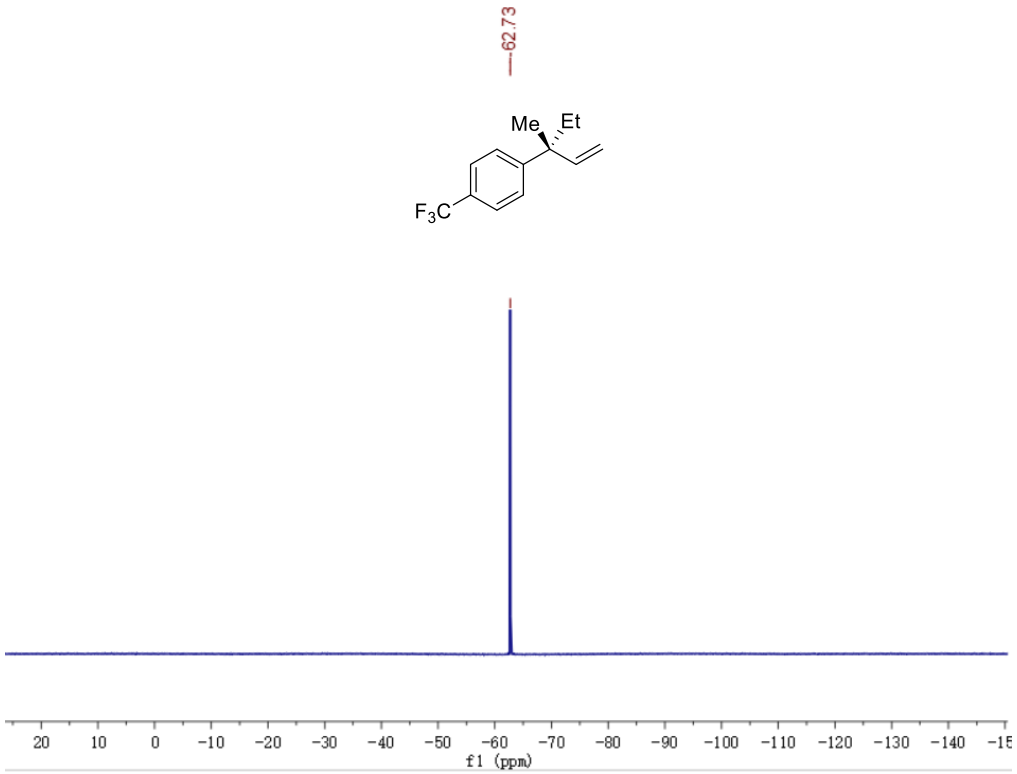

Figure S69: ^{19}F NMR (282 MHz, $CDCl_3$) spectrum of **3ra** and **4ra**

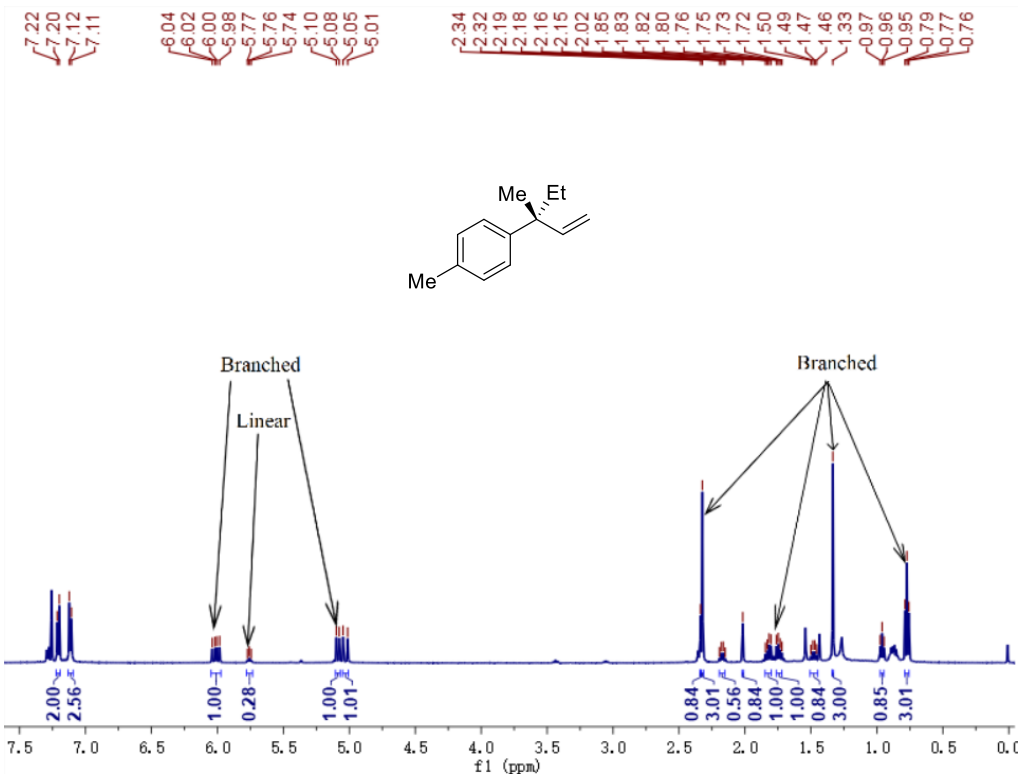

Figure S70: ^{1}H NMR (500 MHz, $CDCl_3$) spectrum of **3sa** and **4sa**

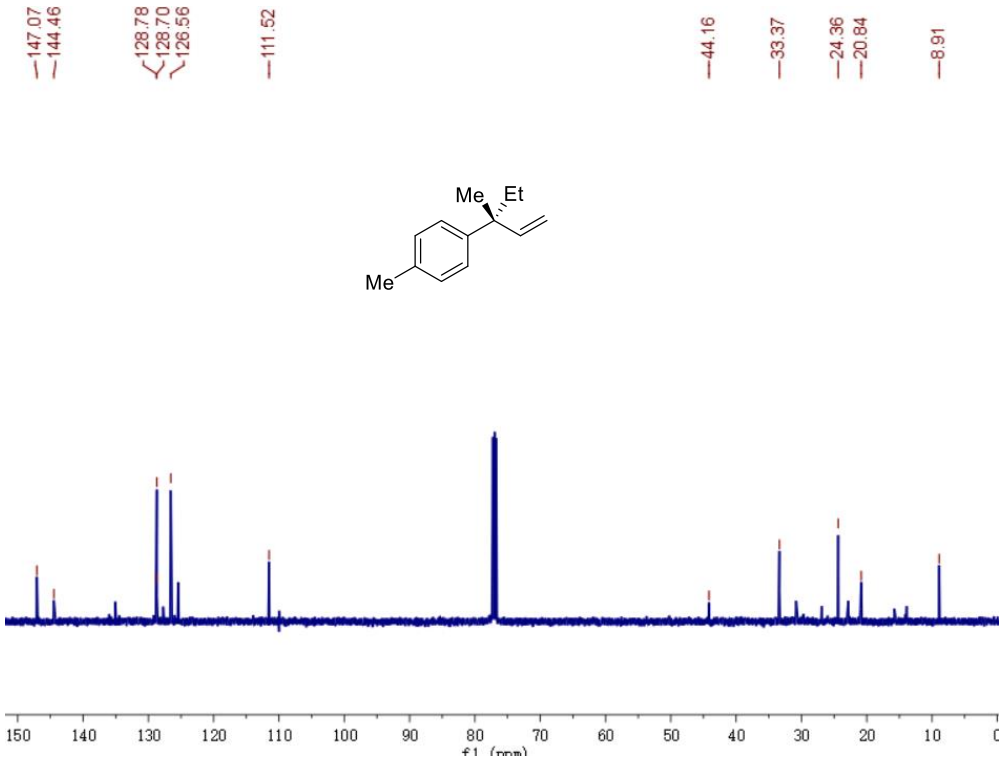

Figure S71: ^{13}C NMR (126 MHz, $CDCl_3$) spectrum of **3sa** and **4sa**

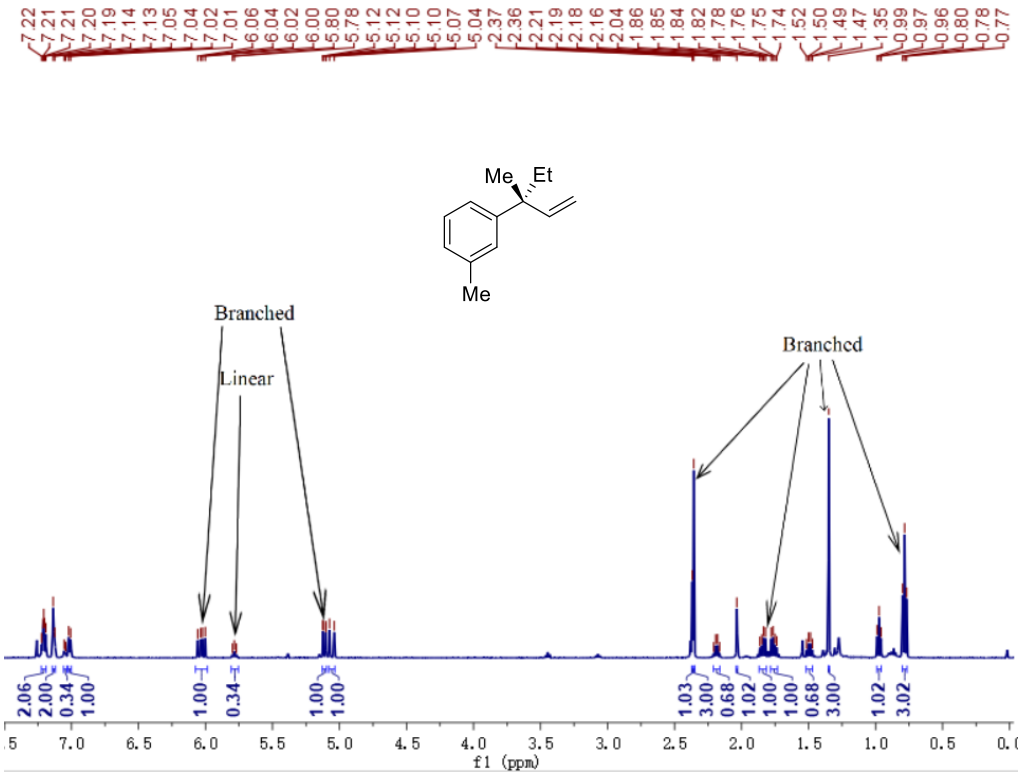

Figure S72: ^{1}H NMR (500 MHz, $CDCl_3$) spectrum of **3ta** and **4ta**

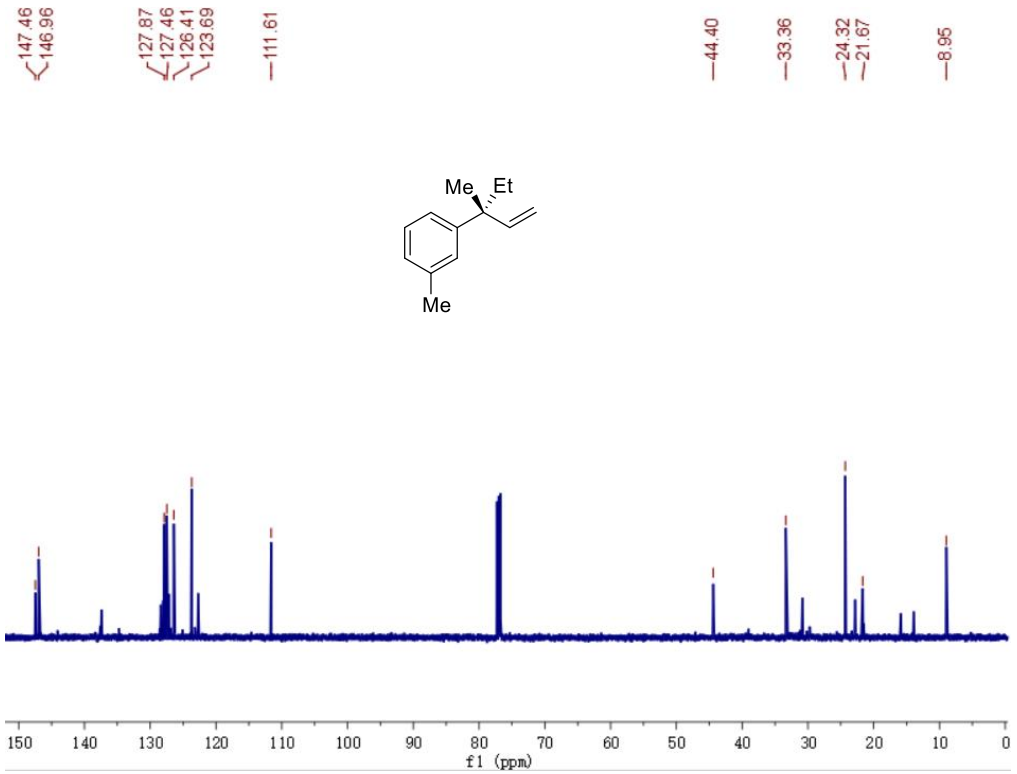

Figure S73: ^{13}C NMR (126 MHz, $CDCl_3$) spectrum of **3ta** and **4ta**

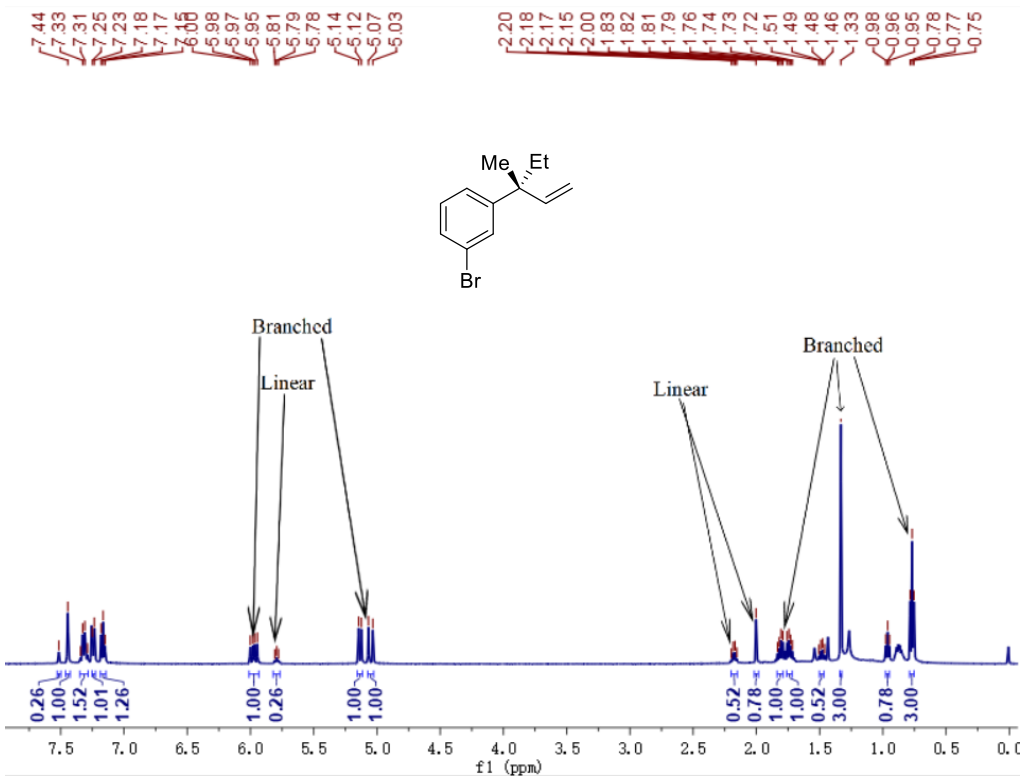

Figure S74: ^{1}H NMR (500 MHz, $CDCl_3$) spectrum of **3ua** and **4ua**

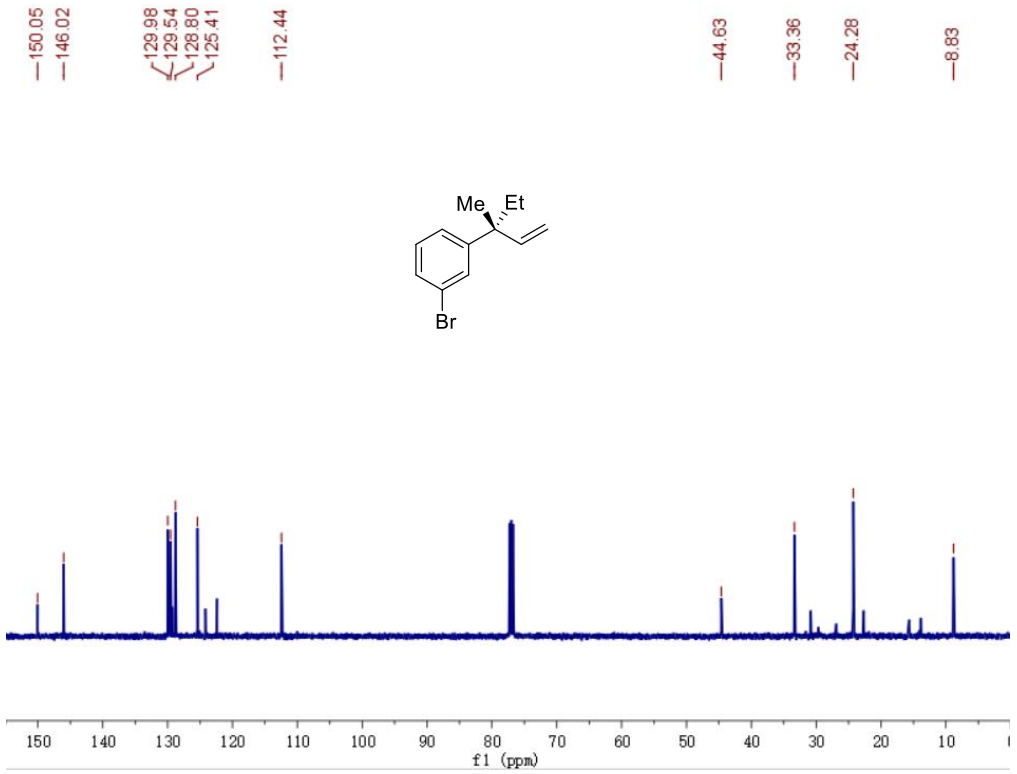

Figure S75: ^{13}C NMR (126 MHz, $CDCl_3$) spectrum of **3ua** and **4ua**

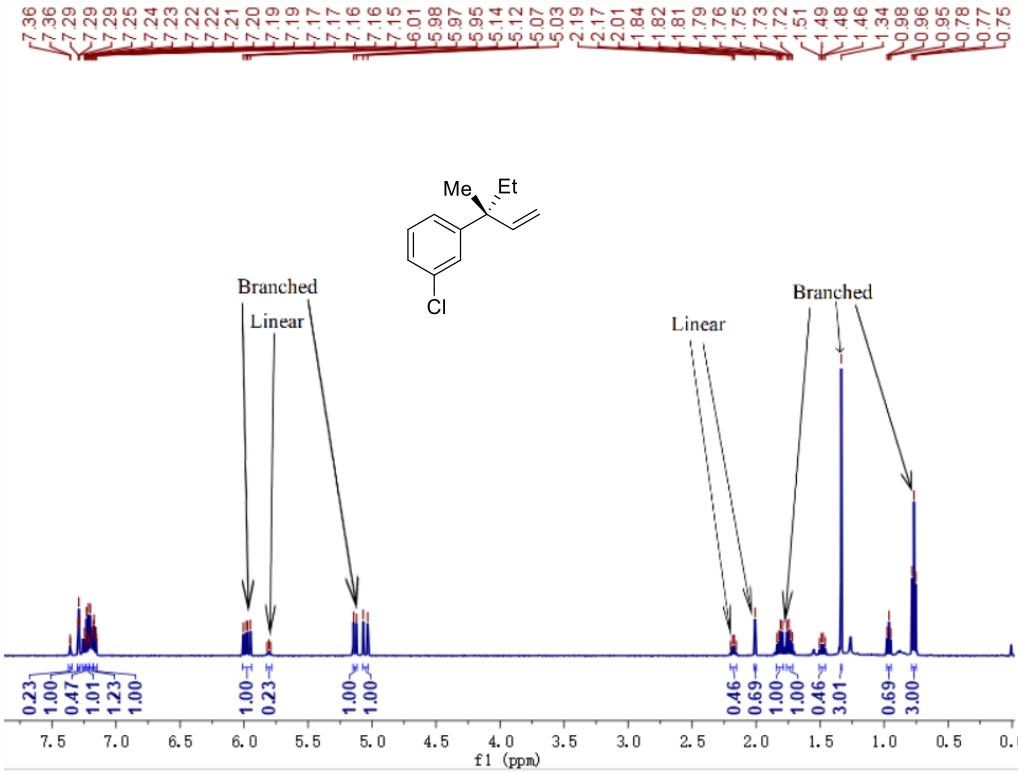

Figure S76: ^{1}H NMR (500 MHz, $CDCl_3$) spectrum of **3va** and **4va**

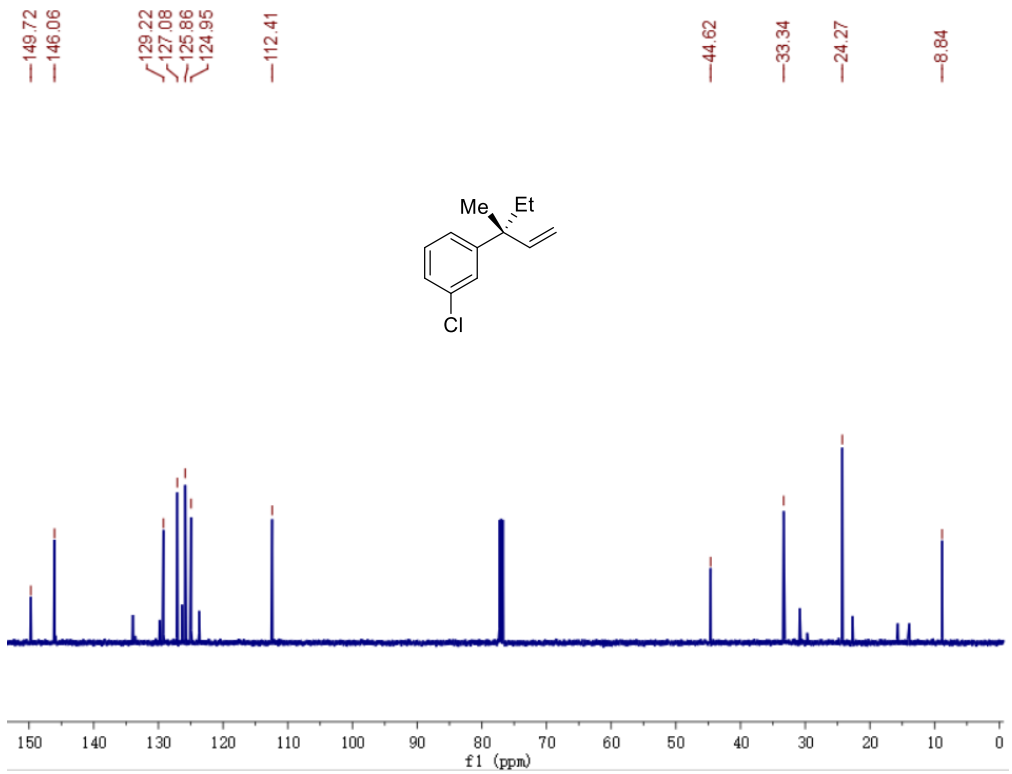

Figure S77: ^{13}C NMR (126 MHz, $CDCl_3$) spectrum of **3va** and **4va**

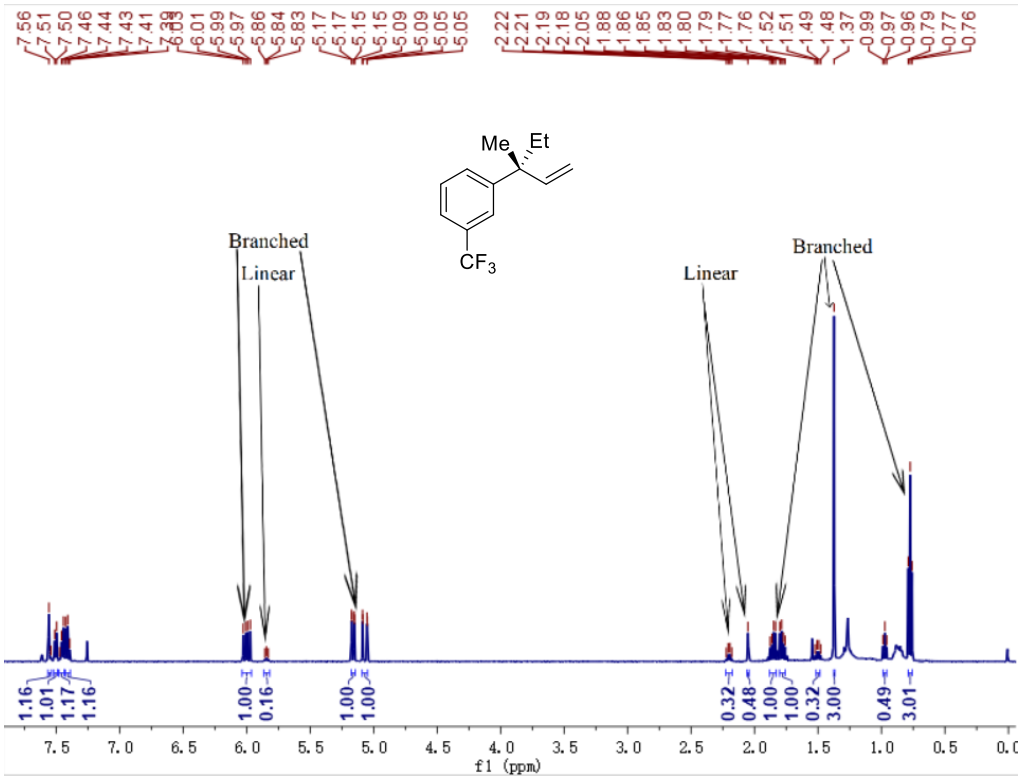

Figure S78: ^{1}H NMR (500 MHz, $CDCl_3$) spectrum of **3wa** and **4wa**

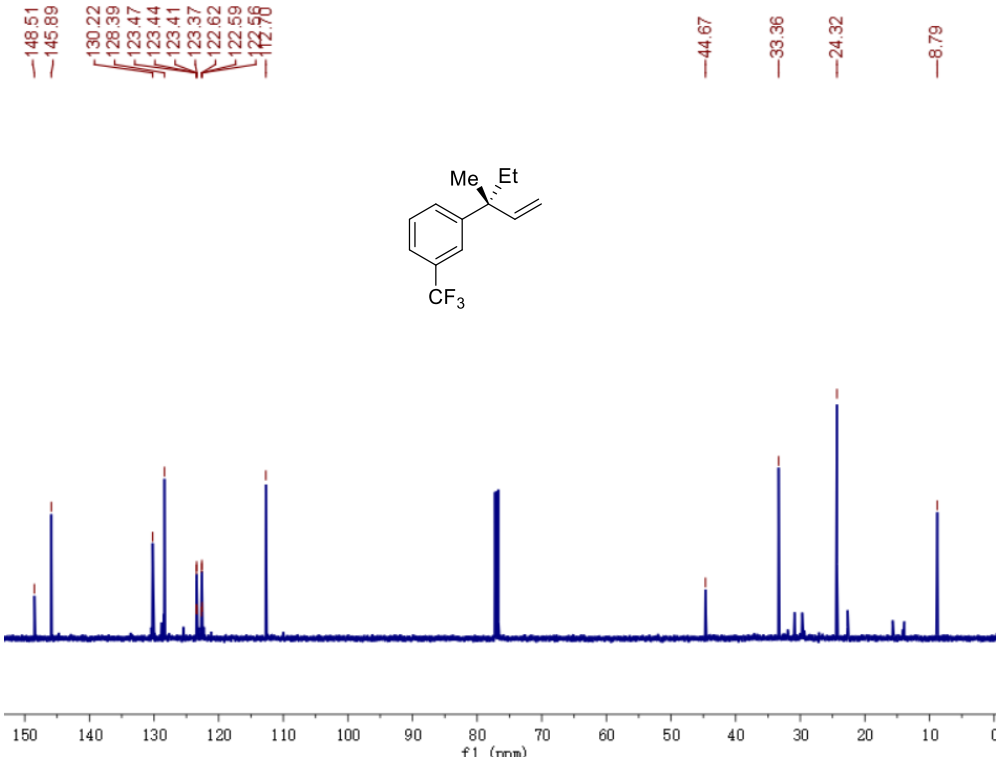

Figure S79: ^{13}C NMR (126 MHz, $CDCl_3$) spectrum of **3wa** and **4wa**

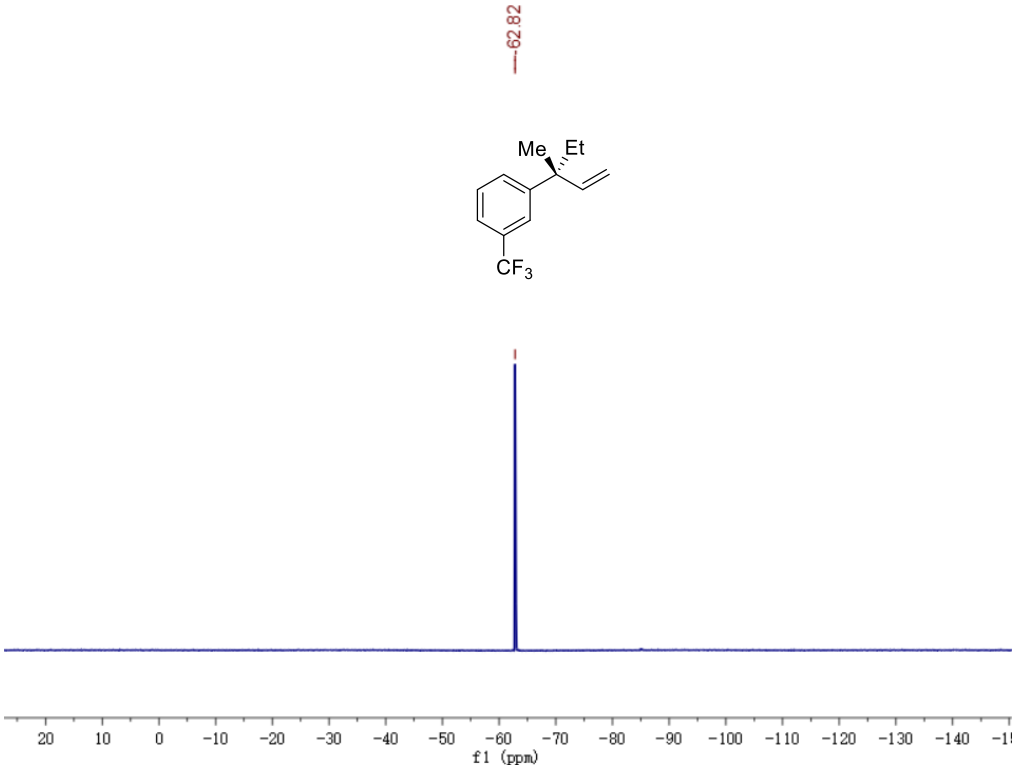

Figure S80: ^{19}F NMR (282 MHz, $CDCl_3$) spectrum of **3wa** and **4wa**

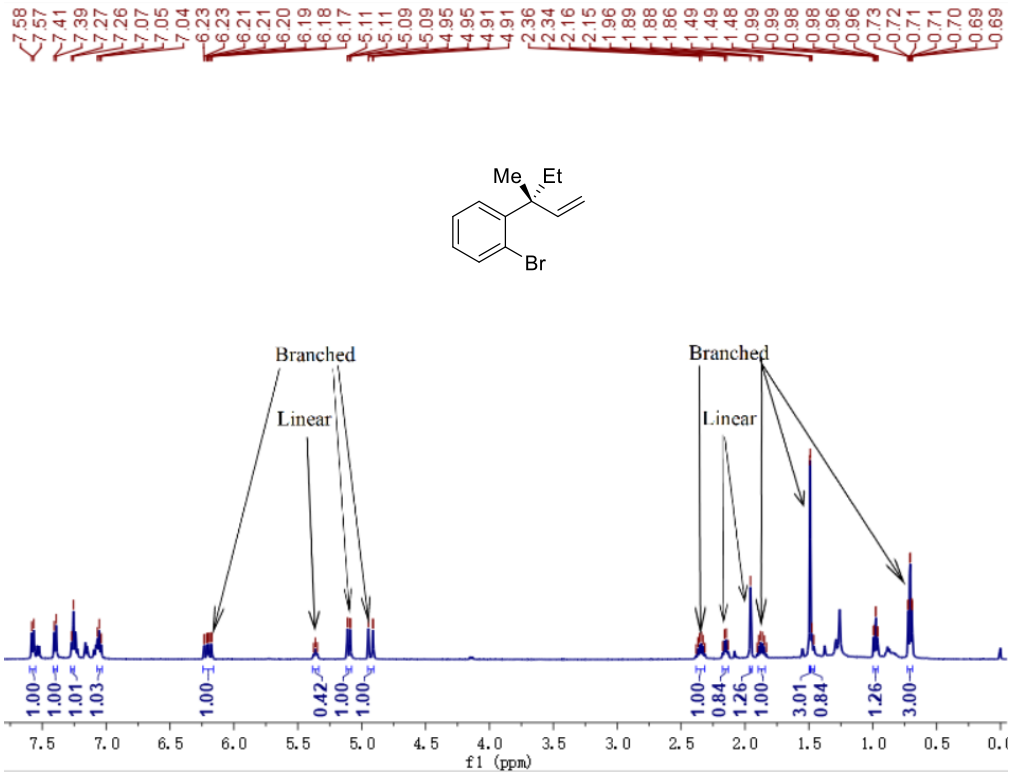

Figure S81: ^{1}H NMR (500 MHz, $CDCl_3$) spectrum of **3xa** and **4xa**

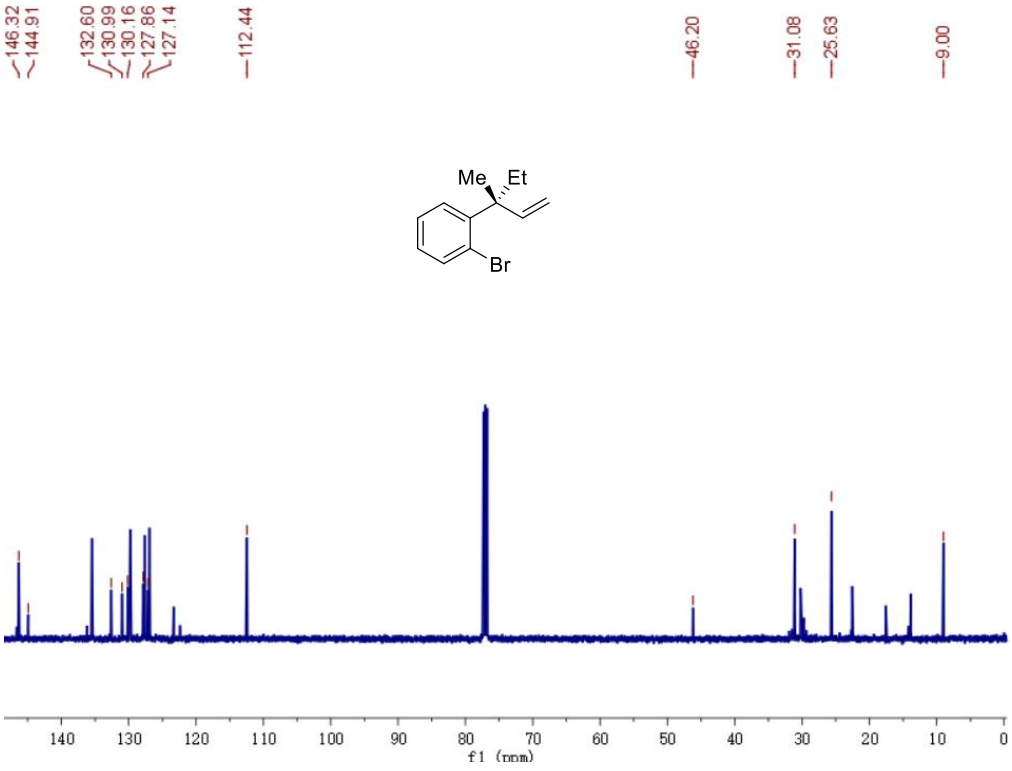

Figure S82: ^{13}C NMR (126 MHz, $CDCl_3$) spectrum of **3xa** and **4xa**

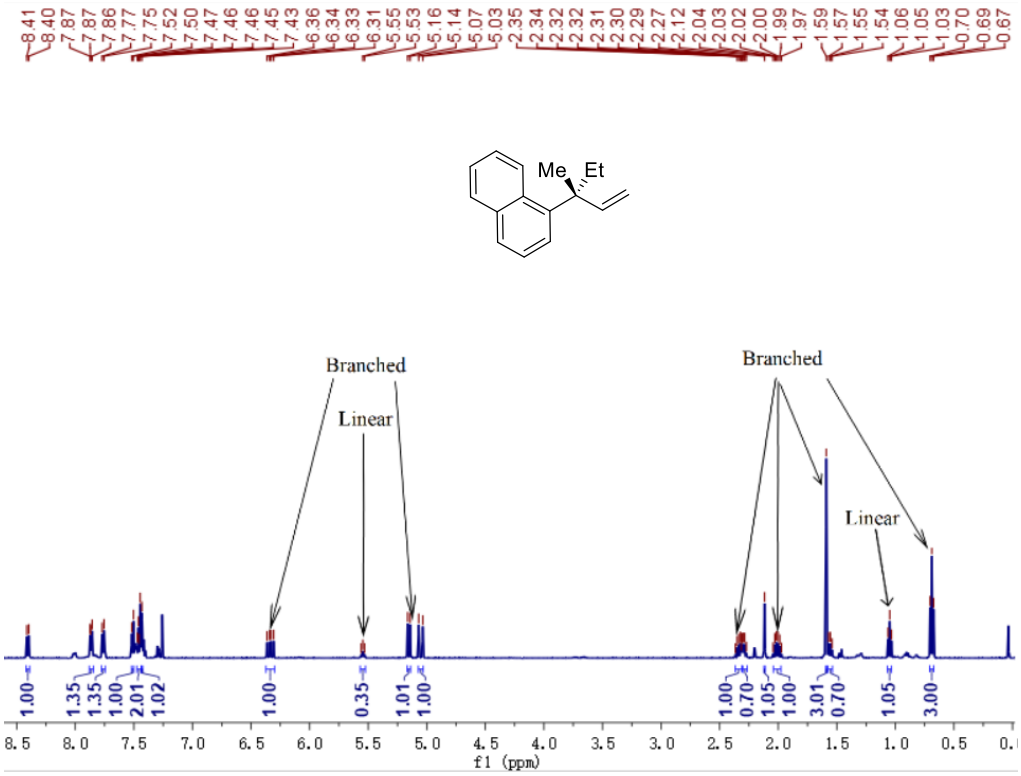

Figure S83: ^{1}H NMR (500 MHz, $CDCl_3$) spectrum of **3ya** and **4ya**

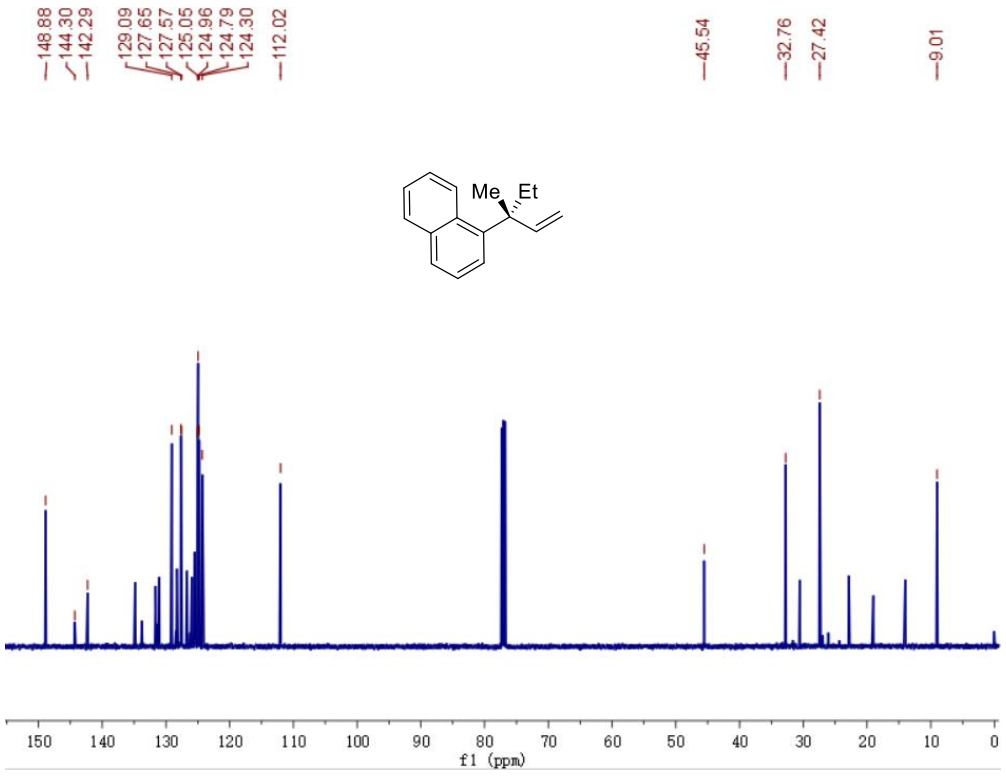

Figure S84: ^{13}C NMR (126 MHz, $CDCl_3$) spectrum of **3ya** and **4ya**

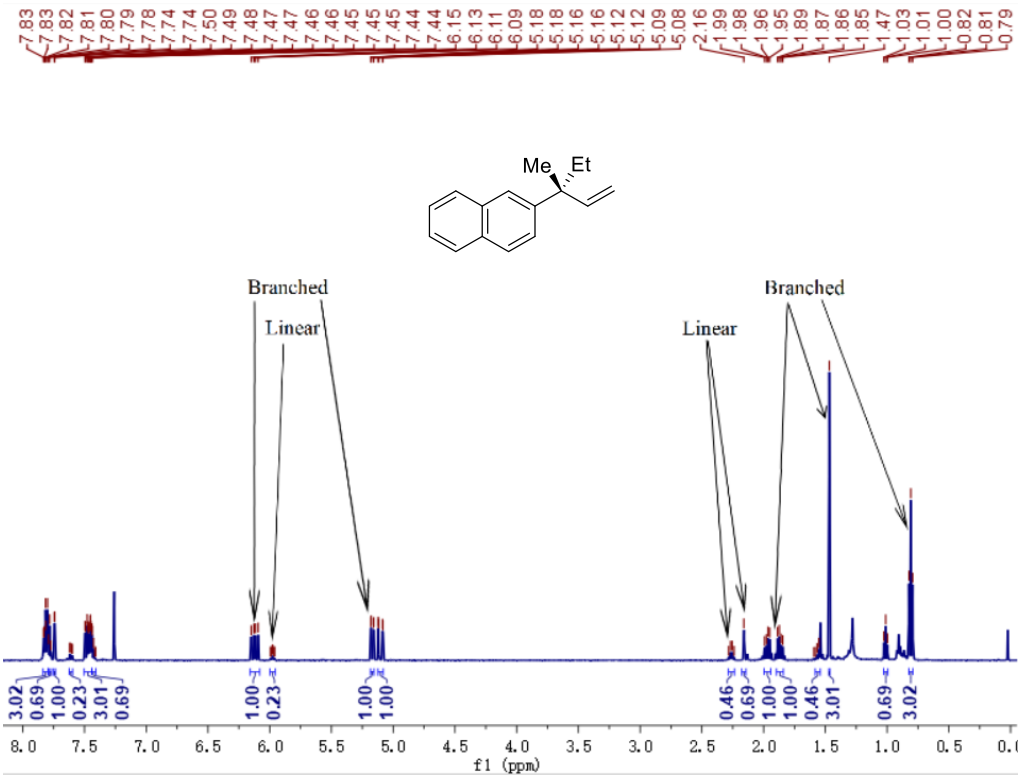

Figure S85: ^{1}H NMR (500 MHz, $CDCl_3$) spectrum of **3za** and **4za**

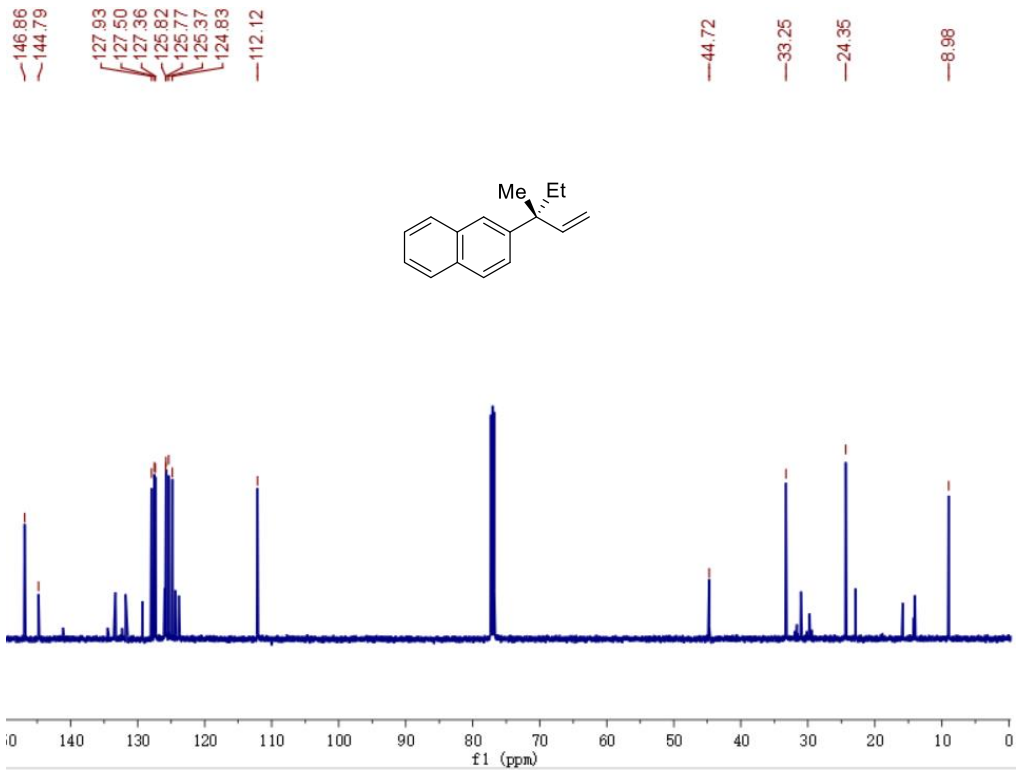

Figure S86: ^{13}C NMR (126 MHz, $CDCl_3$) spectrum of **3za** and **4za**

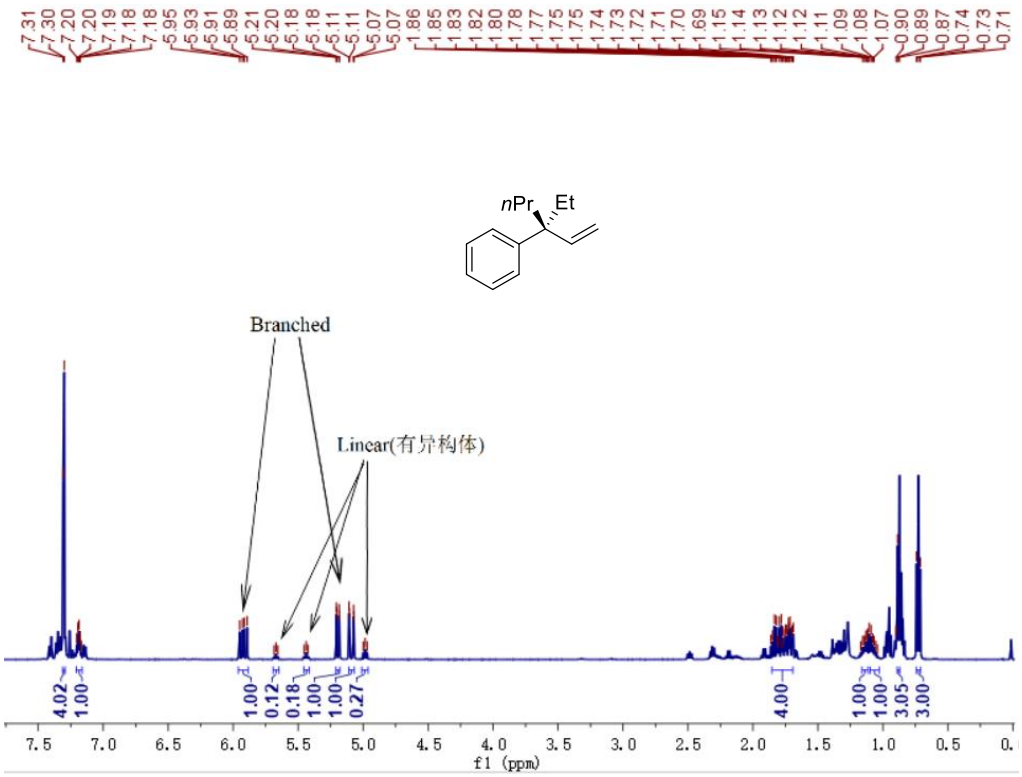

Figure S87: ^{1}H NMR (500 MHz, $CDCl_3$) spectrum of **3x'a** and **4x'a**

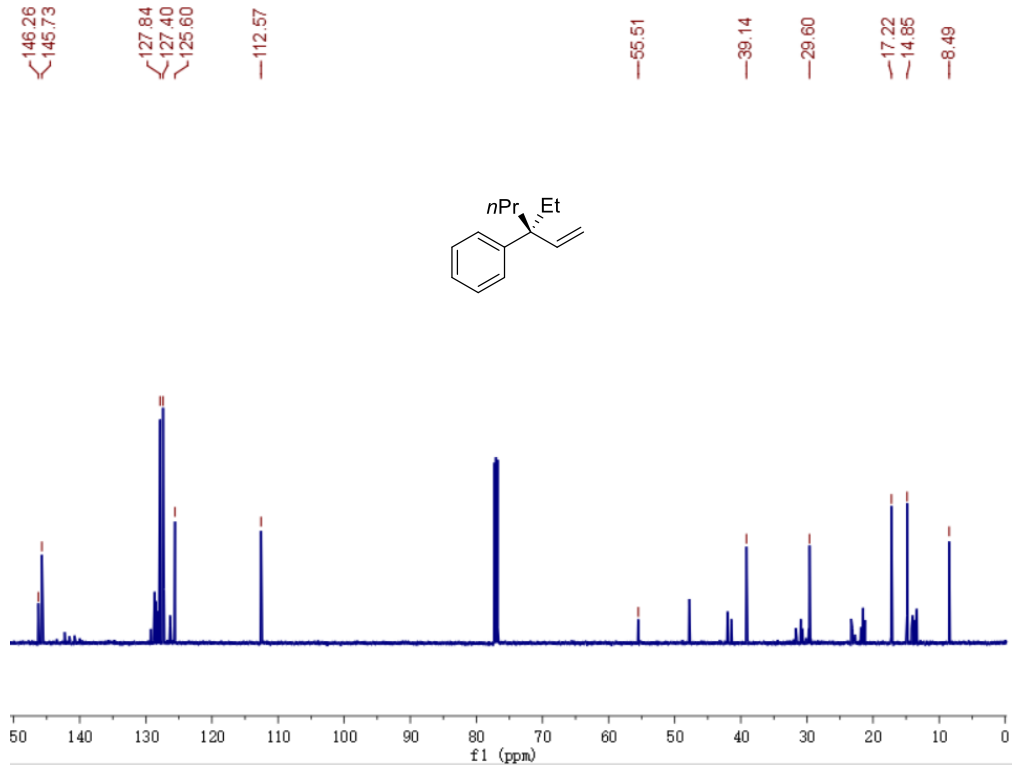

Figure S88: ^{13}C NMR (126 MHz, $CDCl_3$) spectrum of **3x'a** and **4x'a**

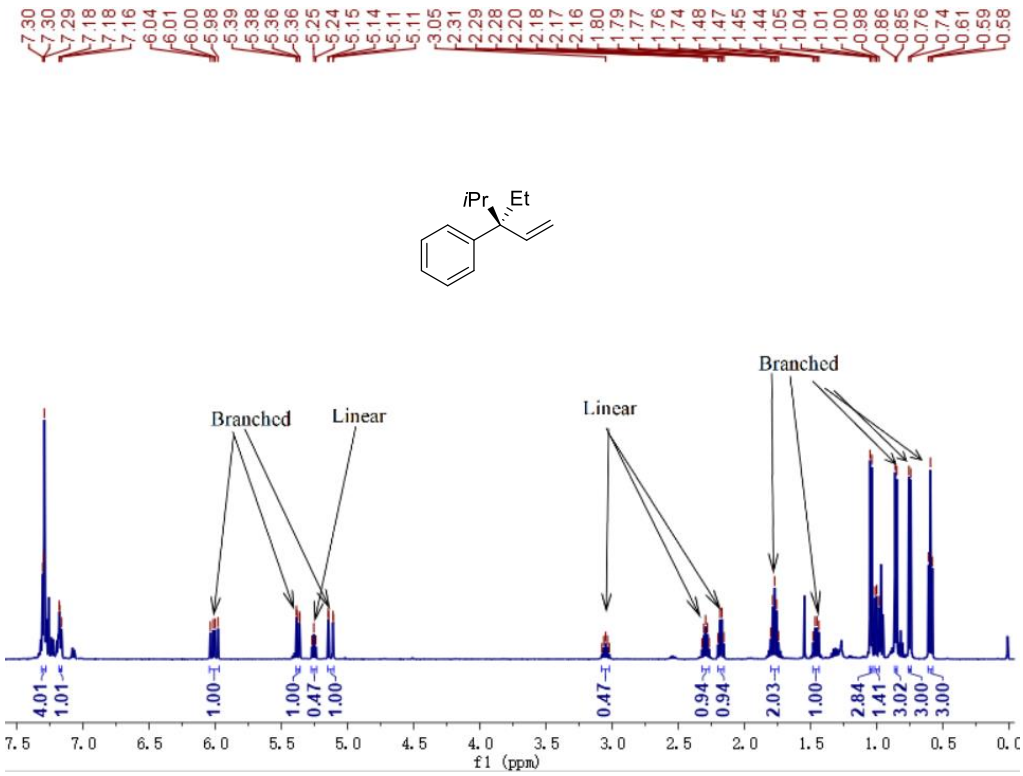

Figure S89: ^{1}H NMR (500 MHz, $CDCl_3$) spectrum of **3y'a** and **4y'a**

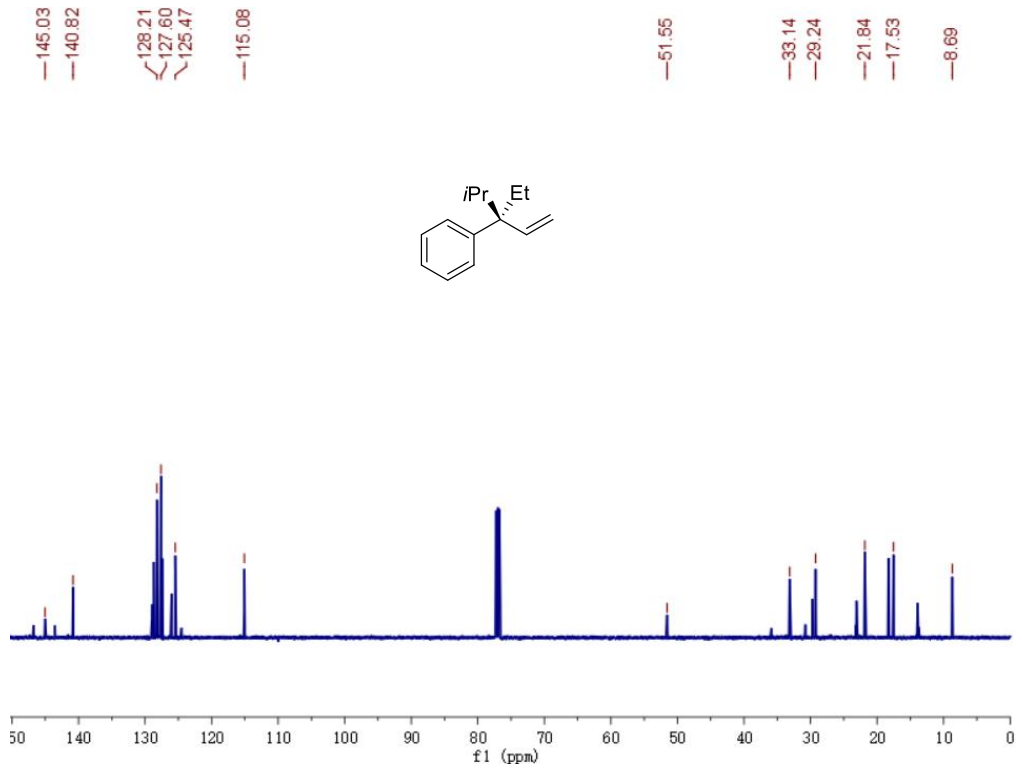

Figure S90: ^{13}C NMR (126 MHz, $CDCl_3$) spectrum of **3y'a** and **4y'a**

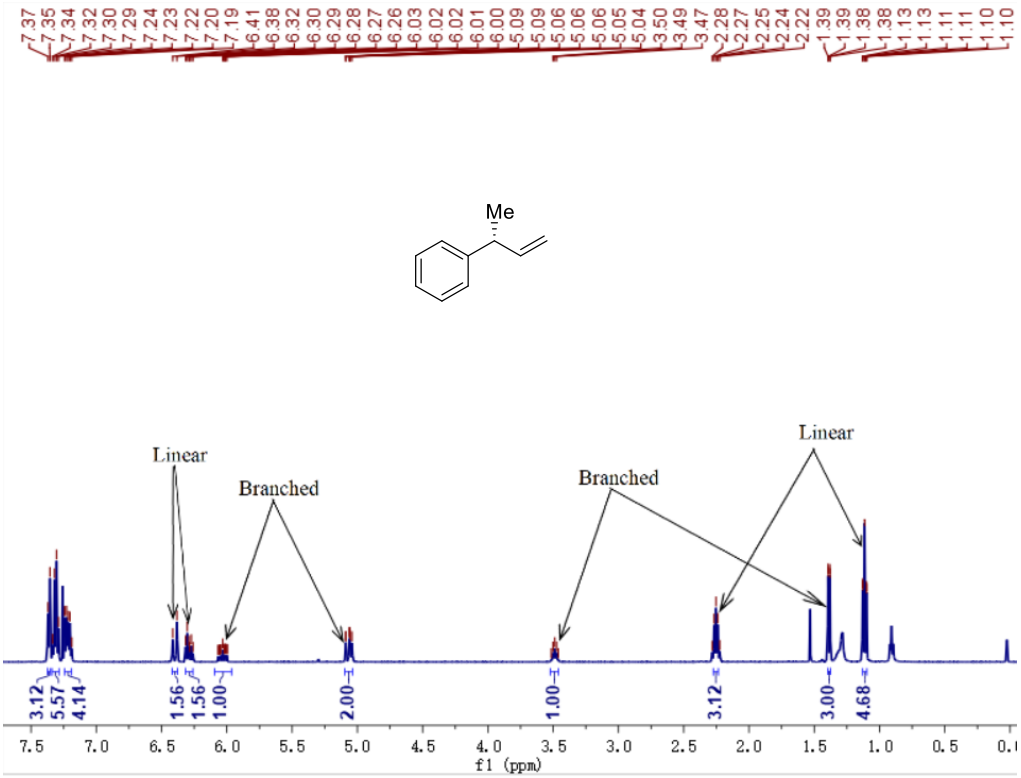

Figure S91: ^{1}H NMR (500 MHz, $CDCl_3$) spectrum of **3ab** and **4ab**

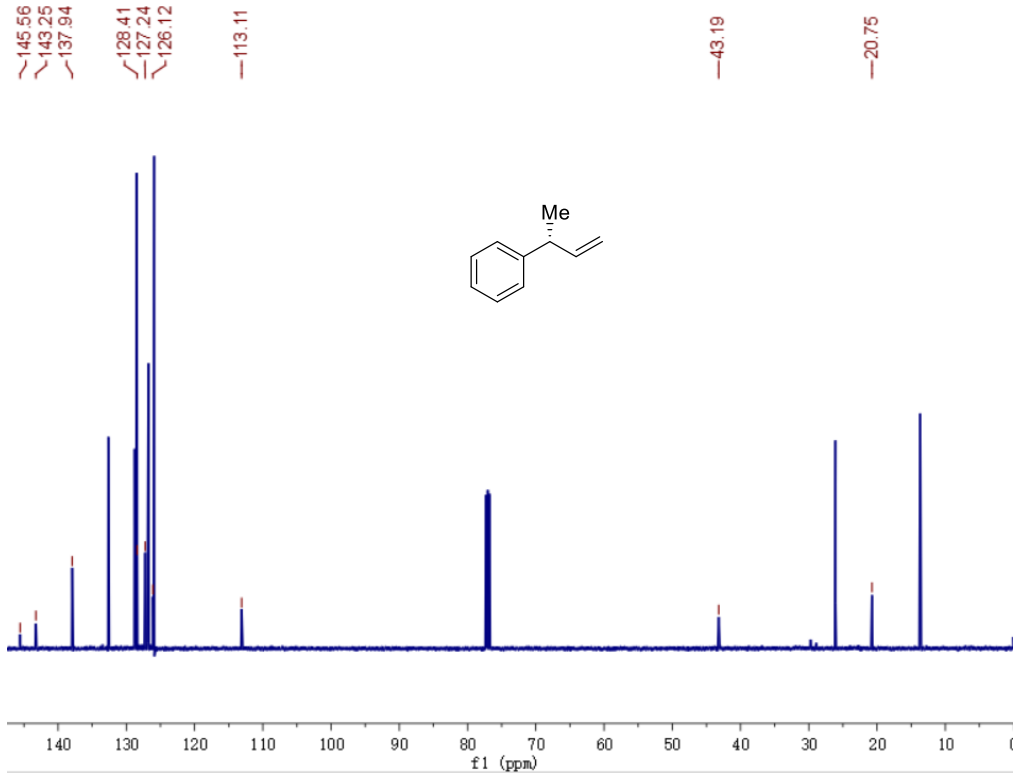

Figure S92: ^{13}C NMR (126 MHz, $CDCl_3$) spectrum of **3ab** and **4ab**

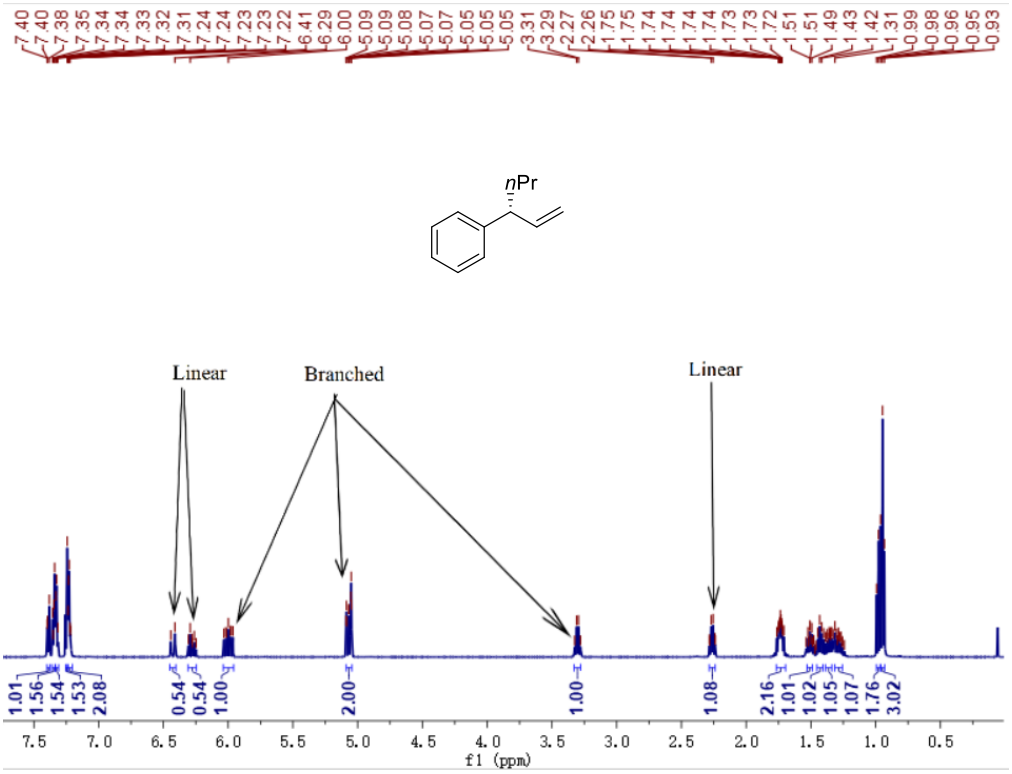

Figure S93: ^{1}H NMR (500 MHz, $CDCl_3$) spectrum of **3ac** and **4ac**

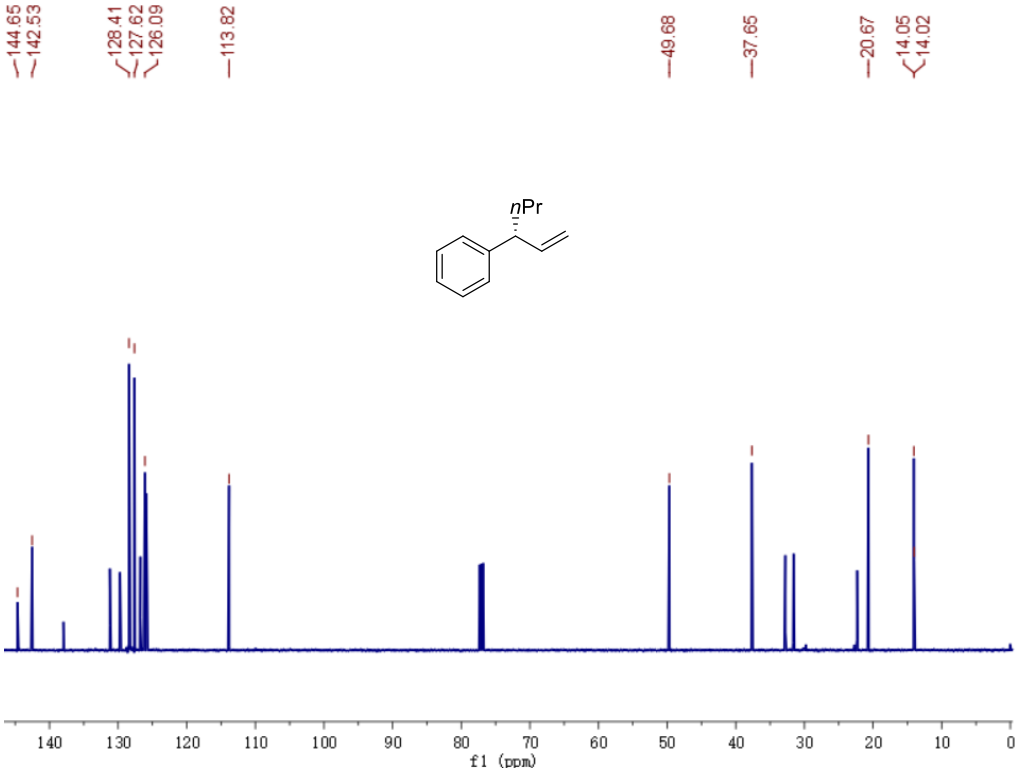

Figure S94: ^{13}C NMR (126 MHz, $CDCl_3$) spectrum of **3ac** and **4ac**

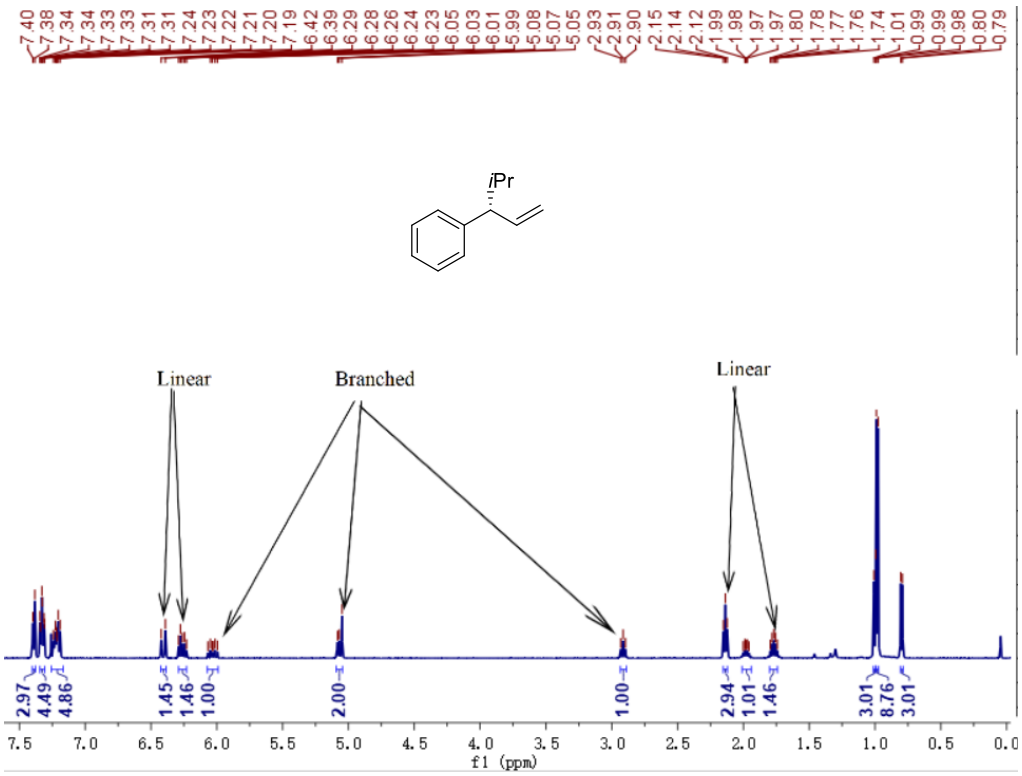

Figure S95: ^{1}H NMR (500 MHz, $CDCl_3$) spectrum of **3ad** and **4ad**

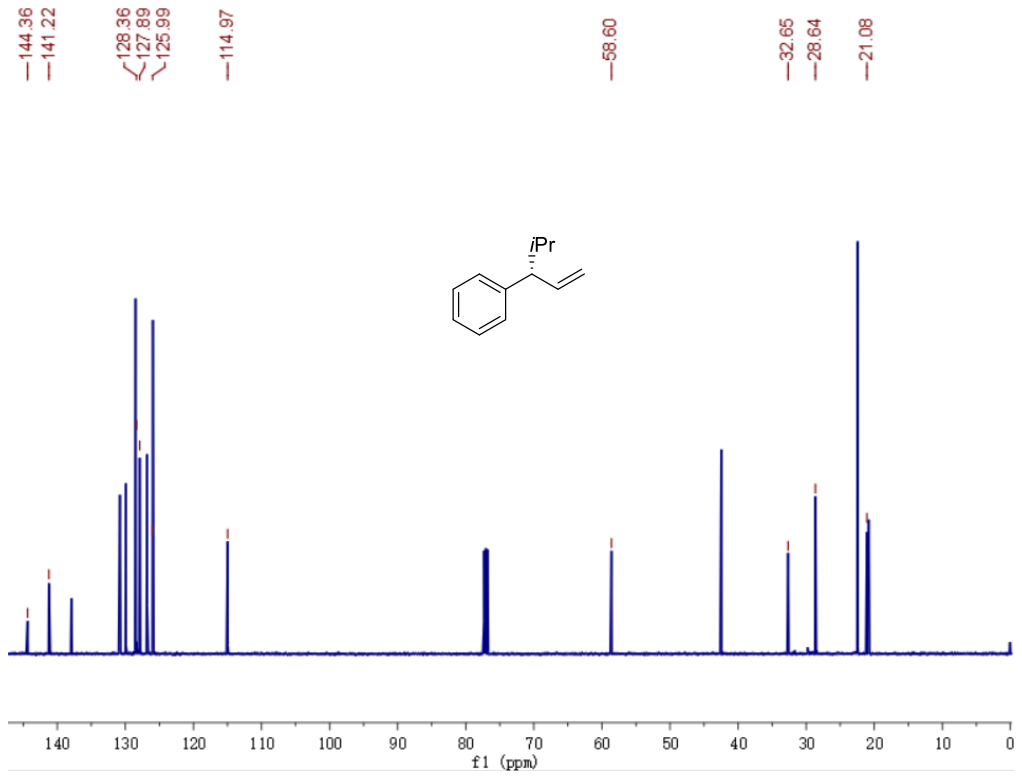

Figure S96: ^{13}C NMR (126 MHz, $CDCl_3$) spectrum of **3ad** and **4ad**

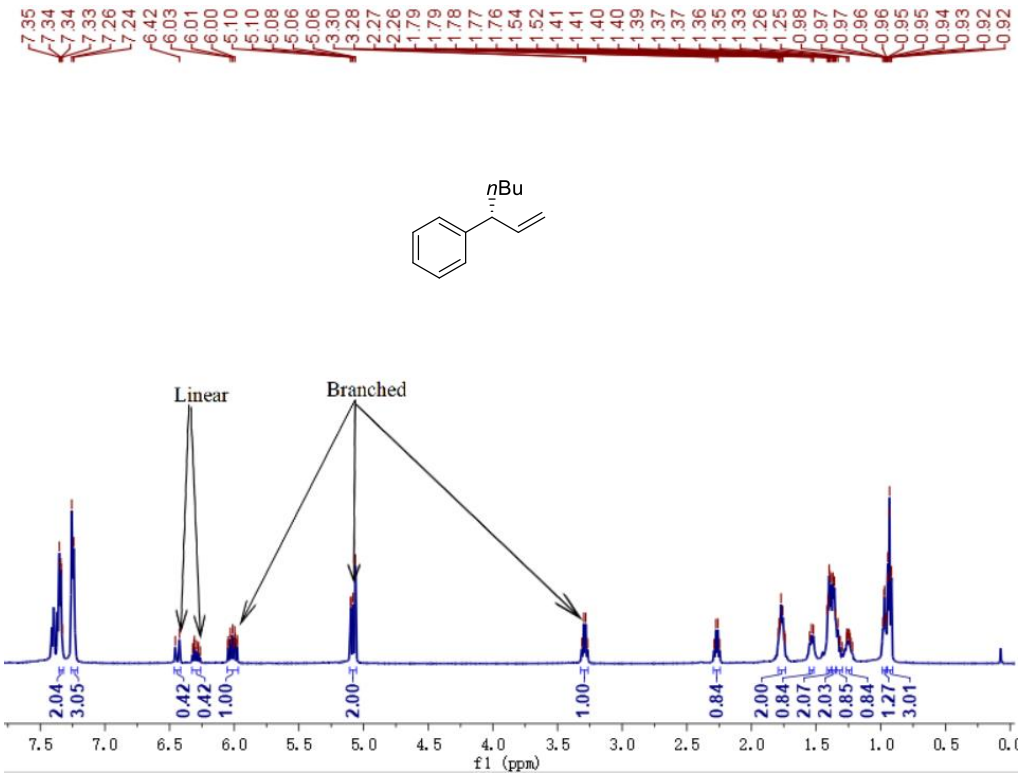

Figure S97: ^{1}H NMR (500 MHz, $CDCl_3$) spectrum of **3ae** and **4ae**

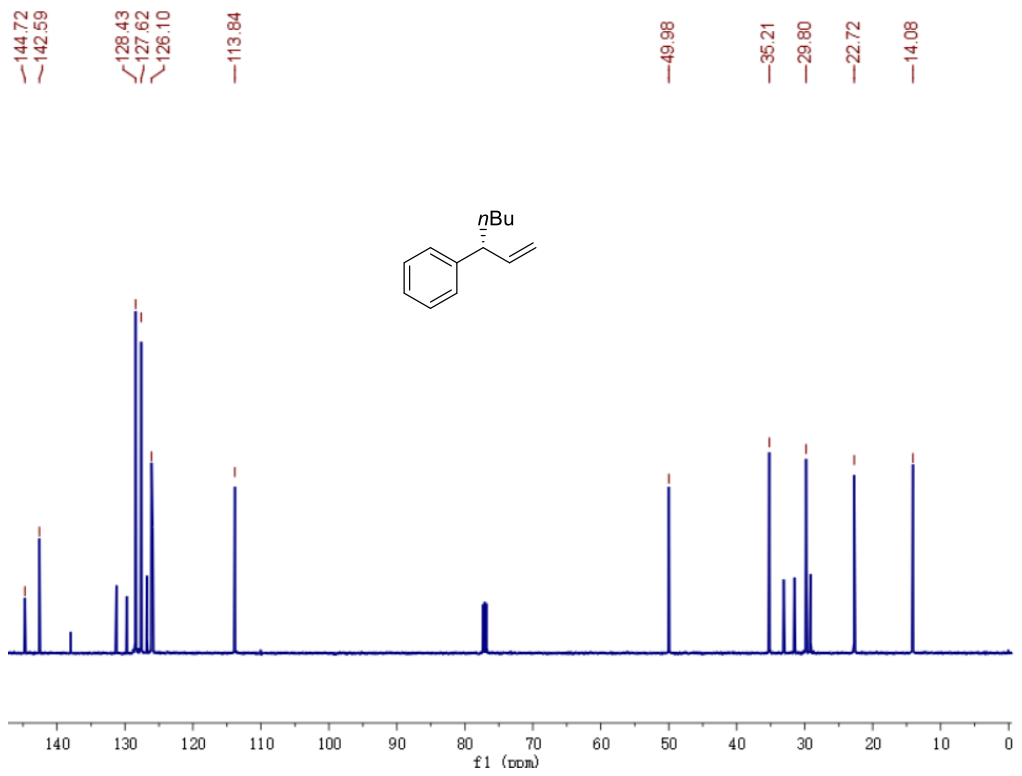

Figure S98: ^{13}C NMR (126 MHz, $CDCl_3$) spectrum of **3ae** and **4ae**

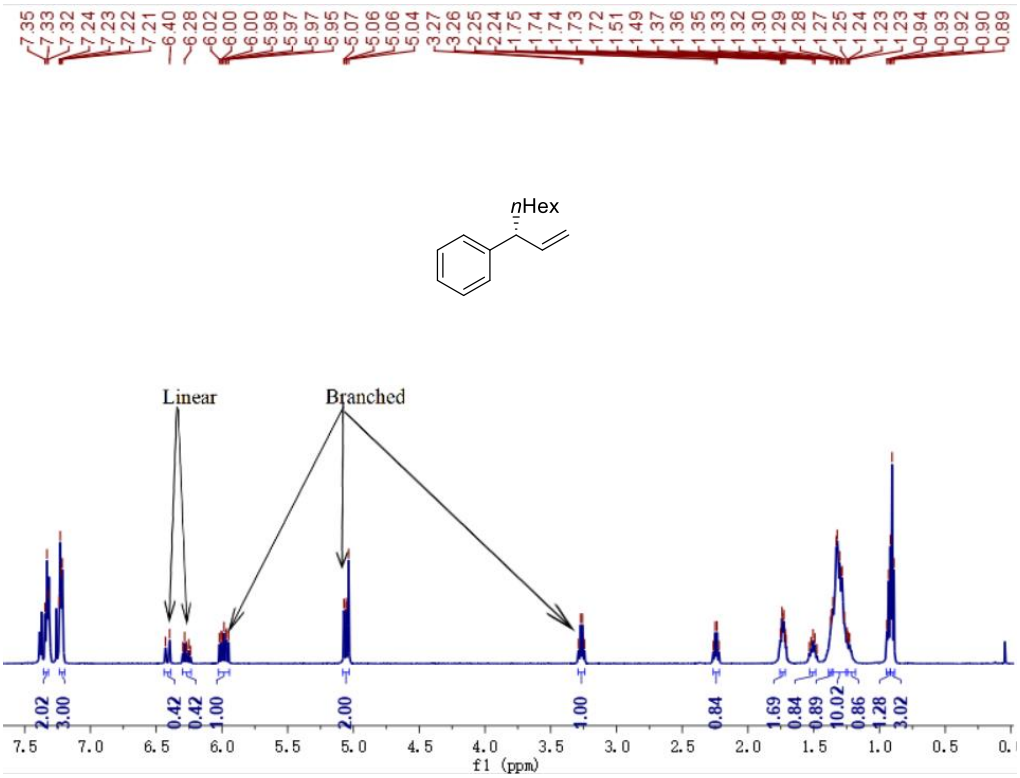

Figure S99: ^{1}H NMR (500 MHz, $CDCl_3$) spectrum of **3af** and **4af**

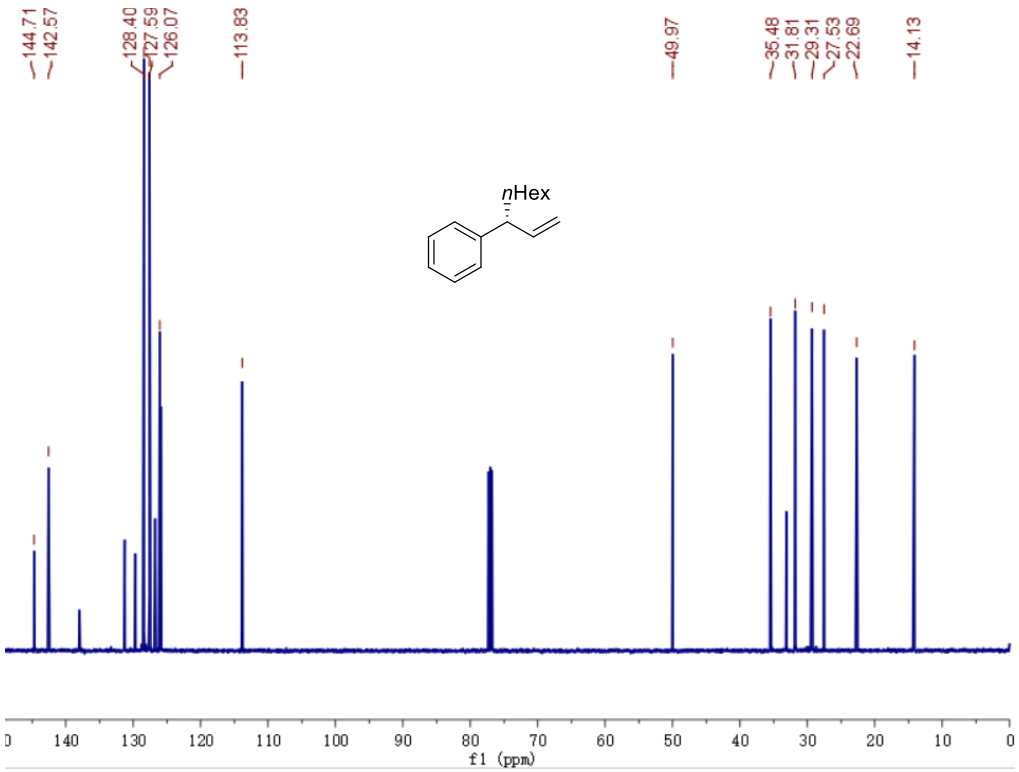

Figure S100: ^{13}C NMR (126 MHz, $CDCl_3$) spectrum of **3af** and **4af**

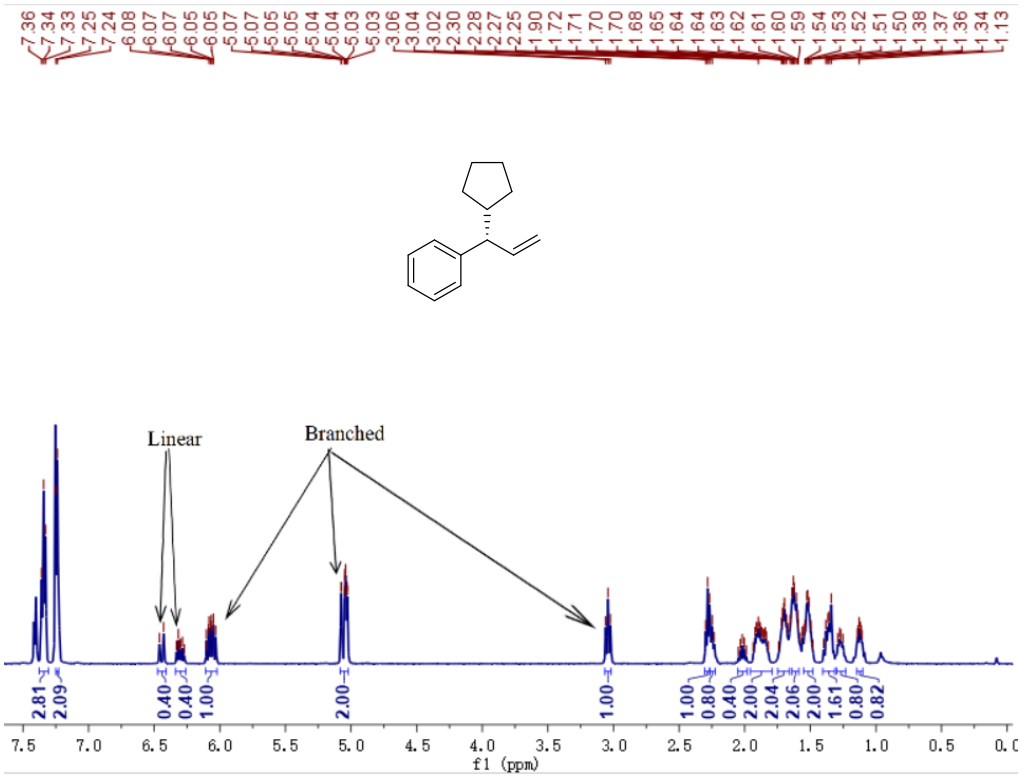

Figure S101: ^{1}H NMR (500 MHz, $CDCl_3$) spectrum of **3ag** and **4ag**

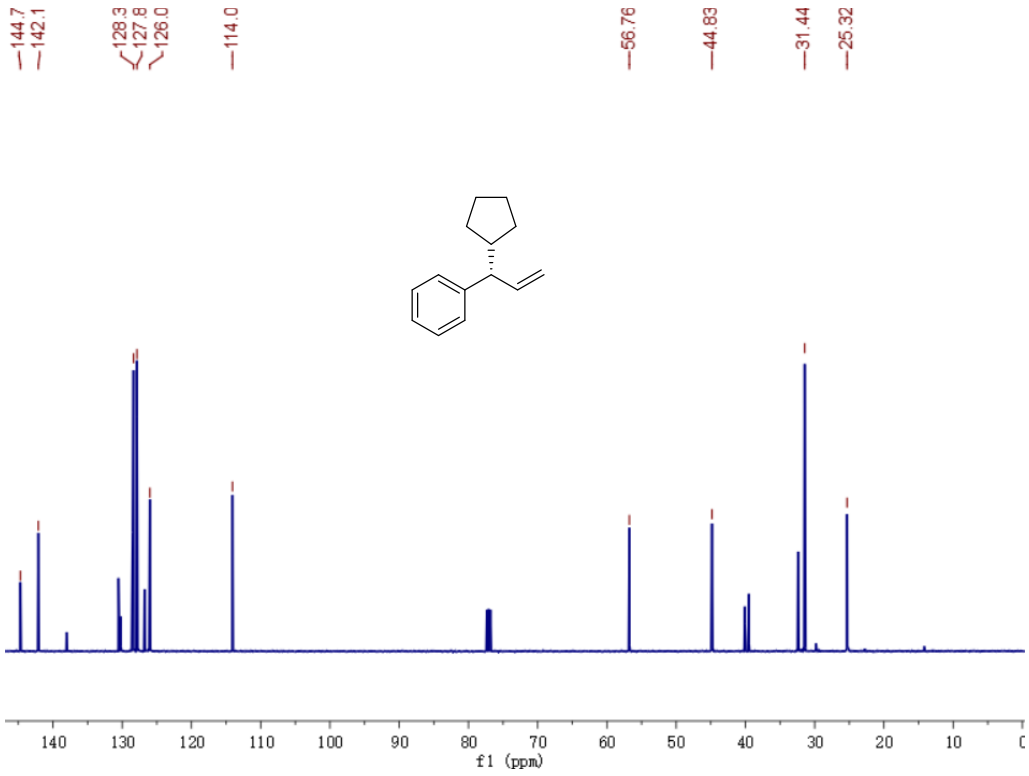

Figure S102: ^{13}C NMR (126 MHz, $CDCl_3$) spectrum of **3ag** and **4ag**

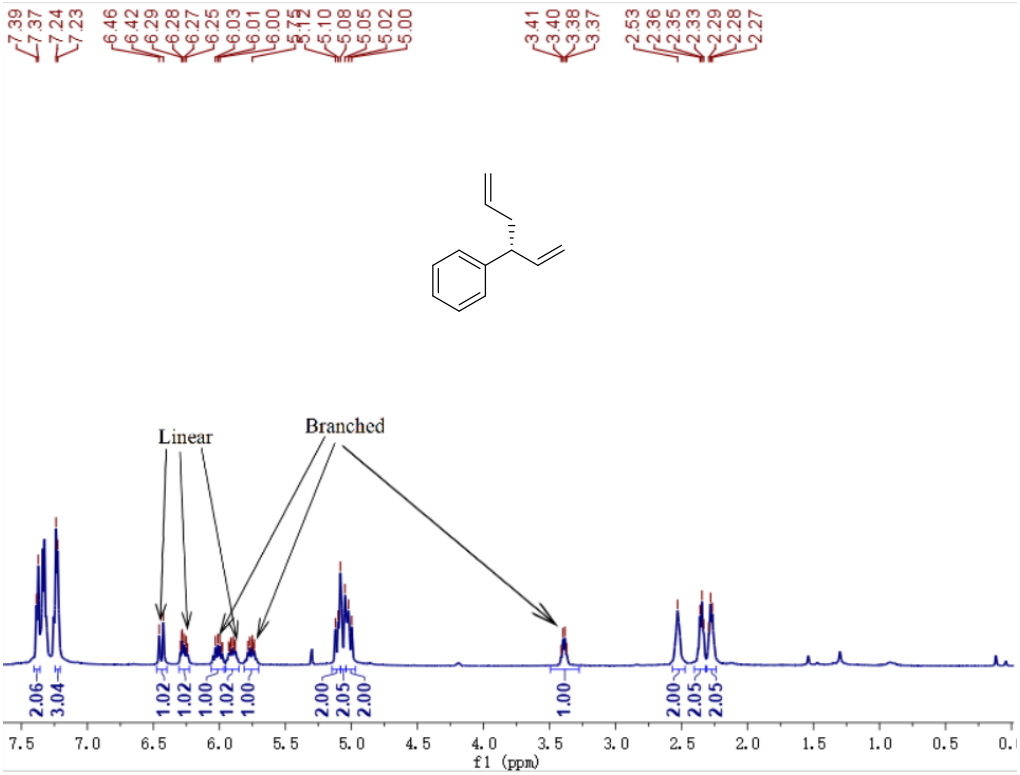

Figure S103: ^{1}H NMR (500 MHz, $CDCl_3$) spectrum of **3ah** and **4ah**

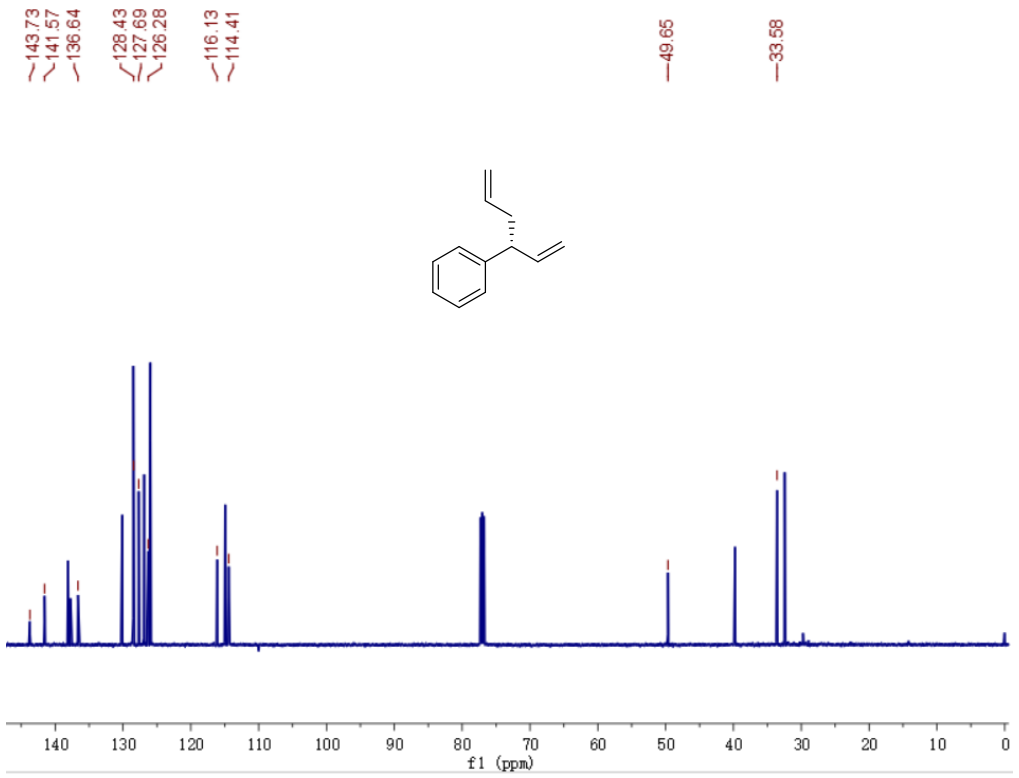

Figure S104: ^{13}C NMR (126 MHz, $CDCl_3$) spectrum of **3ah** and **4ah**

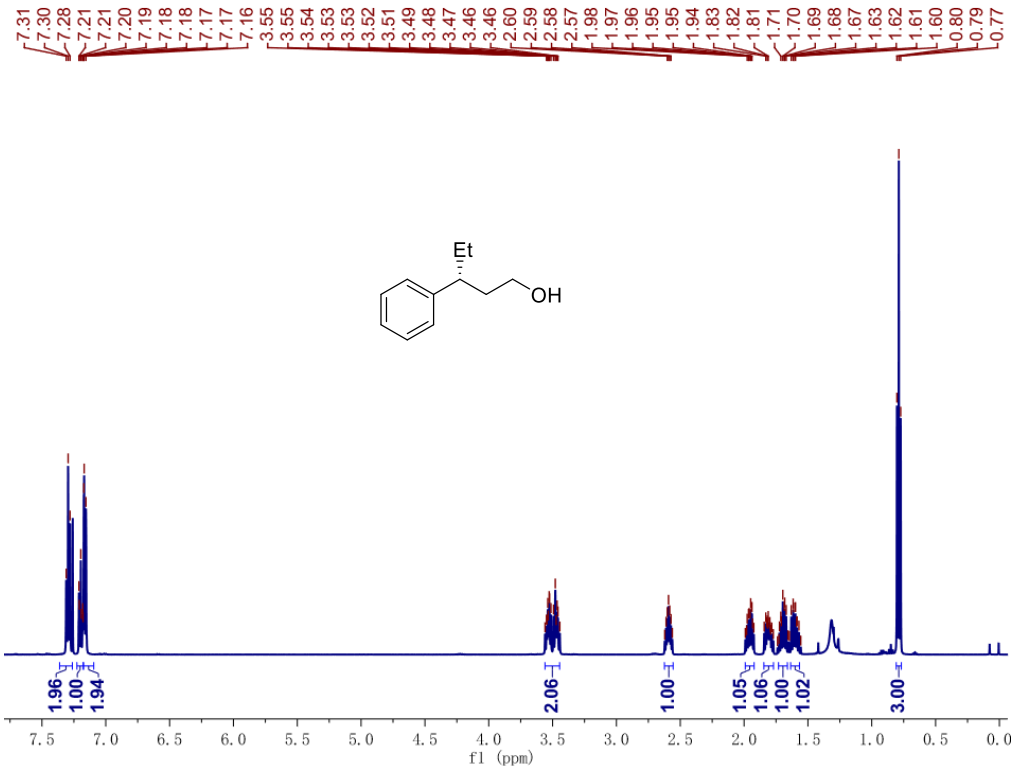

Figure S105: ^{1}H NMR (500 MHz, $CDCl_3$) spectrum of **5a**

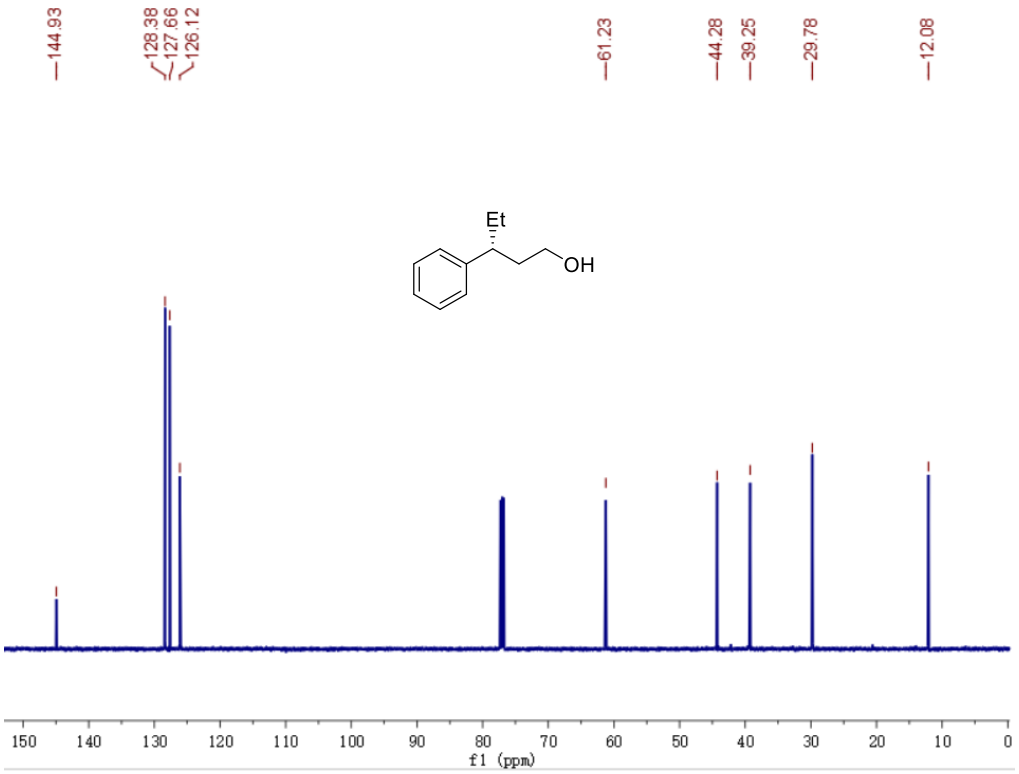

Figure S106: ^{13}C NMR (126MHz, $CDCl_3$) spectrum of **5a**

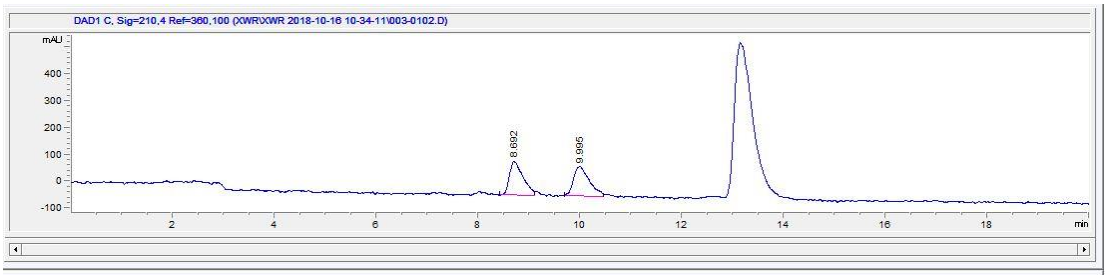

#	时间	峰面积	峰高	峰宽	对称因子	峰面积 %
1	8.692	2413.5	128.9	0.2344	0.461	50.057
2	9.995	2408	110.4	0.2705	0.659	49.943

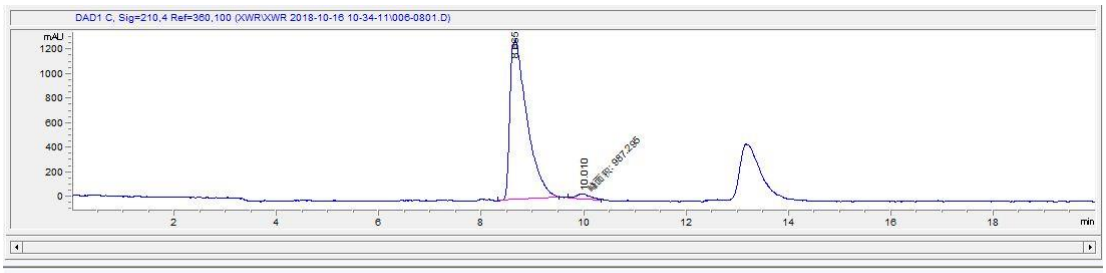

#	时间	峰面积	峰高	峰宽	对称因子	峰面积 %
1	8.665	30328.3	1306.5	0.2828	0.469	96.847
2	10.01	987.3	43.5	0.378	0.901	3.153

Figure S107: HPLC chromatographs of **3aa**

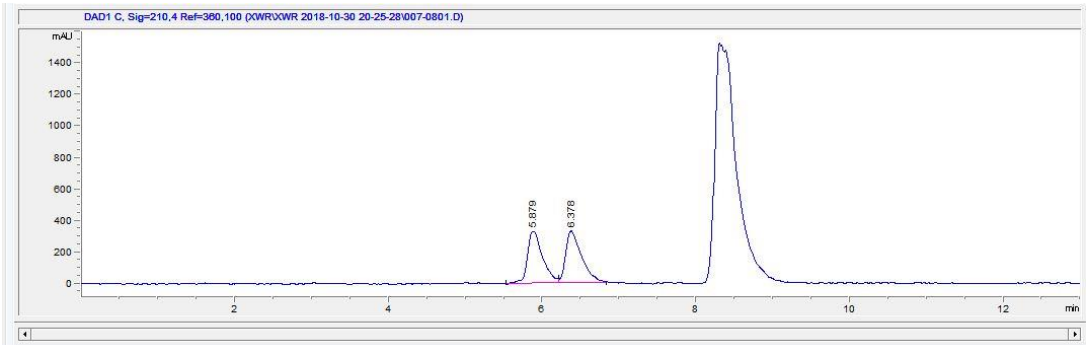

#	时间	峰面积	峰高	峰宽	对称因子	峰面积 %
1	5.879	4560.7	332.6	0.2	0.584	49.028
2	6.378	4741.5	330.5	0.1994	0.521	50.972

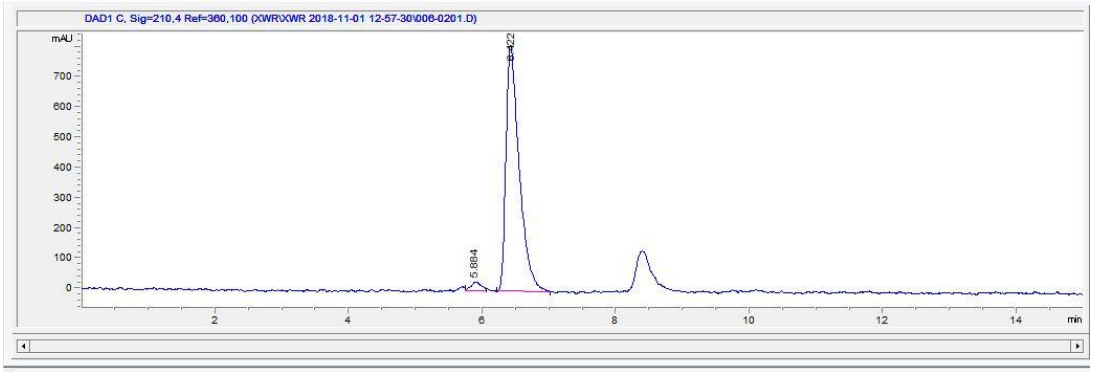

#	时间	峰面积	峰高	峰宽	对称因子	峰面积 %
1	5.884	345.8	31.3	0.1389	0.613	2.967
2	6.422	11310.6	815.8	0.1998	0.495	97.033

Figure S108: HPLC chromatographs of **3ba**

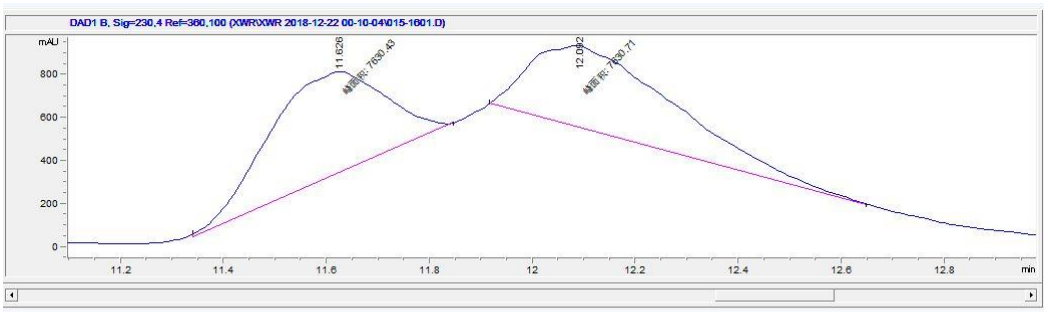

#	时间	峰面积	峰高	峰宽	对称因子	峰面积 %
1	11.626	7630.4	473.7	0.2685	1.697	49.999
2	12.092	7630.7	378.3	0.3361	0.403	50.001

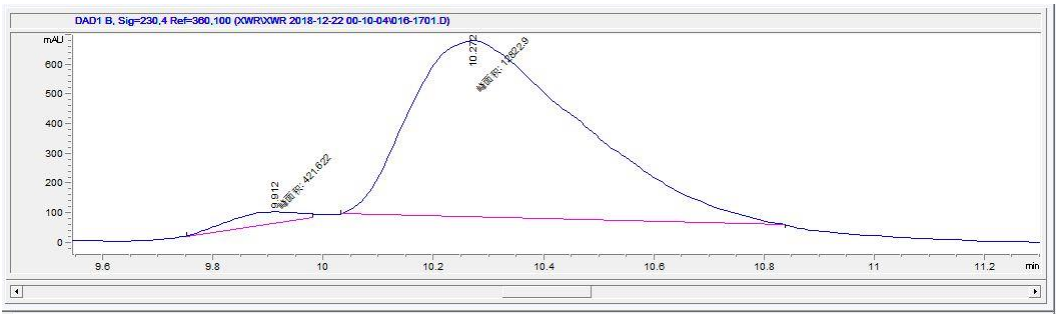

#	时间	峰面积	峰高	峰宽	对称因子	峰面积 %
1	9.912	421.6	42.6	0.1651	2.411	3.183
2	10.272	12822.9	595.1	0.3591	0.563	96.817

Figure S109: HPLC chromatographs of **3ca**

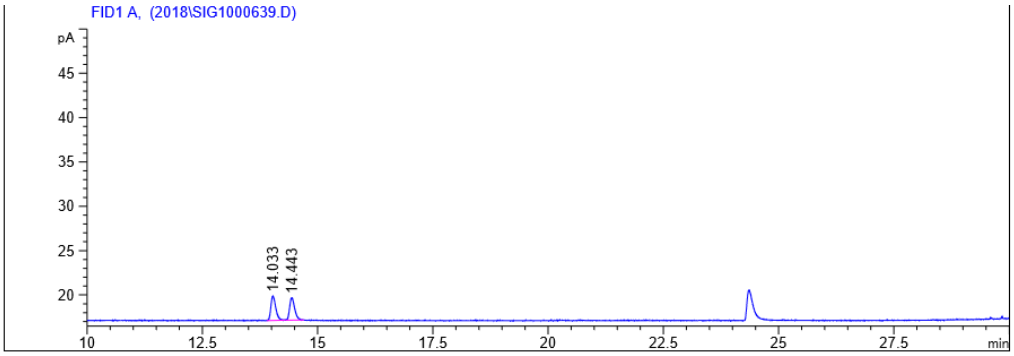

Peak #	RetTime [min]	Type	Width [min]	Area [pA*s]	Height [pA]	Area %
1	14.033	BB	0.1159	20.26668	2.75307	51.52841
2	14.443	BB	0.1192	19.06440	2.52065	48.47159

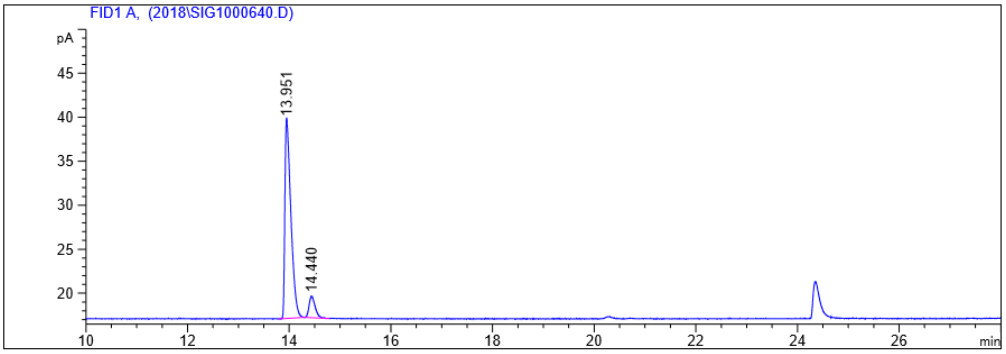

Peak #	RetTime [min]	Type	Width [min]	Area [pA*s]	Height [pA]	Area %
1	13.951	BB	0.1245	186.31029	22.52155	90.25405
2	14.440	BB	0.1283	20.11844	2.43716	9.74595

Figure S110: HPLC chromatographs of **3da**

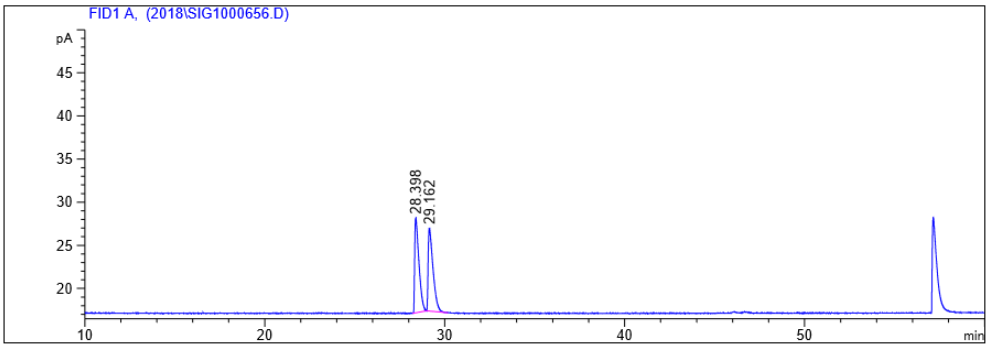

Peak #	RetTime [min]	Type	Width [min]	Area [pA*s]	Height [pA]	Area %
1	28.398	BB	0.2233	180.40466	11.00275	49.89987
2	29.162	BB	0.2501	181.12866	9.59916	50.10013

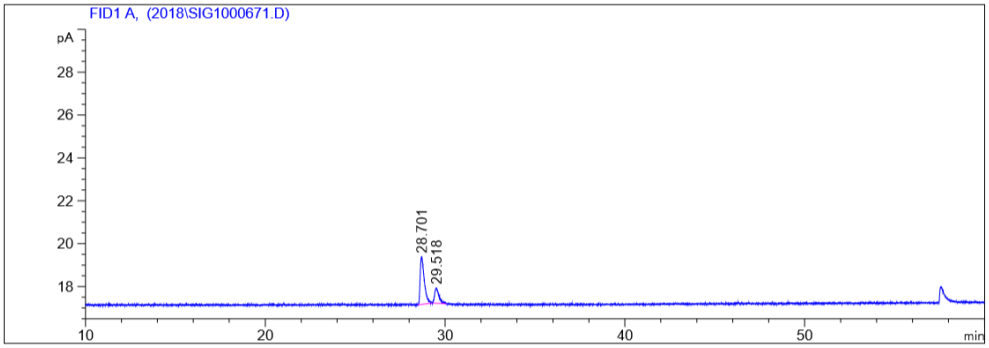

Peak #	RetTime [min]	Type	Width [min]	Area [pA*s]	Height [pA]	Area %
1	28.701	BB	0.2268	34.88015	2.20212	74.39054
2	29.518	BB	0.2120	12.00773	7.00317e-1	25.60946

Figure S111: HPLC chromatographs of **3ea**

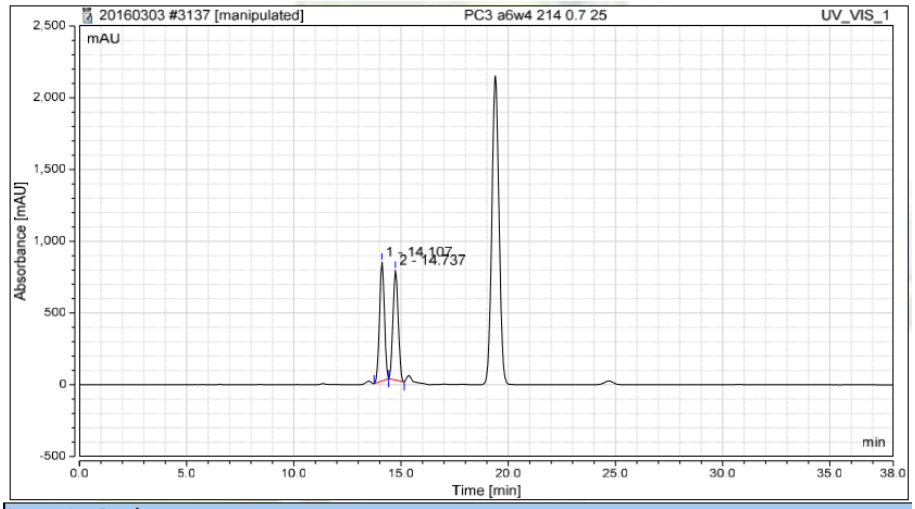

Integration Results

No.	Retention Time min	Retention Time min	Area mAU*min	Height mAU	Relative Area %
1	14	14.107	220.472	829.608	50.54
2	15	14.737	215.726	766.046	49.46

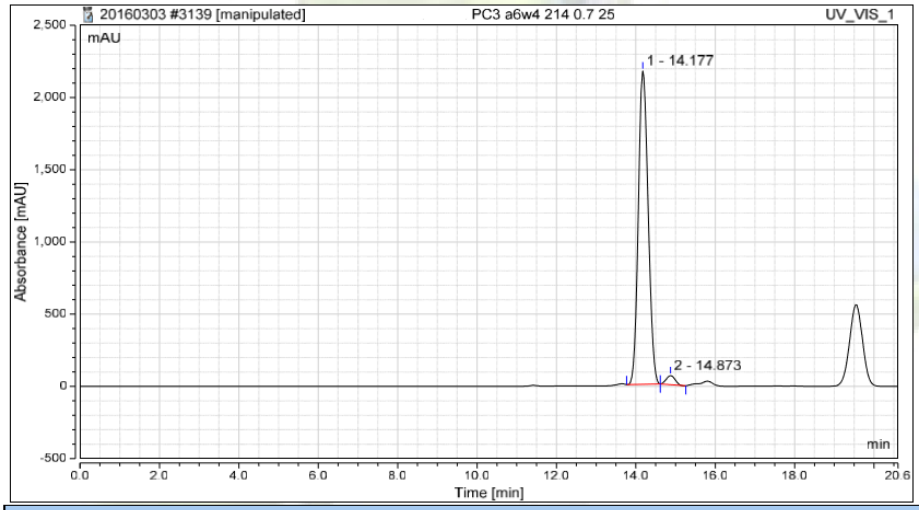

Integration Results

No.	Retention Time min	Retention Time min	Area mAU*min	Height mAU	Relative Area %
1	14	14.177	615.672	2170.815	97.48
2	15	14.873	15.924	63.264	2.52

Figure S112: HPLC chromatographs of **3fa**

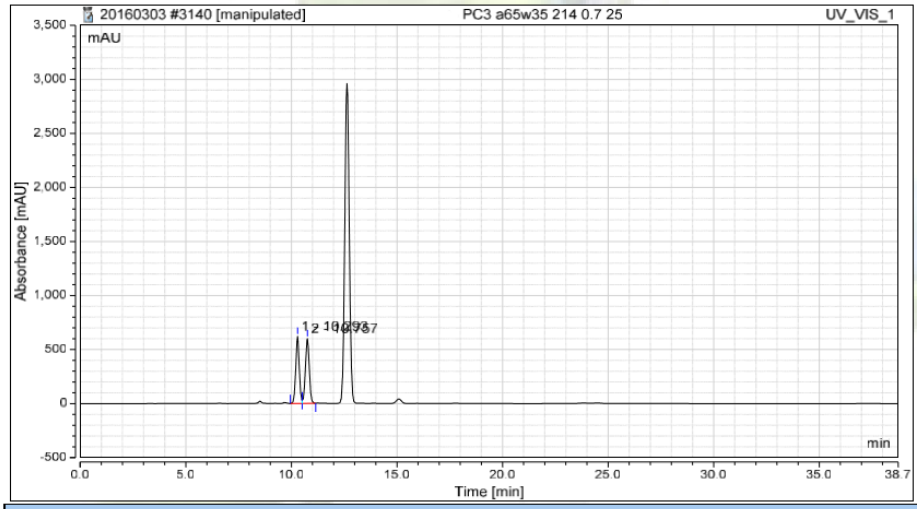

Integration Results

No.	Retention Time min	Retention Time min	Area mAU*min	Height mAU	Relative Area %
1	10	10.293	119.357	622.507	48.93
2	11	10.757	124.580	600.002	51.07

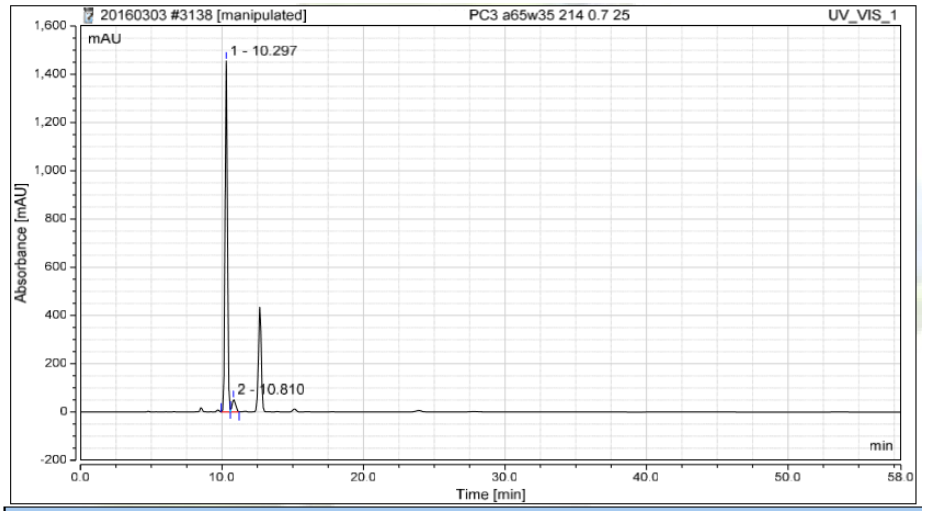

Integration Results

No.	Retention Time min	Retention Time min	Area mAU*min	Height mAU	Relative Area %
1	10	10.297	281.592	1455.817	94.80
2	11	10.810	15.442	51.750	5.20

Figure S113: HPLC chromatographs of **3ga**

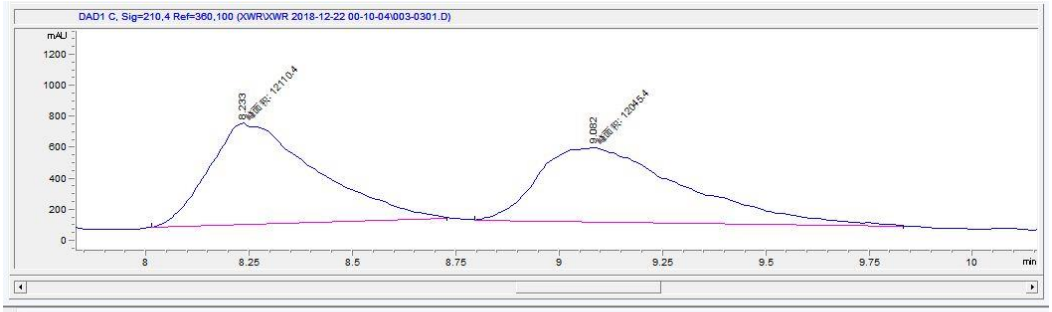

#	时间	峰面积	峰高	峰宽	对称因子	峰面积 %
1	8.233	12110.4	661.2	0.3053	0.462	50.134
2	9.082	12045.4	480.9	0.4174	0.569	49.866

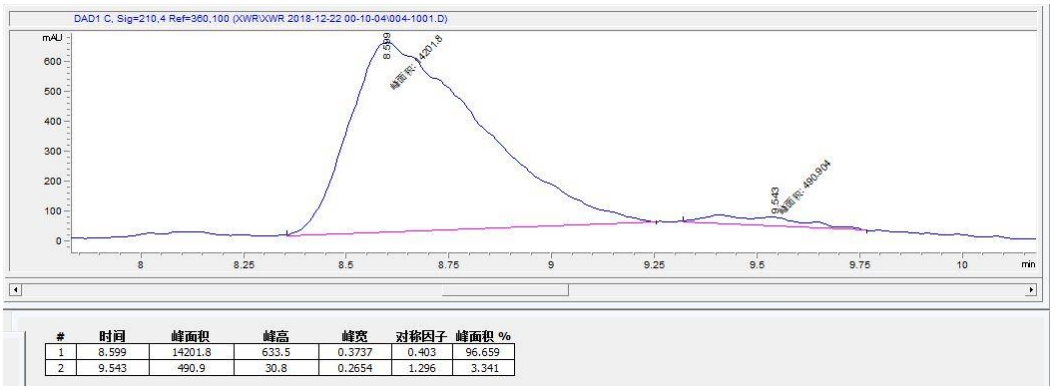

#	时间	峰面积	峰高	峰宽	对称因子	峰面积 %
1	8.599	14201.8	633.5	0.3737	0.403	96.659
2	9.543	490.9	30.8	0.2654	1.296	3.341

Figure S114: HPLC chromatographs of **3ha**

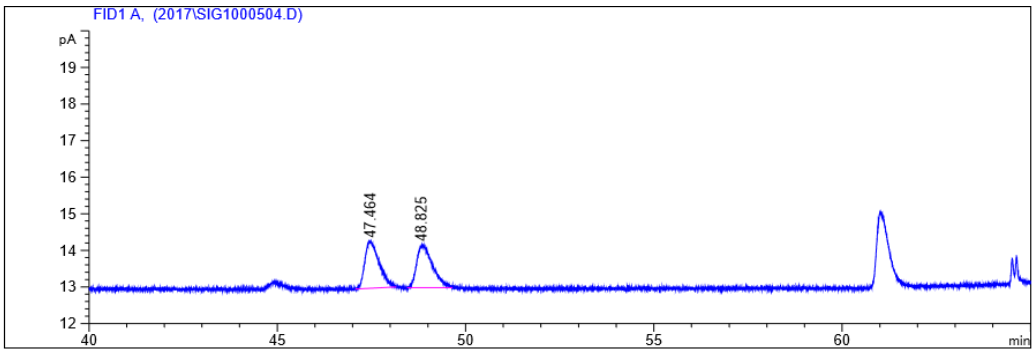

Peak #	RetTime [min]	Type	Width [min]	Area [pA*s]	Height [pA]	Area %
1	47.464	BB	0.3325	33.75562	1.26849	49.84428
2	48.825	BB	0.3472	33.96654	1.15461	50.15572

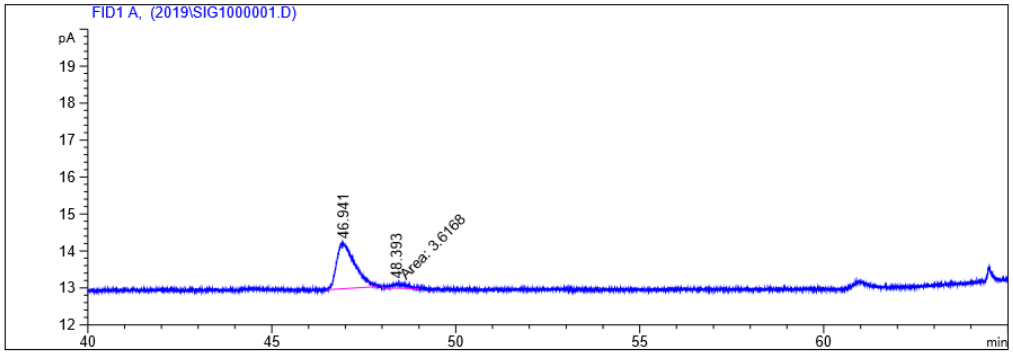

Peak #	RetTime [min]	Type	Width [min]	Area [pA*s]	Height [pA]	Area %
1	46.941	BB	0.4021	42.47622	1.24477	92.15326
2	48.393	MM	0.3889	3.61680	1.55002e-1	7.84674

Figure S115: HPLC chromatographs of **3ia**

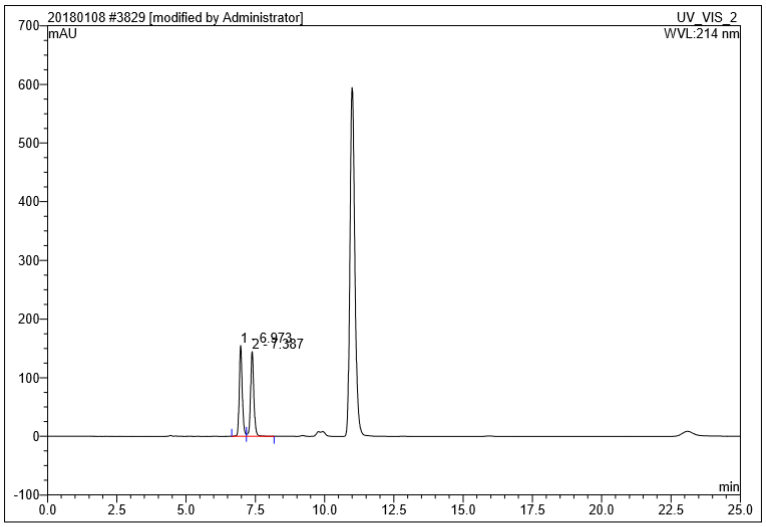

No.	Ret.Time min	Peak Name	Height mAU	Area mAU*min	Rel.Area %	Amount	Type
1	6.97	n.a.	155.163	19.479	49.66	n.a.	BM
2	7.39	n.a.	144.625	19.746	50.34	n.a.	MB

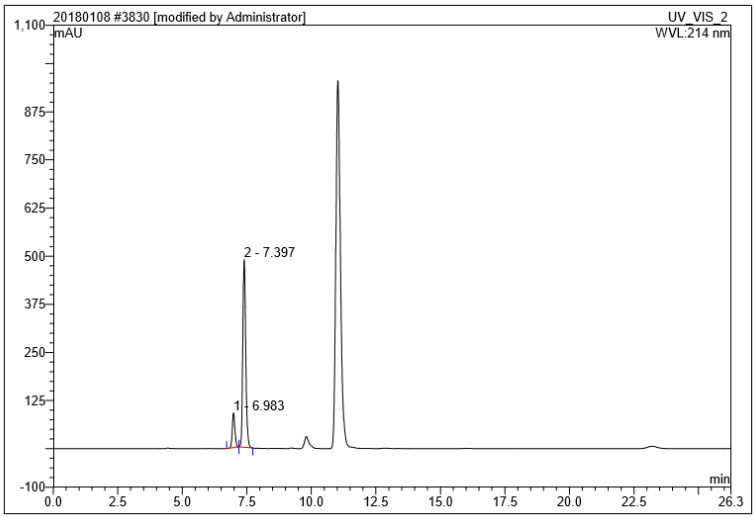

No.	Ret.Time min	Peak Name	Height mAU	Area mAU*min	Rel.Area %	Amount	Type
1	6.98	n.a.	90.381	10.778	14.35	n.a.	BMb*
2	7.40	n.a.	487.751	64.337	85.65	n.a.	bMB*

Figure S116: HPLC chromatographs of **3ja**

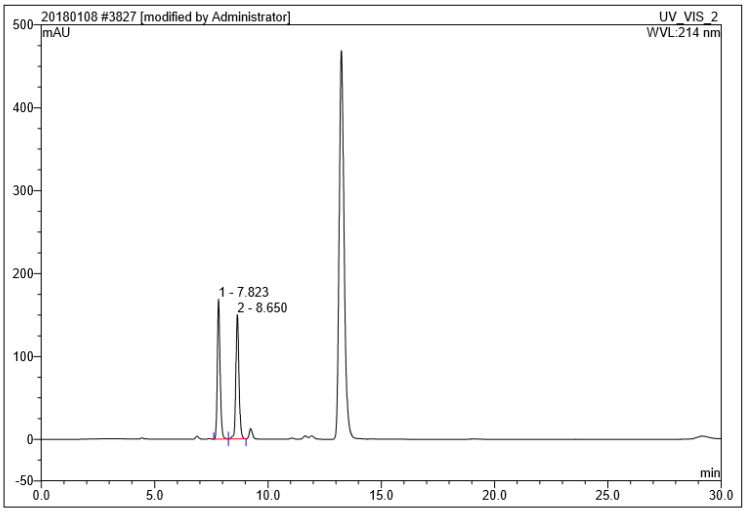

No.	Ret.Time min	Peak Name	Height mAU	Area mAU*min	Rel.Area %	Amount	Type
1	7.82	n.a.	168.969	24.180	50.20	n.a.	BM *
2	8.65	n.a.	149.962	23.988	49.80	n.a.	MB*

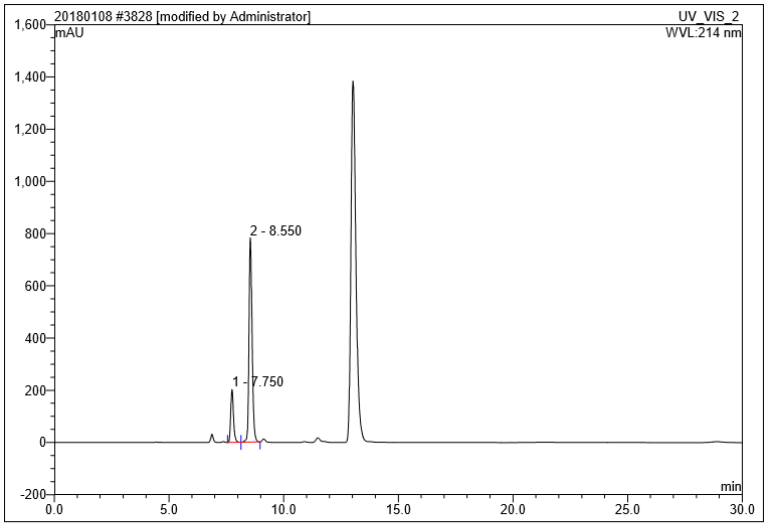

No.	Ret.Time min	Peak Name	Height mAU	Area mAU*min	Rel.Area %	Amount	Type
1	7.75	n.a.	203.005	28.489	18.66	n.a.	BM *
2	8.55	n.a.	782.960	124.199	81.34	n.a.	MB*
Total:			985.965	152.688	100.00	0.000	

Figure S117: HPLC chromatographs of **3ka**

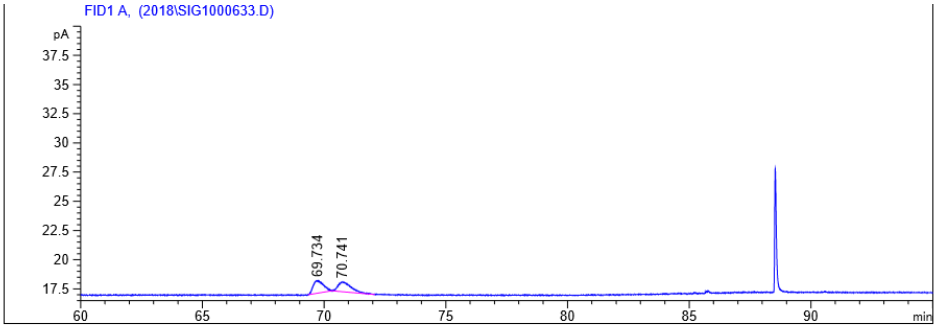

Peak #	RetTime [min]	Type	Width [min]	Area [pA*s]	Height [pA]	Area %
1	69.734	BB	0.3511	31.47605	1.05806	50.66784
2	70.741	BB	0.4427	30.64629	8.18688e-1	49.33216

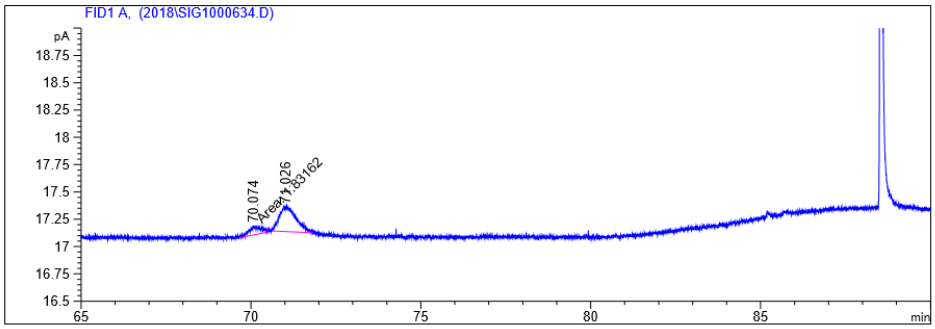

Peak #	RetTime [min]	Type	Width [min]	Area [pA*s]	Height [pA]	Area %
1	70.074	MM	0.3811	1.83162	8.00932e-2	18.74358
2	71.026	BB	0.4261	7.94035	2.21558e-1	81.25642

Figure S118: HPLC chromatographs of **3la**

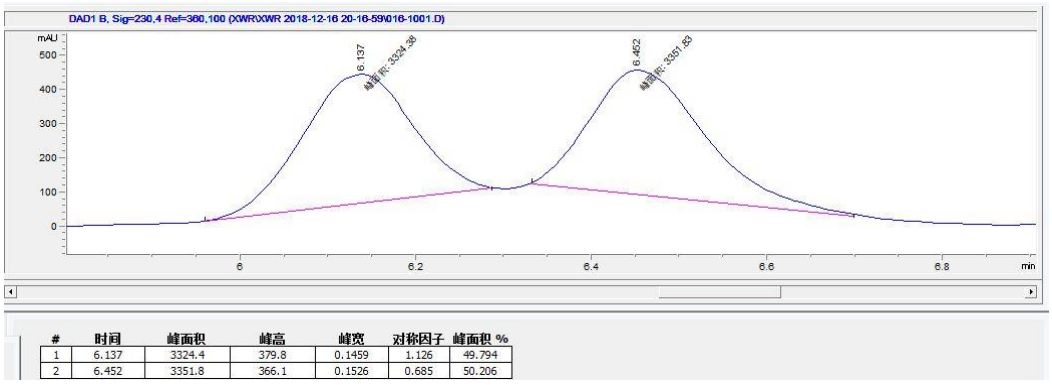

#	时间	峰面积	峰高	峰宽	对称因子	峰面积 %
1	6.137	3324.4	379.8	0.1459	1.126	49.794
2	6.452	3351.8	366.1	0.1526	0.685	50.206

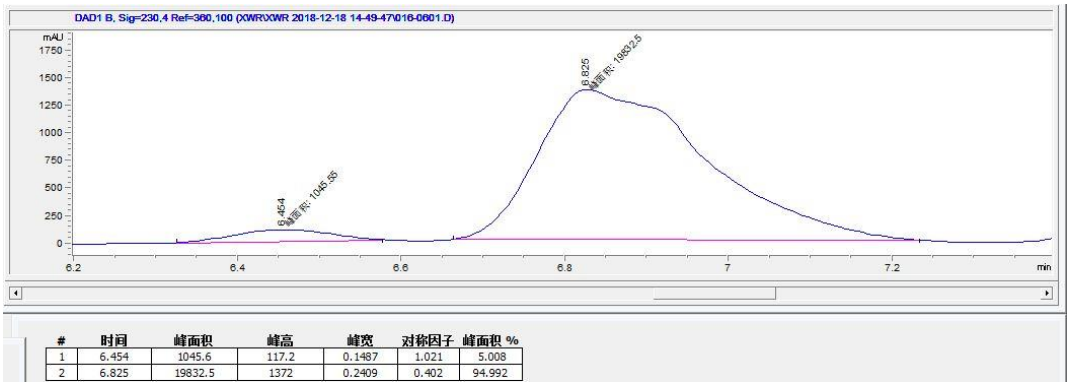

#	时间	峰面积	峰高	峰宽	对称因子	峰面积 %
1	6.454	1045.6	117.2	0.1487	1.021	5.008
2	6.825	19832.5	1372	0.2409	0.402	94.992

Figure S119: HPLC chromatographs of **3ma**

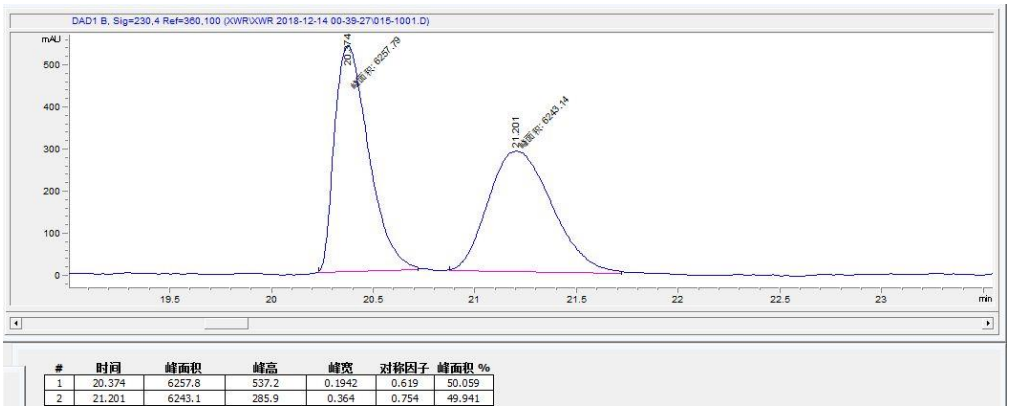

#	时间	峰面积	峰高	峰宽	对称因子	峰面积 %
1	20.374	6257.8	537.2	0.1942	0.619	50.059
2	21.201	6243.1	285.9	0.364	0.754	49.941

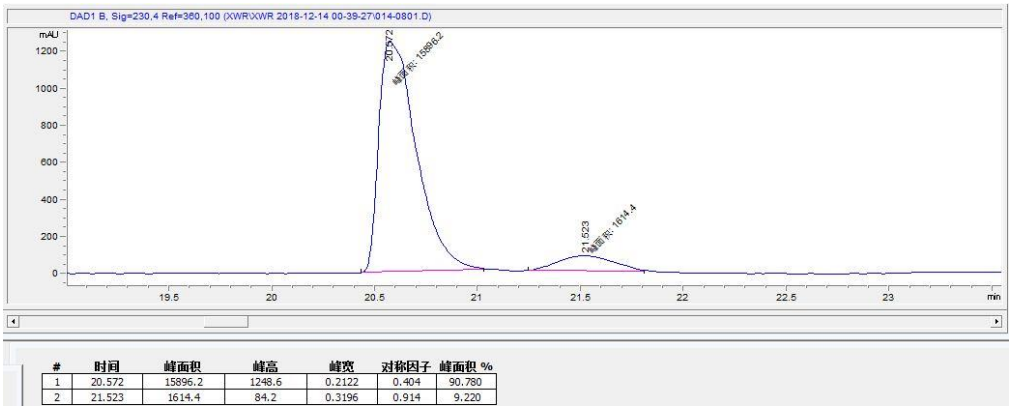

#	时间	峰面积	峰高	峰宽	对称因子	峰面积 %
1	20.572	15896.2	1248.6	0.2122	0.404	90.780
2	21.523	1614.4	84.2	0.3196	0.914	9.220

Figure S120: HPLC chromatographs of **3na**

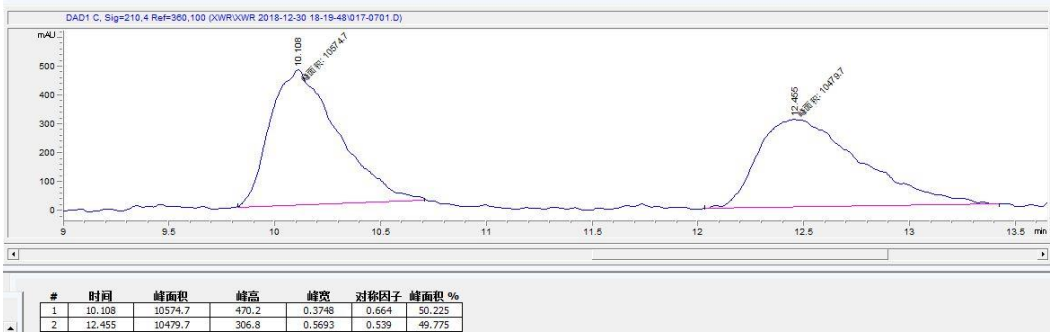

#	时间	峰面积	峰高	峰宽	对称因子	峰面积 %
1	10.108	10574.7	470.2	0.3748	0.664	50.225
2	12.455	10479.7	306.8	0.5693	0.539	49.775

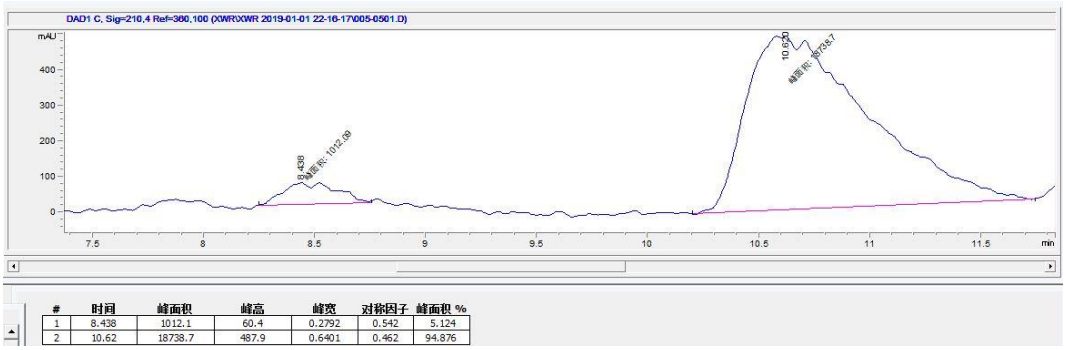

#	时间	峰面积	峰高	峰宽	对称因子	峰面积 %
1	8.438	1012.1	60.4	0.2792	0.542	5.124
2	10.62	18738.7	487.9	0.6401	0.462	94.876

Figure S121: HPLC chromatographs of **3oa**

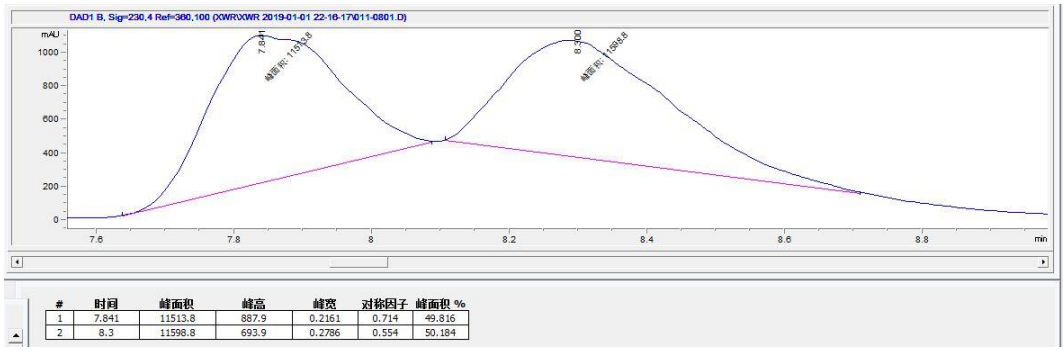

#	时间	峰面积	峰高	峰宽	对称因子	峰面积 %
1	7.841	11513.8	887.9	0.2161	0.714	49.816
2	8.3	11598.8	693.9	0.2786	0.554	50.184

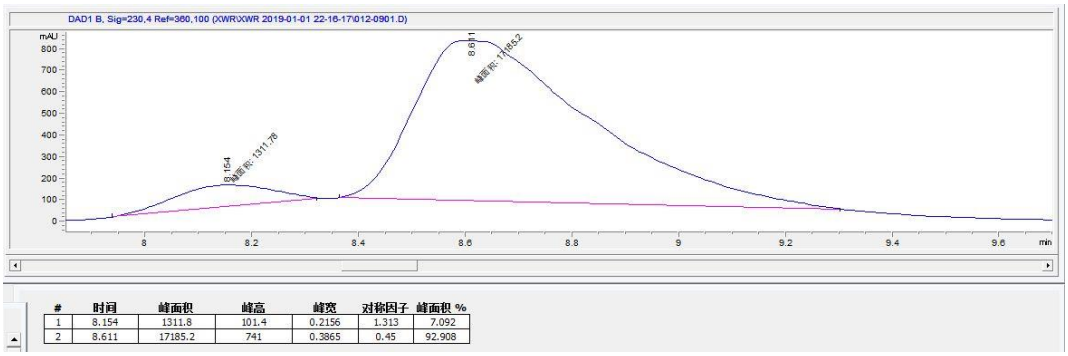

#	时间	峰面积	峰高	峰宽	对称因子	峰面积 %
1	8.154	1311.8	101.4	0.2156	1.313	7.092
2	8.611	17185.2	741	0.3865	0.45	92.908

Figure S122: HPLC chromatographs of **3pa**

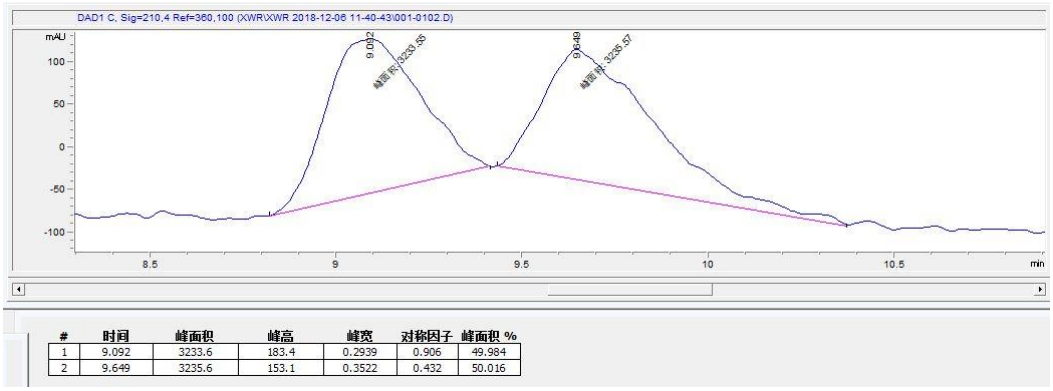

#	时间	峰面积	峰高	峰宽	对称因子	峰面积 %
1	9.092	3233.6	183.4	0.2939	0.906	49.984
2	9.649	3235.6	153.1	0.3522	0.432	50.016

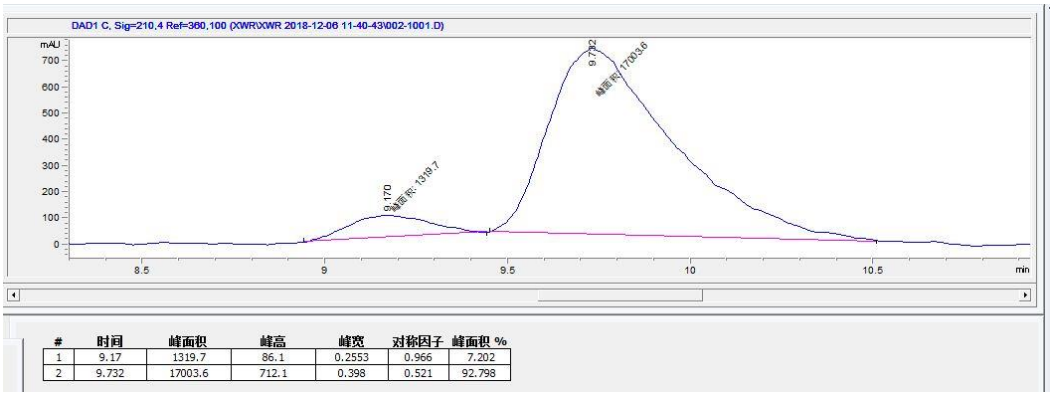

#	时间	峰面积	峰高	峰宽	对称因子	峰面积 %
1	9.17	1319.7	86.1	0.2553	0.966	7.202
2	9.732	17003.6	712.1	0.398	0.521	92.798

Figure S123: HPLC chromatographs of **3qa**

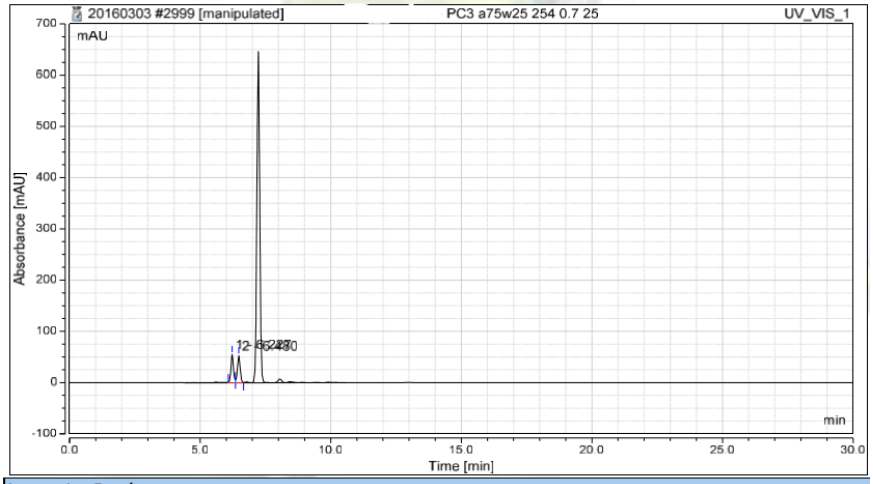

Integration Results

No.	Retention Time min	Retention Time min	Area mAU*min	Height mAU	Relative Area %
1	6	6.227	6.243	55.910	49.73
2	6	6.480	6.310	53.161	50.27

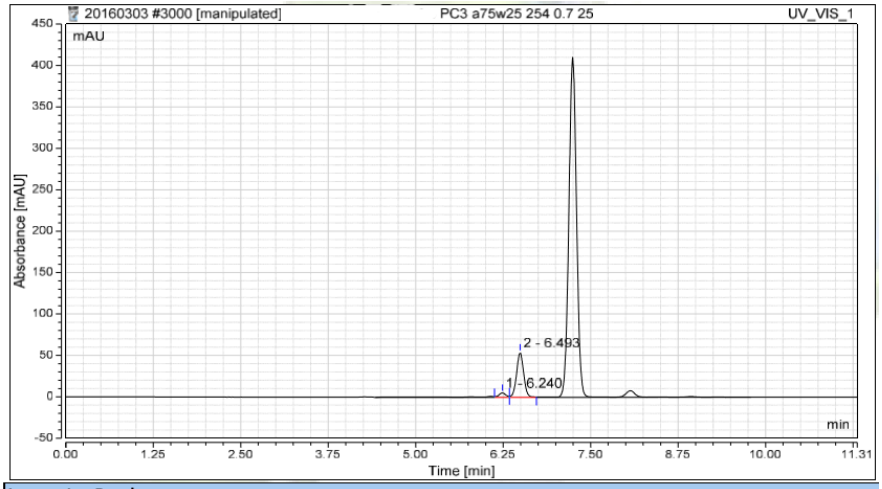

Integration Results

No.	Retention Time min	Retention Time min	Area mAU*min	Height mAU	Relative Area %
1	6	6.240	0.621	5.375	8.90
2	6	6.493	6.348	54.228	91.10

Figure S124: HPLC chromatographs of **3ra**

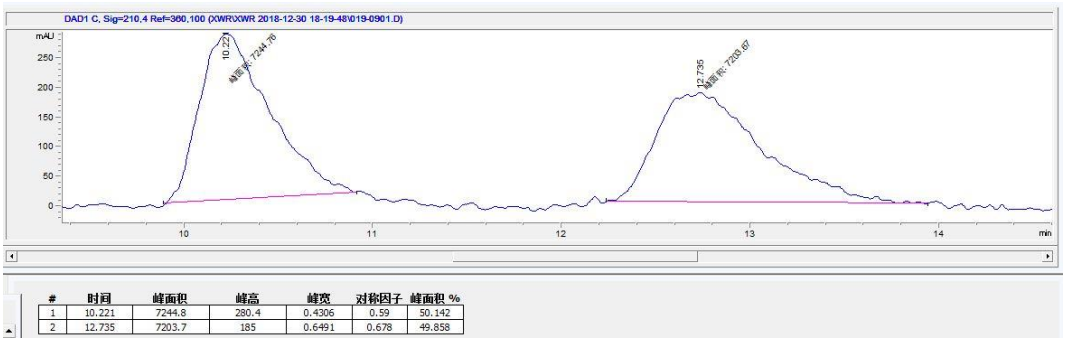

#	时间	峰面积	峰高	峰宽	对称因子	峰面积 %
1	10.221	7244.8	280.4	0.4306	0.59	50.142
2	12.735	7203.7	185	0.6491	0.678	49.858

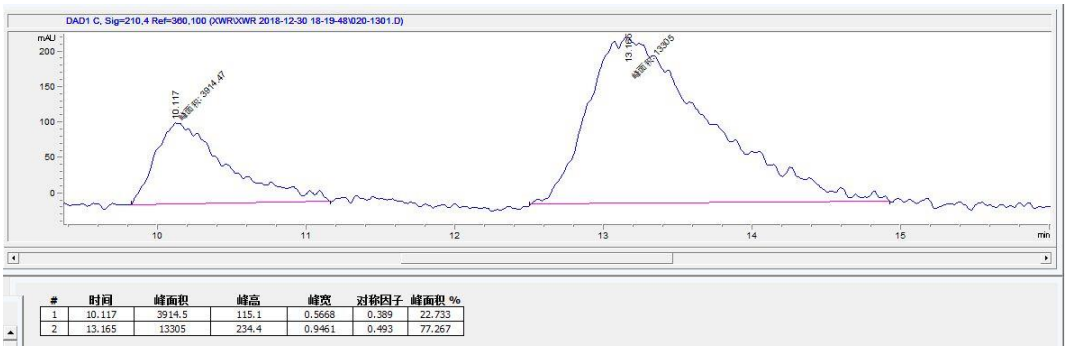

#	时间	峰面积	峰高	峰宽	对称因子	峰面积 %
1	10.117	3914.5	115.1	0.5668	0.389	22.733
2	13.165	13305	234.4	0.9461	0.493	77.267

Figure S125: HPLC chromatographs of **3sa**

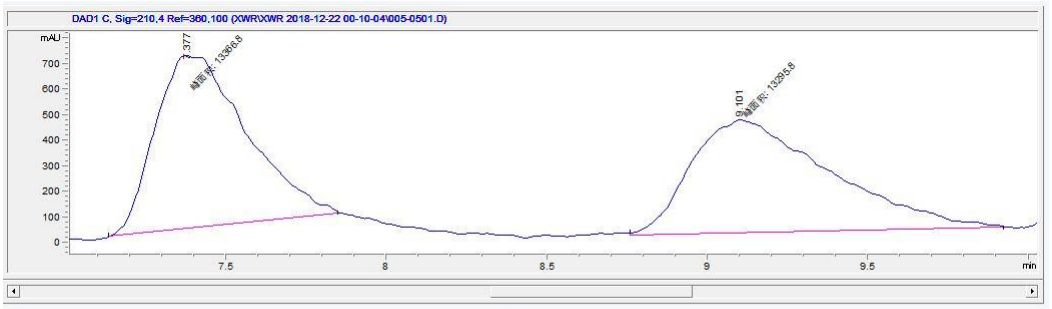

#	时间	峰面积	峰高	峰宽	对称因子	峰面积 %
1	7.377	13366.8	678.1	0.3285	0.53	50.133
2	9.101	13295.8	441.4	0.502	0.536	49.867

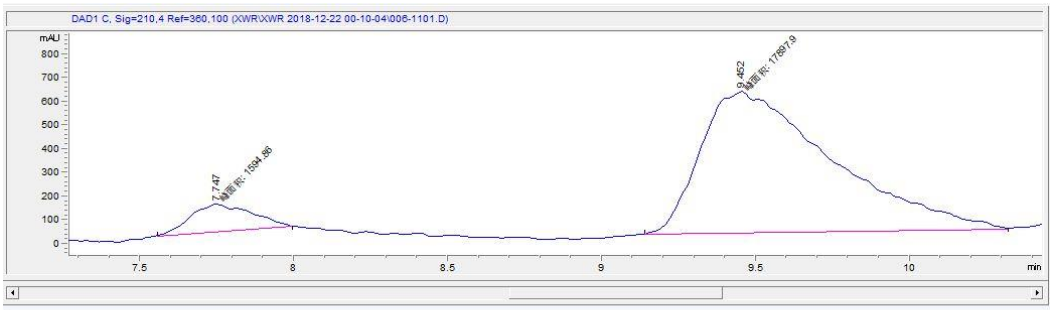

#	时间	峰面积	峰高	峰宽	对称因子	峰面积 %
1	7.747	1594.9	117.4	0.2265	0.759	8.182
2	9.452	17897.9	597.6	0.4992	0.43	91.818

Figure S126: HPLC chromatographs of **3ta**

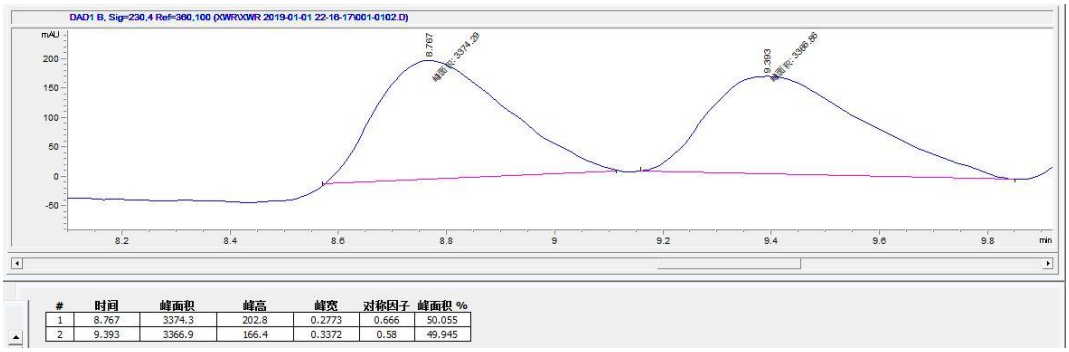

#	时间	峰面积	峰高	峰宽	对称因子	峰面积 %
1	8.767	3374.3	202.8	0.2773	0.666	50.055
2	9.393	3366.9	166.4	0.3372	0.58	49.945

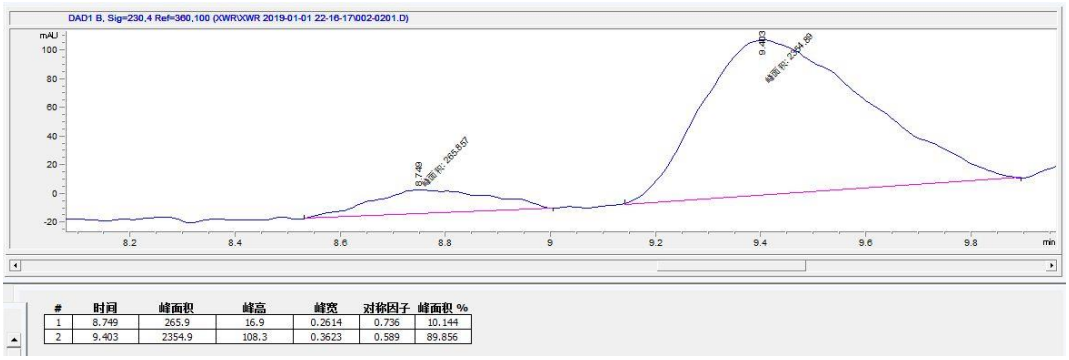

#	时间	峰面积	峰高	峰宽	对称因子	峰面积 %
1	8.749	265.9	16.9	0.2614	0.736	10.144
2	9.403	2354.9	108.3	0.3623	0.589	89.856

Figure S127: HPLC chromatographs of **3ua**

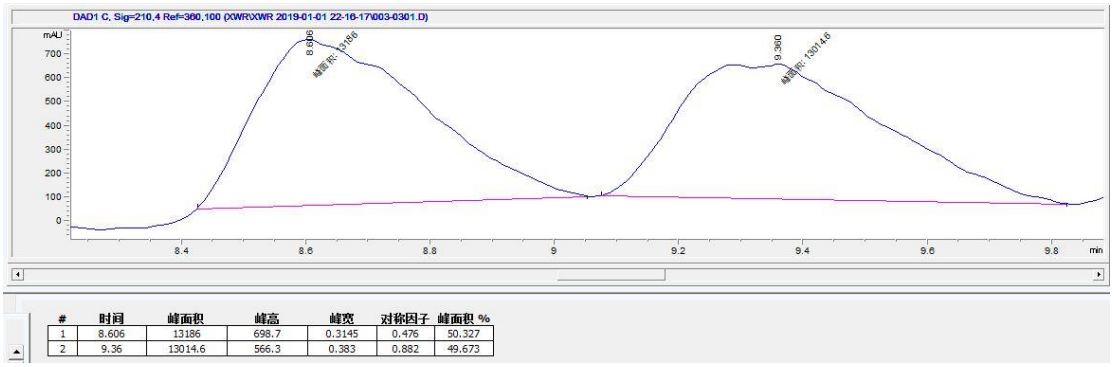

#	时间	峰面积	峰高	峰宽	对称因子	峰面积 %
1	8.606	13186	698.7	0.3145	0.476	50.327
2	9.36	13014.6	566.3	0.383	0.882	49.673

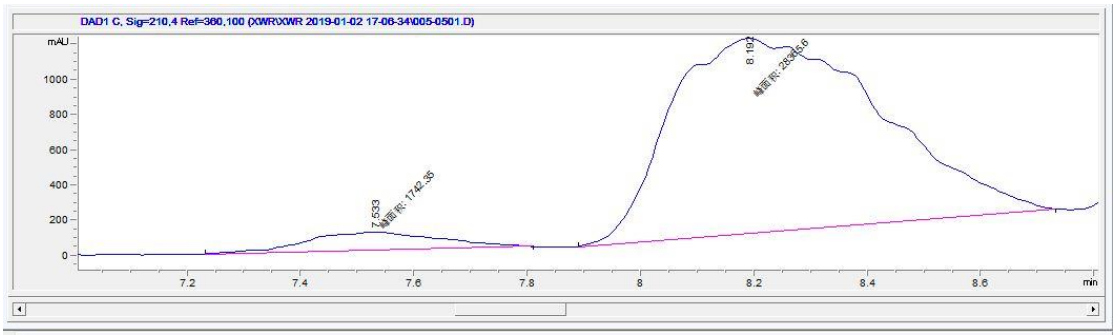

#	时间	峰面积	峰高	峰宽	对称因子	峰面积 %
1	7.533	1742.4	105.9	0.2743	1.231	5.787
2	8.192	28365.6	1108.7	0.4264	0.604	94.213

Figure S128: HPLC chromatographs of **3va**

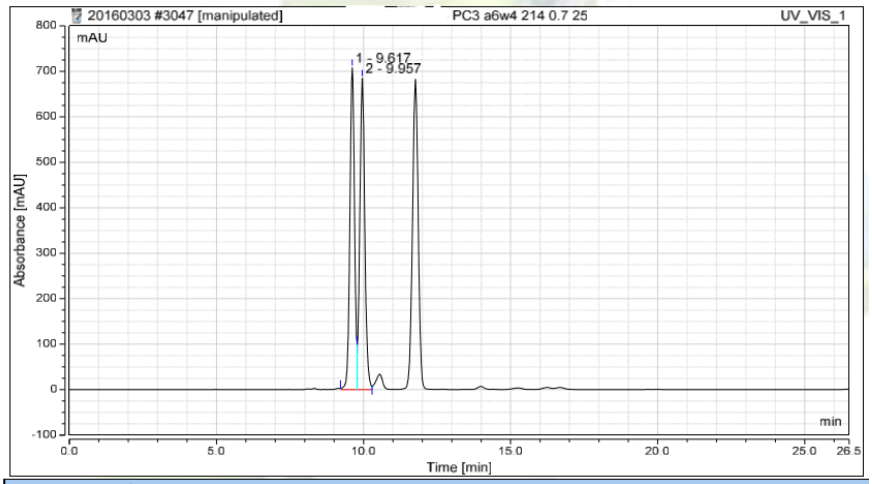

Integration Results

No.	Retention Time min	Retention Time min	Area mAU*min	Height mAU	Relative Area %
1	10	9.617	128.644	708.044	48.83
2	10	9.957	134.819	685.106	51.17

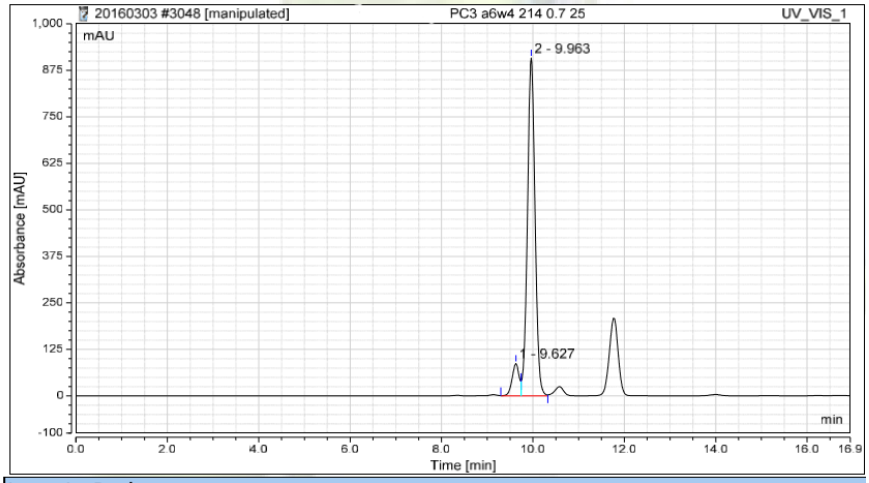

Integration Results

No.	Retention Time min	Retention Time min	Area mAU*min	Height mAU	Relative Area %
1	10	9.627	15.397	87.353	8.07
2	10	9.963	175.497	908.190	91.93

Figure S129: HPLC chromatographs of **3wa**

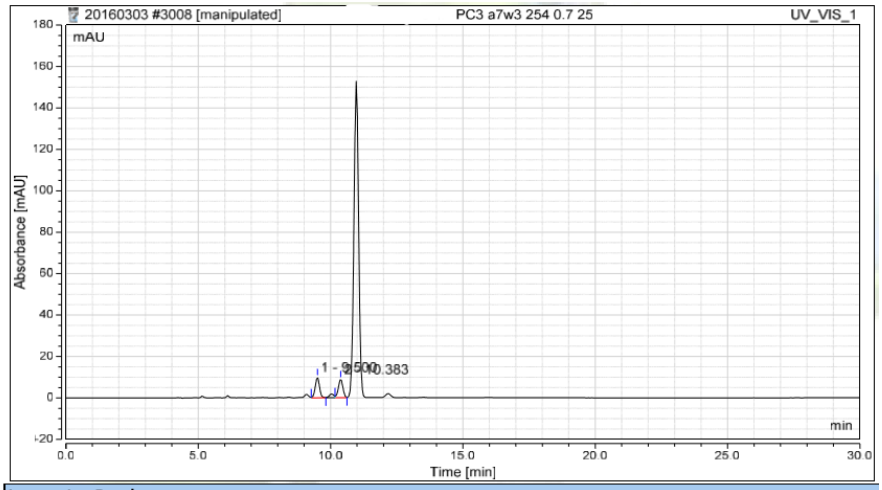

Integration Results

No.	Retention Time min	Retention Time min	Area mAU*min	Height mAU	Relative Area %
1	10	9.500	1.816	9.988	50.79
2	10	10.383	1.760	8.916	49.21

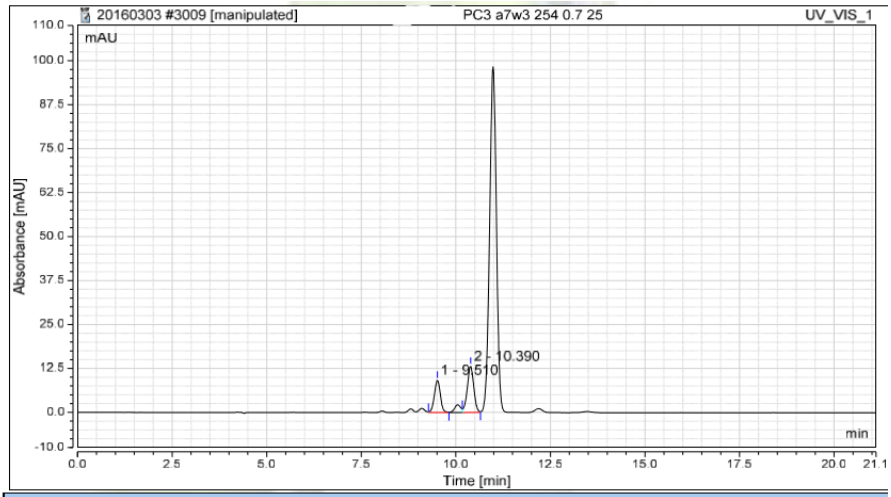

Integration Results

No.	Retention Time min	Retention Time min	Area mAU*min	Height mAU	Relative Area %
1	10	9.510	1.679	9.283	38.88
2	10	10.390	2.640	13.228	61.12

Figure S130: HPLC chromatographs of **3xa**

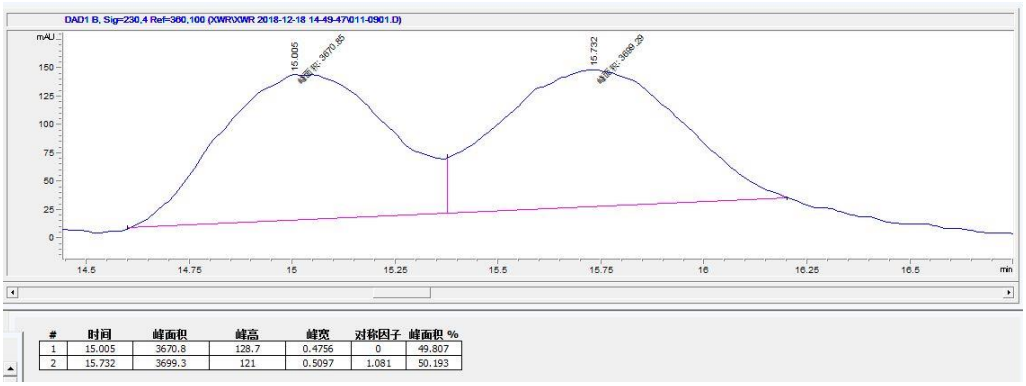

#	时间	峰面积	峰高	峰宽	对称因子	峰面积 %
1	15.005	3670.8	128.7	0.4756	0	49.807
2	15.732	3699.3	121	0.5097	1.081	50.193

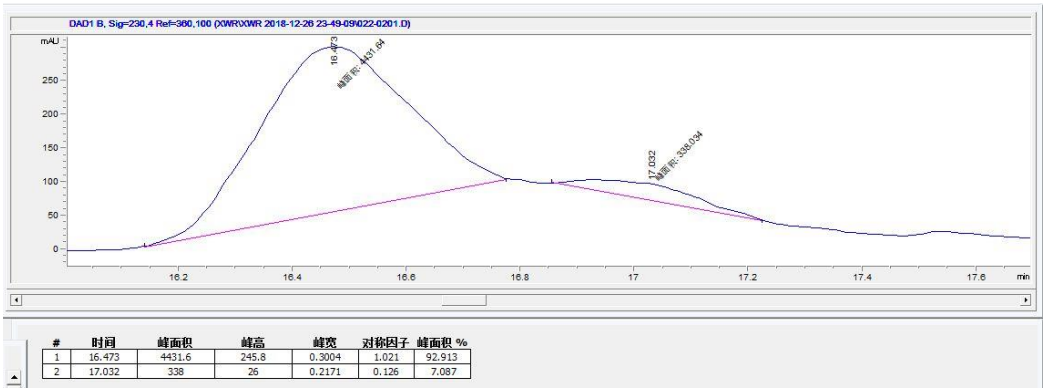

#	时间	峰面积	峰高	峰宽	对称因子	峰面积 %
1	16.473	4431.6	245.8	0.3004	1.021	92.913
2	17.032	338	26	0.2171	0.126	7.087

Figure S131: HPLC chromatographs of **3ya**

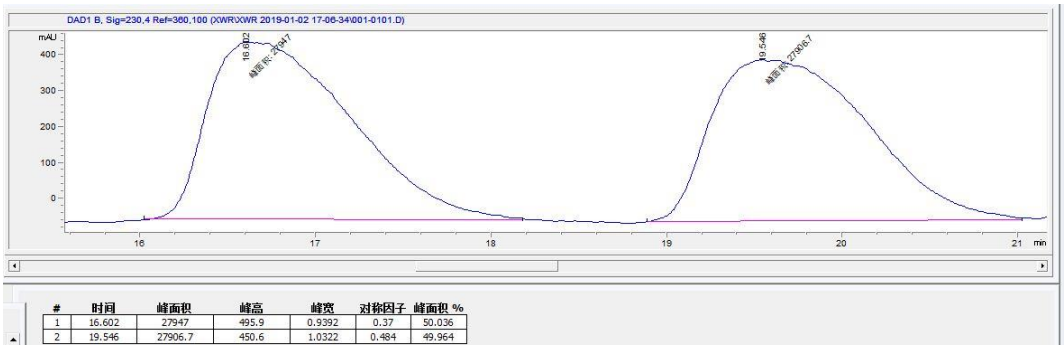

#	时间	峰面积	峰高	峰宽	对称因子	峰面积 %
1	16.602	27947	495.9	0.9392	0.37	50.036
2	19.546	27906.7	450.6	1.0322	0.484	49.964

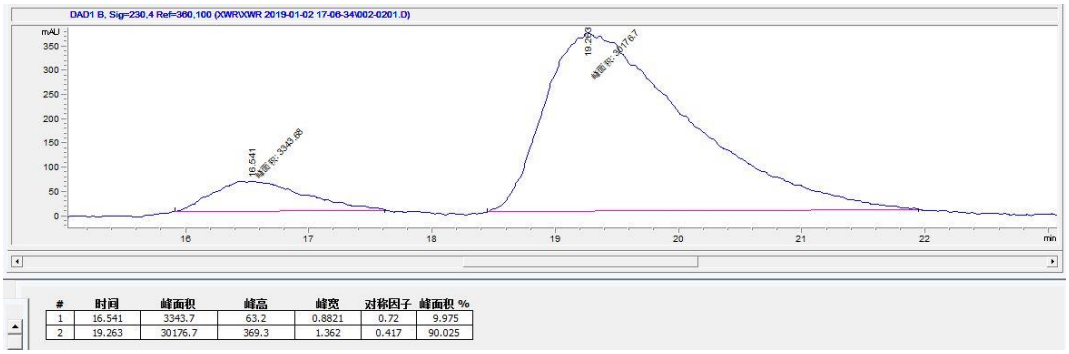

#	时间	峰面积	峰高	峰宽	对称因子	峰面积 %
1	16.541	3343.7	63.2	0.8821	0.72	9.975
2	19.263	30176.7	369.3	1.362	0.417	90.025

Figure S132: HPLC chromatographs of **3za**

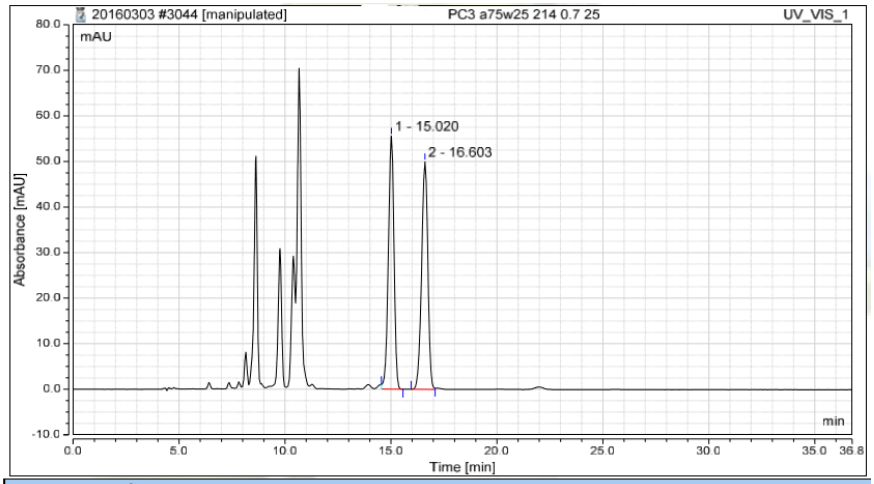

Integration Results

No.	Retention Time min	Retention Time min	Area mAU*min	Height mAU	Relative Area %
1	15	15.020	17.106	55.570	50.07
2	17	16.603	17.060	49.961	49.93

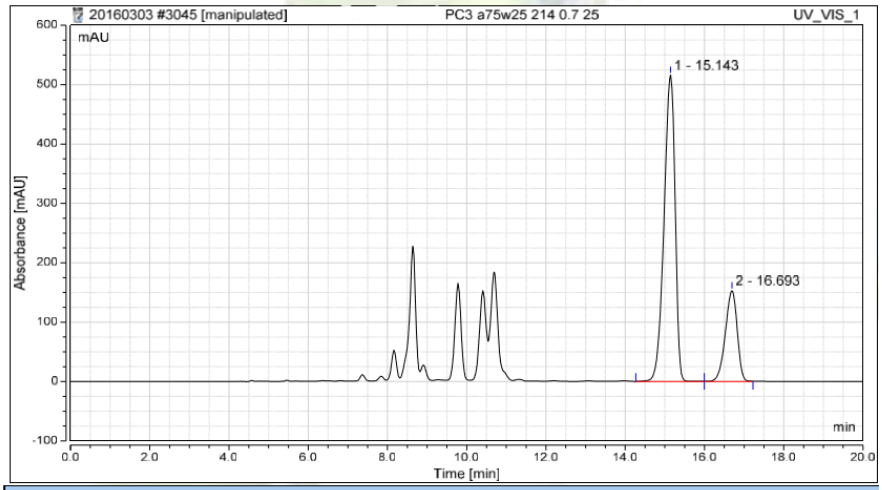

Integration Results

No.	Retention Time min	Retention Time min	Area mAU*min	Height mAU	Relative Area %
1	15	15.143	168.520	516.256	75.93
2	17	16.693	53.430	153.392	24.07

Figure S133: HPLC chromatographs of **3x'a**

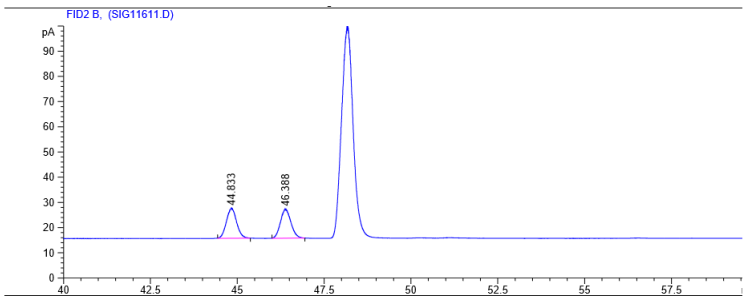

Peak #	RetTime [min]	Type	Width [min]	Area [pA*s]	Height [pA]	Area %
1	44.833	BBA	0.2470	242.47057	11.83693	50.18971
2	46.388	BBA	0.2457	240.63754	11.61718	49.81029

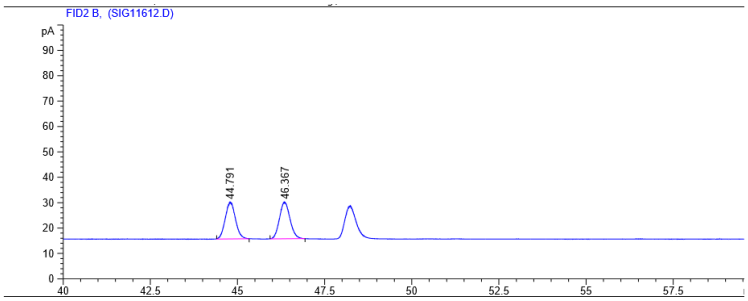

Peak #	RetTime [min]	Type	Width [min]	Area [pA*s]	Height [pA]	Area %
1	44.791	BBA	0.2425	292.43338	14.42415	49.11993
2	46.367	BBA	0.2507	302.91229	14.44002	50.88007

Figure S134: HPLC chromatographs of **3y'a**

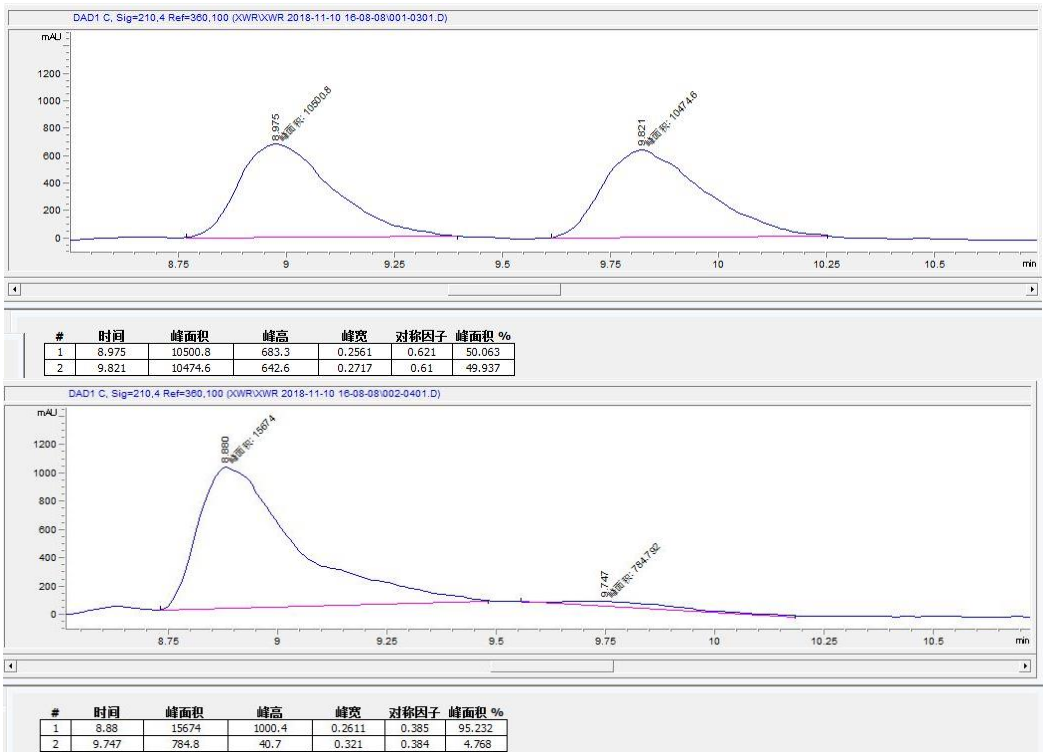

#	时间	峰面积	峰高	峰宽	对称因子	峰面积 %
1	8.975	10500.8	683.3	0.2561	0.621	50.063
2	9.821	10474.6	642.6	0.2717	0.61	49.937

#	时间	峰面积	峰高	峰宽	对称因子	峰面积 %
1	8.88	15674	1000.4	0.2611	0.385	95.232
2	9.747	784.8	40.7	0.321	0.384	4.768

Figure S135: HPLC chromatographs of **3ab**

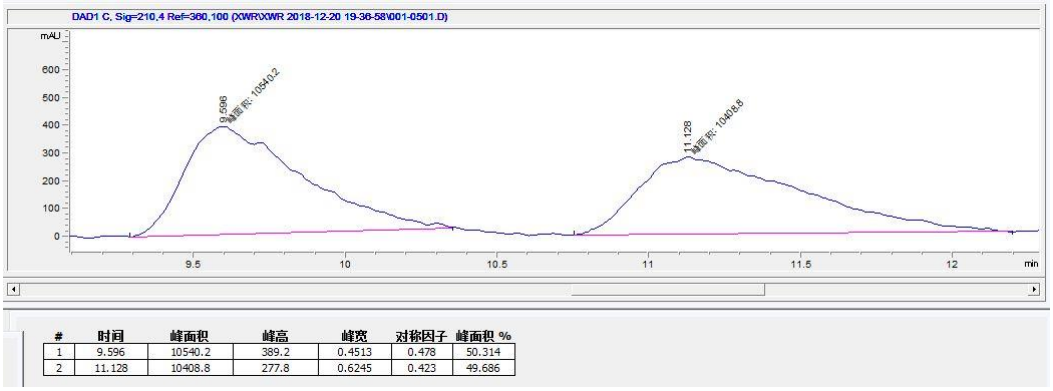

#	时间	峰面积	峰高	峰宽	对称因子	峰面积 %
1	9.596	10540.2	389.2	0.4513	0.478	50.314
2	11.128	10408.8	277.8	0.6245	0.423	49.686

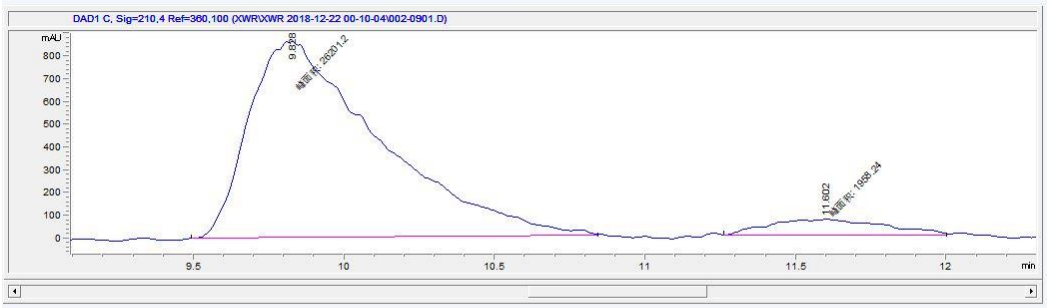

#	时间	峰面积	峰高	峰宽	对称因子	峰面积 %
1	9.828	26201.2	863.1	0.5059	0.483	93.046
2	11.602	1958.2	71.2	0.4586	0.979	6.954

Figure S136: HPLC chromatographs of **3ac**

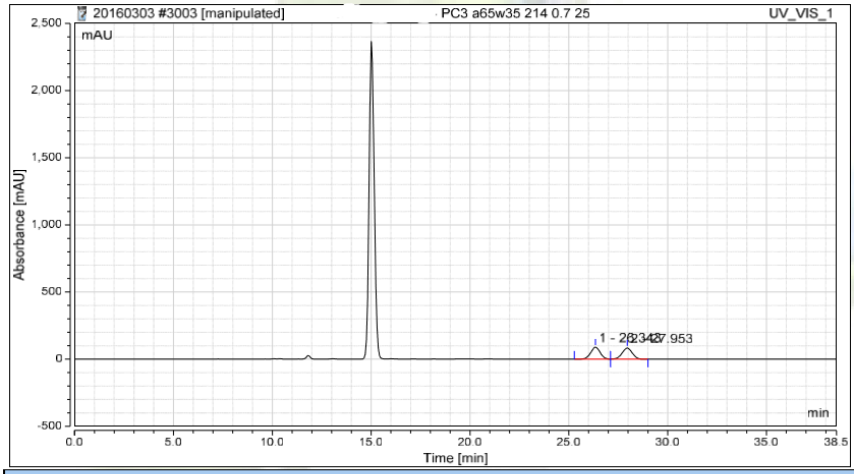

Integration Results

No.	Retention Time min	Retention Time min	Area mAU*min	Height mAU	Relative Area %
1	26	26.343	49.688	89.331	50.04
2	28	27.953	49.599	83.030	49.96

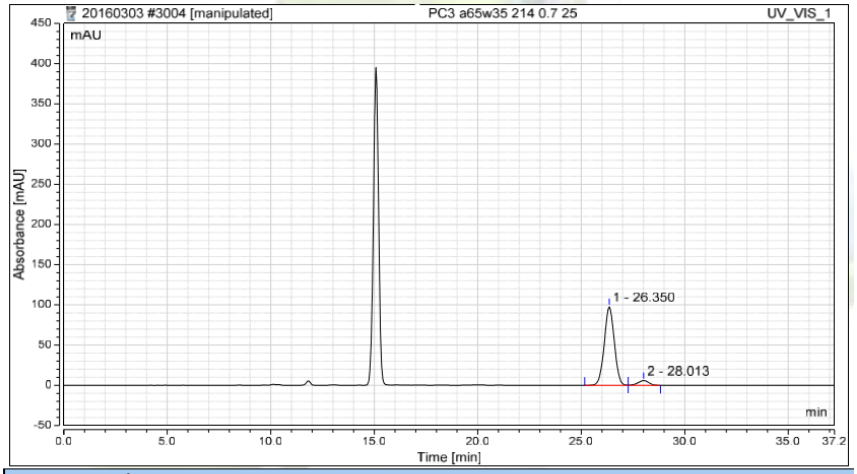

Integration Results

No.	Retention Time min	Retention Time min	Area mAU*min	Height mAU	Relative Area %
1	26	26.350	54.881	97.872	93.99
2	28	28.013	3.508	5.804	6.01

Figure S137: HPLC chromatographs of **3ad**

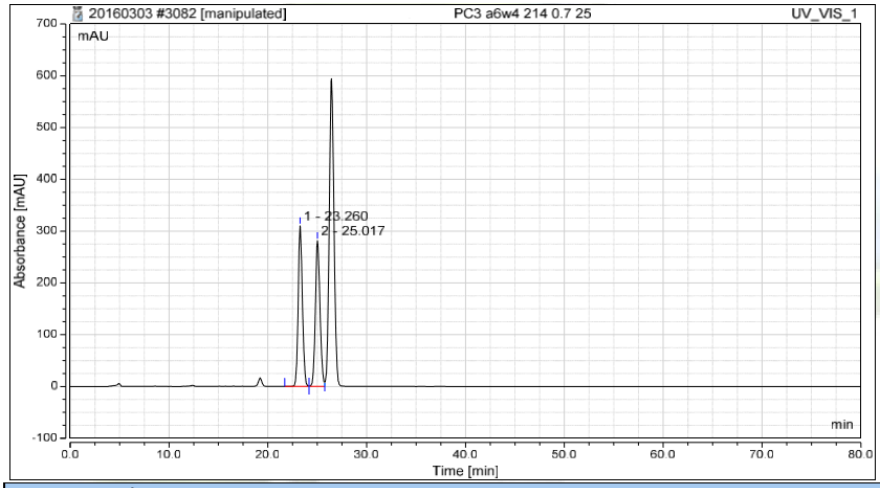

Integration Results

No.	Retention Time min	Retention Time min	Area mAU*min	Height mAU	Relative Area %
1	23	23.260	151.544	310.204	50.02
2	25	25.017	151.452	281.710	49.98

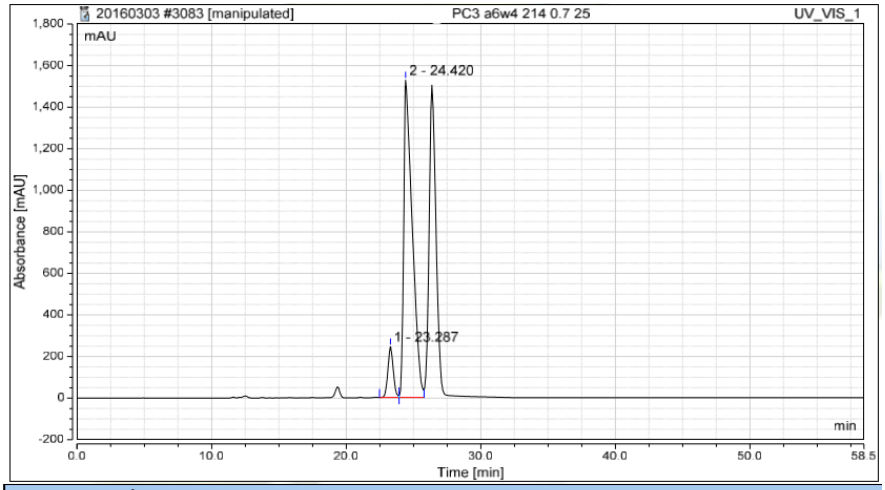

Integration Results

No.	Retention Time min	Retention Time min	Area mAU*min	Height mAU	Relative Area %
1	23	23.287	113.351	244.333	9.20
2	24	24.420	1118.747	1527.322	90.80

Figure S138: HPLC chromatographs of **3ae**

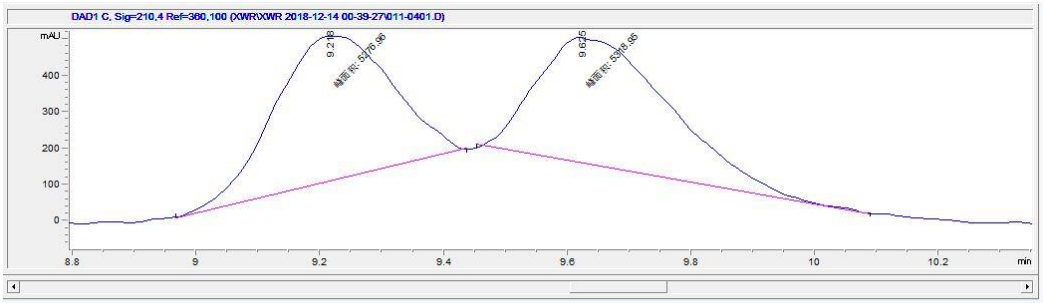

#	时间	峰面积	峰高	峰宽	对称因子	峰面积 %
1	9.218	5277	400.8	0.2194	0.969	49.802
2	9.625	5318.9	347.3	0.2553	0.458	50.198

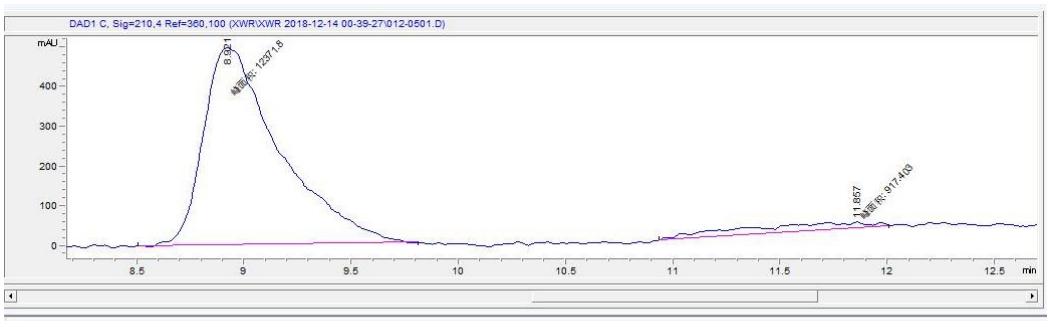

#	时间	峰面积	峰高	峰宽	对称因子	峰面积 %
1	8.921	12371.8	497.7	0.4143	0.453	93.097
2	11.857	917.4	16.5	0.9272	9.997	6.903

Figure S139: HPLC chromatographs of **3af**

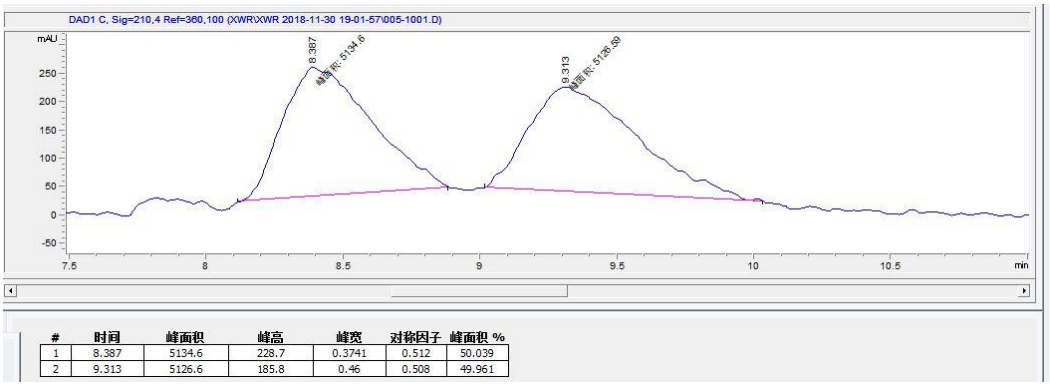

#	时间	峰面积	峰高	峰宽	对称因子	峰面积 %
1	8.387	5134.6	228.7	0.3741	0.512	50.039
2	9.313	5126.6	185.8	0.46	0.508	49.961

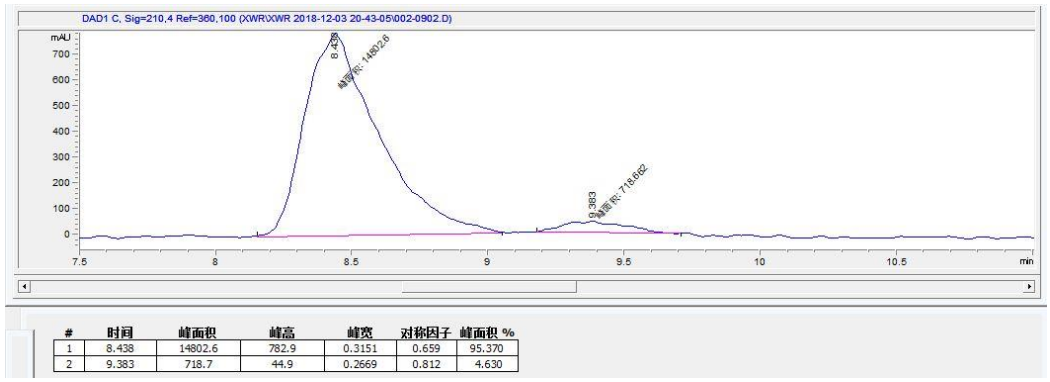

#	时间	峰面积	峰高	峰宽	对称因子	峰面积 %
1	8.438	14802.6	782.9	0.3151	0.659	95.370
2	9.383	718.7	44.9	0.2669	0.812	4.630

Figure S140: HPLC chromatographs of **3ag**

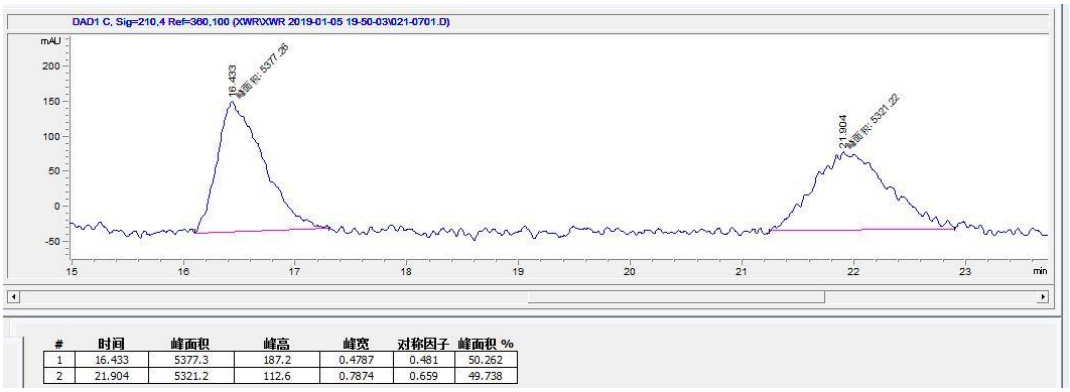

#	时间	峰面积	峰高	峰宽	对称因子	峰面积 %
1	16.433	5377.3	187.2	0.4787	0.481	50.262
2	21.904	5321.2	112.6	0.7874	0.659	49.738

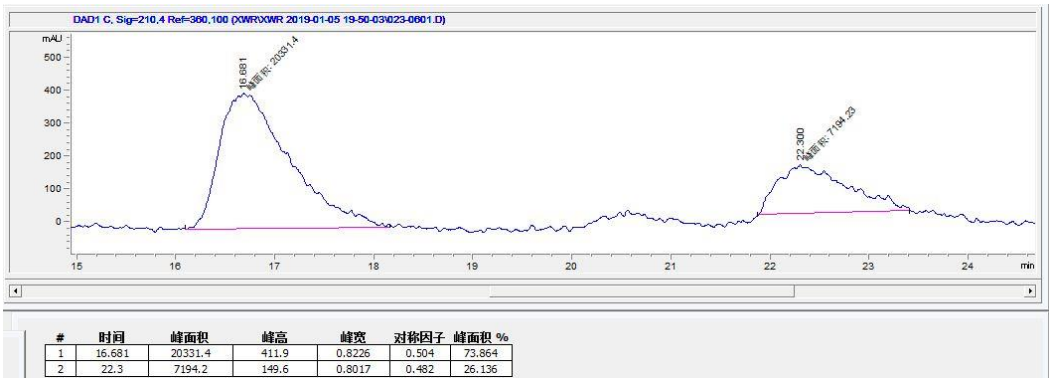

#	时间	峰面积	峰高	峰宽	对称因子	峰面积 %
1	16.681	20331.4	411.9	0.8226	0.504	73.864
2	22.3	7194.2	149.6	0.8017	0.482	26.136

Figure S141: HPLC chromatographs of **3ah**

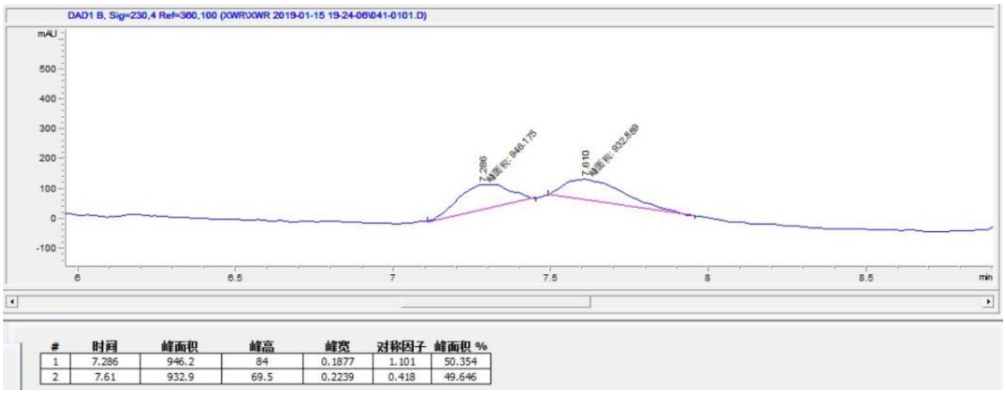

#	时间	峰面积	峰高	峰宽	对称因子	峰面积 %
1	7.286	946.2	84	0.1877	1.101	50.354
2	7.61	932.9	69.5	0.2239	0.418	49.646

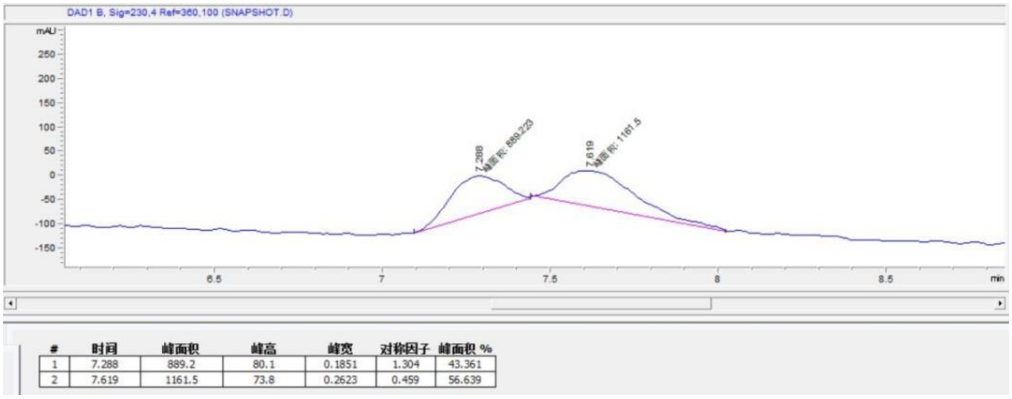

#	时间	峰面积	峰高	峰宽	对称因子	峰面积 %
1	7.288	889.2	80.1	0.1851	1.304	43.361
2	7.619	1161.5	73.8	0.2623	0.459	56.639

Figure S142: HPLC chromatographs of **3cj**

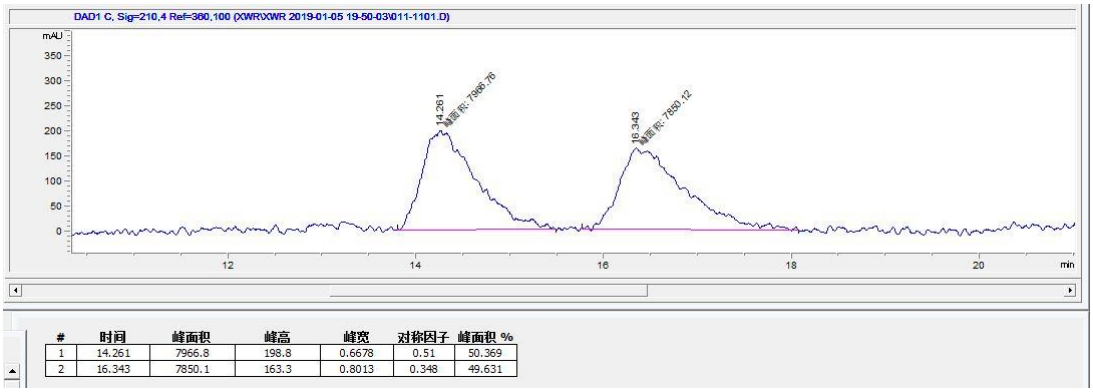

#	时间	峰面积	峰高	峰宽	对称因子	峰面积 %
1	14.261	7966.8	198.8	0.6678	0.51	50.369
2	16.343	7850.1	163.3	0.8013	0.348	49.631

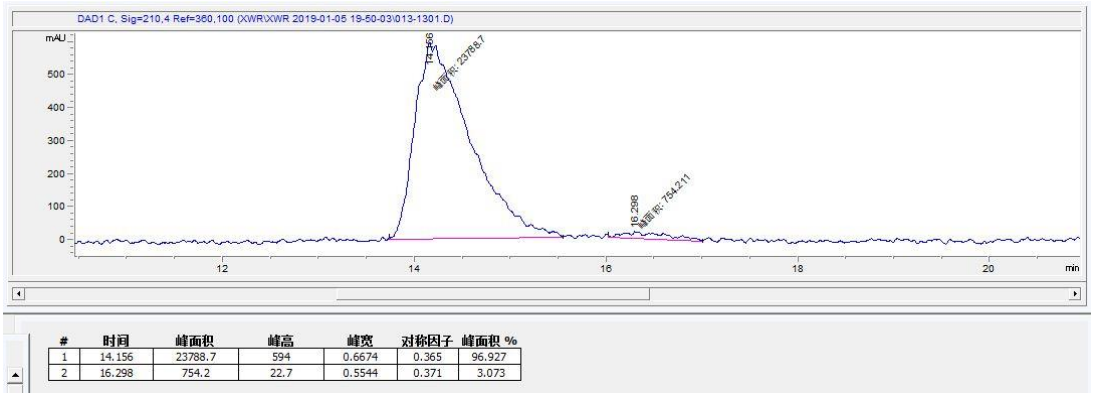

#	时间	峰面积	峰高	峰宽	对称因子	峰面积 %
1	14.156	23788.7	594	0.6674	0.365	96.927
2	16.298	754.2	22.7	0.5544	0.371	3.073

Figure S143: HPLC chromatographs of **3aa** of gram-scale experiment

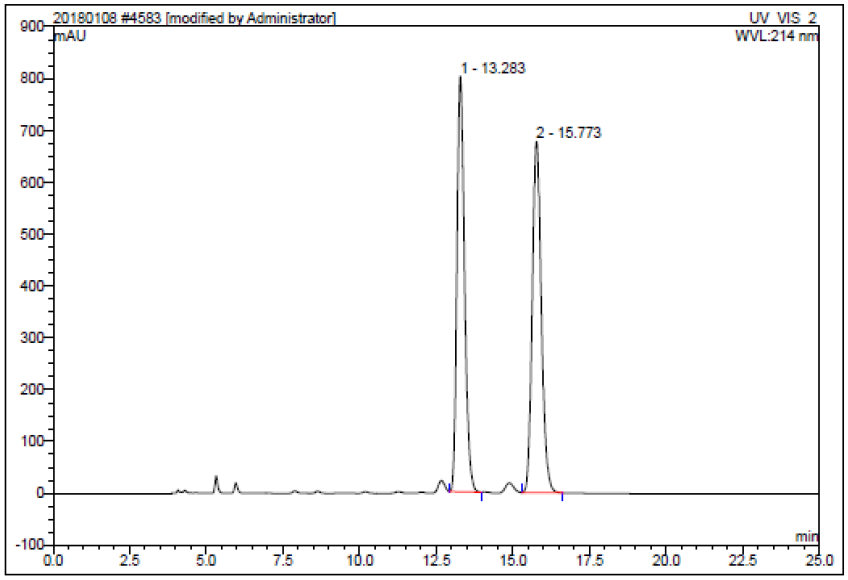

No.	Ret.Time min	Peak Name	Height mAU	Area mAU*min	Rel.Area %	Amount	Type
1	13.28	n.a.	801.713	229.791	49.63	n.a.	BMB*
2	15.77	n.a.	677.572	233.213	50.37	n.a.	BMB*
Total:			1479.286	463.004	100.00	0.000	

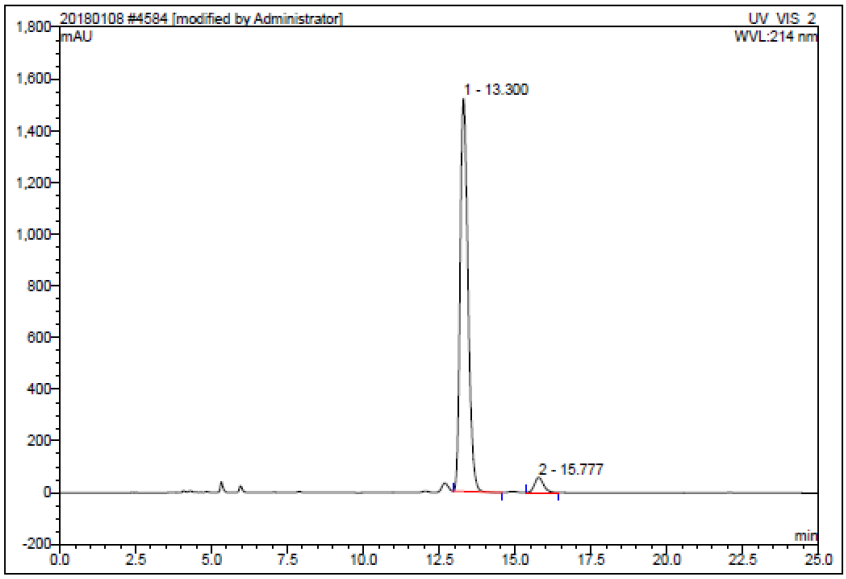

No.	Ret.Time min	Peak Name	Height mAU	Area mAU*min	Rel.Area %	Amount	Type
1	13.30	n.a.	1520.266	456.125	95.88	n.a.	BMB*
2	15.78	n.a.	57.823	19.601	4.12	n.a.	BMB*
Total:			1578.090	475.726	100.00	0.000	

Figure S144: HPLC chromatographs of **5a**